HABILITAČNÍ PRÁCE

2020 RNDr. Lucie Korecká, Ph.D.

UNIVERZITA PALACKÉHO V OLOMOUCI

Přírodovědecká fakulta

Enzymy v cílené modifikaci a diagnostice biologicky aktivních látek

RNDr. Lucie Korecká, Ph.D.

UNIVERZITA PARDUBICE

Fakulta chemicko-technologická

Katedra biologických a biochemických věd

HABILITAČNÍ PRÁCE

Obor: Biochemie

2020

Prohlášení:

Prohlašuji, že jsem tuto habilitační práci vypracovala samostatně s využitím citovaných literárních zdrojů.

V Pardubicích 1. 7. 2020 ……

Poděkování

Těch, kterým patří mé díky, a bez kterých by nejen tato práce, ale ani moje vědecká a akademická kariéra nebyly, je mnoho. Zejména bych chtěla zmínit prof. Zuzanu Bílkovou, která ve mně vkládá svou důvěru již od mých prvních vědeckých krůčků při diplomové páci. A těším se na další společné vědecké výzvy. Díky patří i panu prof. Karlu Vytřasovi a jeho kolegům za to, že mi ukázali, že elektrochemie má své kouzlo. Prof. Jean-Loius Viovymu a jeho týmu za možnost strávit nezapomenutelných deset měsíců v laboratořích Curie Institutu. Díky patří také Mgr. Michaele Šeligové (Čadkové) za její odvahu být mou první Ph.D. studentkou. Děkuji i mým nejbližším kolegyním, kolegům a našim současným postgraduálním studentům ze skupiny imunochemie naší katedry za příjemné a inspirativní pracovní prostředí.

Ten největší dík však patří mému manželovi a dětem, a také rodičům, za jejich lásku a podporu. A nerada bych zapomněla na své nejbližší přátele, se kterými vždy ráda zapomenu na pracovní starosti.

OBSAH

Úvod

Enzymy jako biokatalyzátory hrají v živých organismech klíčovou roli a díky svým vysoce specifickým vlastnostem nachází uplatnění v celé řadě *in vitro* aplikací. Pracují za mírných, ale přesně definovaných podmínek, a odráží i nepatrné změny v dějích, které katalyzují. Své pevné místo mají nejen v biochemické laboratorní diagnostice, ale díky snadné regulovatelnosti mohou být využívány i v široké škále biotechnologických aplikací.

V oblasti cílené katalýzy a modifikace biologicky aktivních látek jsou enzymy často imobilizovány na pevnou fázi a lze tak plně těžit z výhod, které tento způsob přináší. Nejen komerční dostupnost inertních nosičů, ale i možnost syntézy přímo v laboratoři, nabízí velkou variabilitu v přípravě imobilizovaných enzymových systémů. Díky široké škále materiálů, velikostí, tvarů a různých povrchových funkčních skupin lze systém cíleně přizpůsobit konkrétní aplikaci. Pro imobilizaci molekul enzymů jsou využívány různé metody zahrnující adsorpci, enkapsulaci, či pevnou kovalentní vazbu. Z pohledu orientace imobilizované molekuly enzymu lze využít metody neorientované neboli náhodné vazby, nebo metody orientované vazby. Při té je zohledněna konformace molekuly enzymu a jeho aktivního místa tak, aby vazbou nedošlo k negativnímu ovlivnění jeho výsledné aktivity. Imobilizací enzymu je často dosaženo také jeho větší stability a lepší kontrolovatelnosti katalyzované reakce. Další předností imobilizovaných enzymů je možnost opakovaného použití enzymu a minimalizace kontaminace produktu molekulami enzymu, což je důležité zejména pro biotechnologické nebo farmaceutické aplikace.

V oblasti laboratorní diagnostiky jsou enzymy využívány jako indikátory přítomnosti vybraných látek v analyzovaném materiálu. Jako jeden z možných příkladů metod využívajících enzymy lze uvést imunoanalytické metody s indikátory (ELISA, EIA), ve kterých jsou indikátorem právě enzymy. Jsou konjugovány se specifickými protilátkami a prostřednictvím konverze substrátu generují signál úměrný koncentraci sledovaného analytu v reakční směsi. Tyto metody patří, vzhledem k vysoké citlivosti a specifitě, mezi metody využívané ve farmacii a toxikologii pro monitorování hladin léčiv či při vývoji vakcín. V biochemických laboratořích pak pro stanovení hormonů či biomarkerů různých onemocnění. V potravinářském průmyslu pro detekci a kvantifikaci alergenů, toxinů apod. Obvyklá spektrofotometrická, fluorimetrická nebo chemiluminiscenční detekce může být v těchto metodách nahrazena i méně běžnou

elektrochemickou detekcí. Přestože tyto biosenzory, založené na principu ELISA, zatím nejsou v klinické praxi rutinně využívány, mají velký potenciál a již nyní přináší řadu výhod. Je asi pouze otázkou času, kdy taková zařízení najdou širší praktické uplatnění. Konstrukce takových imunosenzorů spočívá v kombinaci citlivé elektrochemické detekce se specifickou a selektivní reakcí antigen-protilátka. Navíc mohou být tyto systémy díky moderním technologiím miniaturizovány a splňují tak požadavky na „point-of-care“ zařízení.

Využití enzymů v kombinaci s magnetickými nosiči je průsečíkem všech prací uvedených v přílohách, které jsou souhrnem výsledků mé vědecké činnosti. Práce je rozdělena do dvou ucelených částí, z nichž první shrnuje výsledky týkající se přípravy imobilizovaných enzymových systémů pro cílenou *in vitro* modifikaci biologicky aktivních látek. Druhá část ukazuje možnosti využití enzymů pro značení protilátek v elektrochemických imunosenzorech určených pro detekci alergenů nebo biomarkerů asociovaných s nádorovým onemocněním.

1. Enzymy

Enzymy jsou přírodní katalyzátory, které při mírných podmínkách (teplota, pH, tlak) usnadňují nebo vůbec umožňují biochemické děje v organismu. To vše s vysokou rychlostí a bez trvalé změny vlastní molekuly. Je pro ně typická vysoká specifita a selektivita, díky které je zajištěna dokonalá kontrola nad průběhem katalyzovaných reakcí i nad výsledným produktem. Ačkoliv i některé molekuly RNA (tzv. ribozymy) vykazují katalytickou aktivitu, v naprosté většině se jedná o proteiny [1- 5].

Specifita enzymů je dána jednak typem substrátu, který je při enzymové reakci přeměňován, a jednak typem katalyzované reakce. V závislosti na reakčním mechanismu byly dosud enzymy děleny do šesti základních tříd (obrázek 1)

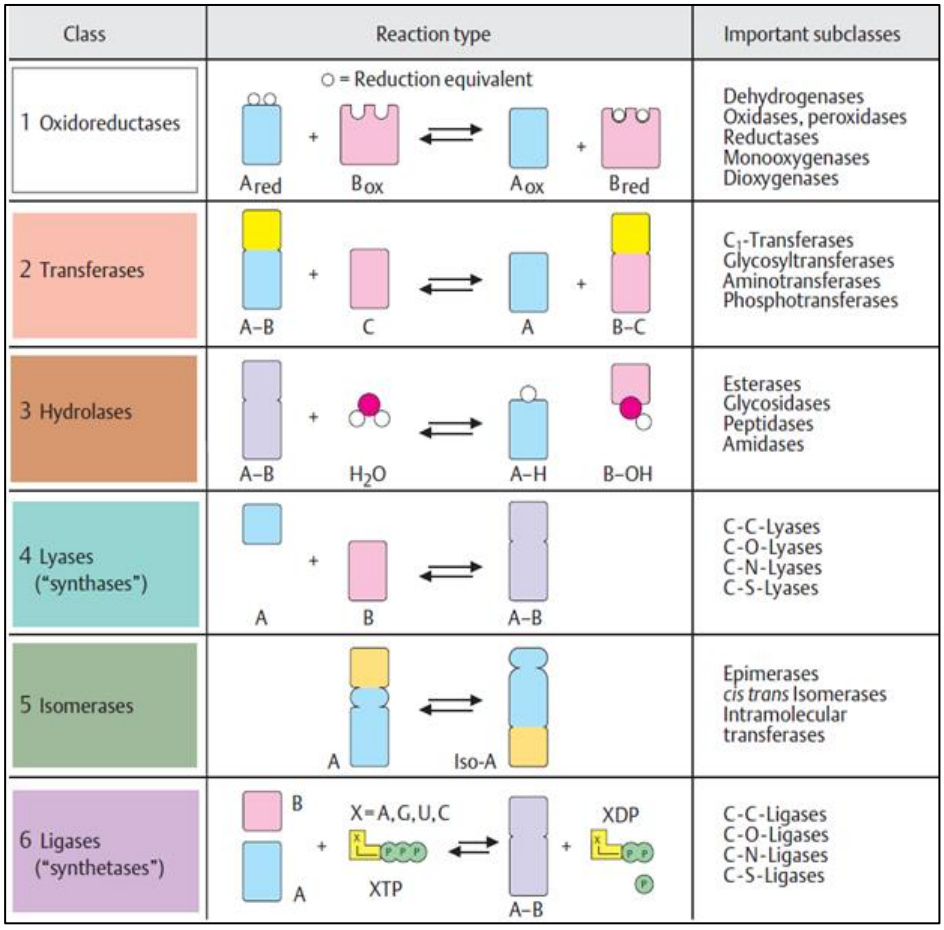

Obrázek 1. Klasifikace enzymů podle typu katalyzované reakce [https://ramneetkaur.com/enzyme-classification-mnemonic/]

V roce 2018 byla Mezinárodní unií pro biochemii a molekulární biologii (IUBMB) klasifikována sedmá třída enzymů, a to translokasy, které katalyzují přenos iontů a molekul přes membrány. Na základě lokalizace v organismu rozeznáváme enzymy membránově vázané, které jsou integrální součástí buněčných nebo organelových membrán, a solubilní, přítomné v cytoplazmě nebo sekretované do extracelulárních tekutin [2]. Podle původu pak rozlišujeme enzymy rostlinné, živočišné a mikrobiální [6].

Za substrátovou specifitu enzymu je zodpovědná proteinová část molekuly, označovaná jako apoenzym. Některé z enzymů mají povahu jednoduchých proteinů a pro vlastní katalytickou reakci nevyžadují přítomnost dalších skupin nebo molekul. Velké množství enzymů jsou však složené proteiny, u kterých je pro účinnou katalýzu nezbytná přítomnost koenzymu, části vykazující enzymovou aktivitu, a tvořící s apoenzymem kompletní aktivní molekulu enzymu. Koenzymy jsou malé molekuly neproteinové povahy, podléhající v průběhu katalyzované reakce změnám, které kompenzují transformace v molekule substrátu. Koenzymy hrají důležitou roli v přenosu vodíků, elektronů nebo skupin atomů [1].

V systémové biologii jsou enzymy využívány pro kinetická měření za simulovaných *in vivo* podmínek s cílem vytvořit komplexní prediktivní modely metabolických drah. Kinetika enzymů v těchto aplikacích poskytuje informace o aktivitě enzymu, reverzibilitě dané reakce či allosterii. Měla by být použitelná pro enzymové reakce s více substráty. Vytvořené modely pak pomáhají pochopit i nejsložitější biochemické procesy, které v organismu probíhají. Nejen v těchto aplikacích je pro optimální simulaci katalyzovaných reakcí důležitá charakterizace enzymů z pohledu jejich aktivity, kinetických parametrů a reakčních podmínek [7].

Enzymová aktivita udává rychlost katalyzované reakce vyjádřenou jako množství substrátu (v mol) přeměněné za 1 sekundu při definovaných reakčních podmínkách (pH, teplota). Jednotkou katalytické aktivity zavedenou v soustavě SI je katal ($mol.s^{-1}$) a nahrazuje jednotku enzymové aktivity U ($\mu mol.min^{-1}$), která je však často používána. Reakční rychlost vždy závisí jak na koncentraci enzymu, tak konvertovaného substrátu. Vztah mezi koncentrací substrátu a rychlostí enzymové reakce popisuje rovnice Michaelis-Mentenové. Z té lze vypočítat tzv. maximální (meznou) rychlost dané reakce (V_{max}), které je dosaženo při maximální saturaci enzymu substrátem, a Michaelisovu konstantu (K_m). Ta odpovídá koncentraci substrátu v polovině maximální rychlosti a je nepřímo úměrná afinitě daného substrátu k enzymu

(obrázek 2) [1, 4, 8]. Tyto veličiny charakterizují daný enzym a patří mezi základní parametry, které jsou hodnoceny při kinetických studiích, charakterizaci nových enzymů či při testování inhibičních látek.

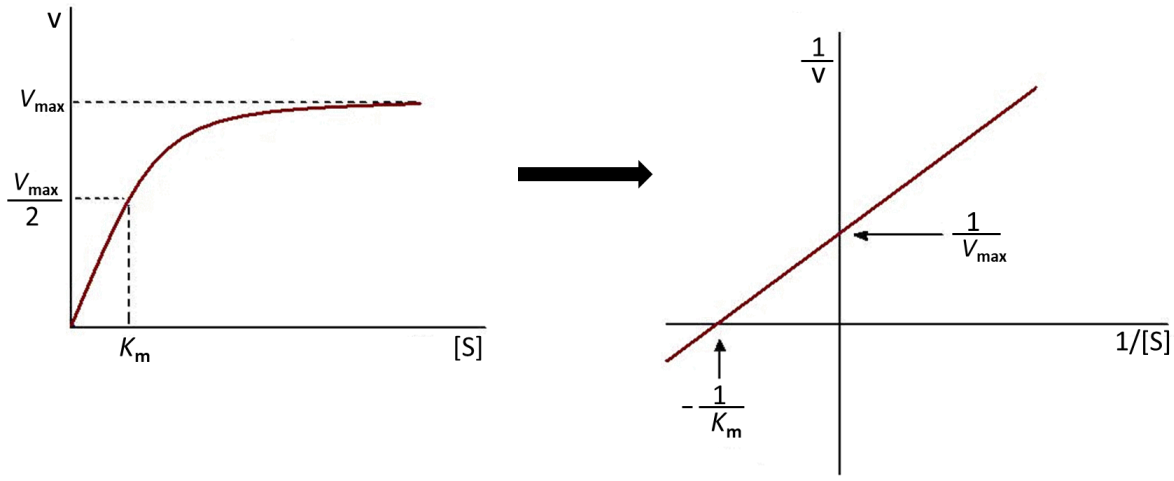

saturační křivka Linearizace Lineweaver-Burk

Obrázek 2. Grafické vyjádření kinetických parametrů enzymové reakce

Aktivita enzymů může být ovlivněna jak pozitivně (aktivátory), tak negativně (inhibitory). Ke zvýšení aktivity enzymů dochází vlivem post-translačních modifikací, jako je glykosylace [9,10] či fosforylace [11] nebo prostřednictvím kovalentně vázaných nízkomolekulárních aktivátorů [12,13]. Velkou roli hraje i mikroprostředí v bezprostřední blízkosti aktivního místa enzymu, např. přítomnost ligandů, které navozují jakousi enzymovou paměť [14]. Je obecně známé, že aktivita a stabilita enzymu může být zvýšena také imobilizací enzymu na pevnou fázi, která při vhodně zvolené metodice přispívá ke stabilizaci konformace molekuly enzymu. Inhibitory jsou definovány jako látky, které blokují aktivní místo enzymu, snižují reakční rychlost, nebo katalytickou reakci zastavují úplně. Na základě mechanismu je popisována inhibice kompetitivní, nekompetitivní, akompetitivní a smíšená. Ne vždy je inhibice nežádoucím jevem. *In vivo* fungují inhibitory u řady organismů v metabolických drahách jako součást jakési zpětné vazby, která umožňuje přirozenou regulaci těchto pochodů. Při využití enzymů v *in vitro* aplikacích je schopnost inhibitorů vázat se do aktivního místa s výhodou využívána pro izolaci a purifikaci enzymů, a také jako ochrana aktivního místa.

1.1 Enzymy jako nástroj pro *in vitro* modifikaci biologicky aktivních látek

Vzhledem k unikátním vlastnostem nachází enzymy uplatnění v celé řadě aplikací. V klinické laboratorní diagnostice patří monitorování vybraných enzymů mezi základní biochemická vyšetření. Změny v aktivitě některých orgánově/tkáňově specifických enzymů mohou poukazovat na vznik onemocnění, v jehož důsledku jsou enzymy ve zvýšené míře uvolňovány do tělních tekutin [15,16]. Monitorování hladin vybraných enzymů je důležité např. v diagnostice onemocnění jater, ledvin, pankreatu, některých nádorových onemocnění, infarktu myokardu a dalších [15].

Vedle klinické diagnostiky, biochemie, enzymologie či metabolomiky, kde jsou enzymy molekulou, která je monitorována, nebo přímo zasahuje do sledovaných dějů, jsou enzymy využívány i v jiných oblastech. Zde slouží jako nástroj pro modifikaci nebo přípravu jiných biologicky aktivních látek. Ve farmaceutickém či potravinářském průmyslu, stejně jako v oblasti biotechnologických aplikací, umožňují přípravu čistých produktů a nahrazují chemické metody syntézy. Oproti chemickým metodám jsou enzymy v těchto procesech výhodné pro jejich vysokou specifitu, možnost regulovat celý proces a eliminovat vznik případných nežádoucích vedlejších meziproduktů. Své pevné místo mají enzymy i v řadě metod, kde se uplatňují mj. v preanalytické fázi k úpravě vzorku.

V následujících částech jsou zmíněny některé konkrétní enzymy, na které jsem se zaměřila nebo se nadále zaměřuji ve své vědecké práci, včetně jejich konkrétních nebo potenciálních aplikací.

Jedním z enzymů, které jsou v literatuře nejvíce citovány, je proteolytický enzym trypsin, neboť je asi nejrozšířenějším enzymem proteomických studiích. Proteomika jako taková je obor, který se zaměřuje na systematické studium proteomu, tj. kompletní sklady proteinů, které se nachází v buňce nebo tkáni. Zohledňuje jejich strukturu, veškeré modifikace, vzájemné interakce i lokalizaci [17]. Klíčovými metodami jsou v proteomice vysoce účinné separační metody, 2D elektroforéza a kapalinová chromatografie ve spojení s tandemovou hmotnostní spektrometrií (LC-MS/MS, nanoLC-MS/MS). MS pak umožňuje vlastní identifikaci specifických peptidů [18-22]. Ať je využit kterýkoliv ze dvou základních přístupů v těchto experimentech („bottom-up“ či „top-down“), vždy zahrnuje enzymovou fragmentaci studovaných proteinů (obrázek 3) [23-25].

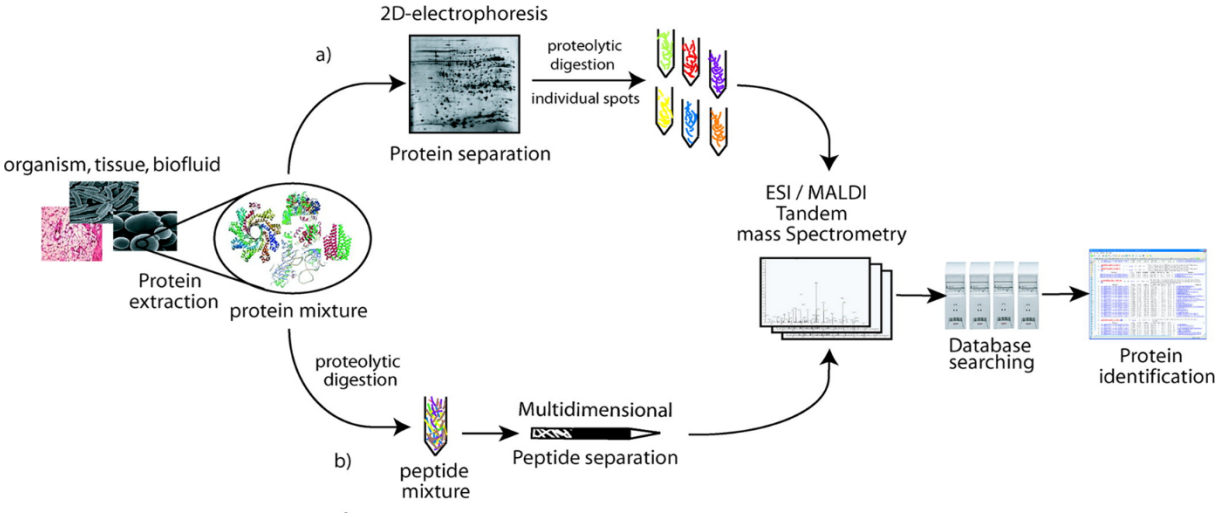

Obrázek 3. Schéma proteomické strategie pro identifikaci proteinů [26]

Právě pro tyto fragmentace je využíván trypsin, přestože jsou pro stejné účely popsány i jiné proteázy. Výhodou trypsinu je, že poskytuje peptidové fragmenty, které nesou na obou koncích pozitivní náboj a jsou pomocí MS snadno identifikovatelné [18,27-30]. Pro zvýšení účinnosti fragmentace, resp. pro přesnější finální identifikaci je trypsin využíván v kombinaci s dalšími proteinasami, jako jsou endoproteinasy Arg-C [27-29], Lys-C [18,27-31], Glu-C [27,29,30], Lys-N [29], Asp-N [29] nebo chymotrypsin [29,30] či subtilisin [27]. Pro identifikaci některých post-translačně modifikovaných proteinů, zejména fosfoproteinů, byly charakterizovány prolyl-endoproteasy (PEPs) [32], které jsou často kombinovány s trypsinem [33,34].

V proteomice méně využívanou proteázou je papain. Pomáhá při charakterizaci a identifikaci terapeutických protilátek, resp. jejich Fab fragmentů připravených z celých molekul imunoglobulinů pomocí papainu [35,36], nebo antigenů vázaných v komplexu [37]. Ten štěpí molekuly protilátek v tzv. pantové oblasti na dva Fab fragmenty a jeden Fc fragment. Uplatňuje se i při vlastní výrobě terapeutických protilátek [38,39] Díky chybějícímu Fc fragmentu mají protilátky lepší schopnost penetrace do tkání než původní celé molekuly, a tím lze zvýšit jejich terapeutický efekt [39,40]. Nebo v oblasti přípravy reagencií pro imunoanalytické nebo zobrazovací metody [41]. Papain je využíván také v potravinářském průmyslu pro redukci proteinových alergenů [42] nebo pro úpravu potravin (maso, mouka apod.) [37,43]. Zajímavou vlastností papainu je, že vedle jeho primární proteolytické funkce vykazuje i vedlejší glykosidasovou aktivitu, což bylo prokázáno již v minulosti. Tato aktivita je

uváděna nejen u již zmiňovaného papainu, ale také pepsinu, bromelainu či pronasy E. Tyto enzymy jsou využívány pro přípravu oligomerů glykosaminoglykanů, zejména chitosanu, chondroitinsulfátu a kyseliny hyaluronové. Tento proces je označován jako depolymerizace [44-49].

Kyselina hyaluronová (HA) a ostatní glykosaminoglykany jsou v posledních letech v popředí zájmu zejména v medicíně, farmaceutickém a kosmetickém průmyslu. Je to dáno vlastnostmi těchto biopolymerů a jejich účinky na živé organismy. HA je zkoumána zejména v oblasti protinádorových léčiv, kde se cílí na její specifické interakce s receptorem CD44, ve zvýšené míře exprimovaným nádorovými buňkami. Díky biokompatibilitě je vhodným kandidátem pro vývoj systémů pro cílenou distribuci léčiv (tzv. drug delivery systems), kdy bývá kombinována s dalším glykosaminoglykanem, chitosanem [50-52]. HA hraje v organismu řadu důležitých rolí, které se odvíjí od velikosti molekuly. Vysokomolekulární kyselina hyaluronová (HMW-HA, M_r > 800 kDa) se podílí se udržení integrity pojivových tkání, má hydratační, protizánětlivé a imunosupresivní účinky. Naopak nízkomolekulární HA je produkována při poškození tkání, podporuje produkci prozánětlivých mediátorů a podílí se na aktivaci imunitního systému a na procesech hojení ran [53-56]. Pro biologické aplikace, kdy jsou kladeny vysoké nároky na čistotu výsledných produktů, je pro přípravu kyseliny hyaluronové o různých molekulových hmotnostech výhodnější enzymová fragmentace než degradace chemickými nebo fyzikálními metodami. Chemická degradace spočívá v kyselé nebo alkalické hydrolýze [57] a její nevýhodou je nejen nezbytné přečištění získaných produktů, ale i obvykle široká distribuce velikostí fragmentů. Oproti tomu enzymová degradace umožňuje zisk fragmentů s užší distribucí molekulových hmotností a celý proces je lépe kontrolovatelný z pohledu reakčních podmínek. V případě kyseliny hyaluronové jsou specifickými enzymy, které štěpí glykosidické vazby v její molekule tzv. hyaluronidasy. Ty se podle reakčního mechanismu se rozdělují do tří skupin. Dvě z nich jsou endo-β-N-acetyl-hexosaminidasy, třetí je endo-β-glukuronidasa. Endo-β-N-acetyl-hexosaminidasy zahrnují eukaryotní hydrolasy (hovězí testikulární, lysozomální, či ze včelího jedu) a prokaryotní lyasy (produkované např. *Staphylococcus sp.*, *Streptococcus pyogenes* nebo *Streptococcus pneumoniae)* [58-61]. Hyaluronanlyasy mohou být pro tento účel připravovány rekombinantní technologií, a to nejčastěji pomocí geneticky modifikované

E. coli. Zdrojovými mikroorganismy bývají *Streptococcus pneumoniae* [62] nebo *Streptococcus pyogenes* [60,63], které přirozeně produkují tento enzym jako faktor virulence.

Cílená enzymová modifikace sfingolipidů může být uvedena jako další z příkladů *in vitro* modifikace biologicky aktivních látek. Modifikované sfingolipidy, konkrétně lyso-sfingolipidy, jsou využívány při analýze sfingolipidů v souvislosti s některými onemocněními. Sfingolipidy jsou komplexní molekuly složené z hydrofobního ceramidu, tvořeného mastnou kyselinou a sfingosinem (*N*-acylsfingosin), a hydrofilní hydrofilní sacharidové nebo fosforylcholinové části [64,65]. Jejich gykosylované formy, glykosfingolipidy (GLs) jsou složkou lipidů buněčných membrán eukaryot. Hrají důležitou roli v mezibuněčné signalizaci, ovlivňují procesy buněčné diferenciace, proliferace, adheze. Patogenní mikroorganismy je také využívají jako povrchové receptory při napadení hostitelské buňky [64,66-69]. Molekuly sfingolipidů mohou být v řetězci ceramidu *N*-deacylovány za vzniku lyso-sfingolipidů. Ty jsou v normálních tkáních a buňkách přítomné v nízkých koncentracích, ale dochází k jejich akumulaci v buňkách a tkáních v důsledku dědičných metabolických chorob tzv. lysosomálních „střádavých" onemocnění (Gaucherova choroba, Krabbeho choroba, metachromatická leukodystrofie aj.) [64,66,69,70]. Deacylace sfingolipidů může být provedena buď chemicky nebo působením enzymů. Chemické metody, konkrétně alkalická hydrolýza a hydrazinolýza, vedou k oddělení mastné kyseliny gangliosidů a tvorbě lyso-forem. Navíc však dochází i k nežádoucímu odštěpení *N*-acetylhexosaminu [71]. Jinou možností může být enzymová modifikace sfingolipidů, která umožňuje získat čistý reakční produkt, a navíc probíhá za mírných reakčních podmínek [72]. Hydrolýzu *N*-acylové vazby sfingolipidů mezi mastnou kyselinou a sfingosinem řetězce ceramidu za tvorby jejich lyso-forem katalyzuje enzym sfingolipid ceramid *N*-deacylasa (SCDasa).

Odkloníme-li se od hydrolytických enzymů, zajímavým enzymem, který může nalézt širší uplatnění zejména v biotechnologických procesech, a se kterým jsme pracovali, je lakasa. Spektrum aplikací lakáz je poměrně široké, od dekolorizace a detoxikace odpadních barviv v textilním průmyslu, přes zábranu oxidace některých látek v potravinářském průmyslu až po uplatnění v oblasti biosenzorů pro analýzu fenolických látek [73-78]. V posledních letech je lakasa testována i v souvislosti se syntézou biopolymerních materiálů pro medicínské využití, a to zejména hydrogelů. Hydrogely jsou syntetizovány z výše zmiňované kyseliny hyaluronové nebo chitosanu intramolekulárním zesítěním. Lakasa může

sloužit buď jako činidlo, které zprostředkovává polymeraci hydrogelu [78,79], nebo pro modifikaci již syntetizovaných hydrogelů. Lakasa je schopná selektivně oxidovat polární hydroxylové skupiny za vzniku karboxylových skupin. Takto modifikované hydrogely vykazují lepší biologické vlastnosti (hydratační nebo absorpční účinky) [80,81].

1.2 Enzymy jako signál generující značky v analýze biologicky významných látek

Vedle využití enzymů v přípravě vzorků a usnadnění vlastní analýzy konkrétních biomolekul, fungují enzymy v dnešní době rutinně v laboratorní diagnostice jako signál generující molekuly v indikátorových imunoanalytických metodách. V závislosti na tom, zda se jedná o látky nízkomolekulární nebo vysokomolekulární, se odvíjí uspořádání těchto metod, kdy pro nízkomolekulární analyty je využíváno uspořádání kompetitivní, pro vysokomolekulární pak tzv. sendvičové (obrázek 4).

Společným principem imunoanalytických metod s indikátory je reakce mezi protilátkou a antigenem, která je vysoce specifická, proto jsou tyto metody citlivé a vhodné pro kvantifikaci analytů přítomných ve vzorku v nízkých koncentracích. Za výsledný signál, který je monitorován, je zodpovědný indikátor (nebo značka) konjugovaný s jednou z reagujících složek. Podle typu indikátoru jsou pak tyto metody klasifikovány do několika skupin. Nejstaršími metodami jsou radioimunoanalytické (RIA z angl. Radioimmunoassay), využívající jako indikátor radioizotop. RIA metody jsou vysoce citlivé, nicméně jsou v nahrazovány metodami s jinými indikátory, zejména enzymy (EIA z angl. Enzyme immunoassay, ELISA, Enzyme-linked immunosorbent assay), fluorofory (FIA z angl. Fluoroimmunoassay) nebo luminofory (CLIA z angl. Chemiluminiscent immunoassay) [82,83]. Nejrozšířenějšími z nich jsou ELISA metody. Přehled metod a nejčastěji používaných indikátorů je uveden v tabulce 1.

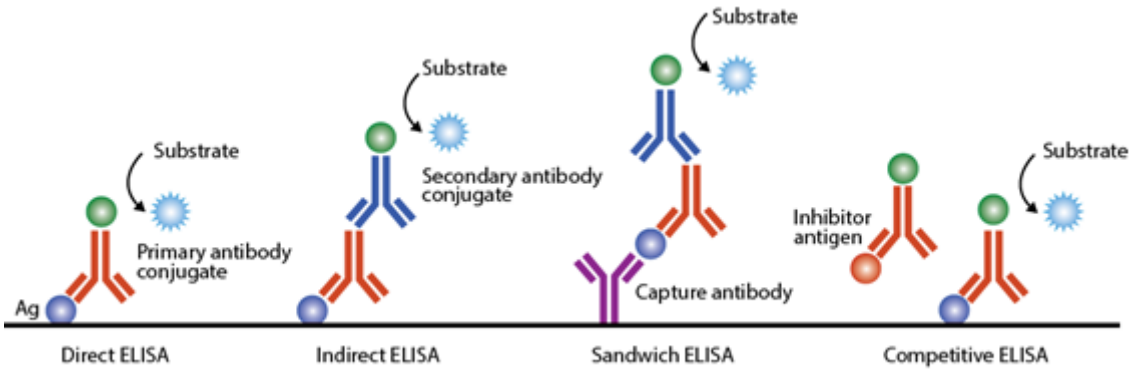

Obrázek 4. Možná uspořádání indikátorových imunoanalytických metod [84]

Enzymová imunoanalýza je dnes v biochemické laboratorní diagnostice využívána rutinně pro stanovení hormonů, biomarkerů různých onemocnění, alergenů, dále monitorování hladin léčiv ve farmacii a toxikologii [85]. Pro malé molekuly s jednou antigenní determinantou, jako jsou léčiva, steroidy, hormony štítné žlázy je běžné zejména kompetitivní uspořádání [86-88]. Pro velké molekuly nesoucí vice antigenních determinant je pak vhodnější nekompetitivní neboli sendvičové, uspořádání. Příkladem mohou být nádorové biomarkery proteinové povahy, alergeny, bakteriální toxiny, antigenní molekuly infekčních onemocnění (virových, bakteriálních, mykotických) nebo molekuly protilátek [89,90].

Pro snadnou manipulaci je v heterogenním provedení (ELISA) jedna z reakčních složek fixována na pevnou fázi. Tou bývá nejčastěji jamka mikrotitrační destičky, stěna zkumavky, nebo povrch magnetických částic [91,92]. Základní princip sendvičové ELISA metody sestává z několika kroků, z nichž první je založen na afinitní reakci mezi primární protilátkou a antigenem (stanovovaná molekula). Vzhledem k vysoké specifitě reakce antigenu s protilátkou lze izolovat stanovovanou látku z komplexní biologické matrice bez nutnosti další úpravy vzorku, a to i v případě nízkých koncentrací. Následuje reakce s druhou, enzymem značenou protilátkou, která se specificky váže na jiné epitopy antigenu, a po přídavku substrátu dochází k enzymové konverzi na produkt poskytující signál úměrný koncentraci (obrázek 5).

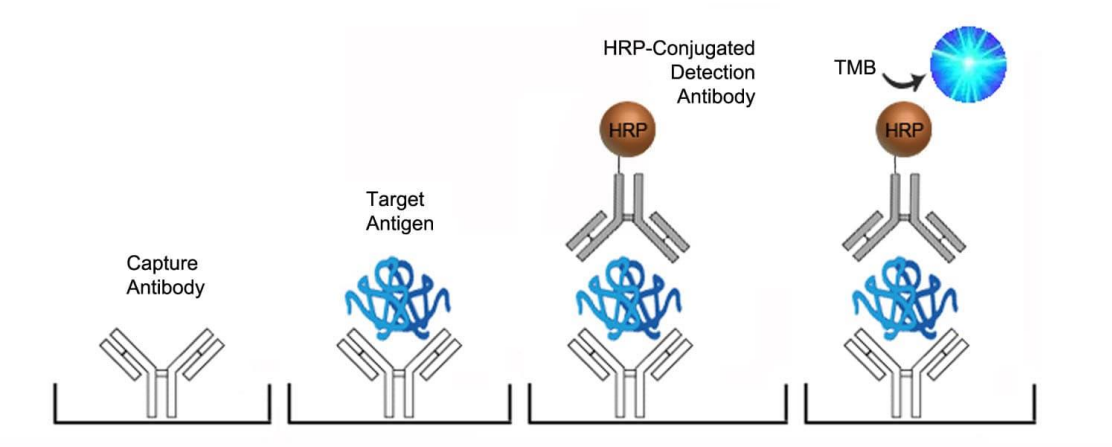

Obrázek 5. Princip a provedení sendvičové ELISA metody [93]

Nejvíce využívanými enzymy pro značení protilátek jsou křenová peroxidasa, alkalická fosfatasa a glukosooxidasa. V závislosti na použitém substrátu je pak detekce spektrofotometrická nebo fluorescenční.

Tabulka 1. Nejčastěji používané značky a substráty v imunoanalytických metodách [94]

metoda	**značka**	**substrát/chromogen**
EIA/ELISA	křenová peroxidasa	peroxid vodíku/OPD (TMB)
	alkalická fosfatasa	*p*-nitrofenylfosfát
	glukosooxidasa	glukosa + O_2
FIA	fluoresceinisothiokyanát (FITC)	
	alkalická fosfatasa	4-methylumbelliferylfosfát
	β-galaktosidasa	4-Methylumbelliferyl β,D –galaktopyranosid
LIA/CLIA	acridiniumslufát	peroxid vodíku
	luminol	peroxid vodíku
ECLIA	rutheniový komplex	tripropylamin
RIA	I^{125}	

Přestože jsou tyto metody běžně zavedené do praxe, v posledních letech se objevuje stále více prací, kdy je princip ELISA metod převeden do oblasti elektrochemických biosenzorů, resp. imunosenzorů. Historie biosenzorů sahá již do 50. let minulého století, kdy L. C. Clark představil kyslíkovou sondu pro měření kyslíku v krvi. Následně byla kombinována s enzymovou elektrodou s imobilizovanou glukózooxidázou pro měření hladiny glukózy v krvi. Tyto objevy daly vznik, v dnešní době běžně rozšířeným, glukometrům, které jsou konstruovány jako jednoduchá, přenosná zařízení. Právě jednoduchost, rychlost a relativně nízká cena jsou důvody vývoje elektrochemických biosenzorů s potenciálem v klinické

diagnostice. Biosenzory jsou analytická zařízení, která ve vhodném uspořádání splňují požadavky na tzv. Point-of-Care zařízení (POCT) [95]. Ta jsou určena pro rychlé testování různých biomarkerů přímo u lůžka pacienta namísto analýzy obvyklými instrumentálně náročnějšími metodami v klinických laboratořích.

Biosenzory jsou typem chemických senzorů tvořených ze dvou základních složek, biologické rozpoznávací složky a fyzikálně-chemického převodníku poskytujícího výsledný signál. Selektivita rozpoznávacích složek umožňuje detekci sledované molekuly i v komplexních biologických matricích bez jakékoliv úpravy vzorku. U enzymových biosenzorů je rozpoznávací složkou molekula enzymu, která je fixována přímo na povrch převodníku, a slouží k selektivní katalýze sledované reakce [96]. Imunosenzory jsou založeny na stejném principu jako ELISA metody, využívají vysoce specifické imunoafinitní reakce mezi protilátkou a antigenem ze vzorku za tvorby imunokomplexu při dosažení vazebné rovnováhy. Za výsledný signál je zodpovědná druhá značená protilátka (tzv. konjugát) se schopností vazby na vzniklý imunokomplex, a to prostřednictvím enzymu, který je s protilátkou konjugován. Enzymy pro konstrukci elektrochemických imunsenzorů jsou, stejně jako v ELISA metodách, křenová peroxidasa (HRP) a alkalická fosfatasa (ALP) [96-98]. Jejich specifické substráty nebo produkty enzymové konverze jsou elektrochemicky aktivní látky.

Aby se mohly elektrochemické imunosensozory rozšířit do praxe ve větším měřítku, je nezbytné, aby dosahovaly srovnatelných parametrů se standardními metodami, zejména citlivosti, selektivity a reprodukovatelnosti. Jsou konstruovány tak, že protilátky, zodpovědné specifické rozpoznání antigenu, jsou fixovány buď přímo na povrch převodníku, nebo jsou s ním v těsném kontaktu, aby byl zajištěn transport elektronů na elektrodě. Pro měření jsou dnes již komerčně dostupné jednorázové tištěné elektrody, nejčastěji v tříelektrodovém uspořádání (pracovní, referentní a pomocná elektroda) (obrázek 6). Lze vybírat z různých materiálů pracovní elektrody v závislosti na stanovované molekule.

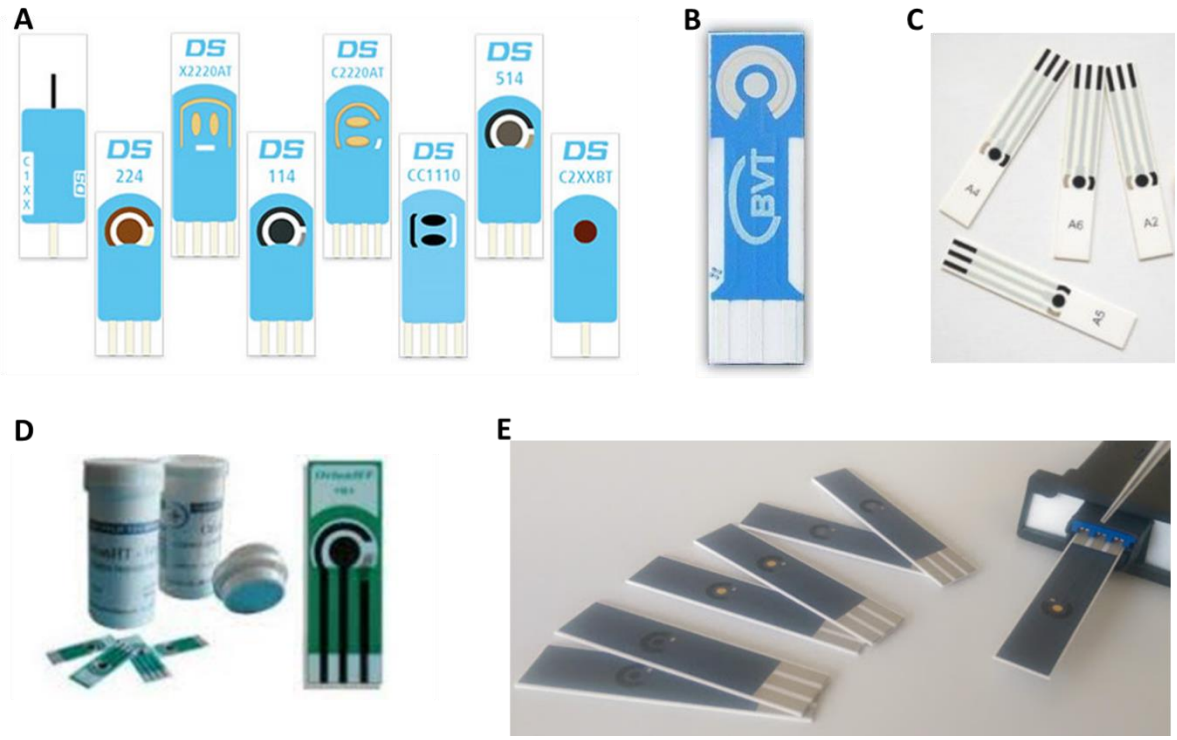

Obrázek 6. Příklady komerčně dostupných jednorázových tištěných senzorů: ***A*** *- Metrohm (Švýcarsko),* ***B*** *– BVT Technologies (ČR),* ***C*** *- ItalSens (Španělsko),* ***D*** *– Orion HighTechnologies (Španělsko),* ***E*** *- Gwent Group (Velká Británie)*

O selektivitě a citlivosti imunosenzoru rozhodují protilátky, a to záchyt antigenu ze vzorku, i značené protilátky, poskytující signál. Jsou-li protilátky pro záchyt antigenu fixovány přímo na povrch pracovní elektrody (tj. převodníku), může být citlivost imunosenzoru negativně ovlivněna v důsledku horšího pohybu elektronů vlivem velikosti molekul protilátek. Proto jsou v posledních letech elektrody modifikovány vrstvami, které uměle zvětšují povrch nebo usnadňují elektronový transport. Často je využívána modifikace grafenem [99,100], či Nafionem [101]. Lze také využít imobilizace protilátek na magnetické částice nebo membrány, kdy veškeré kroky tvorby imunokomplexu probíhají mimo povrch elektrody. Ta je využita pouze pro finální měření.

Více však o citlivost imunosenzoru rozhoduje volba vhodně značené druhé protilátky. Při použití enzymem značených protilátek dosahuje vyšší citlivosti ALP než HRP. HRP většinou vyžaduje ještě přítomnost elektronového mediátoru pro účinný transport elektronů. Jako mediátory bývají využívány thionin [102] nebo methylenová modř [103]. Stále více prací se zaměřuje na amplifikaci výsledného signálu kombinováním enzymů s nanomateriály, které

mají velký specifický povrch a umožňují tak vazbu více molekul enzymu. Jsou využívány různé mesoporézní nanomateriály, zejména nanočástice z oxidu křemičitého (označované také jako silika nanočástice), mesoporézní oxid titaničitý, uhlíkové nanočástice nebo nanotrubice [97,104,105]. Další variantou pro amplifikaci signálu je využití přímo elektroaktivních nanomateriálů pro značení protilátek místo enzymů. Elektroaktivní nanomateriály jsou kovové nanočástice, zejména zlaté (AuNPs), stříbrné (AgNPs), palladiové (PdNPs) [106] či platinové (PtNPs). Kovové nanokrystaly, tzv. kvantové tečky (QDs) jsou také elektroaktivním nanomateriálem. Případně jsou využívány kompozity tvořené kovovými nanočásticemi v kombinaci s oxidem grafenu (GO) [107]. Možné uspořádání imunosenzorů s využitím enzymů, nanomateriálů nebo jejich kombinací, které mají potenciál v klinické laboratorní diagnostice, jsme shrnuli v roce 2018 v přehledovém článku publikovaném v časopise *Current medicinal chemistry* [83].

2. Imobilizované enzymy

Používáme-li enzymy pro cílenou modifikaci látek tak, jak bylo zmíněno výše, je často výhodné enzymy kotvit (tzv. imobilizovat) na pevnou fázi. Imobilizace enzymů umožňuje nejen lepší kontrolovatelnost enzymové reakce, ale také opakované použití enzymu, což je důležité zejména pro biotechnologické využití. Zároveň je po reakci enzym snadno odstraněn ze směsi, takže např. při přípravě čistých produktů již není nutný další krok přečištění získaného produktu. Imobilizací je často dosaženo lepší stability (termostability, větší stability v různých reakčních prostředích), aktivity, zlepšení kinetických parametrů katalyzované reakce i omezení případných inhibičních účinků produktu [6,108-110]. Pro přípravu účinného imobilizovaného enzymu je klíčová volba vhodného nosiče, stejně jako způsob vazby molekul enzymu [111]. Po imobilizaci je pak nezbytná charakterizace z pohledu zachování enzymové aktivity a kinetických parametrů.

2.1 Nosiče pro imobilizaci enzymů

Pevné inertní nosiče vhodné pro imobilizaci enzymů jsou v současné době i komerčně dostupné v široké škále materiálů, velikostí, tvarů, porozity a různých povrchových funkčních skupin, přístupných pro vazbu molekul enzymů. Mohou být ve formě 2D struktur jako pevné

funkcionalizované vrstvy nebo filmy, nebo 3D struktur tvořících sférické částice, vlákna, trubice či sítě (tzv. skafoldy) [112].

Z materiálů jsou využívány nejčastěji anorganické materiály jako oxid křemičitý či oxidy kovů. Anorganické materiály se vyznačují velmi dobrou teplotní, mechanickou a mikrobiální odolností [5,113,114]. Z organických materiálů pak různé biopolymery jako např. celulóza, agaróza [109] chitosan, polydopamin, polyethylenimin (PEI) [115], polyakrylové či polyvinylové materiály. Jsou syntetizovány i anorganicko-organické kompozity [113,116]. Zvláštním typem polymerních materiálů, které lze využít pro imobilizaci enzymů, jsou hydrogely
a tzv. „inteligentní polymery (z angl. Smart polymers)“. Jedná se o biopolymerní materiály, které jsou schopné reagovat na změny vnějšího prostředí, vratnou změnou své konformace. Primárně reagují na změny teploty, pH či iontové síly, vlivem světla nebo magnetického pole. Jsou vyráběny zesítěním různých materiálů, např. alginátu, poly(ε-kaprolaktonu), poly-Lysinu, polyethylenglykolu, akrylamidu, poly-N-isopropylakrylamidu (polyNIPAM) a dalších [109,117-121].

Pro snadnou manipulaci jsou pevné nosiče modifikovány magnetickým materiálem a jsou připravovány magnetické částice. Pro jejich přípravu jsou využívány různé metody v závislosti na požadované výsledné velikosti částic, porozitě, povrchové funkcionalizaci, koloidní stabilitě a hydrofobních/hydrofilních vlastnostech povrchu. Nejběžnějšími metodami pro syntézu jsou mikroemulzní, disperzní, či suspenzní polymerace, chemická koprecipitace, termální dekompozice a další [**P6**,**P7**,6,122,123]. Magnetický materiál nejčastěji tvoří oxidy železa, maghemit (γ-Fe_2O_3) obsahující Fe^{3+} ionty, nebo magnetit (Fe_3O_4) obsahující Fe^{2+} i Fe^{3+} ionty [115,124,125,126]. Ty mohou být inkorporovány do polymerních částic precipitací [**P6,P7**] nebo jsou připravovány tzv. core-shell částice tvořené magnetickým jádrem a polymerním obalem [127-129]. Vlastnosti magnetických částic mohou být upraveny také post-syntetickou modifikací povrchu polymery, hydrofilními biomolekulami či surfaktanty [130].

Z komerčně dodávaných magnetických částic lze zmínit Dynabeads™ (www.thermofisher.com), SiMAG (www.chemicell.de), Sera-Mag™ (www.gelifesciences.com), Magnetická perlová celulóza (www.iontosorb.cz), Micromod (www.micromod.de), ProMAG® (www.bangslabs.com). Obrázek 7 ukazuje snímky některých

komerčních magnetických částic. Zároveň jsou vyvíjeny stále nové materiály či modifikace s ohledem na konkrétní aplikaci.

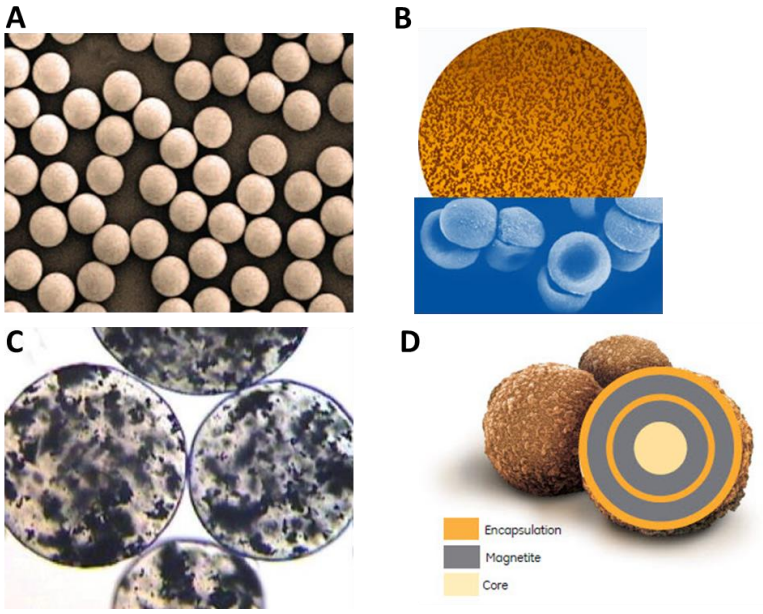

Obrázek 7. Příklady komerčně dostupných magnetických částic: ***A*** *- Dynabeads ™ M-270 (Invitrogen, USA),* ***B*** *- SiMAG částice (Chemicell, Německo),* ***C*** *- Magnetická makroporézní perlová celulosa IONTOSORB MG (Iontosorb, ČR),* ***D*** *– Sera-Mag ™ SpeedBeads ™ (GE Healthcare, Německo)*

Podle našich zkušeností je volba vhodného nosiče při přípravě imobilizovaného enzymu je velice důležitá a může významně ovlivnit výslednou aktivitu enzymu a jeho potenciál pro zamýšlenou aplikaci. S ohledem na molekulovou hmotnost imobilizovaného enzymu nebo jiné biologicky aktivní látky je dobré zohlednit jak velikost, tak porozitu použitých magnetických částic. Denzita a stabilita povrchových funkčních skupin pak ovlivňuje množství navázaných molekul, které však v případě enzymu nemusí odpovídat výsledné enzymové aktivitě.

2.2 Způsoby imobilizace enzymů

Přestože je pro přípravu imobilizovaných enzymů volba vhodného nosiče velice důležitá, o výsledné účinnosti imobilizovaných enzymů rozhoduje i použitý způsob imobilizace. Ten významně ovlivňuje nejen aktivitu enzymu po imobilizaci, ale i přístupnost aktivního místa pro substrát, a celkovou stabilitu. Pro vazbu jsou využívány různé způsoby zahrnující adsorpci,

enkapsulaci, zesíťování, iontovou vazbu nebo vazbu kovalentní. Z pohledu orientace imobilizované molekuly enzymu lze využít metody neorientované nebo orientované vazby, kdy je zohledněna struktura molekuly enzymu a jeho aktivního místa tak, aby vazbou nedošlo k negativnímu ovlivnění jeho aktivity.

Na základě interakce mezi enzymem a pevným nosičem rozdělujeme metody na fyzikální, kam řadíme adsorpci a zachycení v pevném materiálu, a chemické, které jsou založené na pevné vazbě mezi molekulami enzymu a materiálem (obrázek 8) [4,6,16,75,112,126,131,132].

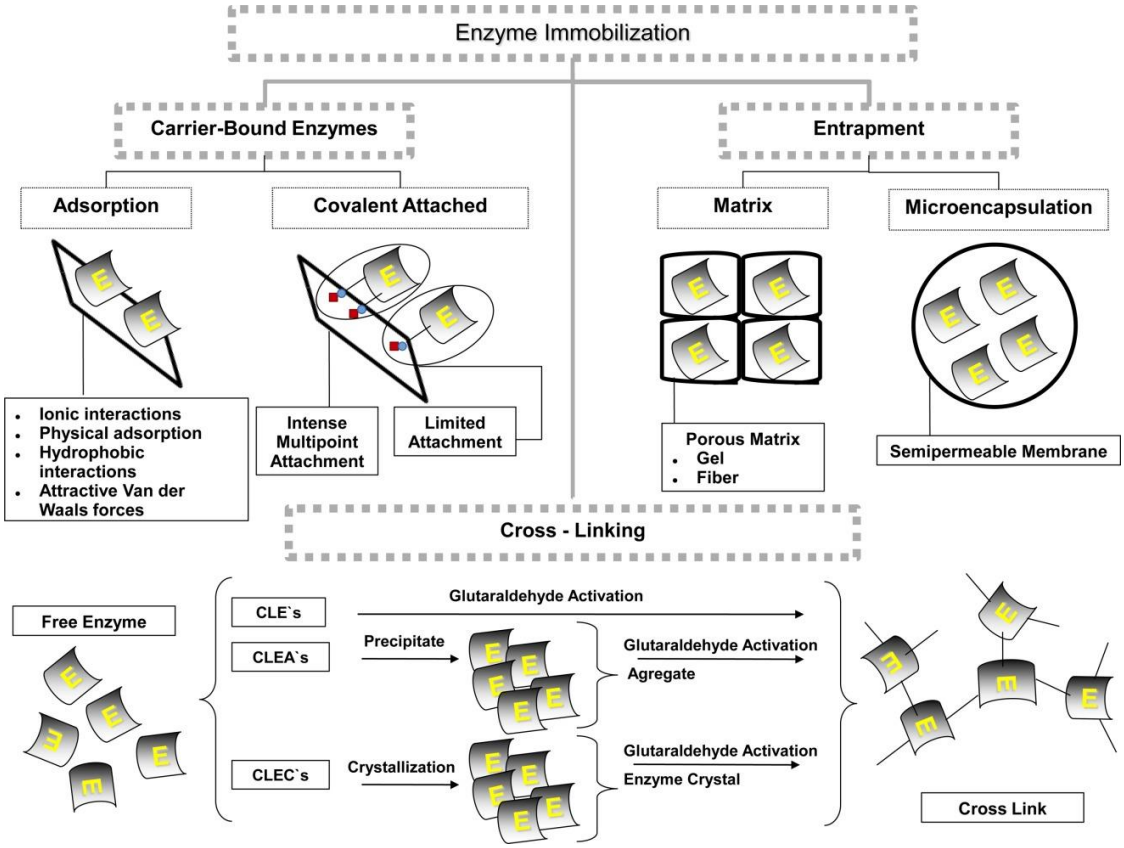

Obrázek 8. Přehled způsobů imobilizace enzymů na pevné nosiče [133]

Imobilizace adsorpcí

Fyzikální adsorpce patří mezi nejstarší imobilizační techniky, ale také nejjednodušší [132]. Zahrnuje fyzikální, iontovou, koordinační a afinitní adsorpci, z nichž nejběžnější je fyzikální. Enzymy jsou s povrchem nosiče poutány vodíkovými můstky, hydrofobními interakcemi, van der Waalsovými nebo elektrostatickými interakcemi [6,132,134]. Imobilizace enzymů nebo proteinů adsorpcí je výhodná také v tom, že probíhá za mírných podmínek a bez nutnosti

přídavku chemických činidel, což přispívá i k zachování vysoké aktivity enzymu. Naopak nevýhodou je, že často dochází k opětovnému uvolnění enzymu vlivem i mírných změn pH, teploty nebo iontové síly.

Při koordinační vazbě interagují kovové ionty (např. Cu^{2+}, Co^{2+}, Ni^{2+}, Zn^{2+}) fixované na nosiči s aminokyselinovými zbytky molekul enzymu. Afinitní chromatografie na imobilizovaných kovových iontech (IMAC) je využívána zejména pro purifikaci rekombinantně připravených enzymů a proteinů nesoucích His-tag. Existují ale i práce, ve kterých je popsáno využití této metody pro imobilizaci enzymů [135-137].

Imobilizace zachycením v polymerní matrici

Technika označovaná jako tzv. "entrapment" spočívá v zachycení molekul enzymu v polymerní síti tvořené z alginátu, chitosanu, polyakrylamidu, celulózy, sol-gel siliky či řady dalších polymerů [138]. Polymerní struktura tvoří buď vláknitou síť nebo obal mikrokapsulí. Vedle polymerů mohou být vytvářeny i kovové organické kostry (z angl. metal-organic frameworks, MOFs), které tvoří trojrozměrné porézní krystaly. Ve všech typech struktur je enzym zachycen, ale je umožněn průchod substrátu a následně produktu po enzymové reakci [6,109,112,132,139]. Stejně jako v případě adsorpce je výhodou zachování vysoké enzymové aktivity. Omezení však tento způsob imobilizace přináší při následném použití pro vysokomolekulární substráty, kde nemusí být zajištěna jejich dostatečná difuze do pórů polymerního materiálu.

Imobilizace kovalentní vazbou

Podstatou chemických technik je kovalentní vazba mezi pevnou fází a molekulami enzymu. Ta je tvořena mezi funkčními skupinami přítomnými na povrchu pevné fáze a ionizovatelnými postranními řetězci aminokyselin lysinu, argininu, histidinu, cysteinu, tyrosinu, kyseliny asparagové a glutamové [112,132,140]. Kovalentní imobilizace vede k tvorbě pevné vazby, odolné vůči opětovnému uvolňování enzymu. Vazba vzniká prostřednictvím chemického činidla, které aktivuje funkční skupiny na povrchu pevné fáze nebo v molekule enzymu před jejich spojením [126,141,142]. Vazbu a následně i vlastnosti imobilizovaného enzymu ovlivňuje řada faktorů, které je třeba zohlednit. Mezi ně patří fyzikálně – chemické vlastnosti

pevné fáze, typ chemické reakce a použitého aktivačního činidla, konformace a orientace molekul enzymu v průběhu imobilizace, i vlastnosti reakčního prostředí.

Fyzikálně – chemické vlastnosti pevné fáze jsou obvykle dobře definovány, a to nejen pro komerčně dodávané nosiče, ale i pro nově vyvíjené. Liší se velikostí a tvarem částic, materiálem použitým pro jejich výrobu, porozitou s definovanou velikostí pórů. U porézních částic je definován celkový povrch, který zahrnuje plochu vnitřního povrchu pórů a vnějšího povrchu. U neporézních materiálů je tedy vnitřní povrch nulový. Pro účinnou imobilizaci enzymů na porézní nosiče platí, že velikost pórů by měla být 3 - 9x větší, než je velikost imobilizované molekuly. Důležitá je informace o povrchových funkčních skupinách, a to nejen typu, ale i množství (hustotě). Podle toho lze volit optimální množství enzymu, které je imobilizováno. Při dostatečném množství funkčních skupin dochází i k tzv. vícebodové kovalentní vazbě molekuly enzymu (z angl. multipoint covalent attachment), která zvyšuje stabilitu imobilizovaného enzymu (z angl. enzyme rigidification) [108,143,144].

Podle typu funkčních skupin je volen *způsob jejich aktivace a reakční prostředí*. Nejčastějšími funkčními skupinami pro vazbu enzymů jsou hydroxylové, karbonylové, karboxylové, amino, epoxy, thiolové, kyanurové či hydrazidové. S těmi pak korespondují funkční skupiny v molekule enzymu, přes které je imobilizován (tabulka 2).

Tabulka 2. Přehled nejčastěji využívaných kombinací funkčních skupin na pevné fázi a molekule enzymu pro kovalentní imobilizace, včetně aktivačních činidel a typu vznikající vazby [142]

funkční skupina nosiče	funkční skupina proteinu	aktivační činidlo (aktivovaná skupina)	vznikající vazba
- COOH	- NH_2	• karbodiimid (- COOH)	amidová
- NH_2	- COOH	• karbodiimid (- COOH) • karbodiimid v kombinaci se sulfo-NHS esterem (- COOH)	amidová
	- NH_2	• autoreaktivní, bez aktivačního činidla	alkylaminová
- NH - NH_2	- OH	• jodistan sodný (- OH), s následnou reduktivní aminací	alkylaminová
- OH	- NH_2	• jodistan sodný (- OH), s následnou reduktivní aminací • karbonyldiimidazol	alkylaminová karbamátová
	- NH_2	• autoreaktivní, bez aktivačního činidla při pH 9	alkylaminová
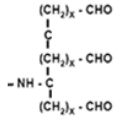	- NH_2	• autoreaktivní, bez aktivačního činidla	alkylaminová
- SH	- SH - NH_2	• autoreaktivní, bez aktivačního činidla • maleinimid	disulfidová thioetherová

V některých případech jsou využívána tzv. distanční raménka (z angl. spacer arms), kterými je modifikován nosič před vlastní kovalentní imobilizací enzymu. Tato raménka zajistí oddálení molekuly enzymu od pevné fáze. Toto oddálení pomáhá minimalizovat případné sterické zábrany a nežádoucí interakce enzymu s nosičem, eliminovat případný negativní vliv mikroprostředí nosiče, ale zároveň zajistí také konformační flexibilitu a mobilitu. Díky té si ve většině případů enzymy zachovávají po imobilizaci vyšší aktivitu z důvodu lepší dostupnosti aktivního místa pro molekuly substrátu. Vliv na výsledné vlastnosti imobilizovaného enzymu má nejen délka raménka (obrázek 9), ale i struktura, tvar a fyzikálně – chemické vlastnosti [132,145-147].

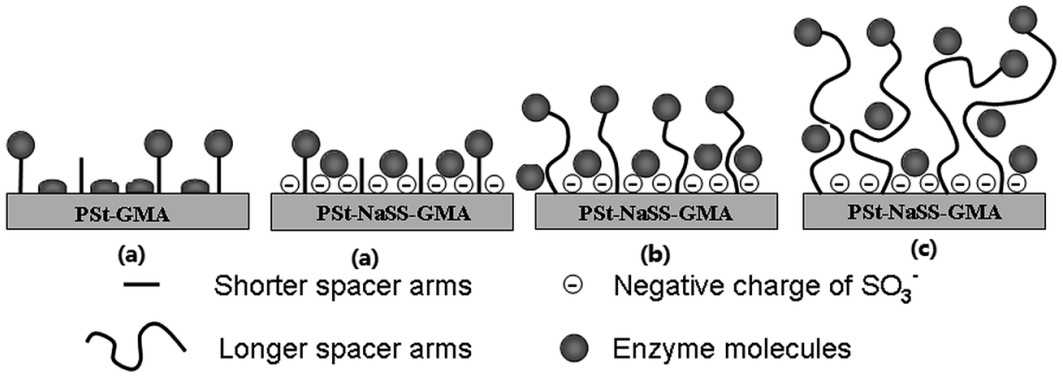

Obrázek 9. Schématické znázornění efektu délky distančního raménka na množství a konformační flexibilitu při imobilizaci enzymu [146]

Dalším parametrem, který ovlivňuje výslednou aktivitu enzymu po imobilizaci, je *orientace molekuly v průběhu imobilizace*. Je-li enzym vázán přes postranní řetězce aminokyselin bez ohledu na orientaci molekuly enzymu, jedná se o tzv. neorientovanou imobilizaci. V případě, že jsou do vazby zapojeny aminokyseliny, které jsou nezbytné pro katalytickou funkci enzymu nebo jsou součástí či v těsné blízkosti aktivního místa, může dojít k významnému poklesu aktivity enzymu po imobilizaci [148,149]. Byly vytvořeny počítačové simulace predikující, které aminokyseliny v rámci molekuly enzymu a s jakou pravděpodobností mohou vytvářet kovalentní vazby [143,150,151].

Proto jsou v některých případech využívány techniky tzv. orientované imobilizace, kdy je zohledněna orientace molekuly enzymu. Způsobů orientované imobilizace je několik. V případě glykosylovaných enzymů může být využita jejich sacharidová část molekuly, která je oxidována za vzniku reaktivních aldehydových skupin a následně tvoří s hydrazidem nebo amino modifikovaným nosičem stabilní vazbu [126,152,153]. Další možností je technika tzv. místně řízené mutageneze (z angl. site-directed mutagenesis), spočívající v substituci nebo zavedení specifické aminokyseliny do polypeptidového řetězce enzymu genetickou modifikací. Jako příklad lze uvést práci Cecchina a kol. (2007), kteří modifikovali penicilin G acylasu zavedením jednoho nebo více lysinů do aminokyselinové sekvence v oblastech různě vzdálených od aktivního místa. Takto modifikované molekuly imobilizovali na glyoxyl agarózu a sledovali vliv orientace enzymu na výslednou aktivitu [154]. Kromě lysinu je k substituci využíván také cystein, který zajistí následnou imobilizaci enzymu tvorbou disulfidové vazby [143,148]. Pro efektivní imobilizaci lipas lze využít systém reverzních micel, tedy na rozhraní vodné a organické fáze. Tento systém zaručuje orientaci aktivního místa k hydrofobní fázi.

Zároveň dochází k aktivaci enzymu. Pro lipasy je charakteristická změna konformace v závislosti na prostředí, kdy ve vodném prostředí jsou v uzavřené formě (tzv. lid/flap konformace). V přítomnosti organické fáze se konformace mění na otevřenou a hydrofilní skupiny vzdálené od aktivního místa míří do vodné fáze, ve které dochází k imobilizaci [155,156].

Vhodné *reakční prostředí* v průběhu imobilizace je důležité nejen v případě lipáz, ale i ostatních enzymů, a má vliv na výslednou účinnost imobilizace i aktivitu enzymu. Důležitá je volba vhodného pH, přítomnost solí. U enzymů náchylných k autolytickému štěpení se využívá imobilizace v přítomnosti kompetitivního inhibitoru nebo substrátu, díky kterým je současně i chráněno aktivní místo enzymu.

Kovalentní vazba je využívána pro imobilizace enzymů nejčastěji. Důvodem je vyšší stabilita imbilizovaných enzymů. Zvláštním typem kovalentní vazby je tzv. zesítění enzymů. Provádí se pomocí bifunkčních činidel, např. glutaraldehydu, dihydrazidu kyseliny adipové, H-hydroxysuccinimidu či derivátů maleimidu. Použití těchto činidel zlepšuje stabilitu imobilizovaného enzymu, ale může mít v některých případech negativní vliv na jeho výslednou aktivitu. Je využíváno k cílené přípravě tzv. zesítěných enzymových krystalů (z angl. cross-linked enzyme crystals – CLECs) a enzymových agregátů (z angl. cross-linked enzyme aggregates – CLEAs). Při tomto způsobu není využíván pevný nosič, na který je enzym imobilizován, ale dochází k intramolekulárnímu provázání enzymu. Tímto způsobem lze provázat i více enzymů s různou substrátovou nebo reakční specifitou. Příprava CLECs a CLEAs spočívá v krystalizaci, resp. nedenaturační agregaci molekul enzymu s následným zesítěním pomocí vhodného činidla. Při přípravě CLECs je důležité zajistit optimální konformaci molekuly, pH či iontovou sílu v průběhu krystalizace. Při tvorbě CLEAs výslednou selektivitu ovlivňují použitá agregační i síťující činidla [6,75,132,157].

2.3 Charakterizace imobilizovaných enzymů

Pro přípravu účinných imobilizovaných enzymů je nezbytná jejich charakterizace po imobilizaci. Pro charakterizaci je využívána řada metod v závislosti na tom, jaký parametr zjišťujeme. Obecně lze metody rozdělit na základní a pokročilé. Běžné metody spočívají ve stanovení absolutního množství navázaného proteinu, enzymové aktivity, kinetických

parametrů srovnávaných se solubilním enzymem. Dále je ověřena operační a skladovací stabilita a účinnost imobilizovaného enzymu za různých reakčních podmínek [110].

Základní metody charakterizace imobilizovaných enzymů využívají monitorování reakce enzymu se specifickým substrátem. Kinetické parametry (V_{max} a K_m) nám poskytují informace o zachování nebo změnách afinity enzymu k danému substrátu. Množství navázaného enzymu lze kvantifikovat pomocí běžných kolorimetrických metod pro stanovení proteinů (metoda dle Bradfordové, bicinchoninová metoda BCA). Nebo lze určit účinnost imobilizace po elektroforetické separaci (SDS-PAGE) porovnáním frakcí před a po imobilizaci.

Pokročilé metody jsou zaměřeny na přímé strukturní charakterizaci imobilizovaného enzymu a potvrzení přítomnosti enzymu na povrchu pevné fáze, případně v pórech. Mezi tyto metody řadíme mikroskopii atomárních sil (Atomic force microscopy; AFM) [130,158], Transmisní elektronovou mikroskopii (Transmission electron microscopy; TEM), termogravimetrii (Thermal gravimetric analysis; TGA) [111], infračervenou spektroskopii s Fourierovou transformací (Fourier transform infrared spectroscopy; FTIR) nebo křemenné mikrovážky (Quartz crystal microbalance; QCM) [110,159]. Imobilizací enzymu může docházet i ke změně koloidální stability pevné fáze v roztoku, proto je další metodou charakterizující imobilizovaný enzym také měření zeta potenciálu [110].

3. Imobilizované enzymy v cílené modifikaci biologicky významných látek

Příprava imobilizovaných enzymů a jejich využití pro cílenou modifikaci biomolekul je průsečíkem prací uvedených v přílohách [**P1-5**]. Pro imobilizaci vybraných enzymů byly využívány komerčně dostupné magnetické částice, jejichž přehled uvádí tabulka 3. V závislosti na zamýšlené aplikaci byla volena velikost částic, podle způsobu imobilizace pak funkční skupiny. Vedle komerčních částic jsme, v rámci spolupráce s Ústavem makromolekulární chemie Akademie věd (Praha, ČR), využívali pro imobilizace enzymů i nově vyvíjené magnetické částice.

Při přípravě imobilizovaných enzymů je nutné optimalizovat množství enzymu pro přípravu nejúčinnějšího nosiče, reakční prostředí a množství činidel pro imobilizaci. V některých

případech je potřebný přídavek detergentu pro zabránění agregace částic, což může negativně ovlivňovat výslednou účinnost imobilizace. Připravené nosiče s imobilizovanými enzymy pak byly charakterizovány z pohledu enzymové aktivity, kinetických parametrů, které byly porovnány se solubilním enzymem. Pro vlastní aplikaci je důležitá také operační a skladovací stabilita, aby připravené nosiče byly výhodné i z ekonomického hlediska. Pro finální aplikaci pak bylo optimalizováno i reakční prostředí. Tabulka 4 shrnuje informace o použitých částicích, které byly použity v rámci našich experimentů. Na obrázku 10 jsou fotografie nově vyvíjených magnetických částic.

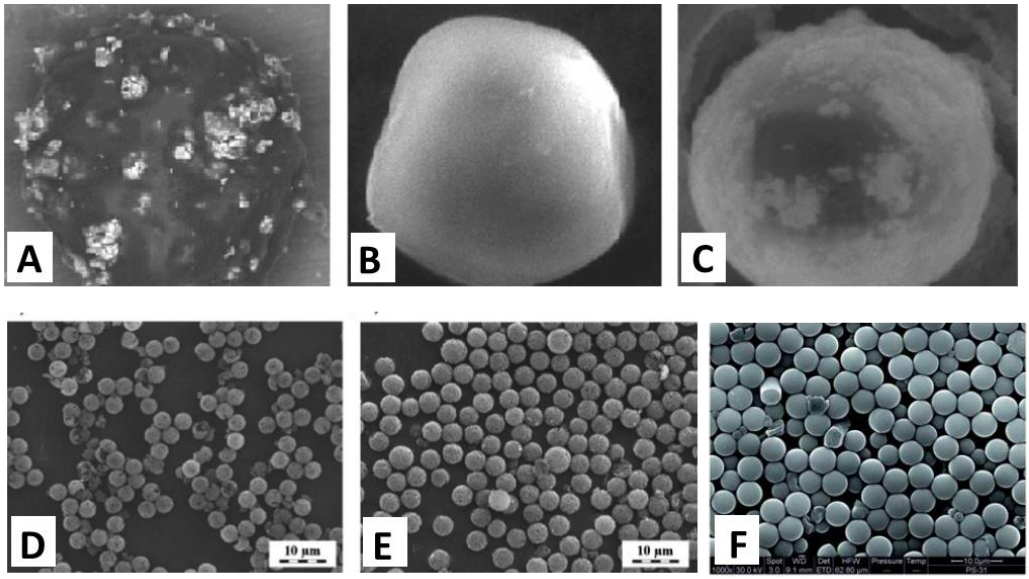

Obrázek 10. Snímky magnetických částic vyvinutých v Ústavu makromolekulární chemie, AV ČR v Praze: ***A*** *– magnetická makroporézní perlová celulosa (80-100 µm),* ***B*** *– alginátem potažené částice (5-10 µm),* ***C*** *– celulosové magnetitové mikročástice (6-8 µm),* ***D*** *– PGMA částice připravené vícenásobným bobtnáním a polymerizaci glycidyl methakrylátu s precipitací oxidů železa (3,9 µm),* ***E*** *– PHEMA částice připravené vícenásobným bobtnáním a polymerizací 2-hydroxyethyl methakrylátu s precipitací oxidů železa (4,4 µm),* ***F*** *– hypersíťované polystyrenové částice připravené kopolymerací styrenu a divinylbenzenu s následnou precipitací oxidů želena (4,8 µm); fotografie ze skenovací elektronové mikroskopie (SEM) [126****, P2, P8****]*

Tabulka 3. Přehled komerčních magnetických částic využitých pro imobilizaci enzymů a jejich konkrétní využití

enzym	magnetické částice (výrobce)	funkční skupina	velikost [µm]	porozita částic	využití	citace
trypsin	SiMAG částice (Chemicell, Německo)	- COOH	1	neporézní	• modifikace proteinů – příprava specifických tryptických peptidů	[25,126,166]
	PolyNIPAM (Ademtech, Francie)			porézní		126
	PolySTYREN (Uptima, Francie)			neporézní		**126**
anhydrotrypsin	SiMAG částice (Chemicell, Německo)	- COOH	80-100	neporézní	• modifikace proteinů – příprava specifických tryptických peptidů • afinitní izolace	[25]
papain	IONTOSORB MG (MBC) (Iontosorb, ČR)	- OH	80-100	makroporézní	• modifikace proteinů • štěpení kyseliny hyaluronové	**P2**
	IONTOSORB MG modifikovaná kyselinou iminodioctovou (MBC-IDA) (Iontosorb, ČR)	- IDA				
hyaluronanlyasa	IONTOSORB MG (MBC) (Iontosorb, ČR)	- OH	0,86	makroporézní	• štěpení kyseliny hyaluronové	**P3**
	IONTOSORB MG modifikovaná kyselinou iminodioctovou (MBC-IDA) (Iontosorb, ČR)	- IDA				

Tabulka 4. Přehled nově vyvinutých magnetických částic použitých pro imobilizaci enzymů a jejich využití

enzym	magnetické částice	materiál	funkční skupina	velikost [µm]	porozita	využití	citace
trypsin	alginátem potažené částice	celulosa povrchově modifikovaná alginátem	- COOH	5-10	neporézní	• modifikace proteinů – příprava specifických tryptických peptidů	**P1**
	PGMA	poly(glycidyl methakrylát)	- COOH	3,9	Porézní		
	PHEMA	poly(2-hydroxyethyl methakrylát)	- COOH	4,4	Porézní		
	poly(HEMA-*co*-GMA)	kopolymer poly(2-hydroxyethyl methakrylátu a glycidyl methakrylátu)	- COOH	3,7	neporézní		
	Fe_3O_4@SiO_2 nanočástice	core/shell Fe_3O_4@SiO_2	- NH_2	0,17-0,29	neporézní		[166]
chymotrypsin	magnetická makroporézní perlová celulosa	celulosa	- OH	125-250	makroporézní	• modifikace proteinů – příprava specifických peptidů	[122,126,131]
papain				80-100			
sfingolipid ceramid *N*-deacylasa (SCDasa)	magnetická makroporézní perlová celulosa	celulosa	- OH	125-250 80-100	makroporézní	• imobilizace trypsinu a IgG protilátek	**P4**, [36]
lakasa	magnetická makroporézní perlová celulosa	celulosa	- NH-NH_2	125-250 80-100	makroporézní	• imobilizace trypsinu a IgG protilátek	**P5**

3.1 Proteolytické enzymy pro modifikaci proteinů

Proteolytické enzymy, konkrétně trypsin a chymotrypsin, využíváme v preanalytické fázi pro štěpení studovaných proteinů před jejich analýzou a identifikací pomocí hmotnostní spektrometrie [160,161]. Oba enzymy jsou řazeny mezi serinové endoproteázy (trypsin, EC 3.4.21.4; chymotrypsin, EC 3.4.21.1) a vykazují velkou podobnost v aminokyselinové sekvenci i terciární struktuře [162]. V organismu mají funkci hlavních enzymů zajišťujících degradaci proteinů. *In vivo* jsou produkovány ve slinivce břišní v inaktivní formě a jejich aktivaci limitovanou proteolýzou dochází v duodenu. Inaktivace je pak zajišťována jejich autolytickým štěpením [163]. Zatímco chymotrypsin štěpí proteinové molekuly specificky za aromatickými aminokyselinami fenylalaninem, tyrosinem a tryptofanem, trypsin štěpí za bazickými aminokyselinami lysinem a argininem [164].

Pro *in vitro* aplikace v proteomických experimentech je právě štěpení za bazickými aminokyselinami výhodné z pohledu snadné identifikace. Proto je trypsin využíván nejčastěji.

Papain využíváme pro modifikaci proteinů, konkrétně molekul imunoglobulinů, které specificky štěpí na Fc a Fab fragmenty v pantové oblasti molekuly. Papain je cysteinová proteasa (EC 3.4.22.2) se širokou specifitou, ale přednostně štěpí za aminokyselinami s hydrofobním postranním řetězcem [164]. Je využíván proteomických experimentech, přípravě fragmentů protilátek [36], I když v podstatně menší míře než trypsin a chymotrypsin.

Pro snadnou manipulaci, kontrolovanou proteolýzu a získání čisté peptidové směsi imobilizujeme tyto enzymy na magnetické nosiče. Jak bylo již uvedeno, využíváme jak magnetické částice komerčně dostupné, tak nově vyvíjené na Ústavu makromolekulární chemie. Testovali jsme magnetické částice různých velikostí, připravené z různých materiálů a povrchově funkcionalizované [126, **P1**]. Na částice byly imobilizovány proteolytické enzymy trypsin, chymotrypsin a papain. Po imobilizaci byly ověřeny jejich aktivity a další parametry ukazující výhodnost imobilizace enzymů [126].

Jako podrobnější příklad porovnání dvou druhů nově syntetizovaných částic bych uvedla naší práci z roku 2012 uveřejněnou v časopise *Macromolecular Bioscience* [**P1**], kde jsme testovali poly-glycidyl methakrylátové (PGMA-COOH) a poly-hydroxyethyl methakrylátové

(PHEMA-COOH) magnetické částice, na které byl imobilizován trypsin. Byly optimalizovány podmínky vlastní imobilizace pro dosažení vysoké účinnosti vazby a po imobilizaci byla ověřena jeho aktivita. Uvedené magnetické částice byly syntetizovány v rámci projektu, kdy bylo vyvíjeno mikrofluidní zařízení na účinnou izolaci cirkulujících nádorových buněk [122]. Trypsin byl pro jejich testování zvolen jako modelový enzym.

Magnetické částice byly připraveny vícestupňovým bobtnáním a polymerací, s následnou precipitací iontů železa a zavedením karboxylových funkčních skupin prostřednictvím kyseliny 2-methakryloyloxy)ethoxy octové (MOEAA) v průběhu procesu polymerace. U připravených částic byla potvrzena porézní struktura a velikost 3,9 µm (PGMA-COOH), resp. 4,6 µm (PHEMA-COOH). Po syntéze byly částice charakterizovány z pohledu morfologie, velikosti a indexu polydisperzity pomocí skenovací elektronové mikroskopie (SEM). Byl stanoven obsah železa pomocí atomové absorpční spektrometrie (AAS) a množství povrchových karboxylových skupin titračně. Stabilita částic byla ověřena měřením zeta potenciálu.

Trypsin byl následně na částice imobilizován kovalentně, s využitím karbodiimidu a sulfo-NHS jako síťujících činidel (tzv. karbodiimidová metoda). Bylo testováno několik kombinací přídavku těchto činidel, různé reakční prostředí a množství trypsinu použitého pro imobilizaci. Pro minimalizaci případného autolytického štěpení trypsinu a ochranu aktivního místa probíhala imobilizace s přídavkem kompetitivního inhibitoru benzamidinu. Po imobilizaci byla ověřena výsledná aktivita enzymu spektrofotometricky pomocí chromogenního nízkomolekulárního substrátu N-α-benzoyl-D,L-arginin-4-nitroanilidu (BApNA), který je běžně využíván. Průměrná aktivita byla 1021 ± 44 U/mg částic pro PGMA-COOH a 1418 ± 32 U/mg pro PHEMA-COOH. Dále byla u nosičů ověřena operační a skladovací stabilita enzymu. Skladovací stabilita byla u obou nosičů srovnatelná (obrázek 11), v případě operační stability vykazoval nosič PGMA-COOH nižší stabilitu, kdy aktivita po pěti použitích klesla na 39 % původní aktivity.

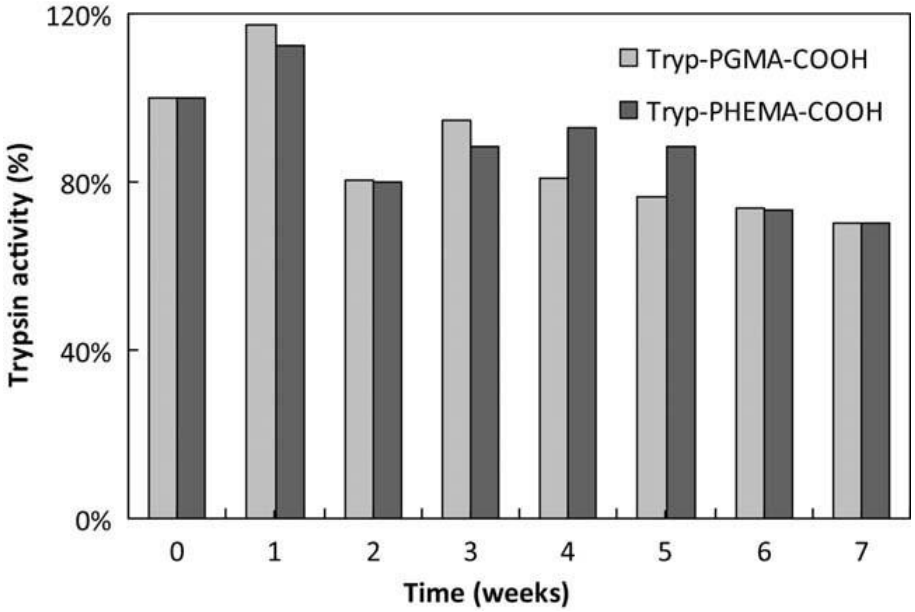

*Obrázek 11. Porovnání skladovací stability PGMA-COOH a PHEMA-COOH částic s imobilizovaným trypsinem [**P1**]*

Byl sledován vliv iontové síly reakčního prostředí měřením zeta potenciálu, který odráží koloidální stabilitu částic. Pro oba typy částic byla největší stabilita v 0,01 M fosfátovém pufru pH 7,3 a je tedy nejvhodnějším reakčním prostředím, částice jsou homogenně rozptýleny v roztoku a lze předpokládat nejlepší dostupnost aktivního místa enzymu (obrázek 12).

Z pohledu enzymové aktivity i stability se jako vhodnější jevily částice PHEMA-COOH. Kromě trypsinu byly na tyto částice imobilizovány i protilátky (lidské IgG), které představovaly modelový systém přípravy afinitních nosičů. I pro imobilizaci protilátek byla vyšší účinnost vazby na částice PHEMA-COOH [**P1**].

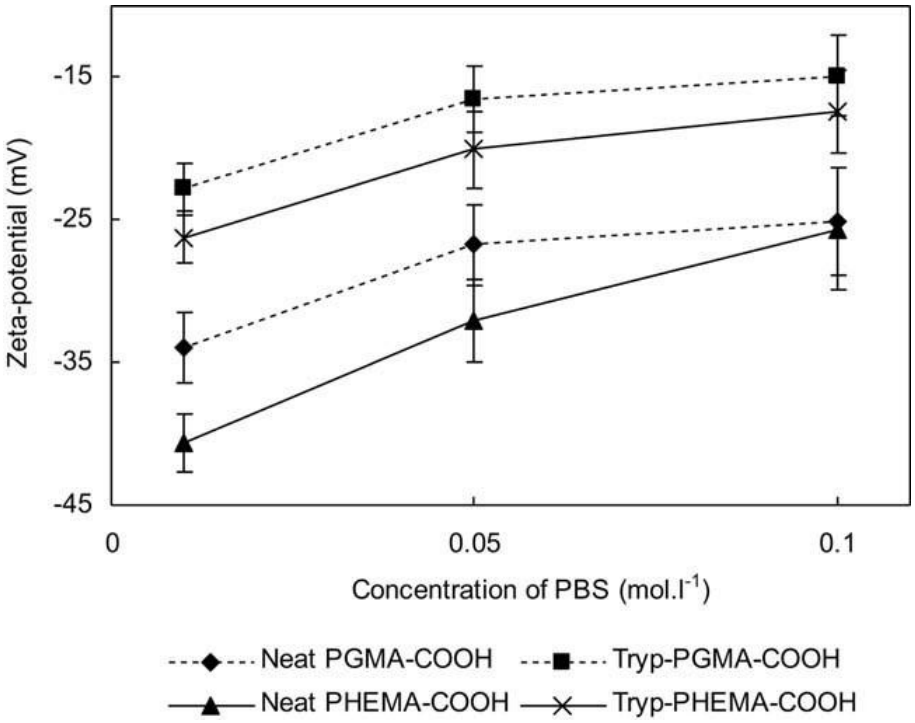

*Obrázek 12. Porovnání zeta potenciálu PGMA-COOH a PHEMA-COOH částic před a po imobilizaci trypsinu měřený ve fosfátovém pufru (PBS) o různých koncentracích (pH = 7,3) [**P1**]*

3.2 Papain a jeho vedlejší glykosidasová aktivita

V případě imobilizovaného papainu jsme se zaměřili jeho vedlejší glykosidasovou aktivitu. Na tomto projektu jsme spolupracovali s firmou Contipro a.s. a jeho cílem bylo připravit magnetický nosič s imobilizovaným enzymem pro přípravu nízkomolekulárních fragmentů kyseliny hyaluronové (HA) s úzkou distribucí velikostí pro účely farmaceutického a kosmetického průmyslu. Přestože pro fragmentaci kyseliny hyaluronové jsou specifické enzymy hyaluronidasy a hyaluronanlyasy, papain, u kterého byla prokázána vedlejší glykosidasová aktivita, je enzym rostlinného původu. To je, v porovnání s hyaluronidasami živočišného původu, výhodnější, protože je minimalizováno riziko kontaminace finálního produktu, který je cílen na bioaplikace. Výhodou je i jeho nízká cena. Papain je izolován z rostliny *Carica papaya.*

Kyselina hyaluronová je vysokomolekulární nesulfatovaný gylkosaminoglykan. Jeho struktura je jednoduchá, je tvořena opakujícími se disacharidovými jednotkami kyseliny β-D-glukuronové a *N*-acetyl-D-glukosaminu spojenými střídavě β-(1→3) a β-(1→4) vazbami.

Glykosidasová aktivita papainu je založena na stejném mechanismu jako mají hyaluronanlyasy (obrázek 15), tedy v postupném štěpení za disacharidovými jednotkami mezi kyselinou glukuronovou a *N*-acetyl-D-glukosaminem.

Papain byl imobilizován na magnetický nosič z důvodů snadného odstranění enzymu z reakční směsi a získání čistého produktu. Navíc se ukázalo, že magnetická forma nosiče a jeho porézní charakter jsou klíčovými parametry pro přípravu účinného nosiče s imobilizovaným papainem. V roce 2014 jsme publikovali článek v časopise *Carbohydrate Polymers* [**P2**].
Velikost, porozita a magnetická forma částic použitých pro imobilizace papainu významnou měrou přispívají k depolymerizaci kyseliny hyaluronové procesem označovaným jako tzv. oxidačně – redukční depolymerizace, který je z literatury již známý [165].

Při přípravě nosiče s imobilizovaným papainem byly testovány tři typy komerčně dostupných částic, konkrétně magnetická makroporézní perlová celulosa IONTOSORB MG-OH (Iontosorb, ČR) o velikosti částic 80 - 100 µm, její nemagnetická forma IONTOSORB NMG-OH (Iontosorb, ČR) a neporézní magnetické mikročástice amorfního oxidu křemičitého (siliky) SiMAG-COOH (Chemicell, Německo) o velikosti částic 1 µm. Při zavedení metody byly optimalizovány nejen podmínky imobilizace papainu, ale podmínky nezbytné pro účinnou a kontrolovanou depolymerizaci vysokomolekulární HA. Papain byl imobilizován kovalentně. V případě karboxylem funkcionalizovaných částic byla využita karbodiimidová metoda, pro MG-OH pak vazba po oxidaci hydroxylových funkčních skupin jodistanem sodným za tvorby reaktivních aldehydových skupin reagujících s aminoskupinami papainu za vzniku stabilního hydrazonu. Připravené nosiče byly využity pro štěpení vysokomolekulární kyseliny hyaluronové. Pro ověření fragmentace byly použity techniky gelově-permeační chromatografie s detektorem víceúhlového rozptylu světla (SEC-MALS) a nativní polyakrylamidové gelové elektroforézy v prostředí tris-borát-EDTA (TBE-PAGE) s detekcí barvením roztokem alciánové modři (barvení specifické pro polysacharidy). Vznik oligomerů je na gelu potvrzen přítomností charakteristického „žebříčku“ (obrázek 13), kdy jednotlivé proužky odpovídají oligomerům zkráceným o disacharidovou jednotku kyseliny D-glukuronové a *N*-acetyl-D-glukosaminu.

Zatímco při použití nemagnetického nosiče a neporézních magnetických částic s imobilizovaným papainem nedošlo ke štěpení vysokomolekulárního substrátu (obrázek 13A, pozice 6 a 7), v případě magnetické perlové celulosy byly získány středně a nízkomolekulární

fragmenty kyseliny hyaluronové (obrázek 13C). Porozita v tomto případě zajistila mechanické rozvolnění vysokomolekulární molekuly HA (obrázek 13B). Ionty železa v magnetických částicích pak vedly k oxidačně - redukční depolymerizaci. V součinnosti s enzymovým působením papainu byly získány fragmenty HA.

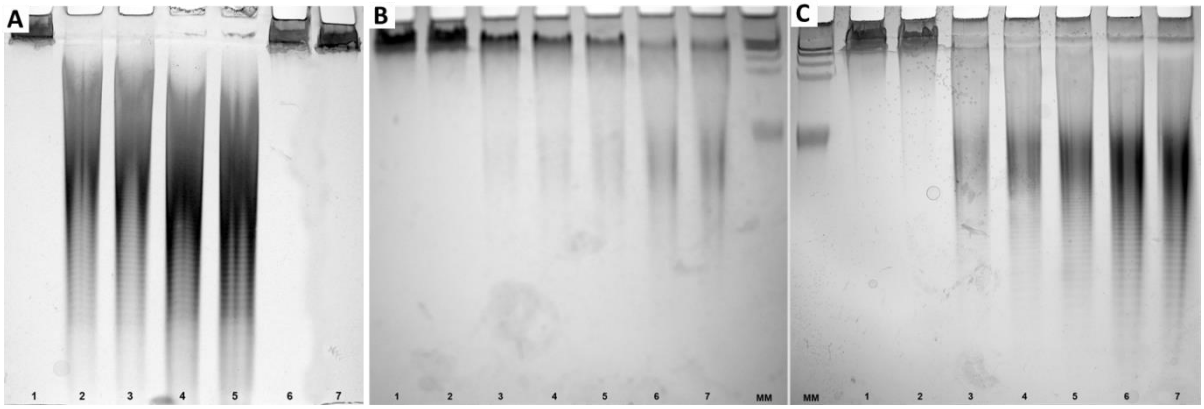

Obrázek 13. Nativní TBE-PAGE pro ověření vlivu parametrů nosiče použitého pro imobilizaci papainu a následnou aplikaci pro štěpení vysokomolekulární kyseliny hyaluronové: ***A*** *– štěpení třemi typy nosičů (1-původní HA, 2-5 – štěpení HA v čase 5-48 hod papainem imobilizovaným na MG-OH, 6-štěpení HA papainem imobilizovaným na neporézní SiMAG-COOH částice 48 hod, 7-štěpení HA papainem imobilizovaným na NMG-OH 48 hod),* ***B*** *– vliv mechanického působení porézní magnetické perlové celulózy bez papainu,* ***C*** *– štěpení HA v čase (1-49 hod) papainem imobilizovaným na MG-OH; nativní Tris-borát-EDTA polyakrylamidová gelová elektroforéza s barvením pomocí Alciánové modři specifickým pro sacharidy [****P2****]*

Účinnost magnetického nosiče s imobilizovaným papainem pro štěpení vysokomolekulární kyseliny hyaluronové ($M_r \approx 1{,}8$ MDa) byla potvrzena i pomocí SEC-MALS analýzy (obrázek 14B).

Připravený nosič kombinující magnetické částice a papain tak může být vhodnou alternativou ke specifičtějším enzymům štěpícím kyselinu hyaluronovou. Zároveň toto využití ukazuje, jaké výhody přináší imobilizované enzymy, jsou-li zohledněny i parametry použitého nosiče.

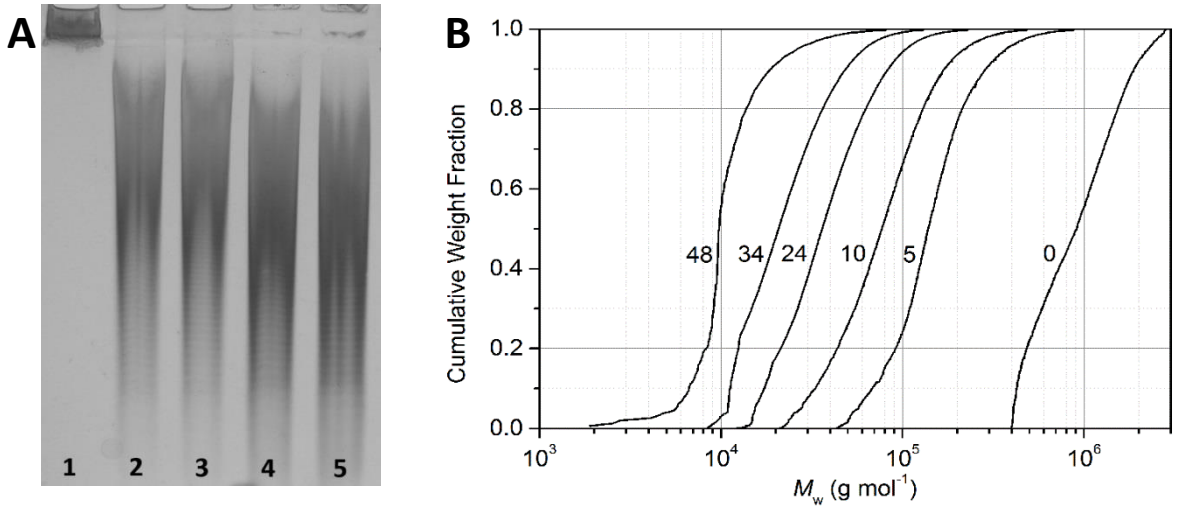

*Obrázek 14. Monitorování fragmentace kyseliny hyaluronové papainem; A - TBE-PAGE frakcí při depolymerizaci vysokomolekulárního hyaluronanu (pozice 1) papainem v čase (pozice 2-5, 5, 10, 24 a 48 hod); B – SEC-MALS analýza frakcí po fragmentaci 0, 5, 10, 24, 34, 48 hod [**P2**]*

3.3 Hyaluronanlyasa pro kontrolovanou fragmentaci kyseliny hyaluronové

Jak bylo uvedeno v kapitole 1.1, hyaluronidasy jsou enzymy, které štěpí kyselinu hyaluronovou. Hyaluronidasy dělíme na tři typy podle jejich rozdílného mechanismu účinku (obrázek 15). První dva jsou endo-β-N-acetyl-hexosaminidasy, hydrolasy živočišného původu a hyaluronanlyasy. Hydrolasy štěpí β-1,4-glykosidickou vazbu za vniku tetrasacharidů a hexasacharidů. Hyaluronanlyasy štěpí β-eliminační reakcí molekuly hyaluronanu na disacharidové jednotky za tvorby dvojné vazby v produktu. Třetí, endo-β-glukuronidasa, štěpí β-1,3-glykosidickou vazbu. Tyto enzymy byly objeveny v korýších, pijavicích a dalších parazitech [1,167].

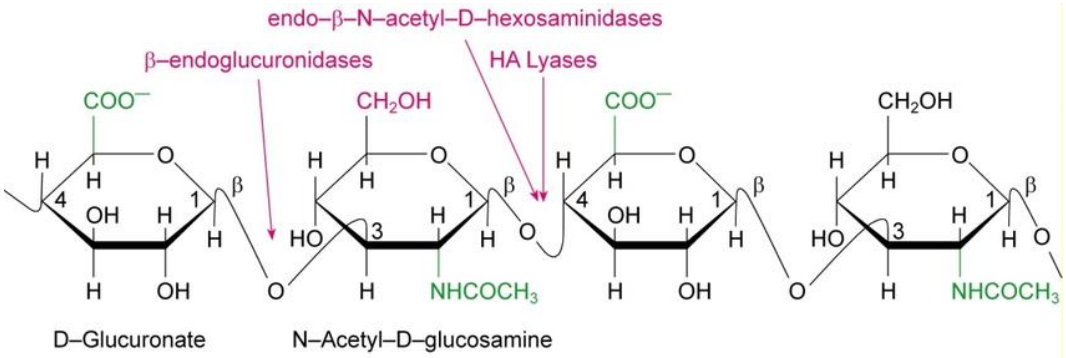

Obrázek 15. Mechanismy účinku hyaluronidas [168]

Hyaluronanlyasy mohou být připraveny rekombinantně, nejčastěji produkované *Streptococcus pneumoniae* nebo *Streptococcus pyogenes*. Tyto rekombinantní enzymy pak splňují požadavky při využití produktů enzymové fragmentace např. ve farmaceutickém průmyslu. Po projektu využívajícím imobilizovaný papain jsme v rámci spolupráce s firmou Contipro a.s testovali nově připravenou rekombinantní hyaluronanlyasu ze *Streptococcus pneumoniae* (SpnHL). Výsledkem byla publikace v časopise *Process Biochemistry* (2018) [**P3**]. Na základě zkušeností s přípravou imobilizovaného papainu byla rekombinantní hyaluronanlyasa imobilizována na dva typy komerčně dostupných magnetických částic, které se lišily povrchovou funkcionalizací, a byl sledován vliv různých způsobů imobilizace na výsledné vlastnosti imobilizovaného enzymu. S ohledem na zamýšlenou aplikaci pro štěpení vysokomolekulární kyseliny hyaluronové, jejíž roztoky jsou viskózní, byly voleny částice s větší velikostí (80 – 100 μm), porézní a s vysokým obsahem železa, neboť tyto vlastnosti napomáhají k homogennímu rozptýlení částic v roztoku a účinné separaci z reakční směsi.

Jedním ze způsobů byla neorientovaná kovalentní vazba na magnetickou makroporézní perlovou celulosu s hydroxylovými funkčními skupinami (MBC). Ty byly oxidovány za tvorby reaktivních aldehydových skupin. Druhou metodou byla orientovaná afinitní sorpce enzymu na stejný nosič, ale modifikovaný kyselinou iminodioctovou (MBC-IDA). Vazba spočívala v prvotní aktivaci nosiče pomocí $CoCl_2$ s afinitou pro histidinové zbytky na molekule enzymu. Rekombinantně připravená SpnHL nese 8 histidinových zbytků (tzv. His-tag kotva).

Vzhledem k tomu, že se jednalo o nově připravený enzym, byla před imobilizací na magnetické částice ověřena jeho čistota pomocí SDS-PAGE a stanovena aktivita a kinetické parametry solubilní formy enzymu jako základní parametry charakterizující připravený enzym. Aktivita SpnHL byla stanovena spektrofotometricky po fragmentaci substrátu (kyseliny hyaluronové). Tento enzym je tzv. procesivní lyasou, z molekuly kyseliny hyaluronové postupně odštěpuje disacharidové jednotky za současné tvorby dvojné vazby v produktu, který byl monitorován spektrofotometricky při 230 nm (obrázek 16A). Vznik disacharidových jednotek byl potvrzen i pomocí polyakrylamidové gelové elektroforézy v prostředí Tris-borát-EDTA (TBE-PAGE) přítomností typické žebříčkové linie (obrázek 16B). Aktivita enzymu byla stanovena 83 U/mg proteinu.

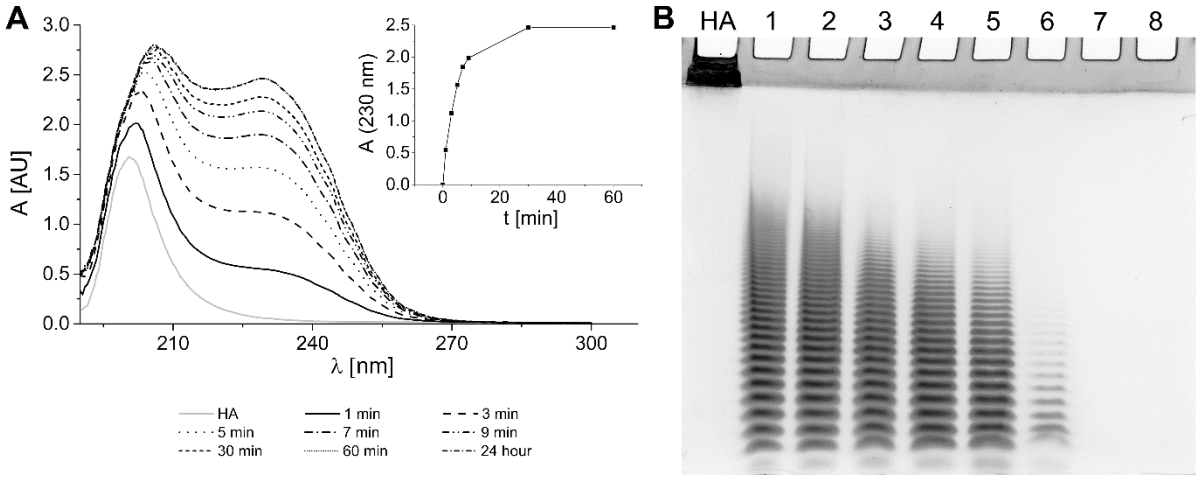

*Obrázek 16. Fragmentace vysokomolekulární kyseliny hyaluronové enzymem SpnHL v čase; A – spektrofotometrická detekce při 230 nm, B – TBE-PAGE [**P3**].*

Po imobilizaci enzymu na oba typy nosičů byla porovnána jejich výsledná aktivita imobilizovaného enzymu a kinetické parametry. Byly testovány různé roztoky, ve kterých imobilizace probíhala, i reakční roztoky pro následné použití. U imobilizovaného enzymu byla ověřena operační a skladovací stabilita, a to pro oba typy nosičů použitých pro imobilizaci.

Přestože jsme předpokládali, že orientovaná vazba bude účinnější a imobilizovaný enzym si zachová vyšší aktivitu, ve srovnání s neorientovanou vazbou, nosič MBC-IDA-SpnHL vykazoval 3x nižší aktivitu než MBC-SpnHL (216 mIU/ml sedimentovaného nosiče pro MBC-IDA vs. 651 mIU/ml pro MBC). I stanovení kinetických parametrů enzymové reakce potvrdilo stejný trend. Byly porovnány kinetické parametry imobilizovaného enzymu se solubilním enzymem (K_m = 0,349 mM; V_{max} = 0,116 s), které potvrdily, že imobilizací došlo ke zlepšení afinity enzymu k danému substrátu (K_m), a to v případě obou typů nosičů (obrázek 17).

Při porovnání operační a skladovací stability obou typů nosičů vykazoval, dle předpokladů, vyšší skladovací stabilitu nosič připravený kovalentní imobilizací (MBC-SpnHL). Lepší operační stabilitu naopak vykazoval enzym imobilizovaný na nosič MBC-IDA (obrázek 18).

	solubilní SpnHL	MBC-SpnHL	MBC-IDA-SpnHL
K_M [mol/l]	3.49 x 10^{-5}	4.35 x 10^{-7}	1.25 x 10^{-6}
v_{max} [s]	1.16 x 10^{-1}	1.45 x 10^{-2}	1.75 x 10^{-2}

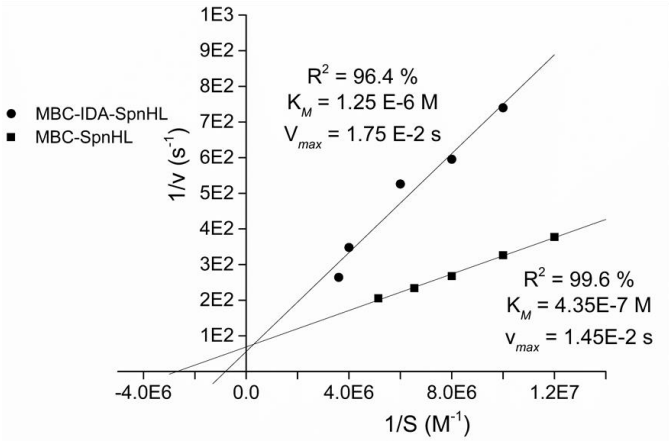

*Obrázek 17. Porovnání kinetických parametrů solubilní a imobilizované rekombinantní hyaluronan lyázy; transformace dat podle Lineweavera a Burka [**P3**]*

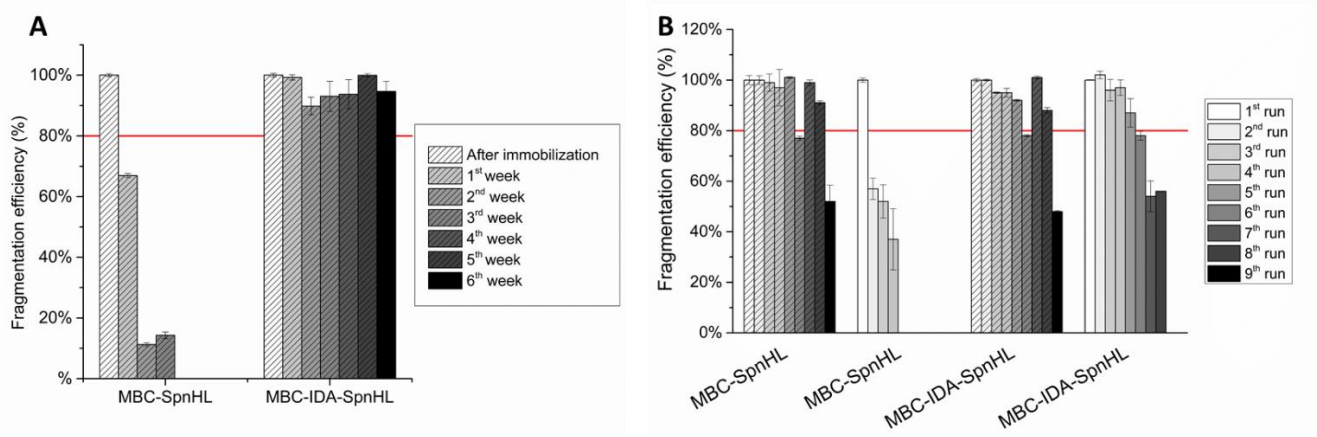

*Obrázek 18. Skladovací (A) a operační (B) stabilita rekombinantní hyaluronan lyázy imobilizované na MBC a MBC-IDA částice [**P3**]*

Oba připravené nosiče byly otestovány pro fragmentaci vysokomolekulární kyseliny hyaluronové a byly účinné i v silně viskózních koncentrovaných roztocích.

3.4 Sphingolipid ceramid N-deacylasa pro modifikaci sfingolipidů

Enzym sfingolipid ceramid *N*-deacylasu (SCDasa, EC 3.5.1.69) hydrolyzuje *N*-acylové vazby sfingolipidů mezi mastnou kyselinou a sfingosinem řetězce ceramidu za tvorby jejich lyso-forem (obrázek 19). Tato reakce probíhá v mírně kyselém prostředí (pH 5-6) a v přítomnosti detergentů [70]. Zároveň katalyzuje i reverzní reakci, tj. reacylaci, nebo výměnu mastných kyselin. Účinnost reakce ovlivňují obě složky, jak typ lyso-sfingolipidu, tak

mastné kyseliny [45]. Hydrolýza substrátů neprobíhá ze 100 %, z důvodu rovnováhy mezi hydrolytickou a kondenzační reakcí [51]. Nejčastějším zdrojem je *Pseudomonas* sp. TK4. Byla popsána i produkce v *Shewanella alga* [70].

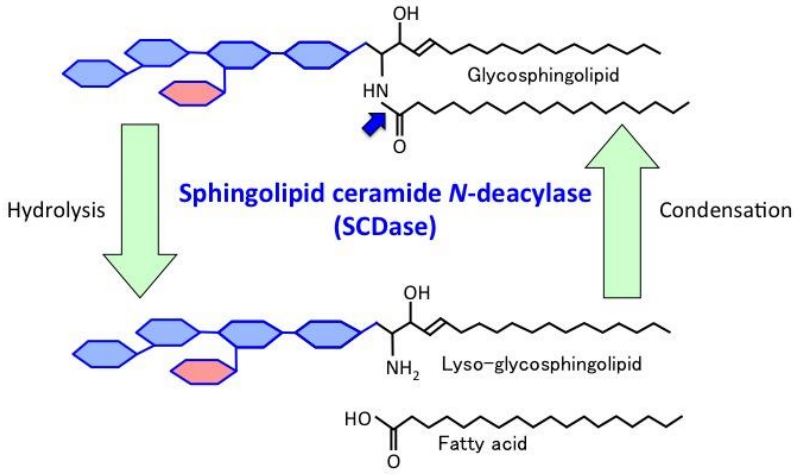

Obrázek 19. Hydrolytická a kondenzační reakce katalyzovaná enzymem Sfingolipid ceramid N-deacylasou [58]

SCDasu jsme využili pro cílenou modifikaci sfingolipidů, kdy byly syntetizovány C17:0 izoformy sulfatidu a glukosylceramidu, které sloužily jako vnitřní standardy pro účely ESI-MS/MS analýzy sfingolipidů. Hladiny sfingolipidů jsou stanovovány v krvi v souvislosti s dědičnými poruchami meabolismu sfingolipodů.

Pro analýzu sfingolipidů lze využít tenkovrstvou chromatografii (TLC, HPTLC), enzymovou imunoanalýzu na pevné fázi (ELISA) nebo tandemovou hmotnostní spektrometrii (MS/MS). Nebo mohou být stanoveny po uvolnění sacharidového řetězce pomocí plynové chromatografie (GC) nebo vysokoúčinné kapalinové chromatografie [68,169]. Pro MS analýzu jsou nezbytné vnitřní standardy sfingolipidů, a to takové, které se v organismu nevyskytují přirozeně [68,170].

Aby byly získány čisté produkty a pro možnost regulace katalyzované reakce, jsme využili opět imobilizace enzymu na magnetické částice. Získané výsledky byly pubikovány v časopise *Rapid communications in mass spectrometry* v roce 2010 [**P4**].

Pro imobilizaci enzymu sfingolipid ceramid *N*-deacylasy (SCDasa) se osvědčila magnetická perlová celulosa s hydroxylovými funkčními skupinami a enzym byl imobilizován stejně jako v případě výše uvedené hyaluronan lyázy po oxidaci magnetických částic za tvorby reaktivních aldehydových skupin.

Po imobilizaci enzymu byla ověřena jeho aktivita, a to pomocí obou typů reakcí, které katalyzuje, tedy hydrolytické i reverzní syntetické. Pro hydrolytickou reakci byl využit substrát Gangliotetraosylceramid (Gg4Cer), kdy v případě aktivního enzymu dochází k odštěpení mastné kyseliny. Pro reverzní syntetickou reakci byl využit lyso-globotriaosylceramid (lyso-Gb3Cer) a kyselina stearová, která je působěním enzymu připojena k lyso-ceramidu. Produkty reakce byly analyzovány pomocí vysokoúčinné tenkovrstvé chromatografie (HPTLC) s vizualizací roztokem orcinolu a denzitometricky byl hodnocen stupeň hydrolýzy, resp. syntézy. Vzniklé produkty pak byly také identifikovány hmotnostní spektrometrií (ESI-MS/MS), tedy metodou, pro kterou byly modifikované sfingolipidy cíleně připravovány. Pro účinnou enzymovou modifikaci byly testovány různé poměry reakčních složek a optimalizováno reakční prostředí. Účinnost enzymové konverze pomocí imobilizovaného enzymu byla také porovnána s jeho solubilní formou, aby bylo ověřeno, zda imobilizace přináší očekávané výhody.

Pro syntetickou reakci C17:0 glukosylceramidu byla imobilizovaná SCDasa účinnější než solubilní forma a při identifikaci produktů bylo prokázáno nižší zastoupení vedlejších kontaminujících produktů C16:0 a C18:0 (obrázek 20).

Navíc při opakovaném použití imobilizovaného enzymu se zastoupení kontaminujících produktů snižovalo (obrázek 21). Čistota modifikovaných sfingolipidů dosahovala 97 %. Imobilizovaný enzym vykazoval vysokou operační stabilitu, kdy ani po 15. použití aktivita výrazně neklesla, a oproti jiným imobilizovaným enzymům extrémní skladovací stabilitu, kdy byl nosič aktivní dokonce po více než roce skladování [**P4**].

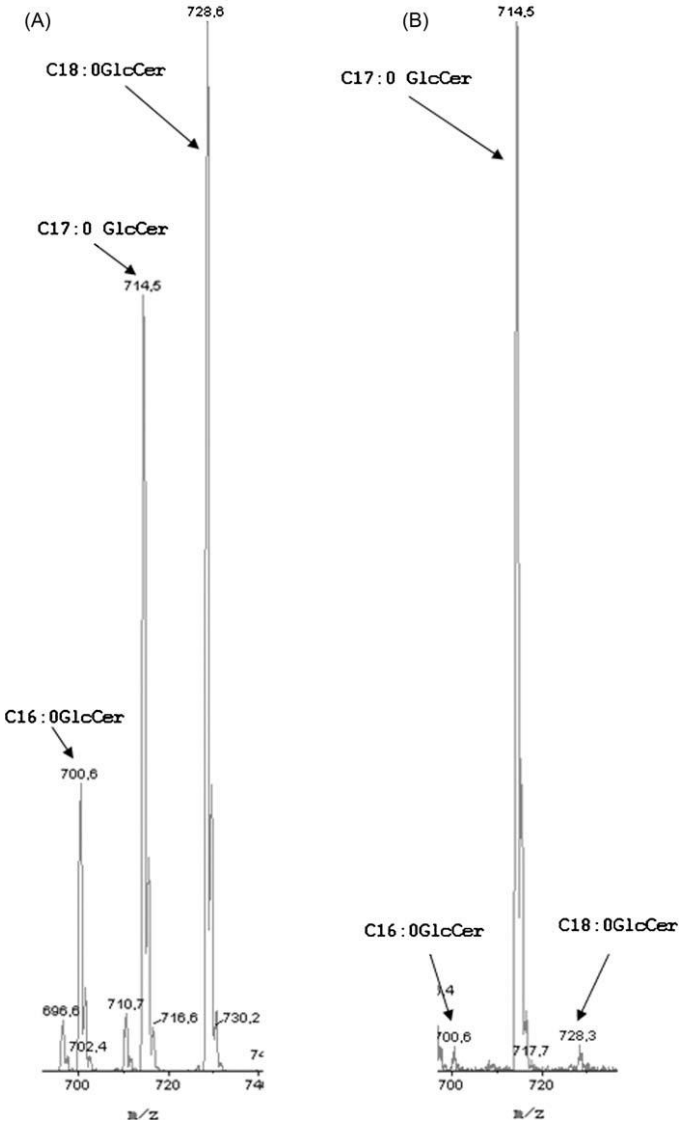

*Obrázek 20. ESI-MS/MS analýza produktu semisyntetické reakce C17:0 glukosylceramidu a vedlejších kontaminujících produktů (C18:0, C16:0) syntetické reakce katalyzované solubilní SCDázou (A) a SCDasou imobilizovanou na magnetické makroporézní perlové celulose (B) [**P4**]*

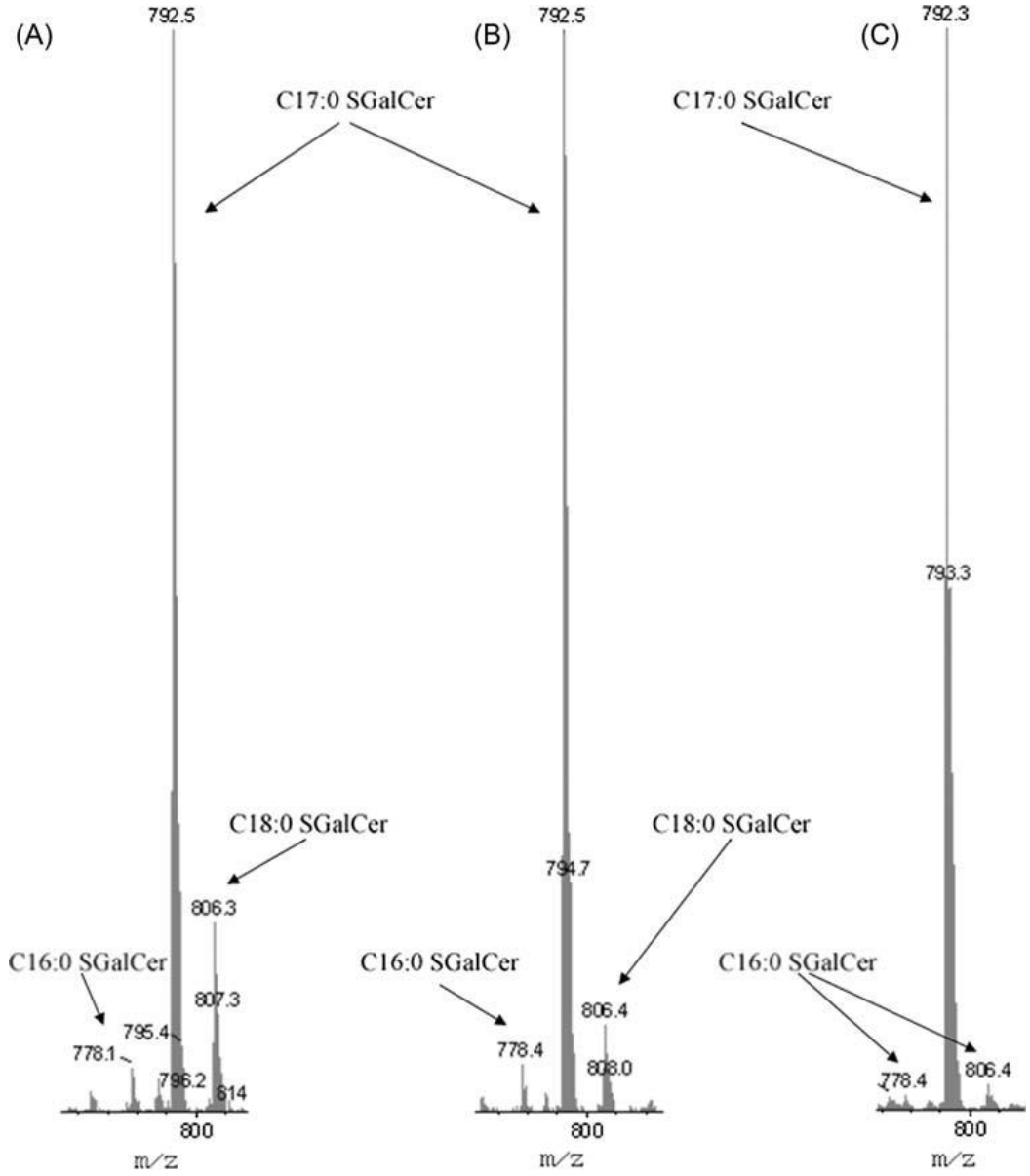

*Obrázek 21. ESI-MS/MS analýza produktu opakované semisyntetické reakce C17:0 sulfatidu a vedlejších kontaminujících produktů (C18:0, C16:0) syntetické reakce katalyzované SCDasou imobilizovanou na magnetické makroporézní perlové celulose; 1. (A), 2. (B) a 3. (C) použití [**P4**]*

Tato aplikace opět ukázala řadu výhod, které přináší imobilizace enzymů na pevnou fázi.

3.5 Lakasa

Lakasy (*p*-difenol: O_2 oxidoreduktasa, EC 1.10.3.2) jsou oxidoreduktasy katalyzující jednoelektronovou oxidaci fenolů, polyfenolů, aromatických aminů se současnou redukcí molekulárního kyslíku na molekulu vody. Vznikající radikály následně prochází radikály, které

procházejí další depolymerizací, repolymerizací, demethylací, dehalogenací nebo tvorbou chinonu. Lakasy jsou charakteristické nízkou substrátovou specifitou, existuje široké spektrum molekul, jejichž oxidaci katalyzují [73,74]. Nejdůležitějším zdrojem lakáz jsou houby bílé hniloby, např. *Trametes versicolor*, *Pycnoporus cinnabarinus*, *Polyorus pinisitus* [74], *Trametes hirsute* [73] aj. Vedle toho jsou produkovány i vyššími rostlinami, některými druhy hmyzu a bakteriemi [75].

Lakasy z *Tramates versicolor* a *Pycnoporus cinnabarinus* byly testovány pro jejich možné využití při dekolorizaci barviv přítomných v odpoadních vodách. Enzym byl testován s modelovým antrachinonovým barvivem a jednoduchým azo barvivem. Pro potenciální průmyslové využití se opět nabízela imobilizace enzymu na pevnou fázi pro snadnou separaci a možnost opakovaného použití. Před vlastní imobilizací byla u obou enzymů v solubilní formě ověřena aktivita pomocí chromogenních substrátů, 2,2´-azino-bis(3-ethylbenzthiazolin-6-sulfonové) kyseliny (ABTS) a syringaldazinu, a byly charakterizovány z pohledu jejich kinetických parametrů (K_m, V_{max}), které byly srovnatelné s dostupnou literaturou. Byly testovány vhodné reakční podmínky (pH, teplota) (obrázek 22), které byly následně použity i pro ověření účinnosti enzymu při dekolorizaci vybraných barviv.

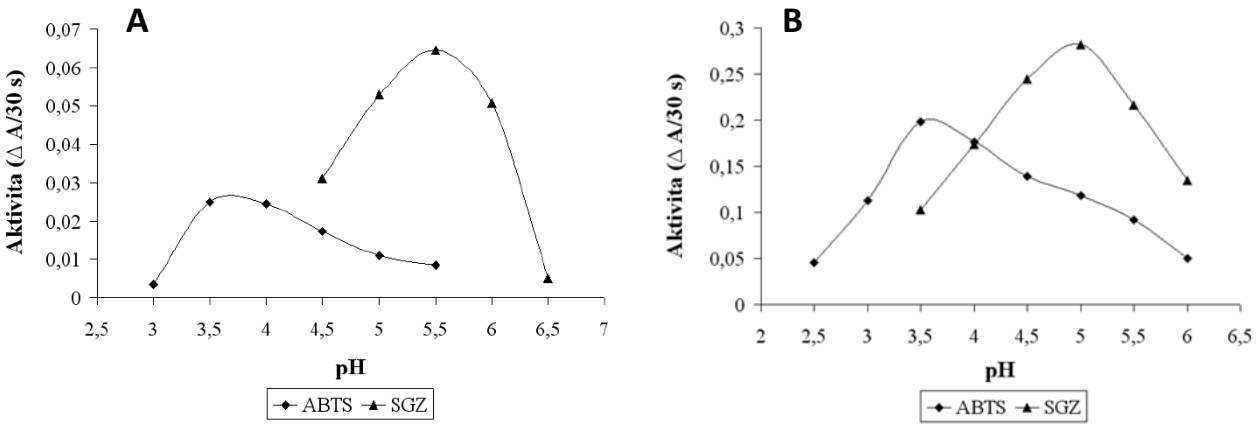

*Obrázek 22. Testování reakčního prostředí enzymu lakasy z **A**-Trametes versicolor, **B**-Pycnoporus cinnabarinus [**P5**] s využitím substrátů ABTS a syringaldazinu (SGZ).*

Ačkoliv v literatuře je uváděno jako optimální pH pro substrát syringaldazin v rozmezí 4–5, pro lakázu izolovanou z *Trametes versicolor* je dle našich výsledků optimum pH až do pH 6,5 (obrázek 22A).

Při testování solubilní lakázy pro dekolorizaci vybraných modelových barviv byly enzymy z obou zdrojů účinné pouze na barvivo antrachinonové (obrázek 23). Při dekolorizaci azo barviva byl efekt minimální.

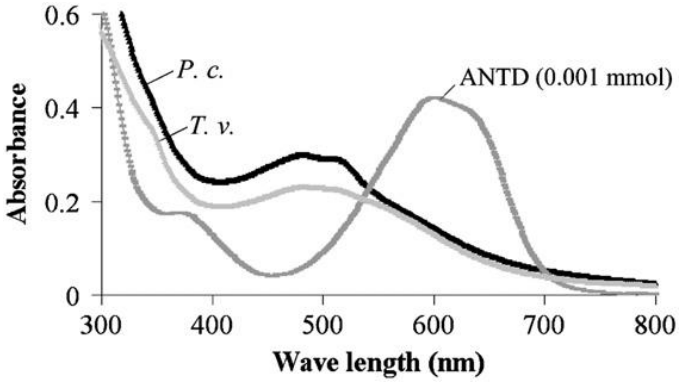

*Obrázek 23. Spektrum dekolorizace antrachinonového barviva solubilní lakasou **T.v.**-Trametes versicolor, **P.c.**-Pycnoporus cinnabarinus [**P5**]*

S ohledem na vlastnosti, zejména rychlou separaci, vysokou vazebnou kapacitu a dobrou stabilitu byla pro imobilizaci lakasy (z *Pycnoporus cinnabarinus*) zvolena magnetická perlová celulosa, a to s hydroxylovými nebo hydrazidovými funkčními skupinami a velikostí částic 125–250 µm. Tak jako v případě ostatních enzymů, které jsme imobilizovali, i v tomto případě byly porovnávány dva zvolené způsoby imobilizace a připravené nosiče byly charakterizovány z pohledu aktivity a stability. Na částice s hydroxylovými funkčními skupinami byl enzym imobilizován neorientovaně po oxidaci funkčních skupin nosiče pomocí jodistanu. Pro imobilizaci na magnetickou perlovou celulosu s hydrazidovými funkčními skupinami byla testována orientovaná vazba, kdy jsme využili toho, že enzym je glykoprotein a glykosylace se vyskytuje v dostatečné vzdálenosti od aktivního místa enzmymu. Při tomto způsobu jsme využili také oxidace jodistanem, ale tentokrát gylkosylované části molekuly enzymu.

Ověření aktivity enzymu po imobilizaci pomocí nízkomolekulárního substrátu syringaldazinu potvrdilo výhody orientované imobilizace. Aktivita lakasy imobilizované orientovaně byla téměř 3x vyšší než aktivita neorientovaně vázaného enzymu (0,63 IU/ml vs. 0,22 IU/ml sedimentovaného nosiče). Pro porovnání byl enzym imobilizován i na nemagnetické formy stejných nosičů, kde byl trend stejný, porovnáme-li způsob imobilizace, nicméně v obou případech nižší než magnetický nosič. Připravený nosič s nejvyšší aktivitou byl následně charakterizován z pohledu operační a skladovací stability. Při skladování nedošlo k výraznému

poklesu ani po měsíci, v případě operační stability pak bylo možné nosič použít opakovaně 7x bez výrazného poklesu aktivity, což opět potvrdilo výhody imobilizovaných enzymů [**P5**].

4. Enzymy jako signál generující molekuly v elektrochemických imunosenzorech

Další oblastí, kde enzymy nachází své široké uplatnění, jsou enzymové imunoanalytické metody, kde jsou enzymy molekuly, které jsou konjugovány s protilátkami pro detekci stanovované látky, a jsou zodpovědné za generování signálu. V rámci dvou projektů GAČR jsme principu ELISA metod využívali v kombinaci s citlivou elektrochemickou detekcí s cílem vyvinout systém pro rychlou detekci potravních alergenů a proteinových biomarkerů asociovaných s ovariálním karcinomem. Výsledky shrnují práce uvedené v přílohách [**P6-P9**].

Obvyklé uspořádání těchto metod je v mikrotitračních destičkách, které tvoří pevnou fázi pro fixaci protilátek pro záchyt stanovované látky ze vzorku. V biosenzorech slouží jako tato pevná fáze přímo povrch pracovní elektrody, kde dochází k finální detekci. Vzhledem k tomu, že povrch pracovní elektrody je limitován její velikostí, využili jsme při vývoji imunosenzorů magnetické částice, kdy lze využít jejich celého specifického povrchu. Na základě zkušeností s imobilizací enzymů byly testovány různé magnetické částice, komerčně dodávané nebo nově syntetizované v rámci spolupráce s Ústavem makromolekulární chemie AV ČR (tabulka 5).

Pro detekci byly využívány komerčně dostupné jednorázové tištěné senzory v tříelektrodovém uspořádání (pracovní/referentní/pomocná elektroda), které umožňují analýzu v malých objemech (40 - 100 µl). V závislosti na stanovované látce byl pak volen metariál pracovní elektrody (tabulka 6).

Tabulka 5. Přehled magnetických částic použitých pro vývoj elektrochemických imunosenzorů pro detekci proteinů.

magnetické částice (Výrobce)	materiál	funkční skupina	velikost [µm]	využití	citace
HPSM (ÚMCH, Praha, ČR)	hypersíťované polystyrenové částice	$-SO_3^-$	4,8	imobilizace anti-ovalbuminových protilátek	**P7**
Sera-Mag™ Double speed (Seradyn, USA)	polystyrenové jádro, dvojitá vrstva magnetitu, polymerní obal	-COOH	0,771	imobilizace: • anti-ovalbuminových protilátek • HRP	**P6**
P(GMA-MOEAA)-NH_2/HA (ÚMCH, Praha, ČR)	poly[glycidylmethakrylát-(methakryloyloxy)ethoxy] octová kys.	$-NH_2$	4,5	imobilizace anti-ovalbuminových protilátek	**P6**
SiMAG (Chemicell, Německo)	silika	$-NH_2$ -COOH	1	Imobilizace: • ALP • anti-HE4 protilátek • anti-ApoE protilátek • Apo E	**P8** **P9** **P10** **P11**

Tabulka 6. Přehled tištěných tříelektrodových senzorů použitých pro vývoj elektrochemických imunosenzorů pro detekci proteinů.

využití	měrná-referentní-pomocná elektroda	výrobce	analyzovaný objem [µl]	
imunosenzor využívající HRP	Pt-Ag/AgCl-Pt	BioSensor Technology (BST, Německo)	40	
imunosenzor využívající ALP	C-Ag-Pt	DropSens (DRP, Španělsko)	50	
imunosenzor využívající QDs	C/Hg-Ag-C	ItalSens (IS-HM1, Španělsko)	50	
	C/Bi-Ag-C	DropSens (DRP, Španělsko)	50	

4.1 Imunosenzor využívající enzym křenovou peroxidázu

Křenová peroxidasa (HRP) je jedním z nejčastěji využívaných enzymů v ELISA metodách. Při elektrochemické detekci je po přídavku substrátu peroxidu vodíku monitorován jeho úbytek vlivem enzymové konverze, který je přímo úměrný koncentraci stanovované látky ve vzorku. HRP byla použita jako značka protilátek v systému pro detekci a kvantifikaci proteinu ovalbuminu, který je potravinovým alergenem [**P6, P7**].

Princip celého systému spočíval v sendvičovém uspořádání, tj. záchytu stanovovaného ovalbuminu specifickými protilátkami, které byly imobilizovány na magnetické částice. Poté byly přidány sekundární protilátky, které byly značené křenovou peroxidasou a v posledním kroku substrát peroxid vodíku (obrázek 24).

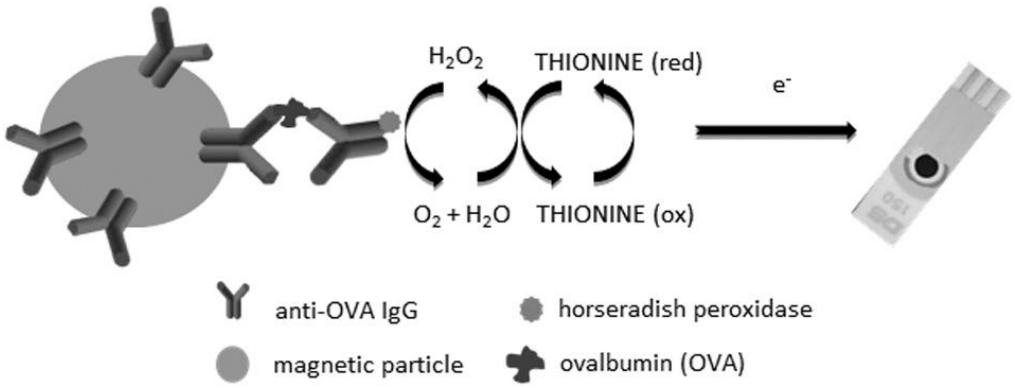

*Obrázek 24. Schéma elektrochemického imunomagnetického biosenzoru pro detekci ovalbuminu [**P6**]*

Stejně jako u enzymů, i protilátky byly na magnetické částice imobilizovány kovalentní vazbou. Pro vazbu protilátek byly použity tři typy částic. V rámci spolupráce s Ústavem makromolekulární chemie byly zkoušeny nejprve hypersíťované polystyrenové částice funkcionalizované sulfoskupinami (SO_3^-). Ty byly výhodné díky jejich autoreaktivitě a vazbě protilátek přes aminoskupinu za tvorby sulfonamidové vazby, a to bez přídavku jakýchkoliv síťujících činidel [**P7**]. Z dalších částic také nově syntetizované P(GMA-MOEAA)-NH_2/HA a pro porovnání komerční Sera-Mag™ částice [**P6**]. Na tyto částice byly protilátky imobilizovány karbodiimidovou metodou. Účinnosti vazby protilátek byla o něco vyšší u nově vyvíjených magnetických částic (90 % a více).

Při vývoji imunosenzoru bylo nutné optimalizovat nejen reakční podmínky vlastního záchytu antigenu mezi primární a sekundární protilátkou, jejich množství, množství substrátu, ale zejména podmínky elektrochemické detekce. Bylo ověřováno, zda u nově vyvíjených částic nedochází při detekci k nežádoucím interferencím vlivem iontů železa z částic. Jako detekční metoda byla zvolena metoda lineární voltametrie, při které je monitorována proudová odezva peroxidu vodíku v závislosti na vloženém potenciálu v rozsahu 0 až 0,8 V. Byly měřeny křivky úbytku peroxidu vodíku v čase v důsledku jeho spotřebování při enzymové reakci s křenovou peroxidázou (obrázek 25).

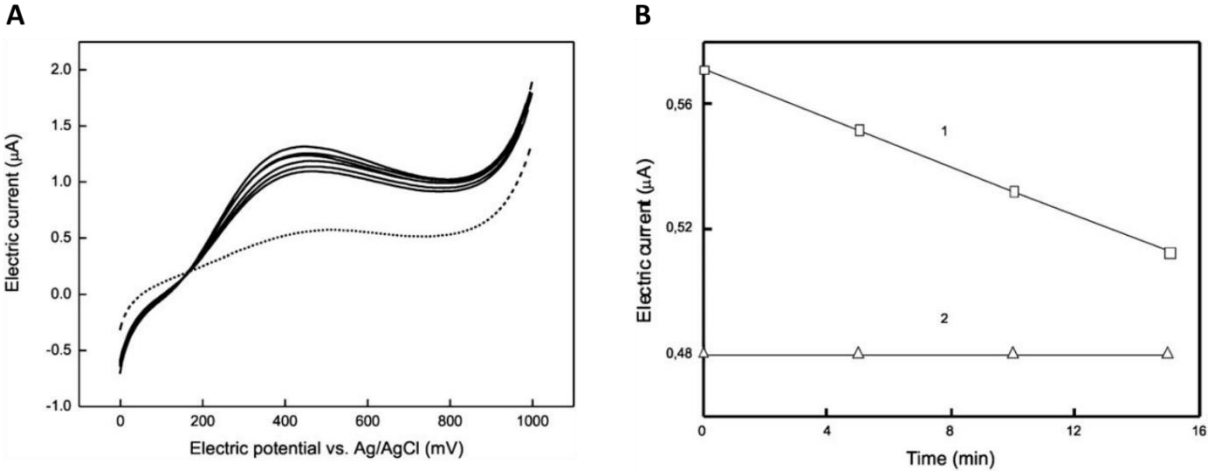

*Obrázek 25. Voltamogram proudové odezvy při úbytku peroxidu vodíku vlivem enzymové konverze křenovou peroxidasou (A); závislost proudové odezvy na čase, hodnota proudu byla odečítána při potenciálu odpovídajícímu maximu píku (B) [**P7**]*

Při použití prvních experimentech vykazoval systém velmi nízkou citlivost, což bylo řešeno přídavkem elektronového mediátoru thioninu. Ten usnadňuje přenos elektronů u povrchu pracovní elektrody a díky němu byly získány vyšší proudové odezvy (obrázek 26A). A v tomto uspořádání jsme dosáhli linearity od 11 do 200 nmol/l s kalkulovaným detekčním limitem 5 nmol/l (obrázek 26B).

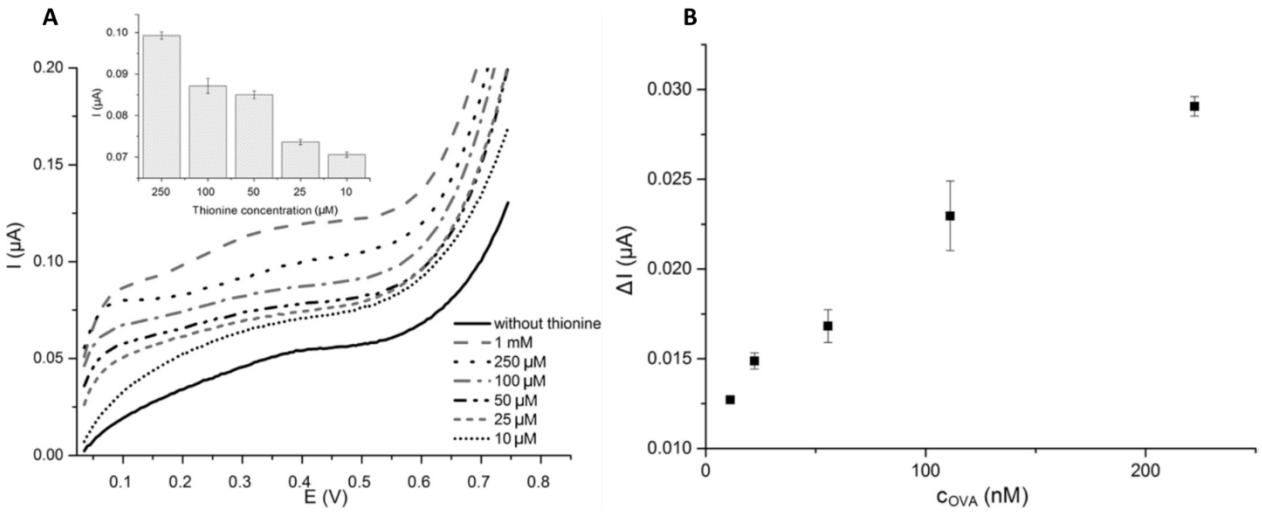

*Obrázek 25. Vliv přídavku elektronového mediátoru thioninu na výšku píku (A); výsledná kalibrační závislost pro kvantifikaci ovalbuminu pomocí elektrochemického imunosenzoru na principu sendvičové ELISA metody (B) [**P6**]*

Přestože některé komerční sestavy pro kvantifikaci ovalbuminu, které jsou založené na běžně využívané ELISA se spektrofotometrickou detekcí, mají nižší detekční limity [116], vyvinutý systém ukázal, jaké možnosti biosenzory přináší.

4.2 Imunosenzor využívající enzym alkalickou fosfatasu

V dalším výzkumu jsme se zaměřili sestavení elektrochemického imunosenzoru pro detekci a kvantifikaci proteinového biomarkeru asociovaného s ovariálním karcinomem, konkrétně lidského epididymálního proteinu 4 (HE4) [**P8**]. HE4 dosahuje, jako jediný nádorový marker, nejvyšší senzitivity pro detekci epiteliálního ovariálního karcinomu, a to již v časných fázích onemocnění. U žen s maligním nádorem, které nemají zvýšené hladiny ostatních markerů, je hladina HE4 zvýšená. Navíc je využíván pro sledování průběhu onemocnění, progrese a odpovědi na terapii.

Vzhledem k tomu, že obvyklá hodnota cut-off pro premenopauzální ženy je 50 pmol/l, a pro postmenopauzální 80 pmol/l [172], s použitím sekundárních protilátek značených HRP bychom nedosáhli potřebné citlivosti.

Proto byl pro značení protilátek zvolen enzym alkalická fosfatasa (ALP). ALP konvertuje řadu substrátů na elektroaktivní produkt s odpovídajícím redox potenciálem, navíc bez nutnosti elektronového mediátoru. K nejběžnějším substrátům patří *p*-aminofenylfosfát (PAPP), *p*-nitrofenylfosfát (PNPP) nebo hydrochinodifosfát (HQDP) [173-175].

Jako nejvhodnější substrát pro ALP a elektrochemickou detekci byl zvolen *p*-aminofenylfosfát, který poskytoval nejvyšší signál. Detekční metodou byla v případě jeho konverze ALP square-wave voltametrie (SWV), pro minimalizaci spotřeby vzorku byly opět využity tištěné tříelektrodové senzory, a to s uhlíkovou pracovní elektrodou, pomocnou platinovou a stříbrnou referentní. Pík odpovídající vznikajícímu elektroaktivnímu produktu (*p*-aminofenol) byl monitorován při potenciálu 0,045V a odečtena proudová odezva v desáté minutě enzymové reakce.

Protože anti-HE4 protilátky značené ALP nejsou komerčně dostupné, byly připraveny s využitím komerčního kitu pro značení protilátek enzymem ALP (Lightning-Link® Alkaline phosphatase conjugation kit, Innova Bioscience), kde konjugace probíhá přes aminoskupiny lysinu v molekule protilátek.

Při vlastním vývoji elektrochemického imunosenzoru pro stanovení HE4 proteinu, byly primární anti-HE4 protilátky imobilizovány na magnetické částice SiMAG s karboxylovými funkčními skupinami pomocí karbodiimidové metody. Celé stanovení v daném uspořádání (obrázek 27), tedy vychytání antigenu pomocí primárních protilátek, vazba sekundárních protilátek a finální enzymové reakce se substrátem PAPP probíhala v celkovém reakčním objemu 1 ml.

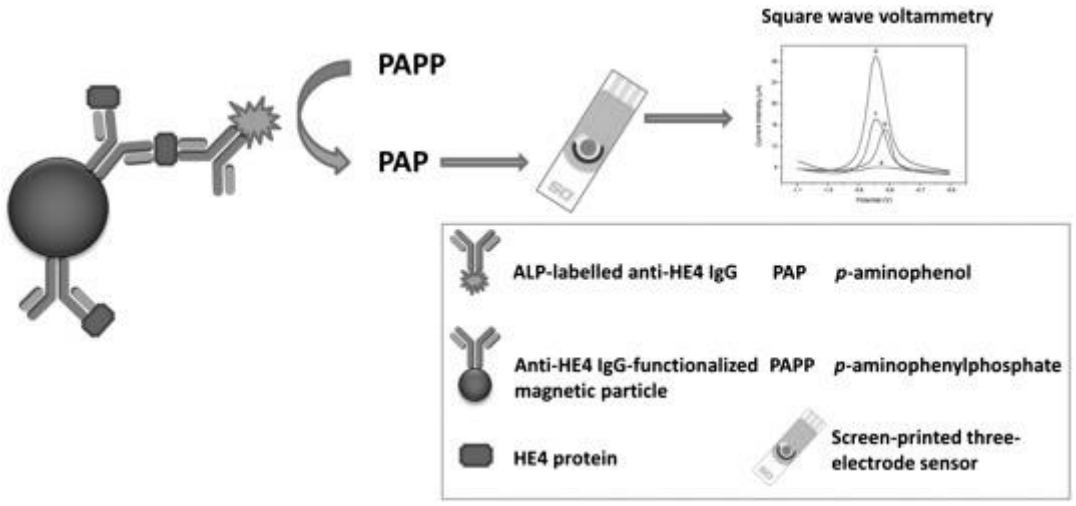

*Obrázek 27. Schéma uspořádání elektrochemického imunosenzoru pro detekci HE4 založeného na magnetických částicích s primárními protilátkami pro záchyt antigenu a protilátkami značenými ALP [**P8**]*

V daném uspořádání jsme dosáhli lineárního rozsahu koncentrací v rozmezí 4 – 400 pmol/l (obrázek 28) s kalkulovaným limitem detekce (LOD) 6,8 fmol/l a limitem kvantifikace (LOQ) 23 fmol/l. Systém v daném uspořádání dosahuje vysoké citlivosti a splňuje podmínky pro kvantifikaci HE4 proteinu i v časných fázích onemocnění. Analýzou standardního lidského séra s definovaným přídavkem standardního proteinu HE4 (s výtěžností 87 – 93 %) byla potvrzena funkčnost systému pro reálné vzorky [**P8**].

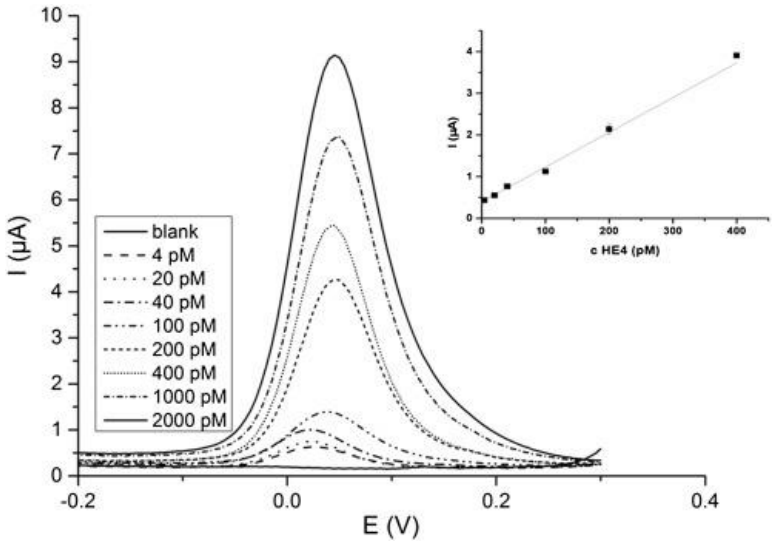

*Obrázek 28. SW voltamogram při detekci HE4 proteinu a kalibrační křivka (insertovaný graf) [**P8**]*

Při sestavení ELISA metody je vždy nezbytná optimalizace dílčích kroků, zejména v případě značených protilátek, které byly připravovány. Je nutné ověřit účinnost značení, ale také zachování vazebné schopnosti připravených značených protilátek a stanovit jejich optimální ředění používané pro sestavení vlastního imunosenzoru.

Pro tyto nezbytné optimalizační kroky jsme využili, z důvodů vysoké ceny vlastních anti-HE4 protilátek, modelový systém s anti-Apo E^{ALP}. Pro ověření schopnosti vazby antigenu a určení optimálního množství značených protilátek byl na magnetické částice imobilizován antigenem (protein Apo E). Pomocí tohoto modelového systému bylo určeno optimální ředění značených protilátek 1:1000, které bylo používáno i pro systém pro detekci proteinu HE4 [**P9**]. Při určení optimálního množství značených protilátek jseme zohlednili i ekonomickou stránku, proto nebylo zvoleno množství, které poskytlo nejvyšší signál (obrázek 29).

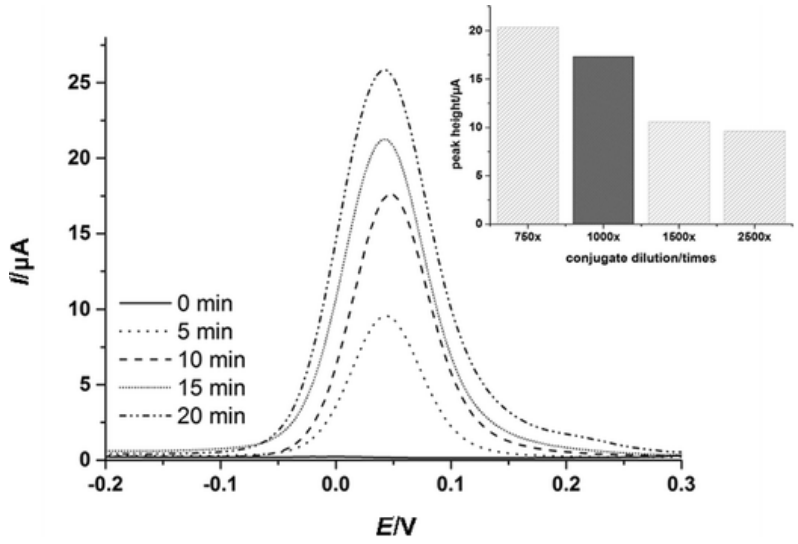

*Obrázek 29. Square-wave voltamogram elektroaktivního produktu konverze PAPP substrátu pomocí anti-Apo E^{ALP}protilátek při ředění 1:1000; insertovaný graf ukazuje proudové odezvy při stanovení optimálního ředění [**P9**]*

Jak je zřejmé z dosažených výsledků, elektrochemické imunosenzory mají potenciál jako jednoduchá zařízení pro analýzu a kvantifikaci biologicky významných proteinů. Kombinace s magnetickými částicemi umožňuje snadnou manipulaci bez ztrát vzorku, kovalentní vazba protilátek zajišťuje dlouhodobou stabilitu připraveného nosiče a celý systém je robustní a není náročný na přístrojové vybavení. Citlivost celého systému je dána citlivostí použité značky protilátek, kdy vyšší citlivosti dosahuje ALP, v porovnání s HRP.

5. Enzymy vs. nanočástice jako signál generující značky v imunosenzorech

V současnosti stále roste uplatnění nově vyvíjených nanomateriálů, a to v různých aplikacích. V případě elektrochemických imunosenzorů nanomateriály buď mohou nahradit enzymy využívané pro značení protilátek, pokud samy o sobě poskytují měřitelný signál. Nebo jsou využívány v kombinaci s enzym. Nanomateriály jsou zaváděny z důvodů požadavků na vyšší citlivost stanovení, což je důležité právě v případě detekce biologicky významných látek. V kombinaci s enzymy se využívá velkého specifického povrchu nanomateriálů, na které jsou enzymy vázány a následně použity jako značky protilátek. Na jednu molekulu protilátky lze tímto způsobem navázat více molekul enzymu a dochází tak k amplifikaci výsledného signálu, a tedy i citlivosti celého stanovení.

Pro tyto účely jsou využívány nejčastěji nanočástice vyrobené z různých materiálů (polymerní, silika, kovové), jednostěnné nebo vícestěnné uhlíkové nanotrubice, dendrony nebo dendrimery [83,176-178]. V kombinaci s elektrochemickými imunosenzory je většinou celý komplex primární protilátka-antigen-značená protilátka sestaven přímo na povrchu pracovní elektrody nebo je opět využíváno výhod magnetických částic.

Jako konkrétní příklad nanočástic v kombinaci s enzymem, které by mohly být využity jako značky protilátek v elektrochemických imunosenzorech lze uvést poly(glycidyl methakrylátové) nanočástice, které byly vyvinuty v Ústavu makromolekulární chemie, AV ČR. Tyto nanočástice jsme testovali, zda mohou přispět k amplifikaci výsledného signálu při sestavení imunosenzoru pro detekci ovalbuminu. Do připravených nanočástic byl po syntéze inkorporován elektronový mediátor thionin, aby nebyl nutný jeho přídavek do roztoku při vlastním měření lineární voltametrií [**P6**]. Následně jsme na nanočástice kovalentně vázali enzym křenovou peroxidasu pomocí karbodiimidové metody. Vedle toho byly připraveny i nanočástice bez thioninu a byl sledován efekt inkorporace thioninu. Při použití částic s inkorporovaným thioninem bylo dosaženo 3x vyšších proudové odezvy v porovnání s částicemi bez thioninu [102].

V případě kombinace nanomateriálů s enzymy dochází ke zvýšení citlivosti stanovení, ale často bývá konstrukce takového systému vícekroková a relativně komplikovaná. Proto se v oblasti

elektrochemických imunosenzorů v dnešní době objevuje řada prací, kde je využíváno takových nanomateriálů, které samy poskytují elektrochemicky měřitelný signál a jsou využívány pro značení protilátek. Nejčastěji se jedná o kovové nanočástice nebo nanokompozity, jako jsou zlaté, stříbrné, platinové nebo palladiové nanočástice, či kvantové tečky [83, **P10**]. Jejich detekce je založena na monitorování proudové odezvy iontů kovu, ze kterého jsou syntetizovány. Pro každý kov je charakteristický potenciál, při kterém je signál monitorován. Z detekčních metod je nejčastější anodická nebo katodická rozpouštěcí voltametrie po rozpuštění nanočástic a uvolnění iontů do roztoku.

Použití nanočástic pro značení protilátek v elektrochemických imunosenzorech je uvedeno v pracích [**P9-P11**]. Z výše zmíněných nanočástic jsme využili pro detekci nádorového markeru HE4 kvantové tečky (QDs). Ty jsou tvořeny selenidem kadmia obalené vrstvou sulfidu zinečnatého a funkcionalizované karboxylovými skupinami (CdSe/ZnS). Uspořádání celého systému bylo stejné jako v případě alkalické fosfatasy (obrázek 30), kdy primární protilátky pro záchyt HE4 ze vzorku byly imobilizovány na magnetické částice. Pro detekci byly připraveny protilátky značené CdSe/ZnS QDs namísto ALP. Finální detekce spočívala v monitorování proudové odezvy Cd(II), které byly uvolněny po rozpuštění QDs v kyselém prostředí. Charakteristicý detekční potenciál pro Cd(II) je -0,75 V. Pro analýzu byly využity opět tištěné tříelektrodové senzory, pro detekci kovů však s uhlíkovou pracovní elektrodou se rtuťovým nebo bizmutovým filmem.

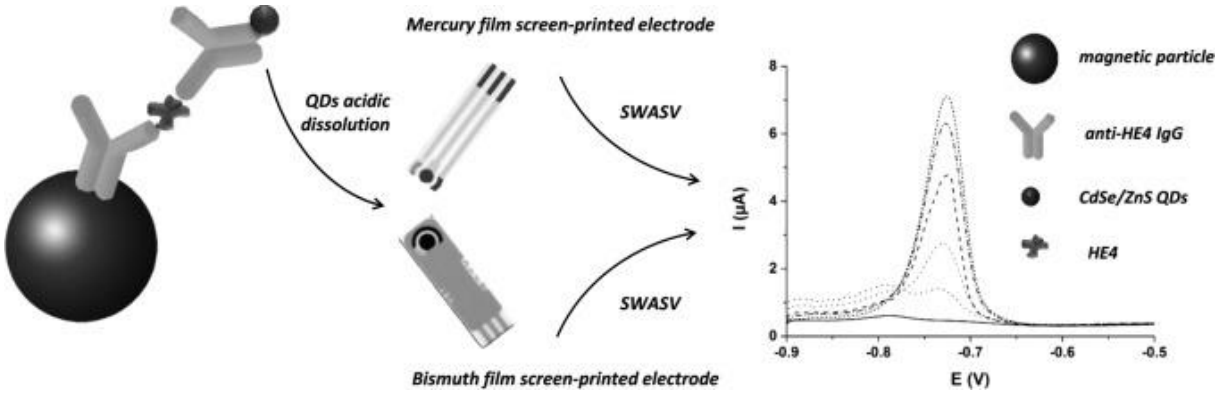

*Obrázek 30. Schéma uspořádání elektrochemického imunosenzoru pro detekci HE4 založeného na magnetických částicích s primárními protilátkami pro záchyt antigenu a protilátkami značenými CdSe/ZnS QDs [**P10**]*

Neboť protilátky značené kvantovými tečkami nejsou komerčně dostupné, byly připravovány cíleně pro daný systém. Byly použity dvě metody značení protilátek. První byla s využitím komerčního kitu SiteClick™ Qdot® 565 Antibody Labeling Kit, která je založena na vazbě přes glykosidickou část protilátek. Druhá metoda značení protilátek, kterou jsme zavedli, vychází z našich zkušeností s využitím magnetických částic [**P11**].

Výhodou komerčního kitu je jednoduchost protokolu, orientovaná vazba v dostatečné vzdálenosti od vazebného místa a relativně vysoká účinnost vazby (75 %). Nevýhodou je, že pro tento způsob vazby je nutná glykosylace protilátek, která se např. u monoklonálních protilátek nemusí vždy vyskytovat. Komerční kit je také určen pouze pro jediný typ kvantových teček, které jsou jeho součástí. A přestože jeho součástí jsou i purifikační kolonky pro oddělení značených protilátek od volných nezreagovaných kvantových teček, nebyly využívány z důvodů vysokých ztrát při purifikaci v důsledku sorpce značených protilátek na purifikační kolonky. Při eleiminaci tohoto kroku pak získaný produkt tak neměl garantovanou čistotu.

Druhý způsob značení protilátek spočívá v afinitním zachycení protilátek na magnetické částice, které byly předem modifikovány antigenem. V dalším kroku jsou na takto fixované protilátky kovalentně navázány kvantové tečky a v posledním kroku jsou značené protilátky uvolněny z imunokomplexu a připraveny k použití bez další nezbytné purifikace [**P11**]. Výhodou této metody je její univerzálnost, lze ji využít pro jakékoliv protilátky. Navíc, fixací protilátky na antigen jsou chráněna vazebná místa protilátky. Protilátky je možné označit jakýmikoliv kvantovými tečkami nebo i jinými nanočásticemi. Metoda byla optimalizována s modelovým systémem Apo E – anti-ApoE. Účinnost značení byla ověřena několika metodami, kapilární elektroforézou s laserem indukovanou fluorescencí (CE-LIF), gelovou elektroforézou (TBE-PAGE, SDS-PAGE) a elektrochemicky (obrázek 31). Je třeba zmínit, že účinnost této metody je oproti komerčnímu kitu nižší, přibližně 30 %.

Protilátky anti-HE4 značené oběma postupy byly úspěšně využity při vývoji elektrochemického imunosenzoru pro detekci proteinu HE4.

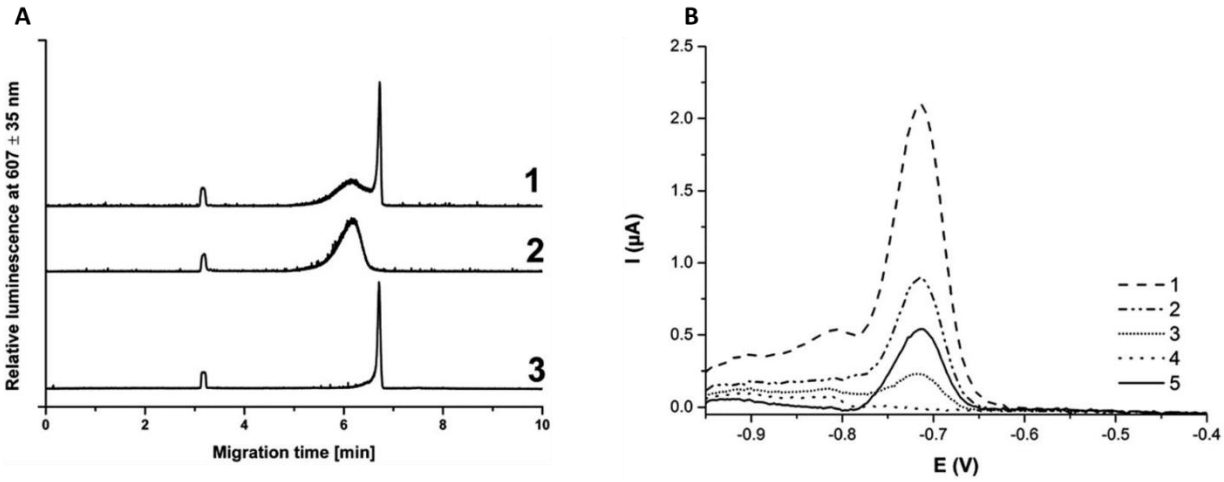

*Obrázek 31. Ověření účinnosti značení protilátek anti-ApoE kvantovými tečkami CdSe/ZnS pomocí karbodiimidové metody s využitím antigenem modifikovaných magnetických částic; (A) CE-LIF analýza frakcí 1 – směs anti-ApoE a QDs, 2- značené anti-ApoE$^{CdSe/ZnS}$, 3-QDs; (B) elektrochemická analýza (SWASV) frakcí 1- čisté QDs, 2-4 – promývací frakce, 5- značené anti-ApoE$^{CdSe/ZnS}$ [**P11**]*

Pro oba typy značených protilátek jsme dosáhli srovnatelných detekčních limitů. V případě protilátek značených námi zavedenou metodou byl širší lineární rozsah koncentrací. Vliv na výslednou citlivost má i typ použité pracovní elektrody, kdy senzory s uhlíkovou pracovní elektrodou s *in situ* vytvořeným bizmutovým filmem poskytly lepší linearitu v širším rozmezí koncentrací (obrázek 32).

Pro potvrzení funkčnosti systému i pro reálné vzorky, bylo analyzováno standardní lidské sérum s definovanými přídavky HE4 proteinu, kde se výtěžnost pohybovala v rozmezí 80 - 91 %. V porovnání s imunosenzorem využívajícím protilátky značené ALP, je systém s kvantovými tečkami méně citlivý, i přesto však splňuje požadavky na detekci proteinu HE4 v koncentracích odpovídajících cut-off hodnotám pro diagnostiku ovariálního karcinomu.

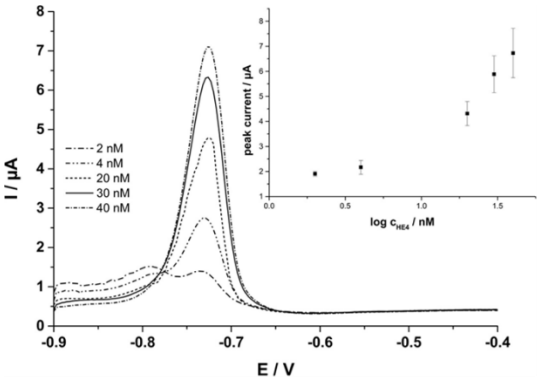

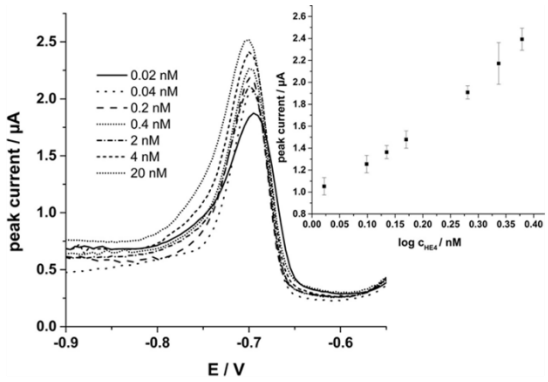

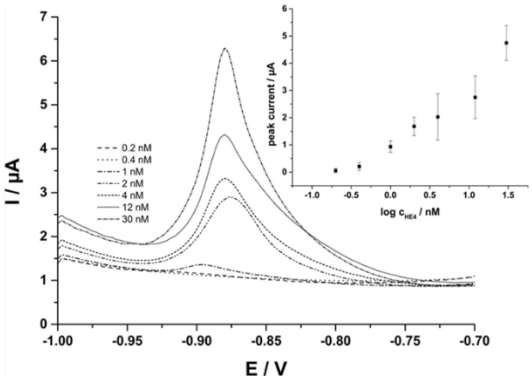

Senzor	LOD [pM]	Lineární rozsah [nM]
Hg-SPCE	2,94[a]	2 – 40
Hg-SPCE	3,7[b]	0,2 – 20
Bi-SPCE	5,27[a]	0,02 - 20

[a]komerční kit; [b]karbodiimidová metoda

*Obrázek 32. SWASV voltamogramy a kalibrační křivky kvantifikace HE4 proteinu pomocí elektrochemických imunosenzorů; senzory se rtuťovým filmem (Hg-SPCE) a protilátkami anti-HE4$^{CdSe/ZnS}$ značenými pomocí komerčního kitu (A), senzory se rtuťovým filmem (Hg-SPCE) a protilátkami anti-HE4$^{CdSe/ZnS}$ značenými karbodiimidovou metodou (B), senzory s bizmutovým filmem (Bi-SPCE) a protilátkami anti-HE4$^{CdSe/ZnS}$ značenými pomocí komerčního kitu (C); kalkulované limity detekce a lineární rozsah pro uvedené systémy [**P10**]*

Benefitem využití kvantových teček a kovových nanočástic v kombinaci s elektrochemickou detekcí je také možnost simultánní detekce více analytů v rámci jedné analýzy. Ta je založena na rozdílných detekčních potenciálech různých kovových iontů. Je-li použita vhodná kombinace kovových nanočástic pro značení protilátek s odlišnou specifitou, lze uvolněné ionty stanovit vedle sebe, a tím i více analytů (obrázek 33). To je výhodné v případě biomarkerů asociovaných s některými onemocněními, kde profil biomarkerů může přispět k přesnější diagnostice nebo monitorování terapeutické odpovědi.

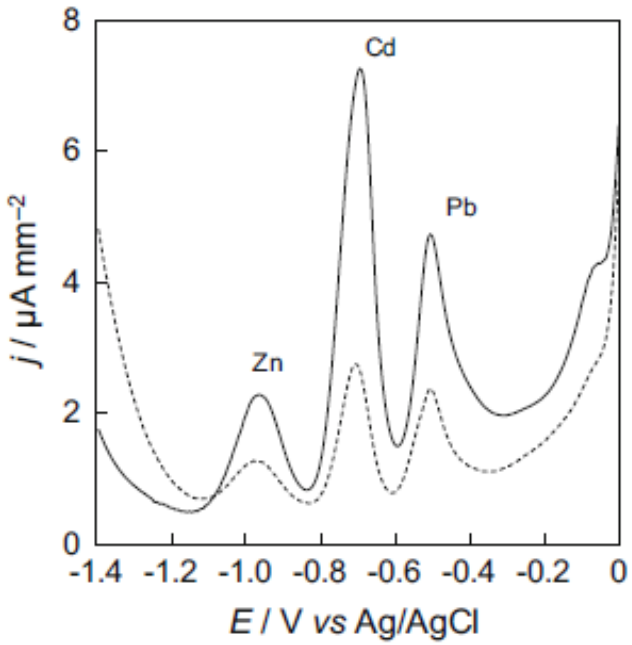

Obrázek 33. SWASV voltamogram simultánní detekce kovových iontů v prostředí acetátového pufru [179]

Elektrochemické imunosenzory, a to jak v kombinaci s enzymy, tak i elektroaktivními nanomateriály, by mohly být vhodnou alternativou k rutinně využívaným, ale přístrojově náročnějším metodám. Přestože tyto metody nenahradí, přináší řadu výhod, které mají potenciál zejména v oblasti screeningu onemocnění.

Závěr

Výsledky prací, které byly v rámci práce popsány, ukazují potenciál využití enzymů v řadě oblastí, od analytického až po možnost využití v oblasti biotechnologií. Jejich imobilizace na pevnou fázi přináší řadu výhod v podobě větší stability enzymu, zlepšení kinetických parametrů katalyzované reakce, nebo možnosti opakovaného použití. Při imobilizaci enzymů bylo nezbytné optimalizovat podmínky vazby, volit vhodnou metodu imobilizace, která může ovlivnit výslednou aktivitu imobilizovaného enzymu a jeho účinnost. Při přípravě imobilizovaných enzymů bylo přistupováno individuálně a s ohledem na jejich finální aplikaci, podle toho byla volena metoda a podmínky imobilizace, a použité magnetické částice. Díky dostupnosti široké škály komerčních magnetických částic, ale i nově vyvíjených v rámci spolupráce s kolegy z Ústavu makromolekulární chemie AV ČR bylo možné porovnat a částice pro přípravu účinných nosičů s imobilizovanými enzymy.

Při využití enzymů v oblasti elektrochemických imunosenzorů se podařilo sestavit imunosenzory pro detekci ovalbuminu a nádorového biomarkeru proteinu HE4. I v této oblasti jsme využili kombinaci s magnetickými částicemi, na které byly imobilizovány specifické protilátky pro snadnou a selektivní izolaci stanovovaného proteinu ze vzorku. Enzymy byly konjugovány se specifickými protilátkami a použity pro elektrochemickou detekci izolovaného proteinu. Alkalická fosfatasa se ukázala jako vhodný enzym pro využití v imunosenzorech, nejen díky několika elektroaktivním substrátům, ale i vyšší citlivosti ve srovnání s křenovou peroxidasou. Pro zvýšení citlivosti byly enzymy kombinovány s nanočásticemi. Nanočástice, konkrétně kvantové tečky byly také pro elektrochemickou detekci nádorového biomarkeru proteinu HE4 použity samostaně, díky jejich elektroaktivním vlastnostem. I v tomto případě bylo dosaženo takové citlivosti, která umožňuje detekci nízkých hladin tohoto proteinu, což je důležité pro včasnou diagnostiku rozvoje nádorového onemocnění.

Perspektiva do budoucna

Výsledky dosažené v oblasti elektrochemických imunosenzorů budou využity ve výzkumu, který probíhá již v současné době a je zaměřen na vývoj multiplexního imunosenzoru pro simultánní kvantifikaci tří proteinových bimarkerů asociovaných s nádorovým onemocněním, případně prozánětlivých biomarkerů. Pro multiplexní analýzu je nutné najít tři vhodné značky protilátek, které umožní analýzu v rámci jednoho měření. Nabízí se tak tři různé typy nanočástic nebo jejich kombinace s enzymy. Díky uspořádání, robustnosti, a možnosti miniaturizace by biosenzory mohly být v budoucnu alternativou splňující kritéria POCT zařízení. Další oblastí, kde již bylo dosaženo prvních výsledků, je detekce bakterií pomocí imunosenzoru, a to na úrovni celých buněk, s potenciálem využití pro screening kontaminace potravin.

Vybrané enzymy budou i v rámci dalšího výzkumu imobilizovány na magnetické částice a využívány v řadě aplikací. Cílem bude i další propojení enzymů s elektrochemickou detekcí. Jedním ze záměrů je charakterizace imobilizovaných kinas z pohledu aktivity a kinetických parametrů enzymové reakce elektrochemicky jako alternativa k metodám využívaným v současnosti.

Seznam použitých zkratek

AAS	Atomová absorpční spektrometrie
ABTS	kyselina 2,2´-azino-bis(3-ethylbenzthiazolin-6-sulfonová)
AFM	Mikroskopie atomárních sil
AgNPs	Stříbrné nanočástice
ALP	Alkalická fosfatasa
AuNPs	Zlaté nanočástice
BApNA	N-α-benzoyl-D,L-arginin-4-nitroanilid
BCA	Bicinchoninová metoda
CE-LIF	Kapilární elektroforéza s laserem indukovanou fluorescencí
CLEAs	Enzymové agregáty (z angl. cross-linked enzyme aggregates)
CLECs	Zesítěné enzymové krystaly (z angl. cross-linked enzyme crystals)
CLIA	Chemiluminiscenční imunoanalýza
ECLIA	Elektrochemiluminiscenční imunoanalýza
EIA	Enzymová imunoanalýza
ELISA	Enzymová imunoanalýza na pevné fázi
ESI-MS/MS	Tandemová hmotnostní spektrometrie s ionizací elektrosprejem
FIA	Fluorescenční imunoanalýza
FITC	Fluoresceinisothiokyanát
FTIR	Infračervená spektroskopie s Fourierovou transformací (z angl. Fourier transform infrared spectroscopy)
Gg4Cer	Gangliotetraosylceramid
GC	Plynová chromatografie
GLs	Glykosfingolipidy
GO	Grafen oxid
HA	Kyselina hyaluronová
HE4	Lidský epididymální protein 4
HMW-HA	Vysokomolekulární kyselina hyaluronová
HPSM	Hypersíťované polystyrenové magnetické částice

HPTLC	Vysokoúčinná tenkovrstvá chromatografie
HQDP	Hydrochinodifosfát
HRP	Křenová peroxidasa
IMAC	Afinitní chromatografie na imobilizovaných kovových iontech
LC-MS/MS	Kapalinová chromatografie ve spojení s tandemovou hmotnostní spektrometrií
LIA	Luminiscenční imunoanalýza
LOD	Limit detekce
LOQ	Limit kvantifikace
lyso-Gb3Cer	Lyso-globotriaosylceramid
MBC	Makroporézní perlová celulosa
MBC-IDA	Makroporézní perlová celulosa modifikovaná kyselinou iminodioctovou
MOEAA	Kyselina (2-methakryloyloxy)ethoxy octová
MOFs	Kovové organické kostry (z angl. metal-organic frameworks)
OPD	*o*-fenylendiamin
PAPP	*p*-aminofenylfosfát
PdNPs	Palladiové nanočástice
PEI	Polyethylenimin
PEPs	Prolyl-endoproteasy
PGMA	Poly-glycidyl methakrylát
PHEMA	Poly-hydroxyethyl methakrylát
PNPP	*p*-nitrofenylfosfát
POCT	Testování v místě péče o pacienta (z angl. Point-of-Care Testing)
PolyNIPAM	Poly-N-izopropylakrylamid
PtNPs	Platinové nanočástice
QCM	Křemenné mikrovážky (z angl. Quartz crystal microbalance)
QDs	Kvantové tečky
RIA	Radioizotopová imunoanalýza
RNA	Kyselina ribonukleová

SCDáza	Sfingolipid ceramid *N*-deacylasa
SDS-PAGE	Polyakrylamidová gelová elektroforéza v prostředí dodecylsulfátu sodného
SEC-MALS	Gelově-permeační chromatografie s detektorem víceúhlového rozptylu světla
SEM	Skenovací elektronová mikroskopie
SGZ	Syringaldazin
SpnHL	Hyaluronanlyasa ze *Streptococcus pneumoniae*
SWV	Square-wave voltametrie
TBE-PAGE	Polyakrylamidová gelová elektroforéza v prostředí Tris-borát-EDTA pufru
TEM	Transmisní elektronová mikroskopie
TGA	Termogravimetrie
TLC	Tenkovrstvá chromatografie
TMB	Tertamethylbenzidin

Seznam použité literatury

1. Blanco A., Blanco G., *Medical Biochemistry*, 2017 (Academic Press, ISBN 9780128035504)
2. Komoda T., Matsunaga T., *Biochemistry for Medical Professionals*, 2015 (Academic Press, ISBN 9780128019184)
3. Bhagavan N. V., Ha C.-E., *Essentials of Medical Biochemistry*, 2011 (Academic Press, ISBN 9780120954612)
4. Bernal C., Rodríguez K., Marínez R., *Biotechnology Advances*, **36**, 2018, 1470-1480
5. DeLuca D. C., York J. L., *Encyclopedia of Genetics*, 2001 (Academic Press, ISBN 978-0-12-227080-2)
6. Liu D.-M., Chen J., Shi Y.-P., *Trends in Analytical Chemistry*, **102**, 2018, 332-342
7. Eicher J. J., Snoep J. L., Rohwer J. M., *Metabolites,* **2(4)**, 2012, 818-43
8. Kenakin T. P., *Pharmacology in Drug Discovery*, 2012 (Academic Press, ISBN 978-0-12-384856-7)
9. Bonzom C., Hüttner S., Mirgorodskaya E., Chong S. L., Uthoff S., Steinbüchel A., Verhaert R. M. D., Olsson L. *AMB Express,* **9(1)**, 2019, 126-139
10. Goettig P., *International Journal of Molecular Sciences*, **17(12)**, 2016, 1969-1993
11. Berg J. M., Tymoczko J. L., Stryer L., *Biochemistry*, 2002 (New York: W H Freeman)
12. Zorn J. A., Wells J. A., *Nature Chemical Biology*, **6(3)**, 2010, 179-188
13. Darby J. F., Atobe M., Firth J. D., Bond P., Davies G. J., O'Brien P., Hubbard R. E., *Chemical Science*, **8(11)**, 2017, 7772-7779
14. Russell A. J., Klibanov A. M., *Journal of Biological Chemistry*, **263(24)**, 1988, 11624-11626
15. Hemalatha T., Maheswari T. U., Krithiga G., Sankaranarayanan P., Puvanakrishnan R., *Indian Journal of Experimental Biology*, **51**, 2013, 777-788
16. Raja M. M. M., Raja A., Imran M. M., Santha A. M. I., Devasena K., *Biotechnology*, **10(1)**, 2011, 51-59
17. Misra A., *Challenges in Delivery of Therapeutic Genomics and Proteomics*, 2011 (Elsevier, ISBN 978-0-12-384964-9)
18. Li Q., Feng Y., Tan M.-J., Zhai L.-H., *Chinese Journal of Analytical Chemistry*, **45(3)**, 2017, 316-321
19. Gaspari M., Cuda G., *Methods in Molecular Biology*, **790**, 2011, 115-126
20. Chmelík J., *Chemické listy*, **99**, 2005, 883-885
21. Michel P. E., Crettaz D., Morier P., Heller M., Gallot D., Tissot J.-D., Reymond F., Rossier J. S., *Electrophoresis*, **27(5-6)**, 2006, 1169-1181
22. Zhu W., Smith J. W., Huang Ch.-M., *Journal of Biomedicine and Biotechnology*, 2010, Article ID 840518
23. Fournier M. L., Gilmore J. M., Martin-Brown S. A. et al. *Chemical Reviews*, **107(8)**, 2007, 3654-3686
24. Šlechotová T., Gilar M., Kalíková K., Moore S. M., Jorgenson J. W., Tesařová E., *Journal of Chromatography A*, **1490**, 2017, 126-132
25. Korecká L., Jankovičová B., Křenková J., Hernychová L., Slovaková M., Le-Nell A., Chmelík J., Foret F., Viovy J.-L., Bílková Z., *Journal of Separation Science*, **31**, 2008, 507-515
26. Kacerovsky M., Lenco J., Musilova I., Tambor V., Lamont R., Torloni M. R., Menon R., *Reproductive Sciences*, **21(3)**, 2014, 283-295
27. Christine L. Gatlin, Jimmy K. Eng, Stacy T. Cross, James C. Detter, John R. Yates, *Analytical Chemistry*, **72(4)**, 2000, 757-763
28. Wu Z., Huang J., Li Q., Zhang X., *Analytical Chemistry*, **90(16)**, 2018, 9700-9707
29. Giansanti, P., Tsiatsiani, L., Low, T. et al. *Nature Protocols*, **11**, 2016, 993–1006
30. Vincent D., Ezernieks V., Rochfort S., Spangenberg G., *International Journal of Molecular Sciences*, **20(22)**, 2019, 5630-5657
31. Batth T. S., Papetti M., Pfeiffer A., Tollenaere M. A. X., Francavilla Ch., Olsen J. V., *Cell reports*, **22(10)**, 2018, 2784-2796

32. Šebela M., Řehulka P., Kábrt J., Řehulková H., Oždian T., Raus M., Franc V., Chmelík J., *Journal of Mass Spectrometry*, **44**, 2009, 1587–1595
33. van der Laarse S. A. M., van Gelder C. A. G. H., Bern M., Akeroyd M., Olsthoorn M. M. A., Heck A. J. R., *The FEBS Journal*, 2020, doi:10.1111/febs.15190
34. Schräder C. U., Lee L., Rey M., Sarpe V., Man P., Sharma S., Zabrouskov V., Larsen B., Schriemer D. C., *Molecular & Cellular Proteomics*, **16(6)**, 2017, 1162-1171
35. Carreño-Tarragona G., Cedena T., Montejano L., Alonso R., Miras F., Valeri A., Rivero A., Lahuerta J. J., Martinez-Lopez J., *Transfusion Medicine*, **29**, 2019, 193-196
36. Korecká L., Bílková Z., Holčapek M., Královský J., Beneš M., Lenfeld J., Minc N., Cecal R., Viovy J.-L., Przybylski M., *Journal of Chromatography B*, **808**, 2004, 15-24
37. Aibara N., Kamohara Ch., Chauhan A. K., Kishikawa N., Miyata Y., Nakashima M., Kuroda N., Ohyama K., *Journal of Immunological Methods*, **461**, 2018, 85–90
38. Bobaly B., D´Atri V., Goyon A., Colas O., Beck A., Fekete S., Guillarme D., *Journal of Chromatography B,* **1060**, 2017, 325-335
39. Kinman A. W. L., Pompano R. R., *Bioconjugate Chemistry*, **30**, 2019, 800-807
40. Wagner-Rousset E., Fekete S., Morel-Chevillet L., Coals O., Corvaïa N., Cianférani S., Guillarme D., Beck A., *Journal of Chromatography A,* **1498**, 2017, 147-154
41. Calzada V., García M. F., Alonso-Martínez L. M., Camachoc X., Goicochea E., Fernández M., Castillo A. X., Díaz-Miqueli A., Iznaga-Escobar N., Leyva Montaña R., Alonso O., Pablo Gambini J., Cabral P., *Current Medicinal Chemistry - Anti-Cancer Agents*, **16(9)**, 2016, 1184-1189
42. Li Y., Yu J., Goktepe I., Ahmedna M., *Food Chemistry*, **196**, 2016, 1338–1345
43. Fernandez-Lucas J., Casta˜neda D., Hormigo D., *Trends in Food Science & Technology*, **68**, 2017, 91-101
44. Kumar, B., Varadaraj, M., Tharanathan, R., *Biomacromolecules*, **8(2)**, 2007, 566–572
45. Muzzarelli, R. A. A., Terbojevich, M., Muzzarelli, C., Francescangeli, O., *Carbohydrate Polymers*, **20**, 2002, 69–78
46. Vishu Kumar, A. B., Tharanathan, R. N., *Carbohydrate Polymers*, **58**, 2004, 275–283
47. Vishu Kumar, A. B., Varadaraj, M. C., Lalitha, R. G., Tharanathan, R. N., *Biochimica et Biophysica Acta*, **1670**, 2004, 137–146
48. Lin, H., Wang, H., Xue Ch Ye, M., *Enzyme and Microbial Technology*, **31**, 2002, 588–592
49. Kang Z., Zhou Z., Wang Y., Huang H., Du G., Chen J., *Trends in Biotechnology*, **36(8)**, 2018, 806-818
50. Jiao Y., Pang X., Zhai G., *Current Drug Targets*, **17(6)**, 2016, 720-730
51. Huang G., Huang H., *Journal of Controlled Release*, **278**, 2018, 122-126
52. Wang T., Hou J., Su C., Zhao L., Shi Y., *Journal of Nanobiotechnology*, **15**, 2017, 7-19
53. Triggs-Raine B., Natowicz M. R., *World Journal of Biological Chemistry*, **6(3)**, 2015, 110-120
54. Bollyky P. L., Bogdani M., Bollyky J. B., Hull R. L., Wight T. N., *Current Diabetes Reports*, **12**, 2012, 471-480
55. Jiang D., Liang J., Noble P. W., *Physiological Reviews*, **91**, 2011, 221-264
56. Rayahin J. E., Buhrman J. S., Zhang Y., Koh T. J., Gemeinhart R. A. *ACS Biomaterials Science & Engineering*, **1(7)**, 2015, 481-493
57. Chen H., Qin J., Hu Y., *Molecules,* **24**, 2019, 617-629
58. Muckenschnabel I., Bernhardt G., Spruss T., Dietl B., Buschauer A., *Cancer Letters*, **131(1)**, 1998, 13-20
59. Pavan M., Beninatto R., Galesso D., Panfilo S., Vaccaro S., Messina L., Guarise C., *Biochimica et Biophysica Acta (BBA) - General Subjects*, **1860(4)**, 2016, 661-668
60. Yang P.-F., Lee C.-K., *Carbohydrate Polymers*, **65**, 2006, 159-164
61. Stern R., Jedrzejas M. J., *Chemical Reviews*, **106(3)**, 2006, 818-39
62. Kelly S. J., Taylor K. B., Li S., Jedrzejas M. J., *Glycobiology*, **11(4)**, 2001, 297-304
63. Baker J. R., Dong S., Pritchard D. G., *Biochemical Journal*, **365(1),** 2002, 317-322
64. Kita K., Kurita T., Ito M., *European Journal of Biochemistry*, **268**, 2001, 592-602

65. Hernandez E. M., *Functional dietary lipids*, 2016 (Woodhead Publishing, ISBN 978-1-78242-247-1)
66. Zama K., Hayashi Z., Ito S., Hirabayashi Z., Inoue T., Ohno K., Okino N., Ito M., *Glycobiology*, **19(7)**, 2009, 767-775
67. Arigi E., Blixt O., Buschard K., Clausen H., Levery S. B., *Glycoconjugate Journal*, **29**, 2012, 1-12
68. Mills K., Eaton S., Ledger V., Young E., Winchester B., *Rapid Communications in Mass Spectrometry*, **19**, 2005, 1739-1748
69. Ito M., Kurita T., Kita K., *Journal of Biological Chemistry*, **270(41)**, 1995, 24370-24374
70. Kurita T., Izu H., Sano M., Ito M., Kato I., *Journal of Lipid Research*, **41**, 2000, 846-851
71. Ando T., Li S-Ch., Ito M., Li Y-T., *Journal of Chromatography A*, **1078**, 2005, 193-195
72. Huang F.-T., Han Y.-B., Feng Y., Yang G.-Y., *Journal of Lipid Research,* **56,** 2015, 1836-1842
73. Abadulla E., Tzanov T., Costa S., Robra K-H., Cavaco-Paulo A., Gübitz G. M., *Applied Environmental Microbiology*, **66(8)**, 2000, 3357-3362
74. Claus H., Faber G., König H., *Applied Microbiology and Biotechnology*, **59**, 2002, 672-678
75. Voběrková S., Solčány V., Vršanská M., Adam V., *Chemosphere*, **202**, 2018, 694-707
76. Wong Y., Yu J., *Water Research*, **33(16)**, 1999, 3512-3520
77. Champagne P-P., Ramsay J. A., *Bioresource Technology*, **101**, 2010, 2230-2235
78. Bersanetti P. A., Escobar V. H., Nogueira R. F., dos Santos Ortega F., Schor P., de Araújo Morandim-Giannetti A., *European Polymer Journal*, **112**, 2019, 610–618
79. Huber D., Grzelak A., Baumann M., Borth N., Schleining G., Nyanhongo G. S., Guebitz G. M., *New Biotechnology*, **40**, 2018, 236-244
80. Pei J., Yin Y., Shen Z., Bu X., Zhang F., *Carbohydrate Polymers,* **135**, 2016, 234–238
81. Bu X., Pei J., Zhang F., Liu H., Zhou Z., Zhen X., Wang J., Zhang X., Chan H., *Carbohydrate Polymers,* **188**, 2018, 151-158
82. Blake C., Gould B. J., *Analyst*, **109**, 1984, 533-547
83. Korecká L., Vytřas K., Bílková Z., *Current Medicinal Chemistry*, **25**, 2018, 3973-3987
84. https://biotechkart.wordpress.com/2015/09/04/all-you-need-to-know-about-elisa/ [2020-05-01]
85. Hosseini S., Vázquez-Villegas P., Rito-Palomares M., Martinez-Chapa S. O*., Springer Briefs in Forensic and Medical Bioinformatics,* 2018, doi.org/10.1007/978-981-10-6766-2_2
86. Mohan S., Lawton R., Palmer Ch., Cadenas Rojas A., *Journal of Immunological Methods,* **474**, 2019, 112671-112677
87. Ram N., Furqan S., Ahmed S., *Case Reports in Endocrinology,* 2019, Article ID 5028534, doi.org/10.1155/2019/5028534
88. Broto M., McCabe R., Galve R., Marco M.-P., *Analyst*, **144**, 2019, 5172-5178
89. Saita T., Yamamoto Y., Hosoya K., Yamamoto Y., Kimura S., Narisawa Y., Shin M., *Analytica Chimica Acta*, **969,** 2017, 72-78
90. Ansari M. R. *Protein-protein Interactions Assays*, 2018, (InTechOpen, ISBN 978-1-78923-390-2)
91. Kourilov V., Steinitz M., *Analytical Biochemistry,* **311(2)**, 2002, 166-170
92. Paleček E., Kizek R., Havran L., Billova S., Fojta M., *Analytica Chimica Acta,* **469(1)**, 2002, 73-83
93. https://www.lsbio.com/elisakits/ [2020-05-01]
94. Darwish I. A., *International Journal of Biomedical Science and Engineering*, **2(3)**, 2006, 217–235
95. Malhotra B. D., Chaubey A., *Sensors and Actuators B*, **91**, 2003, 117–127
96. Li. G., *Nano-inspired Biosensors for Protein Assay with Clinical Applications,* 2019 (Elsevier, ISBN 978-0-12-815053-5)
97. Zhao Y., Zheng Y., Kong R., Xia L., Qu F., *Biosensors & Bioelectronics,* **75**, 2016, 383-388
98. Yin Z., Liu Y., Jiang L.-P., Zhu J.-J., *Biosensors & Bioelectronics*, **26(5)**, 2011, 1890-1894
99. Szunerits S., Boukherroub R., *Interface Focus*, **8**, 2018, 20160132
100. Morales-Narváez E., Baptista-Pires L., Zamora-Gálvez A., Merkoçi A., *Advanced Materials*, **29**, 2017, 1604905
101. Gong Q., Wang Y., Yang H., *Biosensors & Bioelectronics,* **89(1)**, 2017, 565-569

102. Zasonská B., Čadková M., Kovářová A., Bílková Z., Korecká L., Horák D., *ACS Applied Matererials & Interfaces,* **7**, 2015, 24926-24931
103. Chaubey A., Malhotra B. D., *Biosensors & Bioelectronics,* **17(6–7)**, 2002, 441-456
104. Çakıroğlu B., Özacar M., *Electroanalysis*, **32**, 2020, 166–177
105. Gao Z.-D., Guan F.-F., Li Ch.-Y., Liu H.-F., Song Y.-Y., *Biosensors & Bioelectronics,* **41,** 2013, 771-775
106. Rezaei B., Shams-Ghahfarokhi L., Havakeshian E., Ensafi A. A., *Talanta,* **158**, 2016, 42-50
107. Cho I.-H., Lee J., Kim J., Kang M., Paik J. K., Ku S., Cho H.-M., Irudayaraj J., Kim D.-H., *Sensors*, **18**, 2018, 207-225
108. Mateo C., Palomo J. M., Fernandez-Lorente G., Guisan J. M., Fernandez-Lafuente R., *Enzyme and Microbial Technology*, **40**, 2007, 1451-1463
109. Sheldon R. A., *Advanced Synthesis & Catalysis*, **349**, 2007, 1289-1307
110. Bolivar J. M., Eisl I., Nidetzky B., *Catalysis Today*, **259**, 2016, 66-80
111. Mohamad N. R., Marzuki N. H. Ch., Buang N. A., Huyop F., Wahab R. A., *Biotechnology & Biotechnological Equipment*, **29(2)**, 2015, 205–220
112. Rehm F. B. H., Chen S., Rehm B. H. A., *Molecules*, **21**, 2016, 1370-1388
113. Zucca P., Sanjust E., *Molecules*, **19**, 2014, 14139-14194
114. Wang J., Caruso F., *Chemistry of Materials*, **17**, 2005, 953-961
115. Bilal M., Zhao Y., Rasheed T., Iqbal H. M. N., *International Journal of Biological Macromolecules*, **120(B)**, 2018, 2530-2544
116. Sheldon R. A., van Pelt S., *Chemical Society Reviews*, **42**, 2013, 6223-6235
117. Roy N., Saha N., Jelínková L., Sáha P., Sáha T., *Plasty a kaučuk*, **3-4**, 2012, 73-80
118. Zhang S., Shang W., Yang X., Zhang S., Zhang X., Chen J., *Bulletin of the Korean Chemical Society*, **34(9)**, 2013, 2741-2746
119. Macková H., Horák D., Trachtová Š., Rittich B., Španová A., *Journal of Colloid Science and Biotechnology*, **1(2)**, 2012, 235-240
120. Quan Ch.-Y., Wei H., Sun Y.-X., Cheng S.-X., Shen K., Gu Z.-W., Zhang X.-Z., Zhuo R.-X., *Journal of Nanoscience and Nanotechnology*, **8(5)**, 2008, 2377-2384
121. Zhang Y., Yang W., Wang Ch., Wu W., Fu S., *Journal of Nanoscience and Nanotechnology*, **6(9-10)**, 2006, 2896-2901
122. Horák D., Svobodová Z., Autenbert J., Coudert B., Plichta Z., Královec K., Bílková Z., Viovy J.-L., *Journal of Biomedical Materials Research Part A*, **101A**, 2013, 23-32
123. Patsula V., Kosinová L., Lovrić M., Ferhatovic Hamzić L., Rabyk M., Konefal R., Paruzel A., Šlouf M., Herynek V., Gajović S., Horák D., *ACS Applied Matererials & Interfaces*, **8(11)**, 2016, 7238-7247
124. Can M. M., Coşkun M., Fırat T., *Journal of Alloys and Compounds*, **542**, 2012, 241-247
125. Kim W., Suh Ch.-Y., Cho S.-W., Roh K.-M., Kwon H., Song K., Shon I.-J., *Talanta*, **94**, 2012, 348-352
126. Korecká L., Ježová J., Bílková Z., Beneš M., Horák D., Hradcová O., Slováková M., Viovy J.-L. *Journal of Magnetism and Magnetic Materials*, **293**, 2005, 349-357
127. Kalska-Szostko B., Wykowska U., Satuła D., *Colloids and Surfaces A: Physicochemical and Engineering Aspects*, **481**, 2015, 527-536
128. Caruso F., Susha A. S., Giersig M., Möhwald H., *Advanced Materials*, **11**, 1999, 950-953
129. Zhao W., Gu J., Zhang L., Chen H., Shi J., *Journal of the American Chemical Society*, **127(25)**, 2005, 8916-8917
130. Holubová L., Knotek P., Palarcik J., Cadkova M., Belina P., Vlcek M., Korecka L., Bilkova Z., *Materials Science and Engineering C*, **44**, 2014, 345-351
131. Gu Y.-J., Zhu M.-L., Li Y.-L., Xiong Ch.-H., *International Journal of Biological Macromolecules*, **112**, 2018, 1175-1182
132. Cao L., *Carrier-bound Immobilized Enzymes (Principles, Applications and Design)*, 2005 (Wiley-VCH, ISBN 3-527-31232-3

133. Bezerra C. S., de Farias Lemos C. M. G., de Sousa M., Gonçalves L. R. B., *Journal of Applied Polymer Science*, 2015, DOI: 10.1002/APP.42125
134. Kim K. H., Lee O. K., Lee E. Y., *Catalysts,* **8(2)**, 2018, 68
135. Zucca P., Fernandez-Lafuente R., Sanjust E., *Molecules*, **21**, 2016, 1577-1602
136. Zang P. F., Lee C. K., *Biochemical Engineering Journal*, **37**, 2007, 108-115
137. Sun J., Ma H., Liu Z., Su Z., Xia W., Yang Y., *Colloids and Surfaces A: Physicochemical and Engineering Aspects*, **414**, 2012, 190-197
138. Asgher M., Noreen S., Bilal M., *International Journal of Biological Macromolecules*, **95**, 2017, 54-62
139. Nawaz M. A., Rehman H. U., Bibi Y., Aman A., Qader S. A. U., *Biochemistry and Biophysics Reports*, **4**, 2015, 250–256
140. Cirillo G., Nicoletta F. P., Curcio M., Spizzirri U. G., Picci N., Iemma F., *Reactive and Functional Polymers*, **83**, 2014, 62-69
141. Nguyen H. H., Kim M., *Applied Science and Convergence Technology*, **26(6)**, 2017, 157-163
142. Hermanson G. T., *Bioconjugate techniques*, 2008 (Elsevier Inc., ISBN 978-0-12-370501-3)
143. Grazú V., Abian O., Mateo C., Batista-Viera F., Fernández-Lafuente R., Guisán J. M., *Biotechnology and Bioengineering*, **90(5)**, 2005, 597-605
144. Grazú V., López-Gallego F., Montes T., Abian O., González R., Hermoso J. A., García J. L., Mateo C., Guisán J. M., *Process Biochemistry*, **45(3)**, 2010, 390-398
145. Zhang D.-H., Yuwen L.-X., Peng L.-J., *Journal of Chemistry,* 2013, Article ID 946248, http://dx.doi.org/10.1155/2013/946248
146. Peng G., Hou X., Liu B., Chen H., Luo R. *RSC Advances,* **6**, 2016, 91431-91439
147. Mendes A. A., Giordano R. C., Giordano R. de L. C., de Castroc H. F., *Journal of Molecular Catalysis B: Enzymatic*, **68**, 2011, 109-115
148. Mohamad N. R., Marzuki N. H. C., Buang N. A., Huyop F., Wahab R. A., *Biotechnology & Biotechnological Equipment*, **29(2)**, 2015, 205-220
149. Hernandez K., Fernandez-Lafuente R., *Enzyme and Microbial Technology*, **48**, 2011, 107-122
150. Torres-Salas P., Monte-Martinez A., Cutiño-Avila B., Rodriguez-Colinas B., Alcalde M., Ballesteros A. O., Plou F. J., *Advanced Materials*, **23**, 2011, 5275-5282
151. Ferrario V., Ebert C., Knapic L., Fattor D., Basso A., Spizzo P., Gardossi L., *Advanced Synthesis & Catalysis,* **353**, 2011, 2466-2480
152. Bílková Z., Slováková M., Horák D., Lenfeld J., Churáček J., *Journal of Chromatography B: Biomedical Sciences and Applications,* **770**, 2002, 177-181
153. Liu Y., Yu J., *Microchimica Acta*, **183**, 2016, 1-19
154. Cecchini D. A., Serra I., Ubiali D., Terreni M., Albertini A. M., *BMC Biotechnology*, **7**, 2007, 54-64
155. Liu T., Zhao Y., Wang X., Li X., Yan Y., *Bioresource Technology,* **132**, 2013, 99-102
156. Yi S., Dai F., Zhao C., Si Y., *Scientific Reports,* **7**, 2017, Article ID 9806, DOI:10.1038/s41598-017-10453-4
157. Roy J. J., Abraham T. E., Abhijith K. S., Kumar P. V. S., Thakur M. S., *Biosensors & Bioelectronics*, **21**, 2005, 206-211
158. Marcuello C., de Miguel R., Go´mez-Moreno C., Martı´nez-Ju´lvez M., Lostao A., *Protein Engineering, Design & Selection,* **25(11)**, 2012, 715–723
159. Carlsson N., Gustafsson H., Thörn C., Olsson L., Holmberg K., Åkerman B., *Advances in Colloid and Interface Science*, **205**, 2014, 339–360
160. Bílková Z., Stefanescu R., Cecal R., Korecká L., Ouzká Š., Ježová J., Viovy J.-L., Przybylski M., *European Journal of Mass Spectrometry*, **11(5)**, 2005, 489-495
161. Korecká L., Jankovičová B., Křenková J., Hernychová L., Slovaková M., Le-Nell A., Chmelík J., Foret F., Viovy J.-L., Bílková Z., *Journal of Separation Science,* **31**, 2008, 507-515
162. Ma W., Tang Ch., Lai L., *Biophysical Journal*, **89(2)**, 2005, 1183–1193
163. Rawlings N. D., Salvesen G., *Handbook pf Proteolytic Enzymes,* 2013 (Elsevier, ISBN 978-0-12-382219-2)
164. https://www.brenda-enzymes.org/ [2020-02-29]

165. Pigman W., Rizvi S., Holley H. L. *Arthritis Rheumatology*, **4**, 1961, 240-252
166. Slováková M., Sedlák M., Křížková B., Kupčík R., Bulánek R., Korecká L., Drašar Č., Bílková Z., *Process Biochemistry*, **50(12)**, 2015, 2088-2098
167. http://www.enzyme-database.org/news.php [2020-02-29]
168. Dongol Y., Dhananjaya B. L., Kumar Shrestha R., Aryal G., *Pharmacological and Immunological Properties of Wasp Venom*, 2013, DOI: 10.5772/57227
169. Mills K., Johnson A., Winchester B., *FEBS Letters*, **515**, 2002, 171-176
170. Gantner M., Schwarzmann G., Sandhoff K., Kolter T., *Journal of Lipid Research*, **55(12)**, 2014, 2692–2704
171. https://www.antibodies/online.com [2019-01-29]
172. Valík D., Nekulová M., Zdražilová Dubská L., Springer D., Malbohan I., Zima T., Topolčan O., Fuchsová R., Svobodová Š., *Klin. Biochem. Metab.,* **22(43)**, 2014, 22-39
173. Li X. M., Yang X. Y., Zhang S. S., *Trends in Analytical Chemistry*, **27**, 2008, 543-553
174. Pemberton R. M., Hart J. P., Stoddard P., Foulkes J. A., *Biosensors & Bioelectronics,* **14**, 1999, 495-503
175. Wilson M. S., Rauh R. D., *Biosensors & Bioelectronics,* **20**, 2004, 276-283
176. Yang M., Li H., Javadi A., Gong S., *Biomaterials,* **31(12)**, 2010, 3281-3286
177. Malhotra R., Patel Y., Vaqué J. P., Gutkind J. S., Rusling J. F., *Analytical Chemistry*, **82**, 2010, 3118-3123
178. Jeong B., Akter R., Han O. H., Rhee C. K., Rahman M. A., *Analytical Chemistry,* **85(3)**, 2013, 1784-1791
179. Sýs M., Metelka R., Korecká L., Pokorná H., Švancara I., *Monatshefte für Chemie – Chemical Monthly*, **148**, 2017, 505-510

Seznam příloh

P1. Horák D., Kučerová J., **Korecká L.**, Jankovičová B., Palarčík J., Mikulášek P., Bílková Z. New monodisperse magnetic polymer microspheres biofunctionalized for enzyme catalysis and bioaffinity separations. *Macromolecular Bioscience,* **12(5)**, 2012, 647-655

P2. Holubova L., **Korecka L.***, Podzimek S., Moravcova V., Rotkova J., Ehlova T., Velebny V., Bilkova Z. Enhanced multiparametric hyaluronan degradation for production of molar-mass-defined fragments. *Carbohydrate polymers,* **112**, 2014, 271-276

P3. Kašparová J., **Korecká L.***, Pepeliaev S., Bílková Z., Smirnou D., Velebný V., Česlová L. Magnetic macroporous bead cellulose functionalised with recombinant hyaluronan lyase for controllable hyaluronan fragmentation. *Process Biochemistry,* **72**, 2018, 105-111

P4. Kuchař L., Rotková J., Asaw B., Lenfeld J., Horák D., **Korecká L.**, Bílková Z., Ledvinová J. Semisynthesis of C17:0 isoforms of sulphatide and glucosylceramide using immobilised sphingolipid ceramide N-deacylase for application in Analytical mass spectrometry. *Rapid Communications in Mass Spectrometry,* **24**, 2010, 2393-2399

P5. Rotková J., Šuláková R., Korecká L., Zdražilová P., Jandová M., Lenfeld J., Horák D., Bílková Z.: Laccase immobilized on magnetic carriers for biotechnology applications. *Journal of Magnetism and Magnetic Materials*, **321**, 2009, 1335-1340

P6. Čadková M., Metelka R., Holubová L., Horák D., Dvořáková V., Bílková Z., **Korecká L.*** Magnetic beads-based electrochemical immunosensor for monitoring allergenic food proteins. *Analytical Biochemistry*, **484**, 2015, 4-8

P7. Šálek P., **Korecká L.**, Horák D., Petrovský E., Kovářová J., Metelka R., Čadková M., Bílková Z. Immunomagnetic sulfonated hypercrosslinked polystyrene microspheres for electrochemical detection of proteins. *Journal of Materials Chemistry*, **21**, 2011, 14783-14792

P8. Čadková M., Dvořáková V., Metelka R., Bílková Z., **Korecká L.*** Alkaline phosphatase labeled antibody-based electrochemical biosensor for sensitive HE4 tumor marker detection. *Electrochemistry Communications*, **59**, 2015, 1-4

P9. Čadková M., Dvořáková V., Metelka R., Bílková Z., **Korecká L.*** Verification of antibody labelling efficiency as an important step in ELISA/QLISA development. *Monatshefte für Chemie – Chemical Monthly,* **147**, 2016, 69-73

P10. Cadková M., Kovarova A., Dvorakova V., Metelka R., Bilkova Z., **Korecka L.*** Electrochemical quantum dots-based magneto-immunoassay for detection of HE4 protein on metal film-modified screen-printed carbon electrodes. *Talanta,* **182**, 2018, 111-115

P11. Dvorakova V., Cadkova M., Datinska V., Kleparnik K., Foret F., Bilkova Z., **Korecka L.*** An advanced conjugation strategy for the preparation of quantum dot-antibody immunoprobes. *Analytical Methods*, **9,** 2017, 1991-1997

Příloha P1

Horák D., Kučerová J., **Korecká L.**, Jankovičová B., Palarčík J., Mikulášek P., Bílková Z. New monodisperse magnetic polymer microspheres biofunctionalized for enzyme catalysis and bioaffinity separations. *Macromolecular Bioscience,* **12(5)**, 2012, 647-655

IF_{2018} = 2,895; Q2 – Chemical sciences, Biological sciences; 28 citací [1. 7. 2020]

- podíl na experimentální práci a vyhodnocení výsledků 30 %
- dílčí příprava a revize článku

New Monodisperse Magnetic Polymer Microspheres Biofunctionalized for Enzyme Catalysis and Bioaffinity Separations

Daniel Horák,* Jana Kučerová, Lucie Korecká, Barbora Jankovičová, Jiří Palarčík, Petr Mikulášek, Zuzana Bílková

Magnetic macroporous PGMA and PHEMA microspheres containing carboxyl groups are synthesized by multi-step swelling and polymerization followed by precipitation of iron oxide inside the pores. The microspheres are characterized by SEM, IR spectroscopy, AAS, and zeta-potential measurements. Their functional groups enable bioactive ligands of various sizes and chemical structures to couple covalently. The applicability of these monodisperse magnetic microspheres in biospecific catalysis and bioaffinity separation is confirmed by coupling with the enzyme trypsin and huIgG. Trypsin-modified magnetic PGMA-COOH and PHEMA-COOH microspheres are investigated in terms of their enzyme activity, operational and storage stability. The presence of IgG molecules on microspheres is confirmed.

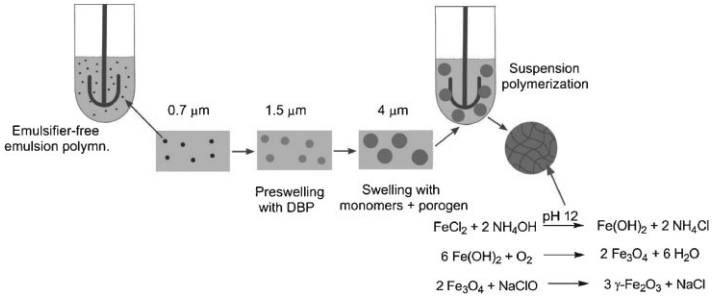

1. Introduction

Interest in superparamagnetic microspheres has been rapidly increasing recently due to their potential in biotechnology and biomedicine. After biofunctionalization, they find practical uses in immunoprecipitations, gentle but highly efficient isolation and purification of biomolecules[1] (proteins, enzymes, antibodies, and nucleic acids), biospecific catalysis,[2] immunomagnetic cell separation,[3] diagnosis and prognosis of malignant diseases,[4] etc. Their main advantages are easy manipulation, high capacity and simple separation from complex heterogeneous biological mixtures including blood, urine, foodstuffs, or tissues. Conventional mechanical methods, such as filtration or centrifugation or multi-step column separation techniques, including size-exclusion chromatography, fractional precipitation, or ion exchange chromatography, can thus be avoided. Moreover, magnetic microsphere-based bioaffinity separation methods enable the effective isolation of viable cells and labile molecules due to the lower mechanical stress than the aforementioned methods.[5]

Several methods are commonly used for the preparation of magnetic polymer microspheres. Encapsulation of magnetic cores with a polymer results in polydisperse particles with irregular shapes,[6] while miniemulsion polymerization in the presence of iron oxide[7] produces

D. Horák
Institute of Macromolecular Chemistry, Academy of Sciences of the Czech Republic, Prague, Czech Republic
E-mail: horak@imc.cas.cz
J. Kučerová, L. Korecká, B. Jankovičová, Z. Bílková
Department of Biological and Biochemical Sciences, Faculty of Chemical Technology, University of Pardubice, Pardubice, Czech Republic
J. Palarčík, P. Mikulášek
Institute of Environmental and Chemical Engineering, Faculty of Chemical Technology, University of Pardubice, Pardubice, Czech Republic

DOI: 10.1002/mabi.201100393

particles <500 nm, emulsion polymerization[8,9] particles <1 μm, dispersion polymerization[10] around 1 μm, and suspension polymerization provides polydisperse particles measuring hundreds of micrometers.[11] An advantage of the multi-step swelling and polymerization technique pioneered by Ugelstad et al.[12] and elaborated by others[13,14] is that it produces strictly monodisperse magnetic particles larger than 1 μm, which are difficult to produce by other techniques. This technique was therefore for the first time adapted in this report on earlier elaborated by us suspension polymerization of glycidyl methacrylate (GMA) and 2-hydroxyethyl methacrylate (HEMA). Another novelty consists in utilization of a new porogen (cyclohexyl acetate) and new stabilizers [2-hydroxyethylcellulose and (hydroxypropyl)methylcellulose] for preparation of macroporous poly(GMA) or poly(HEMA) (PGMA and PHEMA, respectively) microspheres and also in formation of magnetic iron oxide in the pores by oxidation of $Fe(OH)_2$ obtained by precipitation of neat $FeCl_2$ with ammonia.

Despite the wide availability of commercial magnetic carriers, they do not often fulfill all the criteria needed for unique bioanalytical research. The main requirements laid on magnetic microspheres include superparamagnetic behavior, proper size, monodispersity, applicability, and stability in various media (aqueous, organic, and mixed) for a given usage.[15–17] The appropriate type of functional groups on the surface enables the covalent attachment of various biomolecules. The density of functional groups is then one of the key parameters of the microspheres. Even though the number of various applications of magnetic microspheres is continually growing, there are still many areas where the use of newly developed magnetic microspheres with suitable features could be beneficial, e.g., micrototal analysis systems.[18,19] Microspheres need to meet particularly specific requirements in such developing fields as microfluidics. Combining microfluidic devices with magnetic microspheres is creating new possibilities in innovative bioapplications.[19,20] This is the reason why attention has been paid to the development of new types of microspheres.

In order to be able to routinely utilize magnetic microspheres, it is vital to deeply characterize them, verify their stability in various media during the activation process as well as during regular usage and confirm the ability to covalently attach suitable bioactive ligands and subsequently isolate the analyte of interest from the complex mixture in the required purity. Due to the increased stability of immobilized ligands, covalent bonds are preferred for a wide range of applications. Hence, bioactive ligands exemplified by the proteolytic enzyme trypsin and human immunoglobulin G (huIgG) were immobilized on magnetic PGMA and PHEMA microspheres containing carboxyl groups (further denoted as PGMA-COOH and PHEMA-COOH microspheres). Trypsin was selected for the simple quantification of its proteolytic activity. Human IgG served to simulate a biologically active high-molecular-weight biocompound that was immobilized on the magnetic microspheres to form an immunosorbent. The amount of IgG immobilized on the microspheres was quantified by standard bioanalytical methods.

2. Experimental Section

2.1. Materials

Monomers such as styrene (Kaučuk Kralupy, Czech Republic), HEMA (Röhm, Darmstadt, Germany), GMA (Fluka, Buchs, Switzerland), and ethylene dimethacrylate (EDMA; Ugilor S. A., France) were vacuum distilled. 2-[(Methoxycarbonyl)methoxy]ethyl

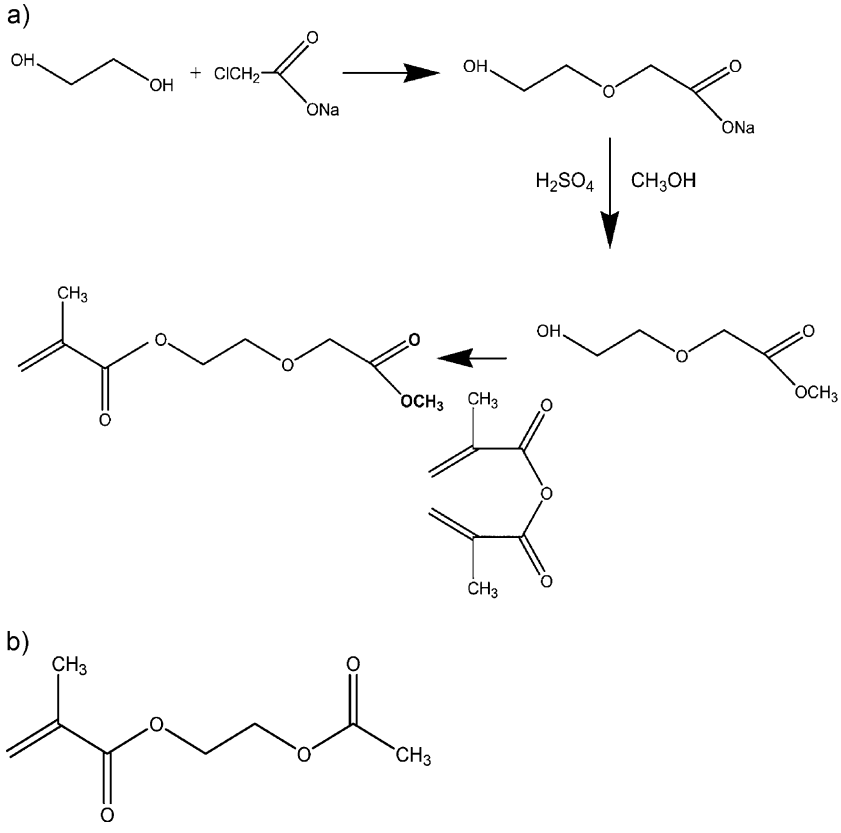

Scheme 1. Synthesis of (a) MCMEMA and (b) HEMA-Ac.

methacrylate (MCMEMA) was prepared from ethylene glycol (300 mL) and chloroacetic acid (94.5 g) in the presence of NaOH (80 g), producing sodium hydroxyethoxyacetate, which was then transformed (in the presence of H_2SO_4 and methanol) to the methyl ester of hydroxyethoxyacetic acid and finally to MCMEMA using methacrylic anhydride (Scheme 1a). 2-(Methacryloyl)oxyethyl acetate (HEMA-Ac; Scheme 1b) was obtained from HEMA and acetic anhydride. Cyclohexyl acetate was obtained from cyclohexanol and acetic anhydride. Trypsin from bovine pancreas (EC 3.4.22.2), bovine serum albumin (BSA), IgG from human serum, benzamidine, 1-ethyl-3-(3-dimethylaminopropyl)carbodiimide (EDC), *N*-α-benzoyl-D,L-arginine-4-nitroanilide (BApNA), and 2-(*N*-morpholino)ethanesulfonic acid (MES) were obtained from Sigma-Aldrich (St. Louis, MO, USA). The Pierce® BCA Protein Assay Kit was produced by ThermoScientific (Rockford, IL, USA). The sodium salt of *N*-hydroxysulfosuccinimide (sulfo-NHS), $FeCl_2 \cdot 4H_2O$, 2-hydroxyethyl cellulose, sodium dodecylsulfate (SDS), benzoyl peroxide (BPO), and Methocel 90 HG [(hydroxypropyl)methyl cellulose] were obtained from Fluka, sodium persulfate was from Lachema (Brno, Czech Republic). Sodium azide was produced by Chemapol (London, United Kingdom). The remaining chemicals were supplied by Sigma-Aldrich, Lachema, or Penta Chemicals (Chrudim, Czech Republic) and were of analytical reagent grade. Ultrapure Q-water ultrafiltered with a Milli-Q Gradient A10 system (Millipore, Molsheim, France) was used for preparing solutions.

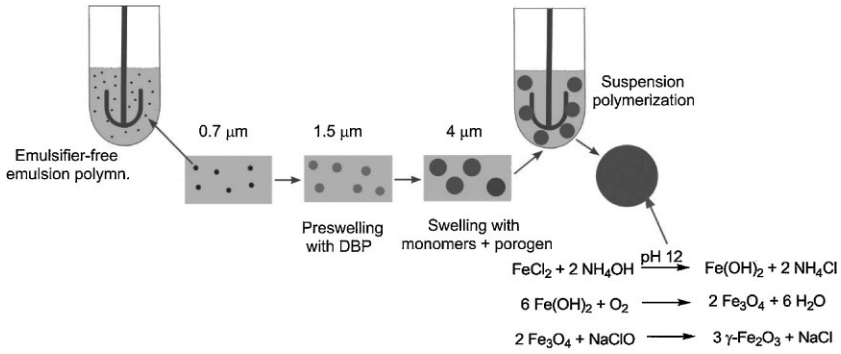

Scheme 2. Preparation of monodisperse magnetic macroporous polymer microspheres by multi-step swelling and polymerization method and precipitation of iron oxide inside their pores.

2.2. Synthesis of Monodisperse Polystyrene (PS) Seeds

PS seeds were obtained by the emulsifier-free emulsion polymerization of styrene in a 150-mL reaction vessel equipped with an anchor-type stirrer. In brief, sodium persulfate (44 mg) and sodium carbonate (39 mg) were dissolved in water (90 mL) to form the aqueous phase. The monomer phase (10 g styrene) was added, the mixture stirred (300 rpm), and the temperature increased to 80 °C. Polymerization proceeded for 20 h under a nitrogen atmosphere. The resulting latex was separated by centrifugation (4000 rpm) and thoroughly washed with a 0.25% aqueous solution of SDS.

2.3. Synthesis of Monodisperse Macroporous PGMA-COOH and PHEMA-COOH Microspheres

Macroporous PGMA-COOH and PHEMA-COOH microspheres were synthesized by the modified multi-step swelling and polymerization method originally developed by Ugelstad et al.[12] (Scheme 2). First, PS latex (0.3 g) was dispersed in 0.25% SDS solution (1 mL) and the mixture sonicated (4710 Series Ultrasonic homogenizer; Cole-Parmer, Chicago, IL, USA) at 15 °C for 3 min. Second, the latex was mixed with an emulsion of dibutyl phthalate (DBP; 0.4 g) in 0.25% SDS (1.2 mL) and 2% $NaHCO_3$ solutions (0.05 mL) under sonication at 15 °C for 4 min. PS latex was swollen with DBP for 4 d with mild stirring (30 rpm); swelling was repeated once more with the same amount of DBP and then four times with double the amount of DBP. The resulting PS latex contained 4.3 g DBP in 17.5 mL of dispersion.

Third, DBP-swollen PS particles were swollen with the monomers, porogen, and initiator in a 30-mL reaction vessel. Briefly, a DBP-swollen PS dispersion (2 mL) was swelled with an emulsion of a solution of BPO (30 mg), GMA (1.5 g), MCMEMA (0.3 g), and EDMA (1.2 g) in 0.1% SDS solution (7.5 mL) for 16 h with gentle stirring (30 rpm). A mixture of cyclohexyl acetate (4 g) in 0.1% SDS solution (10 mL) was then treated with ultrasound at 22 °C for 3 min to form an emulsion and transferred to the above monomer-swollen PS dispersion; swelling proceeded for 3 h under stirring (300 rpm). Alternatively, HEMA-Ac replaced GMA in the swelling solution when PHEMA-COOH microspheres were being prepared.

In the fourth step, a 2 wt% solution of 2-hydroxyethyl cellulose (2 mL), 2 wt% solution of Methocel 90 HG (2 mL), and a solution of citric acid (30 mg) in water (0.5 mL) were mixed with the above monomer-swollen PS latex and the polymerization proceeded at 70 °C for 16 h at stirring rate of 600 rpm under a carbon dioxide atmosphere. The resulting microspheres were removed by filtering, washed with 0.05 wt% Tween 20 solution, ethanol, toluene, and ethanol (five times each), and finally transferred to water. In order to change the methyl ester of MCMEMA to a carboxyl group, the PGMA microspheres were separated by centrifugation and hydrolyzed in 0.2 M H_2SO_4 (50 mL) at 22 °C for 60 h. The microspheres were then washed five times with water with ultrasonic treatment. In order to yield PHEMA microspheres, the acetate of poly[2-(methacryloyl)oxyethyl acetate] was hydrolyzed in 0.5 M NaOH solution (30 mL) in the presence of Tween 20 at 60 °C for 16 h with stirring (300 rpm); the microspheres were purified by washing four times with water and twice with 1,4-dioxane.

2.4. Precipitation of Iron Oxide Inside the Macroporous Microspheres

Macroporous PGMA-COOH or PHEMA-COOH microspheres (1 g) were dispersed in a solution of $FeCl_2 \cdot 4H_2O$ (2 g) in water (10 mL) for 2 min with ultrasonic treatment, removed by filtering, washed again with $FeCl_2$ solution, and left to dry at 40 °C for 30 min. They were then transferred to a 0.5 M NH_4OH solution (20 mL), the mixture stirred (100 rpm) in air at 22 °C for 3 h, the particles separated using a magnet, washed several times with water (100 mL), and mixed with 5 wt% sodium hypochlorite solution

(2 mL) with stirring (100 rpm) for 10 min. Finally, the microspheres were washed with water, ethanol, and water. Before trypsin immobilization, the microspheres were stored in distilled water with 0.1% NaN_3.

2.5. Characterization of Magnetic Microspheres

The microsphere morphology, size, and size distribution were analyzed by scanning electron microscopy (SEM; JEOL JSM 6400, Tokyo, Japan). The number-average diameter (D_n), weight-average diameter (D_w), and uniformity (polydispersity index PDI $= D_w/D_n$) were calculated using Atlas software (Tescan Digital Microscopy Imaging, Brno, Czech Republic) by counting at least 500 individual particles from SEM microphotographs. The D_n and D_w can be expressed as follows:

$$D_n = \frac{\sum n_i D_i}{\sum n_i}$$

$$D_w = \frac{\sum n_i D_i^4}{\sum n_i D_i^3}$$

The microspheres were examined with a Paragon 1000 PC FTIR spectrometer (Perkin-Elmer) with a Specac MKII Golden Gate Single Reflection ATR System with a diamond crystal and a ray angle of incidence of 45°. The iron content was analyzed by atomic absorption spectrometry (AAS Perkin-Elmer 3110) of an extract from a sample obtained by treatment with 70% perchloric and 65% nitric acid at 100 °C for 30 min. A 799 GPT Titrino titrator (Metrohm) was used to evaluate the carboxyl group content of the microspheres by titrating with 0.1 M NaOH.

The electrostatic stability of the microspheres (46 $\mu g \cdot mL^{-1}$ of 0.01–0.1 M phosphate buffer; pH = 7.3) was investigated by zeta-potential measurements using a ZetaPALS apparatus (Brookhaven Instruments; New York, USA).

2.6. Immobilization of Trypsin on Magnetic PGMA-COOH and PHEMA-COOH Microspheres

Three immobilization approaches were investigated for the covalent attachment of trypsin to magnetic microspheres: a one-step procedure using the zero-length crosslinker EDC and sulfo-NHS and a one- or two-step procedure with neat EDC as a coupling agent.

In a typical one-step immobilization using EDC and sulfo-NHS, magnetic PGMA-COOH or PHEMA-COOH microspheres (1 mg) were washed four times with 0.1 M phosphate buffer (pH = 7.3), magnetically separated and mixed with the following agents: EDC (7.5 mg/0.2 mL), sulfo-NHS (1.25 mg/0.2 mL), and trypsin (4 mg/0.5 mL; 0.03 wt% benzamidine). This one-step method can also be carried out without the addition of sulfo-NHS. In a two-step procedure, microspheres were first incubated in buffer with EDC (7.5 $mg \cdot mL^{-1}$) for 10 min, the supernatant with the excess of EDC was removed and trypsin solution (4 mg/0.5 mL) with benzamidine (0.03 wt%) was added to activated microspheres. For all the above-mentioned procedures the reaction proceeded in 0.1 M phosphate buffer (1 mL of total volume; pH = 7.3) at 23 °C for 3 h with gentle stirring. The trypsin-immobilized magnetic microspheres (further denoted as Tryp-PGMA-COOH or Tryp-PHEMA-COOH) were washed ten times with 0.1 M phosphate buffer (pH = 7.3) and stored at 4–8 °C in 0.1 M phosphate buffer (pH = 7.3) containing 0.05% NaN_3 solution.

Trypsin activity was determined using low-molecular-weight chromogenic substrate BApNA according to method modified from the literature.[2] Soluble or immobilized trypsin (0.1 mL) was incubated in 0.1 M NH_4HCO_3 (0.88 mL) and 0.55 M BApNA in *N,N*-dimethylformamide (0.02 mL) at room temperature for 30 min under mild stirring. The reaction was stopped by the addition of acetic acid (30 wt%, 0.2 mL) and the absorbance was measured at 405 nm.

2.7. Immobilization of huIgG on Magnetic PGMA-COOH and PHEMA-COOH Microspheres

Magnetic PGMA-COOH and PHEMA-COOH microspheres (1 mg) were washed five times with 0.1 M MES buffer (pH = 5.0) and incubated with EDC (7.5 $mg \cdot mL^{-1}$ of 0.1 M MES) for 10 min, the excess of unreacted EDC was removed from the activated microspheres by washing with 0.1 M MES buffer (2 × 1 mL) and huIgG (0.2 $mg \cdot mL^{-1}$ of 0.1 M MES) was then added. The immobilization mixture was incubated at 4–8 °C for 16 h. Subsequent washing was identical to that described above. The amount of immobilized huIgG was assessed by absorbance measurement at 260/280 nm (Eppendorf BioPhotometer; Hamburg, Germany) and by BCA test (Pierce® BCA Protein Assay Kit).

3. Results and Discussion

3.1. Synthesis and Characterization of Magnetic Macroporous Microspheres

In this report, carboxyl-terminated microspheres were preferred due to the availability of a range of standardized and optimized protocols for bioconjugating various ligands. Carboxyl groups were introduced in the microspheres by copolymerizing a relatively small amount (10 wt%) of MCMEMA (Scheme 1a) in the feed, which was subsequently hydrolyzed. The microspheres were based both on PGMA and PHEMA. PGMA has the advantage of reactive oxirane groups which can be potentially modified into any functional groups required. In addition to PGMA-COOH microspheres, PHEMA-COOH particles were fabricated as a standard, because PHEMA is commonly used in a range of bioapplications[21] due to its biocompatibility, inertness, and low-protein adsorption.[22] Generally, PGMA microspheres of narrow size distribution can be synthesized by a single-step swelling of PS template (obtained by the dispersion polymerization) with GMA followed by the polymerization.[23]

In this report, however, magnetic PGMA-COOH and PHEMA-COOH microspheres were prepared by a rather complicated multi-step swelling and polymerization method (Scheme 2). In contrast to the single-step method, cyclohexyl acetate could be used as a porogen that dissolved PS seeds. Removal of PS seeds during washing after

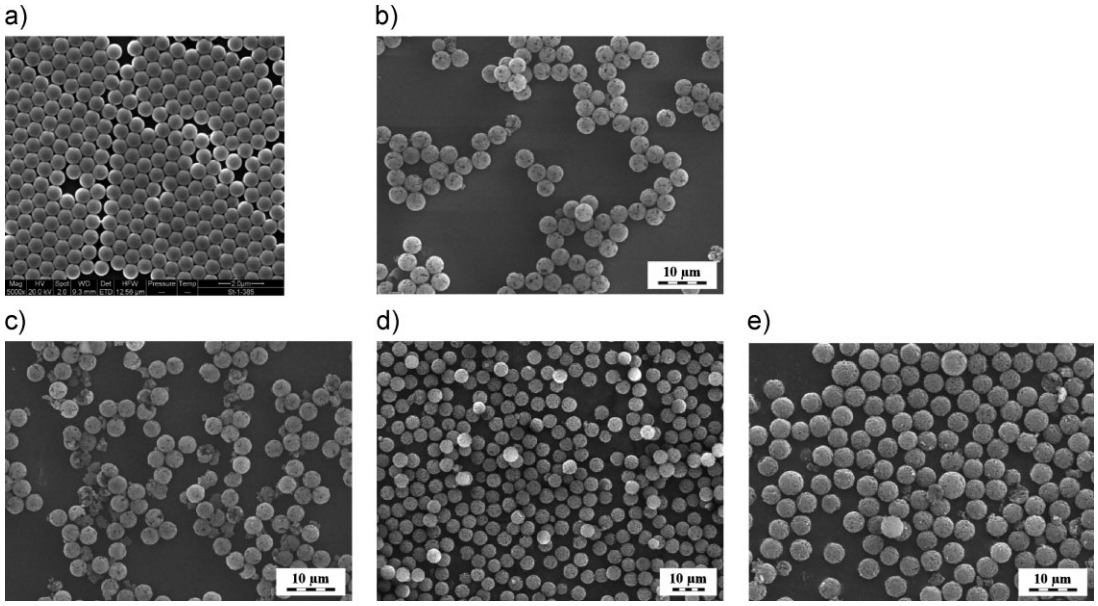

Figure 1. SEM micrographs of (a) PS seeds, (b,c) PGMA-COOH, and (d,e) PHEMA-COOH non-magnetic (b and d) and magnetic (c and e) microspheres.

completion of the polymerization thus did not induce formation of dents so typical for single-step swelling and polymerization method. Moreover, multi-step procedure produced monomer-swollen particles containing much less PS due to much higher swelling of the precursor seed than single-step swelling and polymerization could provide. The multi-step swelling and polymerization method thus produces a highly monodisperse and better quality product than other techniques. First, seeds 0.7 μm in size were prepared by emulsifier-free emulsion polymerization (Figure 1a). Second, the seeds were activated (pre-swelled) with a highly water-insoluble compound (DBP) to enable subsequent swelling with the monomers, initiator, and porogen. In the third step, DBP-swollen PS seeds 1.5 μm in diameter were swelled with the mixture of monomers, initiator, and porogen. This was followed in the fourth step by 2-hydroxyethyl cellulose- and (hydroxypropyl)methyl cellulose-stabilized and BPO-initiated suspension polymerization. In order to introduce carboxyl groups in PGMA and PHEMA microspheres, a MCMEMA comonomer (Scheme 1a) was incorporated in the polymerization feed. After its hydrolysis, [2-(methacryloyloxy)ethoxy]acetic acid (MOEAA) was obtained and 0.19 mmol of carboxyl groups was determined per g of dry PHEMA-COOH microspheres by titration with NaOH solution (Figure 2). This was less than the amount of MCMEMA in the feed (0.5 mmol), which is most likely due to the inaccessibility of some carboxyl groups buried inside the highly crosslinked polymer bulk. Nevertheless, the amount of carboxyl groups available for future modifications was sufficient according to our results. In the synthesis of PHEMA microspheres, HEMA-Ac was a monomer (Scheme 1b), which was hydrolyzed to PHEMA after the polymerization reached completion. An advantage of the HEMA-Ac monomer, compared to HEMA, is its insolubility in water, thus facilitating particle swelling and suspension polymerization in an aqueous phase. Figure 1b and d represents scanning electron micrographs (SEM) of both PGMA-COOH and PHEMA-COOH microspheres prepared by the multi-step swelling and polymerization method. The morphology of the PGMA-COOH and PHEMA-COOH particles was spherical; the particles were monodisperse (PDI = 1.04) and had diameters of 3.9 and

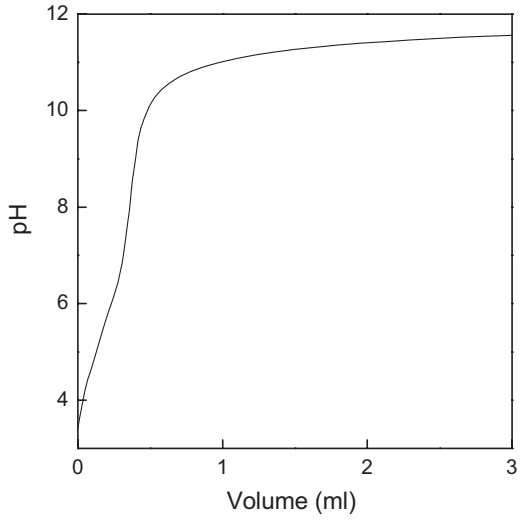

Figure 2. Titration of PHEMA-COOH microspheres (0.2 g) with 0.1 M NaOH.

4.4 μm, respectively. Their surface was rough, containing macropores formed by phase separation during the polymerization in the presence of the porogen (cyclohexyl acetate). Due to the presence of the crosslinking agent (EDMA), the specific surface area of PGMA-COOH and PHEMA-COOH particles amounted to 88.3 and 89.4 $m^2 \cdot g^{-1}$, respectively, according to the dynamic desorption of nitrogen. PGMA microspheres contained oxirane groups, which made additional functionalization possible, resulting in a range of various reactive groups.[24] In this study, oxirane groups were transformed into hydroxyl groups by hydrolysis, thus increasing the hydrophilicity of the product, which is important in reducing non-specific protein adsorption. This was confirmed by attenuation total Fourier-transform reflectance infrared (ATR-FTIR) spectra of initial PGMA-COOH microspheres with the typical transmission peak of oxirane groups at 910 cm^{-1}, which disappeared after the hydrolysis (Figure 3). Moreover, the transmission peak in the region of O–H stretching vibration (≈3400 cm^{-1}) was higher after hydrolysis, signifying that the number of hydroxyl groups had increased.

Both PGMA and PHEMA hydrogels are known to absorb large amounts of water but remain both insoluble and biologically, chemically, and mechanically stable, preserving their shape.[25] The equilibrium water uptake of PGMA-COOH and PHEMA-COOH microspheres was 2.7 and 2.8 $mL \cdot g^{-1}$, respectively, thus reflecting the hydrophilicity of the particles.

To produce magnetic carriers, maghemite (γ-Fe_2O_3) was prepared inside the pores of the macroporous microspheres by a two-step oxidation of $Fe(OH)_2$ with oxygen and sodium hypochlorite (Scheme 2). First, magnetite (Fe_3O_4) was formed by the precipitation of a ferrous salt with ammonium hydroxide and oxidation with oxygen. Second, magnetite was then oxidized with sodium hypochlorite, yielding chemically more stable γ-Fe_2O_3 (maghemite).[26] Neither the morphology nor size of the PGMA-COOH or PHEMA-COOH microspheres substantially changed after the precipitation of iron oxide inside the microsphere pores (Figure 1c and e). Magnetic PGMA-COOH and PHEMA-COOH microspheres contained 13.2 and 19.4 wt% Fe, respectively, according to atomic absorption spectrometry (AAS). This amount of Fe in the microspheres is sufficient to respond quickly to a magnetic field as was confirmed by earlier measurements of magnetic properties of analogous PGMA microspheres (prepared by the dispersion polymerization) with a magnetometer.[27] The advantage of maghemite over magnetite is its oxidation stability. Due to its low solubility in water and ability to form coordination complexes with carboxyl groups, it was not released from the microspheres in aqueous media.

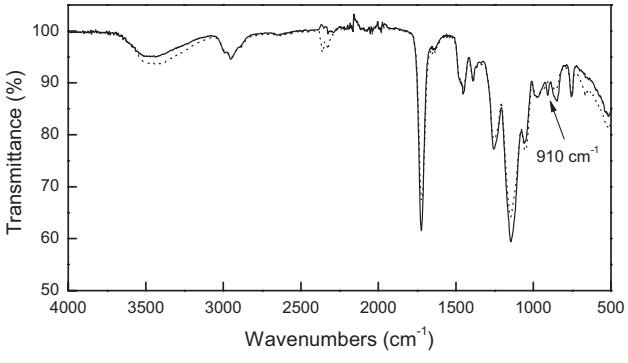

Figure 3. ATR-FTIR spectra of PGMA-COOH microspheres (—) before and (···) after hydrolysis with H_2SO_4.

3.2. Biofunctionalization of Magnetic PGMA-COOH and PHEMA-COOH Microspheres

Trypsin was immobilized on magnetic PGMA-COOH and PHEMA-COOH microspheres via EDC/sulfo-NHS chemistry. The amount of immobilized trypsin was subsequently measured by colorimetric assay with a chromogenic substrate. This approach enables the amount of actually active enzyme molecules to be quantified. Benzamidine is a low-molecular-weight competitive inhibitor of trypsin, which prevents the self-cleavage of trypsin during the immobilization process. Its presence in the immobilization mixture enhances the binding efficiency of trypsin. After the binding procedure, benzamidine is removed by simple washing.

For PGMA-COOH microspheres, the highest activity of immobilized trypsin was achieved with a one-step immobilization using EDC/sulfo-NHS at 23 °C for 3 h (Figure 4). The same trend was observed for magnetic PHEMA-COOH microspheres.

Figure 5 shows the effect of increasing amounts of trypsin in the binding mixture on the amount of enzyme

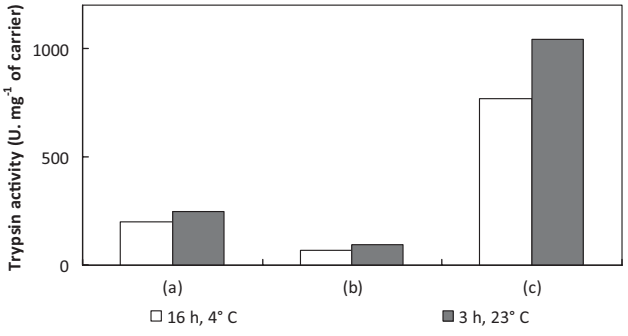

Figure 4. Proteolytic activity of magnetic Tryp-PGMA-COOH microspheres under various reaction conditions (time, temperature, and presence of EDC and sulfo-NHS). (a) One-, (b) two-step protocol with EDC, and (c) one-step immobilization with EDC and sulfo-NHS.

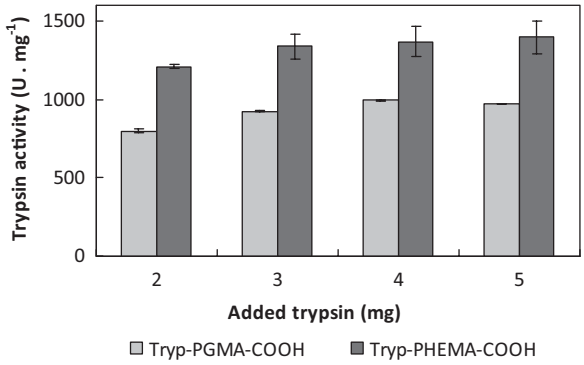

Figure 5. Determination of proper amount of trypsin in binding mixture per mg of magnetic microspheres.

which was immobilized onto the microspheres and simultaneously active. In both types of magnetic carriers, a slight increase in activity was observed as a consequence of increasing the trypsin content in the binding mixture. The optimal amount was found to be 4 mg of trypsin per mg of both magnetic microspheres. Immobilizing higher amounts of enzyme (>5 mg) was not beneficial; the immobilization efficiency slightly decreased (Figure 5).

The average enzyme activity of magnetic Tryp-PGMA-COOH and Tryp-PHEMA-COOH microspheres determined from three repetitions was 1021 ± 44 and $1418 \pm 32\ U \cdot mg^{-1}$ of microspheres, respectively.

To verify that the enzyme molecules were specifically adsorbed, they were washed with 1 M NaCl solution. Enzyme activity then slightly decreased to 99.8 and 99.3% for magnetic Tryp-PGMA-COOH and Tryp-PHEMA-COOH microspheres, respectively. The above-mentioned reduction of trypsin activity is statistically insignificant; hence, the results indicate that more than 99% of the trypsin was coupled to the microspheres through covalent bonds.

Based on good experience with the simultaneous co-immobilization of proteins and other ligands to microspheres, and keeping in mind the aim of covering these hydrophobic clusters, which are responsible for the non-specific adsorption of biomolecules from complex biological mixtures, the addition of inert protein – BSA – could increase the quality of enzyme-biofunctionalized microspheres.[28] BSA solution (33 wt%) was added to the immobilization mixture 10 min after the start of the immobilization. This was followed by a 16-h incubation and subsequent washing with 0.1 M phosphate buffer (pH = 7.3) containing 1 M NaCl for the elimination of eventual non-specifically bound molecules. Magnetic Tryp-PGMA-COOH microspheres achieved a trypsin activity comparable to the procedure without albumin addition (difference <5%).

The chemical as well as biological stability of these newly developed biofunctionalized magnetic microspheres needs to be confirmed before their routine application. Operational and storage stability were therefore verified. The activity of magnetic Tryp-PGMA-COOH and magnetic Tryp-PHEMA-COOH microspheres was repeatedly determined in nine cycles within 1 d (0.1 mg aliquot, using the same one each time). The activity of magnetic Tryp-PHEMA-COOH microspheres decreased only moderately to 60% in the fifth cycle. The activity of magnetic Tryp-PGMA-COOH microspheres decreased more considerably, reaching 39.6% of the original value in the fifth cycle. These results were not what we expected; previous results showed that >50% of the original activity was retained even after the 10th measurement.[2] One of several reasons for the activity decrease could be the absence of BSA during immobilization or the autoproteolytic behavior of trypsin. This issue still needs to be studied in more detail. Storage stability tests, i.e. determination of enzyme activity over one-week periods (0.1 mg aliquot, a fresh one each time) gave excellent results and confirmed the suitability of the prepared biofunctionalized carriers for long-term storage as well as their applicability. More than 70% of the trypsin molecules immobilized on Tryp-microspheres were active after seven weeks of storage, which fulfilled our expectations (Figure 6).

According to the literature, zeta-potential measurements of free and enzyme-modified carriers correlated with enzyme binding efficiency.[29] Thus, we measured the zeta-potential of trypsin-free and trypsin-modified magnetic microspheres in various buffers at various molar concentrations (0.01, 0.05, and 0.1 M). The absolute values of zeta-potential of the microspheres in phosphate buffer decreased after their biofunctionalization with trypsin (Figure 7). A similar tendency was also observed for measurements of the zeta-potential of magnetic Tryp-PGMA-COOH and Tryp-PHEMA-COOH microspheres in NH_4HCO_3 buffer. The lower molar concentrations of buffer

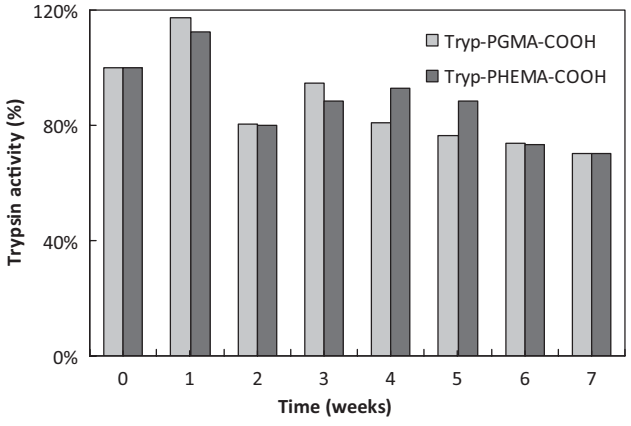

Figure 6. Storage stability of magnetic Tryp-PGMA-COOH and magnetic Tryp-PHEMA-COOH microspheres at 4 °C in 0.1 M phosphate buffer (pH = 7.3) containing 0.03 wt% benzamidine (0.1 mg aliquots).

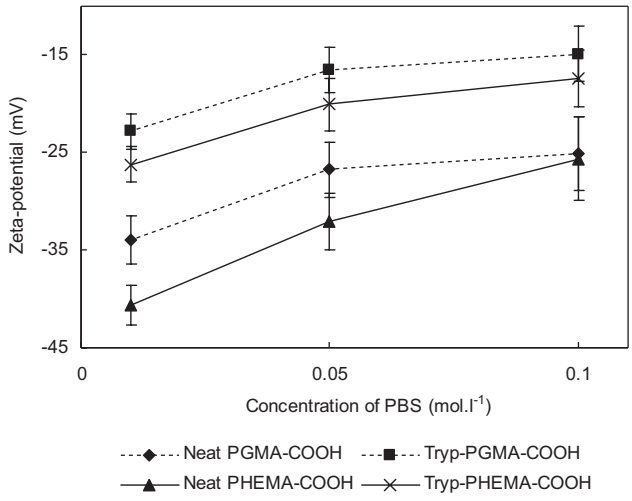

Figure 7. Zeta-potential of magnetic PGMA-COOH and magnetic PHEMA-COOH microspheres before and after biofunctionalization with trypsin in phosphate buffer (pH = 7.3); activity 970 U · mg^{-1} of Tryp-PGMA-COOH and 1417 U · mg^{-1} of Tryp-PHEMA-COOH.

were used, the higher absolute values of zeta-potential of carriers were measured indicating better colloidal stability and lower rate of aggregation due to the repulsion among individual particles. Based on these results, the buffers with a lower molar concentration are preferred for this type of microspheres.

Regarding the potential use of microspheres as carriers of antibodies in the field of immunoprecipitation, human IgG was immobilized on both types of new magnetic microspheres. Based on earlier investigations,[6] an optimized two-step carbodiimide method was chosen for covalently binding huIgG to the microspheres. Two different approaches were used for determining the amount of immobilized huIgG on the microspheres. The total amount of immobilized huIgG was calculated as the difference between the amount of IgG in the binding solution before immobilization and the sum of IgG from all solutions after immobilization, measured by UV spectrophotometry at 260/280 nm. Additionally, the BCA test with IgG-immobilized microspheres was done according to the manufactures' instructions. For both methods, the amount of immobilized IgG was calculated for 1 mg of carrier. Both methods confirmed that the IgG molecules were successfully immobilized onto magnetic PGMA-COOH (76.7 μg of huIgG per mg) and PHEMA-COOH microspheres (124.2 μg of huIgG per mg).

To summarize, both of the newly developed magnetic PGMA-COOH and PHEMA-COOH microspheres presented here can be recommended as suitable carriers for enzyme and also antibodies immobilization.

4. Conclusion

Magnetic monodisperse PGMA-COOH and PHEMA-COOH microspheres were obtained by the multi-step swelling and polymerization method followed by the precipitation of iron oxide inside the pores of the particles. To verify the applicability of the developed magnetic PGMA-COOH and PHEMA-COOH microspheres for immobilizing biocompounds, the proteolytic enzyme trypsin and human IgG were used as model ligands. Trypsin was immobilized on the microsphere surface by the well-known carbodiimide-mediated one-step protocol with heterobifunctional cross-linker EDC and sulfo-NHS agent, and strong bond creation was confirmed. These newly developed biofunctionalized magnetic microspheres demonstrated the possibility of long-term storage without significant changes, which thus indicates great potential for their successful use in bioapplications. Also, IgG-bionfunctionalized microspheres have been shown to be convenient carriers for, e.g., widely used immunoprecipitations.

Acknowledgements: Financial support of the Grant Agency of the Czech Republic (203/09/0857 and P503/10/0664), the Ministry of Education, Youth and Sports (no. MSMT 0021627502), and EU (CaMiNEMS project no. 228980 and NaDiNe project no. 246513) is gratefully acknowledged.

Received: October 6, 2011; Revised: November 29, 2011; Published online: March 13, 2012; DOI: 10.1002/mabi.201100393

Keywords: enzyme catalysis; glycidyl methacrylate; 2-hydroxyethyl methacrylate; magnetic microspheres; trypsin

[1] F. Qu, Y. Guan, Z. Ma, Q. Zhang, *Polym. Int.* **2009**, *58*, 888.
[2] L. Korecká, J. Ježová, Z. Bílková, M. Beneš, D. Horák, O. Hradcová, M. Slováková, J.-L. Viovy, *J. Magn. Magn. Mater.* **2005**, *293*, 349.
[3] S. Cakmak, M. Gumusderelioglu, A. Denizli, *React. Funct. Polym.* **2009**, *69*, 586.
[4] S. Riethdorf, H. Fritsche, V. Muller, T. Rau, C. Schindlbeck, B. Rack, W. Janni, C. Coith, K. Beck, F. Janicke, S. Jackson, T. Gornet, M. Cristofanilli, K. Pantel, *Clin. Cancer Res.* **2006**, *13*, 920.
[5] I. Safarik, M. Safarikova, *BioMag. Res. Technol.* **2004**, *2*, 7.
[6] U. Jeong, X. Teng, Y. Wang, H. Yang, Y. Xia, *Adv. Mater.* **2007**, *19*, 33.
[7] L. P. Ramirez, K. Landfester, *Macromol. Chem. Phys.* **2003**, *204*, 22.
[8] D. Horák, N. Chekina, *J. Appl. Polym. Sci.* **2006**, *102*, 4348.
[9] G. Xie, Q. Zhang, Z. Luo, M. Wu, T. Li, *J. Appl. Polym. Sci.* **2003**, *87*, 1733.
[10] D. Horák, J. Boháček, M. Šubrt, *J. Polym. Sci., Part A: Polym. Chem.* **2000**, *38*, 1161.

[11] D. Horák, E. Pollert, M. Trchová, J. Kovářová, *Eur. Polym. J.* **2009**, *45*, 1009.
[12] J. Ugelstad, T. Ellingsen, A. Berge, B. Helgee, WO 83/03920 (1983).
[13] C. M. Cheng, F. J. Micale, J. W. Vanderhof, M. S. El-Aasser, *J. Polym. Sci., Part A: Polym. Chem.* **1992**, *30*, 235.
[14] V. Smigol, F. Svec, *J. Appl. Polym. Sci.* **1992**, *46*, 1439.
[15] D.-H. Zhang, Y.-F. Zhang, G.-Y. Zhi, Y.-L. Xie, *Colloids Surf. B* **2011**, *82*, 302.
[16] B. Jankovicova, S. Rosnerova, M. Slovakova, Z. Zvěřinova, M. Hubalek, L. Hernychova, P. Rehulka, J.-L. Viovy, Z. Bilkova, *J. Chromatogr. A* **2008**, *1206*, 64.
[17] M. Slováková, J.-M. Peyrin, Z. Bílková, M. Juklíčková, L. Hernychová, J.-L. Viovy, *Bioconjugate Chem.* **2008**, *19*, 966.
[18] A. N. Nel, J. Krenkova, K. Kleparnik, C. Smadja, M. Taverna, J.-L. Viovy, F. Foret, *Electrophoresis* **2008**, *29*, 4944.
[19] M. Slovakova, N. Minc, Z. Bilkova, C. Smadja, W. Faigle, C. Fütterer, M. Taverna, J.-L. Viovy, *Lab Chip* **2005**, *5*, 935.
[20] Z. Bílková, M. Slováková, N. Minc, C. Fütterer, R. Cecal, D. Horák, M. J. Beneš, I. Le Potier, J. Křenková, M. Przybylski, J.-L. Viovy, *Electrophoresis* **2006**, *27*, 1811.
[21] D. Horák, in "*Handbook of Polymer Research: Application of Poly(2-hydroxyethyl methacrylate) in Medicine*", Vol. 19, Eds., R. A. Pethrick, G. E. Zaikov), Nova Science Publishers, New York **2006**, p. 1.
[22] A. Denizli, *J. Appl. Polym. Sci.* **1999**, *74*, 655.
[23] M. Ohmer-Mizrahi, S. Margel, *J. Polym. Sci., Part A: Polym. Chem.* **2007**, *45*, 4612.
[24] *Epoxy Resins: Chemistry and Technology*, (Ed., A. C. May), Marcel Dekker, New York **1988**.
[25] O. Wichterle, in "*Encyclopedia of Polymer Science and Technology*", Vol. 15, Eds., H. F. Mark, N. G. Gaylord, N. M. Bikales), J. Wiley, New York **1971**.
[26] D. Horák, M. Babič, P. Jendelová, V. Herynek, M. Trchová, Z. Pientka, E. Pollert, M. Hájek, E. Syková, *Bioconjugate Chem.* **2007**, *18*, 635.
[27] D. Horák, E. Pollert, H. Macková, *J. Mater. Sci.* **2008**, *43*, 5845.
[28] Z. Bílková, A. Castagna, G. Zanusso, A. Farinazzo, S. Monaco, E. Damoc, M. Przybylski, M. Beneš, J. Lenfeld, J.-L. Viovy, P. G. Righetti, *Proteomics* **2005**, *5*, 639.
[29] N. Schultz, G. Metreveli, M. Franzreb, F. H. Frimmel, C. Syldatk, *Colloids Surf. B* **2008**, *66*, 39.

Příloha P2

Holubova L., **Korecka L.***, Podzimek S., Moravcova V., Rotkova J., Ehlova T., Velebny V., Bilkova Z. Enhanced multiparametric hyaluronan degradation for production of molar-mass-defined fragments. *Carbohydrate polymers,* **112**, 2014, 271-276

IF_{2018} = 6,044; Q1 – Chemical sciences; 10 citací [31. 5. 2020]

- hlavní autor (1. a 2. autor – stejný podíl)
- podíl na experimentální práci a vyhodnocení výsledků 40 %
- dílčí příprava a revize článku, korespondující autor

Carbohydrate Polymers 112 (2014) 271–276

Contents lists available at ScienceDirect

Carbohydrate Polymers

journal homepage: www.elsevier.com/locate/carbpol

Enhanced multiparametric hyaluronan degradation for production of molar-mass-defined fragments

Lucie Holubova[a,b,1], Lucie Korecka[a,*,1], Stepan Podzimek[c], Veronika Moravcova[d], Jana Rotkova[a], Tereza Ehlova[d], Vladimir Velebny[d], Zuzana Bilkova[a]

[a] Department of Biological and Biochemical Sciences, Faculty of Chemical Technology, University of Pardubice, Studentska 573, 3210 Pardubice, Czech Republic
[b] Department of Analytical Chemistry, Faculty of Chemical Technology, University of Pardubice, Studentska 573, 3210 Pardubice, Czech Republic
[c] Synthetic Polymers, Fibres and Textiles Chemistry Unit, Institute of Chemistry and Technology of Macromolecular Materials, Faculty of Chemical Technology, University of Pardubice, Studentska 573, 3210 Pardubice, Czech Republic
[d] Contipro Pharma a.s., Dolni Dobrouc 401, 561 02 Dolni Dobrouc, Czech Republic

ARTICLE INFO

Article history:
Received 12 March 2014
Received in revised form 7 May 2014
Accepted 19 May 2014
Available online 10 June 2014

Keywords:
Hyaluronan fragmentation
Papain
Magnetic particles
SEC-MALS
Pharmaceutics

ABSTRACT

Hyaluronic acid (HA) is known to serve as a dynamic mediator intervening in many physiological functions. Its specific effect has been repeatedly confirmed to be strongly influenced by the molecular size of hyaluronan fragments. However common technological approaches of HA fragments production have their limitations. In many cases, the final products do not meet the strict pharmaceutical requirements, specifically due to size polydispersity and reaction contaminants. We present novel methodology based on combination of unique incidental ability of the plant-derived protease papain to split the glycosidic bonds and an indispensable advantages of biocompatible macroporous material with incorporated ferrous ions serving as carrier for covalent papain fixation. This atypical and yet unpublished highly efficient multiparametric approach allows enhanced HA fragmentation for easily and safely producing molar-mass-defined HA fragments with narrow size distribution. Native polyacrylamide gel electrophoresis (PAGE) and size exclusion chromatography/multi-angle light scattering (SEC-MALS) confirmed the effectiveness of our multiparametric approach.

1. Introduction

Hyaluronic acid (hyaluronan, HA), a common component of synovial fluid and extracellular matrix, is a negatively charged, straight-chain glycosaminoglycan with high molar mass and is composed of alternating $(1\rightarrow 4)$-β linked D-glucuronic acid and $(1\rightarrow 3)$-β linked *N*-acetyl-D-glucosamine residues (Kogan, Soltes, Stern, & Gemeiner, 2007; Kogan, Soltes, Stern, Schiller, & Mendichi, 2008; Maharjan, Pilling, & Gomer, 2011; Segura et al., 2005; Stern, Kogan, Jedrzejas, & Soltes, 2007; Vercruysse, Ziebell, & Prestwich, 1999). It is present in almost all biological fluids and tissues (Kogan et al., 2007; Soltes, Brezova, Stankovska, Kogan, & Gemeiner, 2006). Hyaluronan's high molar mass and its associated unique viscoelastic and rheological properties predispose HA to play important physiological roles in living organisms (Ikegami-Kawai & Takahashi, 2002; Kogan et al., 2007). It already has been confirmed that HA fragments (HAFs) are involved in cell proliferation, differentiation, migration and signal transduction (Ikegami-Kawai & Takahashi, 2002; Kogan et al., 2007; Liu et al., 2004). Modified HA molecules already have found a broad range of biomedical applications even as they are used in cosmetics, pharmaceutics (drug delivery systems, therapeutic reagents) and specialty foods production (DeAngelis, Oatman, & Gay, 2003; Ikegami-Kawai & Takahashi, 2002; Kogan et al., 2007; Kühn, Raith, Sauerland, & Neubert, 2003; Liao, Jones, Forbes, Martin, & Brown 2005; Liu et al., 2004; Stern et al., 2007; Weindl, Schaller, Schäfer-Korting, & Korting, 2004).

Abbreviations: BApNA, Nα-benzoyl-DL-arginine 4-nitroanilide hydrochloride; EDC, 1-ethyl-3(3-dimethylaminopropyl)carbodiimide hydrochloride; EDTA, ethylenediaminetetraacetic acid; HA, hyaluronic acid; HAFs, hyaluronic acid fragments; MBC, magnetic macroporous bead cellulose; M_w, molar mass; NBC, nonmagnetic macroporous bead cellulose; ORD, oxidative–reductive depolymerization; PAGE, polyacrylamide gel electrophoresis; SEC-MALS, size exclusion chromatography/multi-angle light scattering; sulfo-NHS, N-hydroxysulfosuccinimide sodium salt; TBE, Tris/borate/EDTA; TEMED, *N,N,N,N*-tetramethylenediamine.

* Corresponding author at: Department of Biological and Biochemical Sciences, Faculty of Chemical Technology, University of Pardubice, Studentska 573 (HB/C), 532 10 Pardubice, Czech Republic. Tel.: +420 466037711.
E-mail addresses: lucie.korecka@upce.cz, koreckalucie@gmail.com (L. Korecka).
[1] These authors contributed equally to this work.

http://dx.doi.org/10.1016/j.carbpol.2014.05.096
0144-8617/

Despite HA's uniform and simple primary structure, the exact and defined-molar-mass HAFs is clearly of critical importance due to the various biological effects of HAFs differing in size (Cantor & Nadkarni, 2006; Ikegami-Kawai & Takahashi, 2002; Kogan et al., 2007).

Today's technological approaches to producing HAFs with desired properties typically are based on enzymatic (Stern et al., 2007; Vercruysse, Ziebell, & Prestwich, 1999) or free radical (Matsumura, Herp, & Pigman, 1966; Pigman, Rizvi, & Holley, 1961; Soltes et al., 2007; Uchiyama, Dobashi, Ohkouchi, & Nagasawa, 1990) degrading processes, although we also can use methods that disturb the covalent bonds chemically and/or mechanically (Kubo, Nakamura, Takagaki, Yoshida, & Endo, 1993; Miyazaki, Yomota, & Okada, 2001). In many cases, however, the final products do not meet the strict requirements for pharmaceutical products. Polydispersity as well as reaction residues in the final product (e.g., reactive oxidants or enzymes of animal origin) are the main factors limiting the application of such products. The choice among the applied methods is made in practice according to the intended final purpose or use of the HAFs. Still, it is not always possible to guarantee the stability and homogeneity of those fragments produced.

Oxidative–reductive depolymerization (ORD) is a technique based upon the action of such substances as L-ascorbic acid (Harris, Herp, & Pigman, 1972; Pigman et al., 1961; Wong, Halliwell, Richmond, & Skowroneck, 1981), cupric chloride (Harris et al., 1972; Soltes et al., 2006), sodium hypochlorite (Hawkins & Davies, 1998; Uchiyama et al., 1990), photoexcited riboflavin (Frati et al., 1997), cysteine and ferrous salt, in the absence or presence of hydrogen peroxide (Akeel, Sibanda, Martin, Paterson, & Parsons, 2013; Harris et al., 1972; McNeil, Wiebkin, Betts, & Cleland, 1985; Roberts, Roughley, & Mort, 1989; Soltes et al., 2006). Unfortunately, this approach leads to fragments with significant polydispersity in size (McNeil et al., 1985). A frequently neglected fact, moreover, is that final products may be contaminated by such ingredients as metal ions, which not only can adversely affect the immune system but also pose a potential risk for undesirable further decrease in molar mass and subsequent change in the properties of HAFs (Kogan et al., 2007). Thus, subsequent purification processes are necessary.

Similarly to other biopolysaccharides, HA could be degraded chemically using acid or alkaline hydrolysis. However, chemical hydrolysis proceeds in a random fashion and gives rise to a statistical mixture of oligo- and monosaccharides (Kuo, Swann, & Prestwich, 1991; Tokita & Okamoto, 1995).

Depolymerization involving specific scission of the glycosidic linkages is recommended for preparing HAFs. The extent of the reaction can be easily controlled by means of pH, temperature and reaction time. Hyaluronidases, chondroitinases and hexosaminidases are specific endoglycosidases with the ability to degrade glycosaminoglycans efficiently (Frost, Csoka, & Stern, 1996; Furukawa et al., 2013; Highsmith, Garvin, & Chipman, 1975; Kreil, 1995; Maksimenko, Schechilina, & Tischenko, 2003; Stern et al., 2007). The animal origin of all of these combined with their high prices and risk of viral contamination has strongly limited their utilization in the medical, pharmaceutical and even cosmetic industries.

It should be noted that the choice of method for producing HAFs may affect the physicochemical properties and that the resulting biological properties could be slightly altered or even wholly changed. The biotechnology and pharmaceutical industries need to find the simplest possible manner of HAFs production. In particular, they need a process leading to large yields of molar-mass-defined fragments that are generated reliably, at low cost, within a reasonable time, and, of course, in the desired purity and with a narrow size distribution.

Our multiparametric approach that has not been described heretofore combines the ability of plant-derived papain to split the glycosidic bonds with advantages provided by a carrier to which papain is covalently captured and of ferrous ions incorporated into the macroporous material to accelerate the fragmentation of polymeric chains.

2. Materials and methods

2.1. Chemicals and reagents

Papain from papaya latex (EC 3.4.22.2, papainase, buffered aqueous suspension, 16–40 units mg^{-1}); hyaluronic acid sodium salt from *Streptococcus equi* ($1.5–1.8 \times 10^6$ g mol^{-1}); Nα-benzoyl-DL-arginine 4-nitroanilide hydrochloride (BApNA); ethylenediaminetetraacetic acid (EDTA); L-cysteine; saccharide acid-1,4-lacton; polysaccharide standard for electrophoresis select-HA LoLadder; acrylamide; *N,N′*-methylen-bis-acrylamide; and *N,N,N,N*-tetramethylenediamine (TEMED) were purchased from Sigma–Aldrich (St. Louis, MO, USA). Sodium cyanoborohydride was obtained from Fluka (Buchs, Switzerland). Perloza MT 100 nonmagnetic macroporous bead cellulose (NBC; 80–100 μm) and Perloza MG magnetic macroporous bead cellulose (MBC; 80–100 μm) were supplied by Iontosorb (Ústí nad Labem, Czech Republic). SiMAG-Carboxyl microparticles (1 μm) were purchased from Chemicell GmbH (Berlin, Germany). Sucrose and Alcian blue 8GS were obtained from SERVA electrophoresis GmbH (Heidelberg, Germany) and all other chemicals were of reagent grade and produced by PENTA (Chrudim, Czech Republic).

2.2. Immobilization of papain on macroporous bead cellulose

Following Turková, with slight modification (Turková, 1993), 1 ml of Perloza MT 100 (nonmagnetic form, NBC) or Perloza MG (magnetic form, MBC) was washed 5 times with distilled water and then oxidized using 1 ml of 0.2 M $NaIO_4$. The mixture was stirred for 90 min in darkness at room temperature. Perloza was washed 10 times with 0.1 M phosphate buffer (pH 7.0) with 0.002 M EDTA. Thereafter, 4 mg of papain dissolved in the same buffer were added and the reaction mixture was stirred for 10 min at room temperature. Then 5 mg of sodium cyanoborohydride in 0.1 M phosphate buffer (pH 7.0) was added and the reaction was permitted to occur overnight at 4 °C. The carrier with immobilized papain (papain-MBC; papain-NBC) was washed 5 times with 0.1 M phosphate buffer (pH 7.0) with 0.002 M EDTA, then 5 times with 0.1 M phosphate buffer (pH 7.0) with 1.0 M NaCl to remove nonspecifically adsorbed molecules, and again 5 times with 0.1 M phosphate buffer (pH 7.0) with 0.002 M EDTA. The enzyme reactor was stored in fresh 0.1 M phosphate buffer (pH 7.0) with 0.002 M EDTA at 4 °C. The presence of enzyme-active molecules bound to the surface of magnetic particles was verified by a previously published, standard method using the low-molecular-weight substrate BApNA (Bhardwaj et al., 1996; Gaertner & Puigserver, 1992).

2.3. Immobilization of papain on the SiMAG-Carboxyl microparticles

Covalent coupling of papain was performed by the common one-step carbodiimide method using zero-length cross-linker EDC and sulfo-NHS as described by Hermanson (1996), with slight modification. One milligram of SiMAG-Carboxyl was washed 5 times with 1 ml of 0.1 M phosphate buffer (pH 7.3) with 0.002 M EDTA. Then, 7.5 mg of EDC, 1.25 mg of sulfo-NHS and 3 mg of papain in the 0.1 M phosphate buffer (pH 7.3) with 0.002 M EDTA were added and the reaction mixture was stirred at room temperature for 6 h or at 4 °C overnight. Immobilized papain (papain-SiMAG)

was washed 10 times with 0.1 M phosphate buffer (pH 7.3) with 0.002 M EDTA, which was used also as storage buffer. The presence of enzyme-active molecules bound to the surface of magnetic particles was verified by a previously published, standard method using the low-molecular-weight substrate BApNA (Bhardwaj et al., 1996; Gaertner & Puigserver, 1992).

2.4. Determination of papain activity by low molecular-weight substrate BApNA

Determination of papain activity was carried out in accordance with Gaertner and Puigserver (1992) and Bhardwaj et al. (1996), with slight modification. Soluble or immobilized papain (25 μl of sedimented Perloza MT 100 or Perloza MG or 100 μg of SiMAG-Carboxyl) was first activated using 0.02 M L-cysteine in the presence of 0.004 M EDTA for 30 min at 37 °C. The reaction mixture with immobilized papain was stirred. After that, 1 ml of 0.1 M Tris–HCl buffer (pH 7.8) and 0.02 ml of 0.055 M BApNA dissolved in N,N-dimethylformamide were added and the mixture was stirred 30 min at 37 °C. The reaction was stopped with 0.2 ml of 30% acetic acid. The absorbance was measured spectrophotometrically at 405 nm.

2.5. Multiparametric fragmentation of hyaluronic acid

The quantity 1.5 mg of hyaluronic acid sodium salt from *S. equi* ($1.5–1.8 \times 10^6$ g mol^{-1}) was dissolved in 1 ml 0.1 M phosphate buffer (pH 7.0) with 0.1 M NaCl and 1.5 mM saccharide acid-1,4-lacton. The HA solution was stirred overnight at 4 °C for swelling.

One milliliter of sedimented carrier with immobilized papain was washed 5 times with the buffer of composition mentioned above. After the washing steps, 1 ml of swelled HA diluted in 1 ml of the same buffer was mixed with 1 ml of washed carrier. After incubation at 37 °C (using different incubation intervals) under gentle stirring, the supernatant was then separated and HAFs were analyzed by native polyacrylamide gel electrophoresis (PAGE) with specific Alcian blue-silver staining and using size-exclusion chromatography/multi-angle light scattering (SEC-MALS). All steps were carried out at atmospheric pressure.

2.6. Native PAGE analysis of HA molecules

Native PAGE analysis followed by the specific Alcian blue with silver staining was performed according to a working procedure that was adapted for our conditions by combining previously published methods (Cowman et al., 1984; Ikegami-Kawai & Takahashi, 2002; Min & Cowman, 1989). Polyacrylamide gel containing 15% acrylamide and 0.5% N,N-methylenebisacrylamide in 0.1 M TBE buffer (0.1 M Tris/0.1 M borate/0.001 M EDTA; pH 8.3) was used as a separating gel while a polyacrylamide gel containing 5% acrylamide and 0.16% N,N-methylenebisacrylamide in 0.1 M TBE buffer was used as a stacking gel. Electrophoretic separation was performed at 4 °C first at 125 V and 20 mA/gel for 20 min and then at 200 V and 40 mA/gel for approximately 45 min. The specific Alcian blue and silver staining method was employed for visualizing HAFs. After PAGE separation, the gel with separated HAFs was fixed in 0.05% aqueous solution of Alcian blue (which needs to be boiled before use) for 30 min in darkness. After destaining in water (8 times, 5 min each with stirring), the gel with separated HAFs was subjected to silver staining. The gel was placed in 0.03 M potassium dichromate with 0.03 M nitric acid for 5 min and washed with distilled water (6 times, 5 min each). After that, the gel was soaked in 0.01 M silver nitrate for 20 min and then washed with distilled water. The fragments of HA in gel were immediately developed using 0.3 M sodium carbonate with 0.02% formaldehyde. The reaction was stopped with 5% aqueous acetic acid solution. The gel images were captured using a digital camera.

2.7. SEC-MALS analysis of molar-mass-defined HA molecules

Molecular weights (M_w) of hyaluronic acid or hyaluronan fragments were assigned using SEC-MALS. Samples were dissolved overnight in a mobile phase (aqueous 50 mM sodium phosphate containing 0.02% sodium azide). The chromatographic system consisted of an Alliance e2695 separation module, 2414 refractive index detector and 2489 UV-VIS detector (Waters, Milford, MA), and a miniDAWN TREOS light scattering photometer (Wyatt Technology Corporation, Santa Barbara, CA). The injection volume was 100 μl. Each sample was filtered through a 0.22 μm MS nylon syringe filter. The flow rate of the mobile phase was 0.8 ml min^{-1}. Data acquisition and molecular weight calculations were performed using ASTRA software (version 5.3.4, Wyatt Technology Corporation). The specific refractive index increment of 0.155 ml g^{-1} was used for HA (Podzimek, Hermannova, Bilerova, Bezakova, & Velebny, 2010).

3. Results and discussion

The goal was to develop a technology platform for efficient and controllable production of HAFs. As already noted, physical as well as chemical methods of HA polymers degradation lead to producing fragments with high size polydispersity while the enzymatic methods using hyaluronidase of animal origin significantly increase the price of the final products. Additionally, their possible contamination by viral agents can be a risk for biomedical and biotechnological applications. Accordingly, the use of a plant-derived enzyme with the ability to split the glycosidic bond is an eligible alternative.

The ability of such proteases as pepsin (Kumar, Varadaraj, & Tharanathan, 2007; Tao, Wei, Mao, Zhang, & Xia, 2005), papain (Lin, Wang, Xue, & Ye, 2002; Muzzarelli, Terbojevich, Muzzarelli, & Francescangeli, 2002; Terbojevich, Cosani, & Muzzarelli, 1996; Vishu Kumar, Varadaraj, Lalitha, & Tharanathan, 2004;), pronase E (Vishu Kumar & Tharanathan, 2004), bromelain (Muzzarelli et al., 2002), ficin (Pantaleone, Yalpani, & Scollar, 1992), and pancreatin (Yalpani & Pantaleone, 1994) also to split the glycosidic bonds of polysaccharides has been demonstrated many times. In addition, the use of an enzyme in an immobilized form allows continuous monitoring process of HA fragmentation and stopping the reaction at a defined time point. Papain, as a plant-derived enzyme, appears to offer a valuable alternative with an acceptable price and bearing no risk of viral or bacterial contamination.

The first phase of this study was to develop the carrier with immobilized papain. Various types of magnetic microparticles originating in natural or synthetic materials and characterized by high stability in a wide range of reaction conditions were tested. In order to achieve maximum activity and stability of the carrier, the reaction conditions of enzyme immobilization were optimized. The covalent binding of papain onto macroporous bead cellulose was performed via a Schiff base formation between the primary amine groups of the enzyme and the carbonyl functional groups of oxidized cellulose beads. The one-step carbodiimide technique with zero-length cross-linker EDC in combination with sulfo-NHS was applied for papain immobilization to the SiMAG-Carboxyl microparticles as an alternative nonporous carrier. The efficiency of the immobilization procedure, the total amount of papain, and the papain's hydrolytic activity were evaluated by the standard method using low-molecular-mass BApNA substrate.

The carriers' operational characteristics and storage stability were repeatedly tested. Papain immobilized on the magnetic form of macroporous bead cellulose shows high stability with repeated

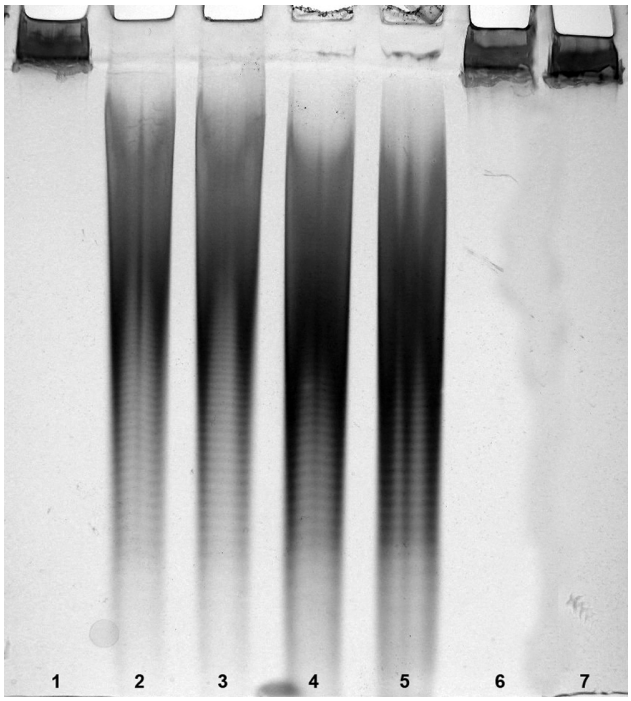

Fig. 1. Native PAGE analysis of HA fragments obtained using immobilized papain (under stirring at room temperature) on various carriers: 1 – native HA without fragmentation, 2 – MBC for 5 h, 3 – MBC for 10 h, 4 – MBC for 24 h, 5 – MBC for 48 h, 6 – SiMAG-Carboxyl for 48 h, 7 – NBC for 48 h; 15% PAA separation gel, 5% focusing PAA gel and Alcian blue-silver staining.

use, as well as during long-term storage. Based on these results, we confirmed that the carrier can be used at least eight times without significant decrease in its activity. Moreover, the bioactive carrier could be stored for more than one month (data not shown) without any significant decline in its activity.

The efficiency of HA polymer chains fragmentation was evaluated by native PAGE, and SEC-MALS was applied for precisely estimating molar mass distribution and monitoring the kinetics of HA polymer degradation.

Fig. 1 demonstrates the efficiency of HA degradation by papain immobilized on 3 carriers differing in certain characteristics. These are magnetic macroporous bead cellulose (papain-MBC) at different times (lanes 2–5), SiMAG (papain-SiMAG) (lane 6), and nonmagnetic macroporous bead cellulose (papain-NBC) (lane 7). After 24 h of incubating HA with carriers, we observed almost zero fragmentation activity of papain immobilized to nonporous SiMAG microparticles (Fig. 1, lane 6) and essentially the same inactivity was obtained from papain immobilized to the nonmagnetic form of macroporous bead cellulose (Fig. 1, lane 7). By contrast, papain-MBC effectively degraded the HA polymers. This proves that the molecular weight of HA polymer chains decrease with increasing incubation time (Fig. 1, lanes 2–5). The efficient fragmentation was confirmed by the presence of discrete ladder-like bands in the gel, which indicate HAFs differing in the numbers of their disaccharide units.

Next, experiments were performed to confirm the supposed positive effect of free soluble ferrous ions added to the reaction medium during the HA fragmentation. Obtained results clearly document the well-defined auxiliary effect of metal ions in relation to fragmentation efficiency (Fig. 2). Nevertheless, for efficient HA fragmentation high concentration of ferrous ions (namely 100 mM) is necessary which leads to an undesired contamination of the final product and thus it is not appropriate for large scale biotechnological exploitation. For this purpose the use of macroporous bead

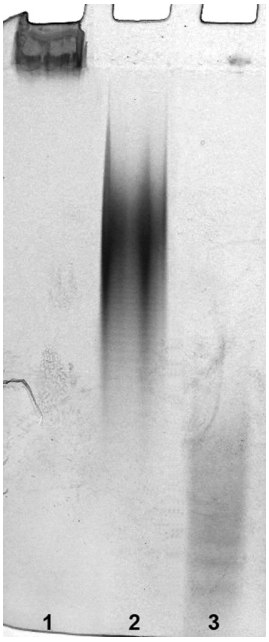

Fig. 2. Native PAGE analysis of HA molecules after incubation while using MBC without or in the presence of ferrous ions (under stirring at 37 °C, 48 h): 1 – MBC, 2 – MBC and 10 mM Fe^{2+}, 3 – MBC and 100 mM Fe^{2+}; 15% PAA separation gel, 5% focusing PAA gel and Alcian blue-silver staining.

cellulose with accessible ferrous ions fixed within the highly porous particles is convenient option.

Additionally we had supposed there to be also a mechanical factor incurred by porous character of MBC involved in the HA fragmentation. The experiments evaluated by native PAGE are presented in Fig. 3. Gel A is for samples of HA fragmented over time (3.5–49 h) by naked MBC and gel B is for samples of HA fragmented over time by the carrier MBC with immobilized papain. Gel A clearly shows the synergy effect of mechanical disentanglement and oxidative–reductive depolymerization reaction due to the carrier that was the magnetic form of macroporous bead cellulose. Even after 32 h of incubation, we still can observe a large amount of long polymer chain that is not penetrating into the gel (Fig. 3A, lanes 1–5). On the contrary, the multiparametric approach combining enzymatic, oxidative–reductive and mechanical effects (gel B) provide intermediate fragments of HA even within 7 h, and their size is reduced with the increasing incubation time. While the presented results definitively prove the positive effect of papain on HA degradation, it is nevertheless important to emphasize that the highest fragmentation efficiency can be obtained using papain along with the supporting effect due to the porous character of the beads, which are produced from a biocompatible, highly hydrophilic material saturated with ferric and ferrous ions accessible for catalysis.

Finally, based on SDS-PAGE analysis used for continuous optimization steps, selected fractions showing the most effective degradation of HA molecules were analyzed by SEC-MALS to obtain more detailed information about degradation efficiency and its dynamics in time and also size polydispersity rate of HAFs. The change of molar mass distribution in the course of degradation is shown in Fig. 4. The distribution curves show no major change in the distribution pattern and polydispersity during time course degradation.

Fig. 5, which show the reaction kinetics, characterized by significant decline in M_w at the beginning of degradation and an approximately linear decrease from the reaction time of about 10 h. The most effective fragmentation that is observed in the initial

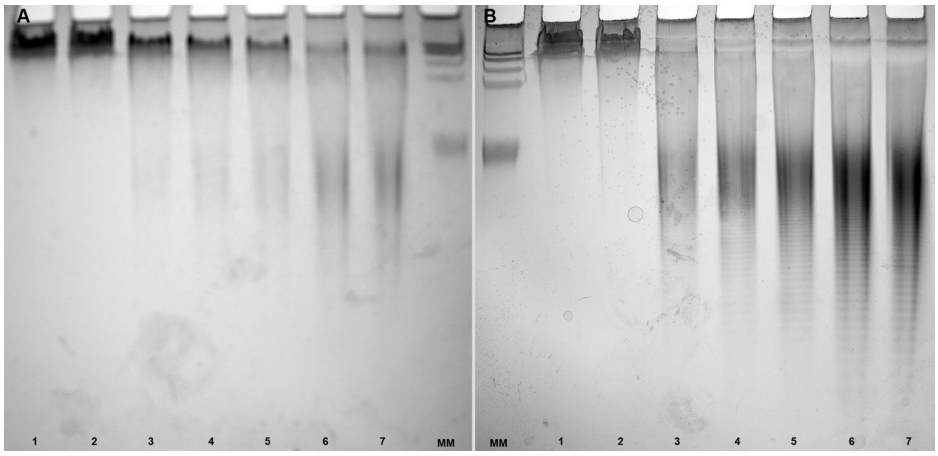

Fig. 3. Native PAGE analysis of HA fragments acquired using MBC without (A) and with (B) papain (papain-MBC) at varying time periods (under stirring at 37 °C, 48 h): (A) 1 – 3.5 h, 2 – 7 h, 3 – 24 h, 4 – 28 h, 5 – 32 h, 6 – 48 h, 7 – 49 h, MM – select-HA LoLadder, (B) MM – select-HA LoLadder, 1 – 3.5 h, 2 – 7 h, 3 – 24 h, 4 – 28 h, 5 – 32 h, 6 – 48 h, 7 – 49 h; 15% PAA separation gel, 5% focusing PAA gel and Alcian blue-silver staining.

phase of the reaction is in accordance with the depolymerization efficiency described by Terbojevich et al. (1996). Mentioned plot allow simple estimation of the fragmentation time needed to obtain HA fragments of requested *Mw*.

In conclusion, by covalent immobilization of the enzyme papain onto magnetic macroporous particles 80–100 μm in size and made from nontoxic and even biocompatible cellulose we prepared an efficient carrier with multiparametric effect promoting the degradation of hyaluronan polymer molecules. This reusable heterogeneous and low-cost biocatalyst enables obtaining a final product in the desired purity in comparison with animal-source enzyme hyaluronidase. Bead cellulose with a defined porosity and permeated by metal ions seems to be the best carrier for mechanical disentanglement and bursting of long HA polymer chains while promoting yields of shorter molecules of interest. The magnetic carrier used in this study contains ferrous and ferric ions homogeneously distributed and strongly fixed within the cellulose. It is known that iron oxides can interact with components of the liquid medium and thereby support long polymer chain degradation through so-called oxidative–reductive depolymerization reaction (ORD) via a mechanism that has been thoroughly described (Uchiyama et al., 1990).

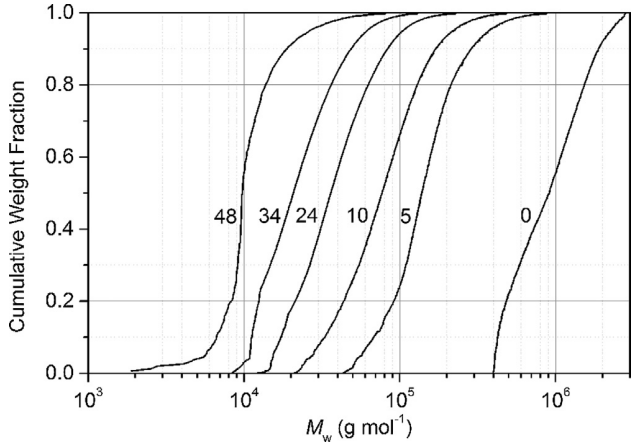

Fig. 4. Chromatogram from size-exclusion chromatography/multi-angle laser light scattering (SEC-MALS) analysis, which proves change in the molar mass distribution of hyaluronan fragments in the course of degradation; the numerical values close to the curve correspond to the reaction time. Hyaluronic acid (1.5–1.8 × 10^6 g mol^{-1}) was fragmented with papain-MBC under stirring at 37 °C for 48 h.

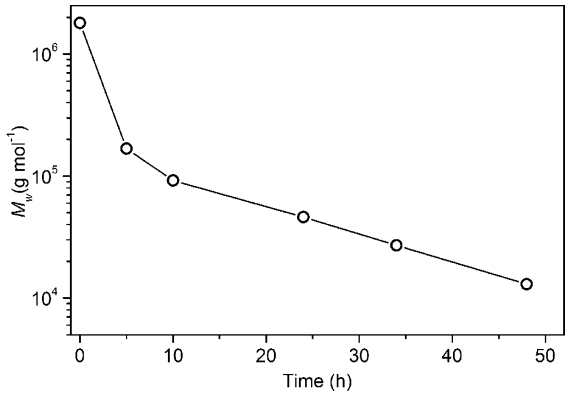

Fig. 5. Weighted-average molar mass (M_w) as a function of degradation time determined using size-exclusion chromatography/multi-angle laser light scattering (SEC-MALS) analysis. Hyaluronic acid (1.5–1.8 × 10^6 g mol^{-1}) fragmented by papain-MBC under stirring at 37 °C for 48 h.

We confirmed that the co-interaction of these three factors (mechanical disentanglement of the long polymer chain due to the macroporous character of used carrier, ORD caused by iron oxides inside the pores of MBC, together with hydrolytic activity of immobilized papain) leads to the efficient and controllable fragmentation that provides molar-mass-defined HAFs.

4. Conclusion

In summary, we have demonstrated an enhanced multiparametric approach for safe and controlled production of molar-mass-defined HAFs with relatively low polydispersity. We do not question the fact that enzyme fragmentation using hyaluronidase is more efficient and rapid, but our multiparametric approach fully solves the problem of contamination in final product while the size of the fragments is readily adjustable by means of quenching the reaction at a defined time point. We confirmed that papain immobilized onto macroporous microparticles, and where iron oxides are fixed within the pores of the microparticles, combined with the mechanical impact of soft cellulose beads and the additional effect of reactive oxygen significantly accelerated the cleavage process.

We assume that a magnetically stabilized fluidized bed within which the continuous and dynamic contact of the carrier with viscous HA molecules driven by an outside magnetic field could

also enhance the fragmentation efficiency. In this case, such an arrangement can be used even for large-scale production in the pharmaceutical or cosmetic industry.

Acknowledgements

This work was supported by The Ministry of Education, Youth and Sports of the Czech Republic, Project CZ.1.07/2.3.00/30.0021 "Enhancement of R&D Pools of Excellence at the University of Pardubice." We gratefully thank Dr. L. Husakova and MSc. I. Urbanova (Department of Analytical Chemistry, Faculty of Chemical Technology, University of Pardubice) for FL-AAS analysis.

References

Akeel, A., Sibanda, S., Martin, S. W., Paterson, A. W. J., & Parsons, B. J. (2013). Chlorination and oxidation of heparin and hyaluronan by hypochlorous acid and hypochloride anions: Effect of sulfate groups on reaction pathways. *Free Radical Biology and Medicine*, *56*, 72–88.

Bhardwaj, A., Lee, J., Glauner, K., Ganapathi, S., Bhattacharyya, D., & Butterfield, D. A. (1996). Biofunctional membranes: An EPR study of active site structure and stability of papain non-covalently immobilized on the surface of modified poly(ether) sulfone membranes through the avidin-biotin linkage. *Journal of Membrane Science*, *119*, 241–252.

Cantor, J. O., & Nadkarni, P. P. (2006). Hyaluronan: The Jekyll and Hyde molecule. *Inflammation & Allergy: Drug Targets*, *5*(4), 257–260.

Cowman, M. K., Slahetka, M. F., Hittner, D. M., Kim, J., Forino, M., & Gadelrab, G. (1984). Polyacrylamide-gel electrophoresis and Alcian Blue staining of sulphated glycosaminoglycan oligosaccharides. *Biochemical Journal*, *221*, 707–716.

DeAngelis, P. L., Oatman, L. C., & Gay, D. F. (2003). Rapid chemoenzymatic synthesis of monodisperse oligosaccharides with immobilized enzyme reactors. *Journal of Biological Chemistry*, *278*, 35199–35203.

Frati, E., Khatib, A.-M., Front, P., Panasyuk, A., Aprile, F., & Mitrovic, D. R. (1997). Degradation of hyaluronic acid by photosensitized riboflavin in vitro. Modulation of the effect by transition metals, radical quenchers, and metal chelators. *Free Radical Biology and Medicine*, *22*(7), 1139–1144.

Frost, G. I., Csoka, T., & Stern, R. (1996). The hyaluronidases: A chemical, biological and clinical overview. *Trends in Glycoscience and Glycotechnology*, *8*, 419–434.

Furukawa, T., Arai, M., Garcia-Martin, F., Amano, M., Hinou, H., & Nishimura, S.-I. (2013). Glycoblotting-based high throughput protocol for the structural characterization of hyaluronan degradation products during enzymatic fragmentation. *Glycoconjugate Journal*, *30*(2), 171–182.

Gaertner, H. F., & Puigserver, A. J. (1992). Increased activity and stability of poly(ethylene glycol)-modified trypsin. *Enzyme and Microbial Technology*, *14*, 150–155.

Harris, M. J., Herp, A., & Pigman, W. (1972). Metal catalysis in the depolymerization of hyaluronic acid by autoxidants. *Journal of the American Chemical Society*, *94*(21), 7570–7572.

Hawkins, C. L., & Davies, M. J. (1998). Degradation of hyaluronic acid, poly- and monosaccharides, and model compounds by hypochlorite: Evidence for radical intermediates and fragmentation. *Free Radical Biology and Medicine*, *24*(9), 1396–1410.

Hermanson, G. T. (1996). *Bioconjugate technique*. San Diego: Academic Press (Part II – Bioconjugate reagents).

Highsmith, S., Garvin, J. H., Jr., & Chipman, D. M. (1975). Mechanism of action of bovine testicular hyaluronidase. *Journal of Biological Chemistry*, *250*(18), 7473–7480.

Ikegami-Kawai, M., & Takahashi, T. (2002). Microanalysis of hyaluronan oligosaccharides by polyacrylamide gel electrophoresis and its application to assay of hyaluronidase activity. *Analytical Biochemistry*, *311*, 157–165.

Kogan, G., Soltes, L., Stern, R., & Gemeiner, P. (2007). Hyaluronic acid: A natural biopolymer with a broad range of biomedical and industrial applications. *Biotechnology Letters*, *29*, 17–25.

Kogan, G., Soltes, L., Stern, R., Schiller, J., & Mendichi, R. (2008). Hyaluronic acid: Its function and degradation in in vivo systems. In Atta-ur-Rahman (Ed.), *Studies in natural products chemistry: Bioactive natural products. Part D* (vol. 34) (pp. 789–882). Amsterdam: Elsevier.

Kreil, G. (1995). Hyaluronidases: A group of neglected enzymes. *Protein Science*, *4*(9), 1666–1669.

Kubo, K., Nakamura, T., Takagaki, K., Yoshida, Y., & Endo, M. (1993). Depolymerization of hyaluronan by sonication. *Glycoconjugate Journal*, *10*(6), 435–439.

Kühn, A. V., Raith, K., Sauerland, V., & Neubert, R. H. H. (2003). Quantification of hyaluronic acid fragments in pharmaceutical formulations using LC-ESI–MS. *Journal of Pharmaceutical and Biomedical Analysis*, *30*, 1531–1537.

Kumar, B., Varadaraj, M., & Tharanathan, R. (2007). Low molecular weight chitosan – Preparation with the aid of pepsin, characterization and its bacterial activity. *Biomacromolecules*, *8*(2), 566–572.

Kuo, J. W., Swann, D. A., & Prestwich, G. D. (1991). Chemical modification of hyaluronic acid by carbodiimides. *Bioconjugate Chemistry*, *2*(4), 232–241.

Liao, Y.-H., Jones, S. A., Forbes, B., Martin, G. P., & Brown, M. B. (2005). Hyaluronan: Pharmaceutical characterization and drug delivery. *Drug Delivery*, *12*(6), 327–342.

Lin, H., Wang, H., & Xue Ch Ye, M. (2002). Preparation of chitosan oligomers by immobilized papain. *Enzyme and Microbial Technology*, *31*, 588–592.

Liu, H., Mao, J., Yao, K., Yang, G., Cui, L., & Cao, Y. (2004). A study on a chitosan–gelatin–hyaluronic acid scaffold as artificial skin *in vitro* and its tissue engineering applications. *Journal of Biomaterials Science, Polymer Edition*, *15*, 25–40.

Maharjan, A. S., Pilling, D., & Gomer, R. H. (2011). High and low molecular weight hyaluronic acid differentially regulate human fibrocyte differentiation. *PLOS ONE*, *6*(10), e26078.

Maksimenko, A. V., Schechilina, Y. V., & Tischenko, E. G. (2003). Role of the glycosaminoglycan microenvironment of hyaluronidase in regulation of its endoglycosidase activity. *Biochemistry (Moscow)*, *68*(8), 862–868.

Matsumura, G., Herp, A., & Pigman, W. (1966). Depolymerization of hyaluronic acid by autoxidants and radiations. *Radiation Research*, *28*(4), 735–752.

McNeil, J. D., Wiebkin, O. W., Betts, W. H., & Cleland, L. G. (1985). Depolymerisation products of hyaluronic acid after exposure to oxygen-derived free radicals. *Annals of the Rheumatic Diseases*, *44*, 780–789.

Min, H., & Cowman, M. K. (1989). Combined Alcian blue and silver staining of glycosaminoglycans in polyacrylamide gels: Application to electrophoretic analysis of molecular weight distribution. *Analytical Biochemistry*, *155*, 275–285.

Miyazaki, T., Yomota, C., & Okada, S. (2001). Ultrasonic depolymerization of hyaluronic acid. *Polymer Degradation and Stability*, *74*, 77–85.

Muzzarelli, R. A. A., Terbojevich, M., Muzzarelli, C., & Francescangeli, O. (2002). Chitosans depolymerized with the aid of papain and stabilized as glycosylamines. *Carbohydrate Polymers*, *20*, 69–78.

Pantaleone, D., Yalpani, M., & Scollar, M. (1992). Unusual susceptibility of chitosan to enzymic hydrolysis. *Carbohydrate Research*, *237*, 325–332.

Pigman, W., Rizvi, S., & Holley, H. L. (1961). Depolymerization of hyaluronic acid by the ORD reaction. *Arthritis Rheumatology*, *4*, 240–252.

Podzimek, S., Hermannova, M., Bilerova, H., Bezakova, Z., & Velebny, V. (2010). Solution properties of hyaluronic acid and comparison of SEC-MALS-VIS data with off-line capillary viscometry. *Journal of Applied Polymer Science*, *116*, 3013–3020.

Roberts, C. R., Roughley, P. J., & Mort, J. S. (1989). Degradation of human proteoglycan aggregate induced by hydrogen peroxide. *Biochemical Journal*, *259*, 805–811.

Segura, T., Anderson, B. C., Chung, P. H., Webber, R. E., Shull, K. R., & Shea, L. D. (2005). Crosslinked hyaluronic acid hydrogels: A strategy to functionalize and pattern. *Biomaterials*, *26*, 359–371.

Soltes, L., Brezova, V., Stankovska, M., Kogan, G., & Gemeiner, P. (2006). Degradation of high-molecular-weight hyaluronan by hydrogen peroxide in the presence of cupric ions. *Carbohydrate Research*, *341*, 639–644.

Soltes, L., Kogan, G., Stankovska, M., Mendichi, R., Rychly, J., Schiller, J., et al. (2007). Degradation of high-molar-mass hyaluronan and characterization of fragments. *Biomacromolecules*, *8*(9), 2697–2705.

Stern, R., Kogan, G., Jedrzejas, M. J., & Soltes, L. (2007). The many ways to cleave hyaluronan. *Biotechnology Advances*, *25*, 537–557.

Tao, H., Wei, W., Mao, Y., Zhang, S., & Xia, J. (2005). Study on degradation characteristics of chitosan by pepsin with piezoelectric quartz crystal impedance analysis technique. *Analytical Sciences*, *21*, 1057–1061.

Terbojevich, M., Cosani, A., & Muzzarelli, R. A. A. (1996). Molecular parameters of chitosans depolymerized with the aid of papain. *Carbohydrate Polymers*, *29*, 63–68.

Tokita, Y., & Okamoto, A. (1995). Hydrolytic degradation of hyaluronic acid. *Polymer Degradation and Stability*, *42*(2), 269–273.

Turková, J. (1993). *Bioaffinity chromatography*. Amsterdam: Elsevier (Chapter 6).

Uchiyama, H., Dobashi, Y., Ohkouchi, K., & Nagasawa, K. (1990). Chemical change involved in the oxidative reductive depolymerization of hyaluronic acid. *Journal of Biological Chemistry*, *265*(15), 7753–7759.

Vercruysse, K. P., Ziebell, M. R., & Prestwich, G. D. (1999). Control of enzymatic degradation of hyaluronan by divalent cations. *Carbohydrate Research*, *318*, 26–37.

Vishu Kumar, A. B., & Tharanathan, R. N. (2004). A comparative study on depolymerization of chitosan by proteolytic enzymes. *Carbohydrate Polymers*, *58*, 275–283.

Vishu Kumar, A. B., Varadaraj, M. C., Lalitha, R. G., & Tharanathan, R. N. (2004). Low molecular weight chitosans: Preparation with the aid of papain and characterization. *Biochimica et Biophysica Acta*, *1670*, 137–146.

Weindl, G., Schaller, M., Schäfer-Korting, M., & Korting, H. C. (2004). Hyaluronic acid in the treatment and prevention of skin diseases: Molecular biological, pharmaceutical and clinical aspects. *Skin Pharmacology and Physiology*, *17*, 207–213.

Wong, S. F., Halliwell, B., Richmond, R., & Skowroneck, W. R. (1981). The role of superoxide and hydroxyl radicals in the degradation of hyaluronic acid induced by metal ions and by ascorbic acid. *Journal of Inorganic Biochemistry*, *14*(2), 127–134.

Yalpani, M., & Pantaleone, D. (1994). An examination of the unusual susceptibilities of aminoglycans to enzymatic hydrolysis. *Carbohydrate Research*, *256*, 159–175.

Příloha P3

Kašparová J., **Korecká L.***, Pepeliaev S., Bílková Z., Smirnou D., Velebný V., Česlová L. Magnetic macroporous bead cellulose functionalised with recombinant hyaluronan lyase for controllable hyaluronan fragmentation. *Process Biochemistry,* **72**, 2018, 105-111

IF_{2018} = 2,883; Q2 – Chemical engineering, Biochemistry; 0 citací [1. 7. 2020]

- koncepce výzkumu, plánování experimentů
- podíl na experimentální práci a vyhodnocení výsledků 30 %
- dílčí příprava a revize článku, korespondující autor

Process Biochemistry 72 (2018) 105–111

Contents lists available at ScienceDirect

Process Biochemistry

journal homepage: www.elsevier.com/locate/procbio

Magnetic macroporous bead cellulose functionalised with recombinant hyaluronan lyase for controllable hyaluronan fragmentation

Jitka Kašparová[a], Lucie Korecká[a,*], Stanislav Pepeliaev[b], Zuzana Bílková[a], Dzianis Smirnou[b], Vladimír Velebný[b], Lenka Česlová[c]

[a] Department of Biological and Biochemical Sciences, Faculty of Chemical Technology, University of Pardubice, Studentska 573, 532 10 Pardubice, Czech Republic
[b] Contipro a.s., 56201 Dolní Dobrouč, Dolní Dobrouč 401, Czech Republic
[c] Department of Analytical Chemistry, Faculty of Chemical Technology, University of Pardubice, Studentska 573, 532 10 Pardubice, Czech Republic

ARTICLE INFO

Keywords:
Hyaluronan
Hyaluronan lyase
Enzyme immobilisation
Magnetic beads

ABSTRACT

Hyaluronic acid (HA) is a component of the extracellular matrix with important potential for biotechnological and pharmaceutical applications. However, the immunological effects of HA are strongly molecular weight-dependent; therefore, production of HA for therapeutic purposes requires control over the molecular weight of the product, as well as mild reaction conditions and elimination of bioactive impurities. Here, we produced and characterised biocompatible magnetic macroporous bead cellulose (MBC) functionalised with *Streptococcus pneumoniae* hyaluronan lyase (SpnHL) that are compatible with these requirements and optimised their reaction and storage conditions. Immobilisation of SpnHL on MBC via reductive amination or MBC with fixed iminodiacetic acid (MBC-IDA) via a His_8-tag had minimal impact on its catalytic activity. The MBC-IDA-SpnHL carrier showed excellent operational and storage stability, and both carriers enabled reproducible time-controlled fragmentation of highly viscous HMW HA solutions, yielding HA fragments of appropriate molecular weight. Thus, these carriers are suitable for numerous industrial and biotechnological applications.

1. Introduction

Hyaluronic acid (HA) is the main component of the extracellular matrix in mammals and is comprised of repeated β-D-glucuronate and *N*-acetyl-D-glucosamine disaccharide units connected by alternating β-(1-3) and β-(1-4) linkages. Despite its structural simplicity, HA has an exceptional role in many important physiological and pathological processes in mammals. The molecular weight of HA has a significant impact on its biological functions [1,2]; while high molecular weight HA (HMW-HA, reaching up to 8000 kDa) occurs in healthy tissues, acting as a space-filling and lubricating agent with immunosuppressive properties, low molecular weight HA (LMW-HA) plays an opposite role in activation of the immune system as a reporter of endogenous danger signals [3,4].

HA is frequently used in pharmaceutical and cosmetic products, including drug delivery systems, day-to-day cosmetic products, and joint supplements, and is one of the most important biocompatible materials used in such products [5–7]. However, because the immunological properties of HA depend on its molecular weight, the molecular weight distribution of HA must be strictly controlled to preserve the desired properties of the product, especially for pharmaceutical applications. Moreover, in the case of HA-based drug delivery systems, which exploit the hydrophilic and immunosuppressive properties of HA, the use of HA with a narrow size distribution enables the therapeutic effect of these systems to be controlled more precisely [8,9].

Several methods for the preparation of HA fragments with different size distributions have been already described [10–13]. However,

Abbreviations: EDTA, ethylenediamine tetraacetic acid; HA, hyaluronic acid; HMW, high molecular weight; IMAC, immobilised metal affinity chromatography; IPTG, isopropyl β-D-1-thiogalactopyranoside; LMW, low molecular weight; MALDI-MS, matrix-assisted laser desorption ionisation-mass spectrometry; MBC, magnetic macroporous bead cellulose; MBC-IDA, magnetic macroporous bead cellulose with fixed iminodiacetic acid; SDS-PAGE, sodium dodecyl sulfate-polyacrylamide gel electrophoresis; SpnHL, *Streptococcus pneumoniae* hyaluronan lyase; TBE-PAGE, Tris-borate EDTA-polyacrylamide gel electrophoresis; TIM, triosephosphate isomerase

* Corresponding author.
E-mail addresses: jitka.kasparova@upce.cz (J. Kašparová), lucie.korecka@upce.cz (L. Korecká), Stanislav.Pepeliaev@contipro.com (S. Pepeliaev), zuzana.bilkova@upce.cz (Z. Bílková), Dzianis.Smirnou@contipro.com (D. Smirnou), Vladimir.Velebny@contipro.com (V. Velebný), lenka.ceslova@upce.cz (L. Česlová).

https://doi.org/10.1016/j.procbio.2018.06.025
Received 22 February 2018; Received in revised form 21 June 2018; Accepted 27 June 2018
Available online 28 June 2018
1359-5113/

commonly used methods such as acid or alkaline hydrolysis and ultrasonic degradation necessitate harsh reaction conditions and result in non-specific fragmentation of HA, offering limited possibility to control the molecular weight distribution of the product. In contrast, enzymatic methods for HA degradation using hyaluronidases, including both eukaryotic hydrolases and prokaryotic lyases, enable HA degradation under mild, biocompatible conditions [13–15].

One limitation of the use of soluble enzymes for catalysis is that the product must be purified to remove the remaining enzyme and to prevent product contamination and uncontrolled substrate conversion. In contrast, enzymes immobilised on solid supports (non-magnetic or magnetic beads based on synthetic or biopolymeric materials) can be removed straightforwardly from the reaction product and offer a number of other advantages over soluble enzymes, including simple and rapid manipulation, reusability, increased enzyme stability, and stable kinetic parameters (Michaelis constant, K_M, and maximal velocity, v_{max}) [10–12]. Moreover, in the case of HA fragmentation, immobilisation of HA-degrading enzymes allows greater control over the fragmentation process, which should enable the production of low polydisperse HA fragments. Thus, immobilised HA-degrading enzymes should be a useful tool to produce HA fragments for therapeutic purposes.

In previous work, recombinant HA lyase from crude unclarified *Escherichia coli* lysate was immobilised on magnetic silica particles based on the principle of immobilised metal affinity chromatography (IMAC), with the goal of one-step purification and immobilisation of HA lyase. HA lyase produce specific fragments with unsaturated bond at its non-reducing end which is advantageously used for rapid spectrophotometric detection (at 232 nm) without necessity of further derivatization [16]. However, immobilised HA lyase systems have not been characterised in detail, and parameters such as the solid phase, immobilisation technique, binding conditions, and reaction conditions, which are crucial for the potential utilisation of immobilised HA lyase in biotechnological applications, have not been optimised. Therefore, the aim of this work was to produce and characterise ready-to-use bioactive carriers consisting of recombinant *Streptococcus pneumoniae* hyaluronan lyase (SpnHL) immobilised on solid-phase supports, and to optimise the conditions for enzyme immobilisation and the subsequent reaction conditions to enable preparation of LMW-HA with a well-defined number of disaccharide units. We used biocompatible macroporous bead cellulose, 80–100 μm in size, with superparamagnetic properties, as these superparamagnetic particles were well-suited to our purposes [17–19].

2. Experimental

2.1. Chemicals

High molecular weight hyaluronic acid sodium salt from *Streptococcus equi* (1.5–1.8 MDa, ≤1% protein), D-saccharic acid 1,4-lactone monohydrate, isopropyl β-D-1-thiogalactopyranoside (IPTG), and sodium periodate were purchased from Sigma Aldrich (St. Louis, MO, USA). Recombinantly prepared *S. pneumoniae* hyaluronan lyase in *E. coli* expression system (estimated enzyme activity, 83 U/mg total protein; protein concentration, 2.1 mg/mL) with a His_8-tag was produced by Contipro, a.s. (Dolní Dobrouč, Czech Republic). Magnetic macroporous bead cellulose (MBC) and MBC with fixed iminodiacetic acid (MBC-IDA) were produced by Iontosorb (100 mg, Fe_3O_4 content ≥30% as a proportion of dry matter, inner diameter 80–100 μm) (Ústí nad Labem, Czech Republic). Protein ladders for gel electrophoresis (Precision Plus Protein™ Unstained Standards 10–250 kDa) were obtained from Bio-Rad (Hercules, CA, USA). All other chemicals were supplied by Lach-Ner (Neratovice, Czech Republic) and were of reagent grade.

2.2. Fermenter expression of S. pneumoniae hyaluronan lyase

Fermenter cultures were prepared in 1-L Multifors and 30-L Techfors fermenters (Infors HT, Bottmingen, Switzerland). Inocula were prepared by cultivating the *E. coli* expression strain BL21-AI transformed with pET-derived plasmid carrying the sequence of hyaluronate lyase gene (Genbank ID ACO21275.1 lacking first 285 amino acids) in 100 mL (for 1-L Multifors) or 400 mL (for 30-L Techfors) Terrific Broth medium (12 g/L tryptone, 24 g/L yeast extract, 5 g/L glycerol, 2.3 g/L KH_2PO_4, 12.5 g/L K_2HPO_4). The inocula were incubated at 37 °C overnight with shaking at 150 rpm. Cells were cultivated in 0.5 L or 20 L Terrific Broth medium for the Multifors and Techfors fermenters, respectively. The cells were cultured until the A_{600} reached 0.1, then expression was induced by the addition of 1 mM IPTG. Simultaneously, to support expression, an additional 20 g/L glycerol was added as a carbon source. During cultivation, the temperature and pH were maintained at 37 °C and 7.0, respectively. To maintain cell growth, the oxygen level was monitored and adjusted by glycerol feed; approximately 1 kg glycerol was used for one 20-L culture.

2.3. Isolation, purification, and characterisation of recombinant hyaluronan lyase

E. coli biomass was harvested by centrifugation at 17,600 × *g* for 10 min in a Sorvall Lynx 6000 centrifuge (Thermo Fisher Scientific, Waltham, MA, USA) precooled to 4 °C. Cells were resuspended in lysis buffer (50 mM sodium phosphate buffer, 500 mM NaCl, pH 8) at a 1:3 ratio and then disrupted by sonication in 200 mL batches (10 × 1 min cycles, with 5 min cooling on ice between each cycle). The enzyme-containing soluble fraction of the lysate was separated from cell debris by centrifugation at 17,600 × *g* for 10 min at 10 °C.

The lysate was then subjected to IMAC purification on a 50-mL column filled with IDA/Ni 100 resin (Iontosorb, Ústí nad Labem, Czech Republic). Prior to purification, the IMAC column was equilibrated with three volumes of loading buffer (50 mM sodium phosphate buffer, 500 mM NaCl, pH 8; constant flow rate of 5 mL/min). The lysate was diluted three-fold in loading buffer and loaded onto the column at a ratio of 20 mg total protein per 1 mL sorbent. The column was thoroughly washed with loading buffer containing 20 mM imidazole, and the protein was eluted in loading buffer supplemented with 200 mM imidazole. The fraction containing the eluted enzyme was concentrated and exchanged into loading buffer using a 50 kDa ultrafilter (Spectrum Laboratories, Inc., Rancho Dominguez, CA, USA). The concentrated sample was diluted in glycerol to give a final glycerol concentration of 50% (w/w). The resulting enzyme solution with concentration of 2.1 mg/mL was stable for months when stored at −20 °C.

The total protein concentration in the samples was determined using a standard Bradford assay [20] with bovine serum albumin (BSA) as standard protein. The identity of the enzyme was confirmed by matrix-assisted laser desorption ionisation mass spectrometry (MALDI-MS) using a MALDI LTQ Orbitrap XL instrument (Thermo Scientific, Waltham, MA, USA), and the purity of the enzyme was assessed by sodium dodecyl sulfate-polyacrylamide gel electrophoresis (SDS-PAGE).

2.4. SpnHL activity assay

Determination of enzyme activity was performed as described previously, with slight modifications [21–23]. Enzyme activity was measured by spectrophotometric monitoring of the increase in absorbance at 230 nm caused by enzymatic degradation of the HA substrate using a Biochrom Libra S22 UV/Vis spectrophotometer (Biochrom Ltd., Cambridge, UK). One unit of enzyme activity was defined as the amount of enzyme required to catalyse the conversion of 1 μmol substrate in 1 min. The product concentration was evaluated using the Lambert-Beer equation, assuming an extinction coefficient of 5.5×10^3 L mol^{-1}

cm^{-1} [22]. For determination of SpnHL enzyme activity, 0.125– 0.66 μM substrate and 1 μg soluble enzyme or 20 μL settled carrier containing immobilised enzyme (MBC-SpnHL, MBC-IDA-SpnHL) was used. 0.1 M sodium phosphate buffer pH 7.0 was used as the reaction buffer and as a diluent for the enzyme. HA was dissolved in 0.1 M phosphate buffer pH 6.0 containing 1 M NaCl and 1.5 mM D-saccharic acid 1,4-lactone monohydrate to eliminate incidental β-glucuronidase activity and to ensure that substrate conversion occurred via a lyase mechanism [24]. The products of enzymatic substrate conversion were additionally confirmed by native Tris-borate EDTA-polyacrylamide gel electrophoresis (TBE-PAGE) combined with alcian blue and silver staining according to a previously published protocol [25,26]. The following conditions were used for separation: 200 V, 30 mA, 45 min, 15% gel.

2.5. Immobilisation of SpnHL on magnetic macroporous bead cellulose

Immobilisation of SpnHL on magnetic macroporous bead cellulose (MBC) was performed using a standard method based on periodate oxidation of MBC according to a previously published protocol with slight modifications [25,27]. One millilitre of settled MBC was washed 10 times with deionised water to remove storage stabilisers. Hydroxyl functional groups were oxidised by the addition of 1 mL 0.2 M sodium periodate and incubation at room temperature for 90 min with gentle mixing. The beads were washed 10 times with deionised water, and then functionalised by the addition of 250 μg SpnHL (equivalent to 21 mU) dissolved in deionised water, followed by gentle mixing and incubation for 1 h at room temperature. The resulting carrier (MBC-SpnHL) was washed 10 times with deionised water and stored at 4 °C. The SpnHL immobilisation efficiency was estimated using standard Tris/glycine SDS-PAGE with silver staining.

2.6. Immobilisation of SpnHL on magnetic macroporous bead cellulose with fixed iminodiacetic acid

Standard IMAC chemistry was used for immobilisation of SpnHL on magnetic macroporous bead cellulose with fixed iminodiacetic acid (MBC-IDA), according to a previously published protocol with some modifications [28]. MBC-IDA was pre-activated using $CoCl_2$ as a chelating agent rather than the commonly used $NiSO_4$. Firstly, magnetic beads were washed 10 times with deionised water to remove storage stabilisers. MBC-IDA beads were then charged by the addition of 0.4 M $CoCl_2$ followed by gentle mixing for 3 min. After chelation, oxidation was achieved by the addition of 1 mL 0.05% hydrogen peroxide. Next, the magnetic beads were washed 10 times with deionised water and functionalised by the addition of 250 μg SpnHL (equivalent to 21 mU) dissolved in deionised water and incubation at room temperature for 1 h with gentle mixing. The resulting carrier (MBC-IDA-SpnHL) was washed 10 times with deionised water and stored at 4 °C. The SpnHL immobilisation efficiency was estimated using standard Tris/glycine SDS-PAGE with silver staining.

2.7. Kinetic parameters of MBC-SpnHL and MBC-IDA-SpnHL

The kinetic parameters of MBC-SpnHL and MBC-IDA-SpnHL were evaluated using the enzyme assay described in Section 2.4. The substrate, HA, was used in the concentration range 0.1–0.5 μM, together with 6 mU (72.3 ng) soluble enzyme or 20 μL settled beads (5 μg SpnHL) for the carriers (MBC-SpnHL and MBC-IDA-SpnHL). Assays were performed at room temperature in 0.1 M phosphate buffer pH 7.0 in a final reaction volume of 1 mL, and the reaction was monitored by measuring the increase in absorbance of the HA degradation products at 10 s intervals for 400 s or at 2 min intervals for 20 min for the soluble and immobilised enzymes, respectively. All samples were measured in triplicate. Kinetic parameters (K_M and v_{max}) were evaluated using a standard Lineweaver-Burk plot.

3. Results and discussion

3.1. Purification and characterisation of recombinant hyaluronan lyase

Recombinant hyaluronan lyase from *S. pneumoniae* (SpnHL) was selected for immobilisation and HA fragmentation not only because this enzyme is well-characterised, and its mechanism and catalytic parameters are known [23], but also for its bacterial origin, which is instead of a mammalian enzyme (e.g. Hyaluronidase form bovine testes) more advantageous for bioapplications. Recombinant SpnHL was expressed in an *E. coli* expression system by fermenter cultivation. The enzyme was expressed with a His_8-tag for purification by IMAC and for oriented attachment of the enzyme onto magnetic beads. The identity of the purified enzyme was confirmed by MALDI-MS, and its purity was evaluated by SDS-PAGE. Both methods confirmed presence of SpnHL with approximate molecular weight 78 kDa and highlighted the presence of contaminating proteins, principally triosephosphate isomerase (TIM), which is a typical contaminant of recombinant enzymes prepared in *E. coli* expression systems [29]. Nevertheless, given that the amount of TIM in the SpnHL preparation was low and that the substrate and reaction mechanism of TIM are entirely different to those of SpnHL, further purification of the enzyme was considered unnecessary. Another unidentified contaminant with size about 35 kDa is presented in the sample which identity was repeatedly not able to prove by same technique probably due to insufficient tryptic cleavage.

The enzyme activity of SpnHL was evaluated spectrophotometrically by measuring the increase in absorbance at 230 nm resulting from release of disaccharide units during fragmentation of the HMW-HA substrate (Fig. 1A). The activity of the purified SpnHL sample was 83 U/mg protein, where one unit is defined as the amount of enzyme required to catalyse the conversion of 1 μmol substrate in 1 min. Formation of HA fragments composed of various numbers of disaccharide units was also confirmed by the appearance of ladder-like bands on native TBE-PAGE gels. Electrophoretic separation of reaction mixtures incubated for various time periods (1 min to 24 h) showed a gradual shift in the size distribution of the HA substrate from HMW-HA to LMW-HA and even HA oligosaccharides (Fig. 1B).

3.2. Immobilisation of SpnHL on magnetic beads

Two types of magnetic beads, hydrophilic magnetic macroporous bead cellulose (MBC) and macroporous bead cellulose with fixed iminodiacetic acid (MBC-IDA), were used for non-oriented and oriented immobilisation of SpnHL, respectively. These biocompatible magnetic beads have several features that are highly useful for biomedical applications, including hydrophilicity, non-toxicity, low non-specific sorption, and high surface area for specific binding. The high content of ferrous oxides (minimum 30% as a percentage of dry matter) in these magnetic beads provides a strong magnetic response, which can be used to efficiently separate the product from the immobilised enzyme. Covalent linkage of recombinant SpnHL onto MBC was performed using a standard reductive amination strategy, in which hydroxyl functional groups on the magnetic beads are converted via periodate oxidation to aldehyde groups, which react with amine groups on the enzyme; the mechanism for this reaction has been described in detail by Hermanson [30]. In the case of MBC-IDA, the His_8-tag of the enzyme was exploited for site-directed immobilisation, based on the interaction between the Co^{3+} ions of the MBC-IDA beads and the His_8-tag of the enzyme. This method has the advantage of combining immobilisation and affinity purification in a single step.

To achieve the highest possible immobilisation efficiency, we optimised the conditions for the immobilisation reaction by varying the buffer composition (phosphate buffer, acetate buffer, and deionised water alone), buffer pH, amount of enzyme, and reaction time. The suitability of each condition for the immobilisation reaction was assessed in terms of binding efficiency, which was evaluated by SDS-

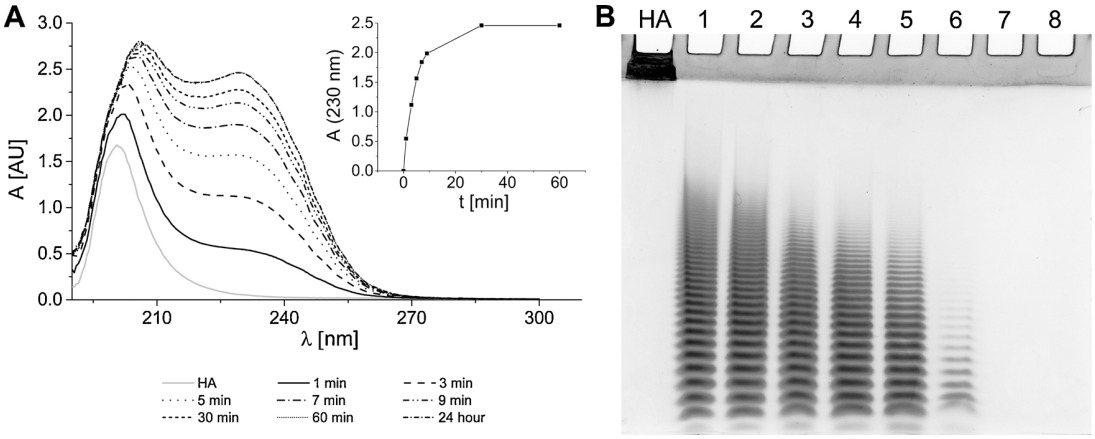

Fig. 1. Monitoring of time-dependent high molecular weight hyaluronic acid (HA) fragmentation by recombinant *Streptococcus pneumoniae* hyaluronan lyase. A) UV spectrum of HA (190–300 nm) as a function of reaction time; inset graph, absorbance at 230 nm as a function of reaction time, indicative of formation of the fragmentation product containing unsaturated bonds, B) Changes in the molecular weight of HA during enzymatic fragmentation monitored by TBE-PAGE showing typical ladder. HA, original HA sample; (1) 1 min; (2) 3 min; (3) 5 min; (4) 7 min; (5) 9 min; (6) 30 min; (7) 60 min; (8) 24 h.

PAGE of the reaction mixture after SpnHL immobilisation combined with silver staining, and enzyme activity, which was evaluated by spectrophotometric enzyme assays. To identify the optimal amount of SpnHL for immobilisation on each type of beads (MBC, MBC-IDA), varying amounts of SpnHL (10 µg to 1.25 mg) were immobilised on 1 mL of settled beads. The optimal amount of SpnHL for immobilisation on both types of beads was determined to be 250 µg, reflecting the protein consumption vs. enzyme activity (data not shown). Possible release of the enzyme from the beads was assessed by application of 1% trifluoroacetic acid to 20–100 µL settled beads for 30 min at room temperature followed by SDS-PAGE. SDS-PAGE analysis did not reveal release of the enzyme from any of the carriers (data not shown).

Comparison of the enzyme activities obtained after immobilisation of SpnHL on MBC and MBC-IDA under different conditions showed that the pH, molarity, and ion composition of the binding solution had little impact on the enzyme activity of the functionalised beads (Table 1). Indeed, use of deionised water rather than a buffer as the binding solution resulted in comparable enzyme activity; thus, given its versatility, deionised water was used for both enzyme immobilisation and storage of the beads. Furthermore, approximate immobilisation efficiency was estimated by comparative densitometric SDS-PAGE analysis of samples collected before and after the immobilisation procedure (Fig. 2). The SDS-PAGE analysis confirmed the results of the enzyme assays and showed that the immobilisation efficiency reached nearly 100% when deionised water was used as the binding solution (97% for MBC-SpnHL, 99% for MBC-IDA-SpnHL). Moreover, a reaction time of 1 h was sufficient for near-complete immobilisation (Fig. 2).

Table 1
Spectrophotometric evaluation of MBC-SpnHL and MBC-IDA-SpnHL binding efficiency by measurement of enzyme activity following immobilisation under different conditions. Reaction conditions: 225 µg hyaluronic acid, 20 µL settled MBC-SpnHL or MBC-IDA-SpnHL, reaction time 50 min, reaction buffer 0.1 M phosphate buffer pH 7.0. Enzyme activity was assessed by monitoring the increase in absorbance at 230 nm. Immobilisation medium: PB, 0.1 M phosphate buffer pH 7.0; AcB, 0.1 M acetate buffer pH 5.0; PBS, phosphate-buffered saline pH 7.0; DIW, deionised water.

	A (230 nm)					
Binding solutions	0.1 M PB pH 7.0	0.01 M PB pH 7.0	0.1 M AcB pH 5.0	0.01 M AcB pH 5.0	PBS	DIW
MBC-SpnHL (20 µL)	0.814	2.295	2.293	2.435	0.977	2.354
MBC-IDA-SpnHL (20 µL)	1.774	2.438	2.489	2.236	1.441	2.429

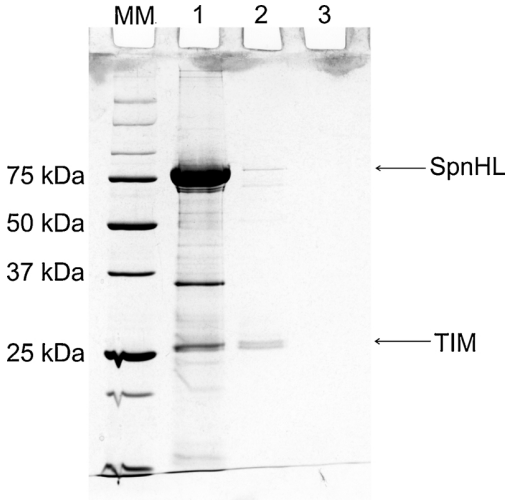

Fig. 2. SDS-PAGE analysis for estimation of the efficiency of hyaluronan lyase immobilisation on MBC and MBC-IDA beads. MM, protein molecular weight standard (10–250 kDa, BioRad); 1, *Streptococcus pneumoniae* hyaluronan lyase (SpnHL; 1 µg); 2, residual unbound enzyme after immobilisation on MBC beads (250 µg SpnHL/mL settled beads); 3, residual unbound enzyme after immobilisation on MBC-IDA beads (250 µg SpnHL/mL settled beads). TIM – triosephosphate isomerase. Ten microliters were applied to each well. Separation conditions: 180 V, 30 mA, 45 min, 12% gel, silver staining.

3.3. Characterisation of MBC-SpnHL and MBC-IDA-SpnHL carriers

Enzyme assays were performed to measure the enzyme activity per mL of settled carrier and the kinetic parameters of the MBC-SpnHL and MBC-IDA-SpnHL carriers. Given the potential biotechnological and pharmaceutical applications of the immobilised enzyme, we performed the enzyme assays under a variety of relevant reaction conditions, using phosphate buffers at neutral pH with varying molarity and with or without the chelating agent ethylenediamine tetraacetic acid (EDTA). Deionised water was also tested as a non-salting reaction medium. For both carriers, the highest enzyme activity was observed when 0.1 M phosphate buffer pH 7.0 without any chelating agent was used as the reaction buffer (Table 2), and all subsequent experiments were performed using this reaction buffer. Unexpectedly, the enzyme activity of

Table 2
Spectrophotometric evaluation of MBC-SpnHL and MBC-IDA-SpnHL enzyme activity measured in various reaction solutions. MBC-IDA-SpnHL was immobilised in deionised water. Reaction conditions: 225 µg hyaluronic acid, 20 µL settled MBC-SpnHL and MBC-IDA-SpnHL, reaction time 50 min. Reaction medium: PB – phosphate buffer pH 7.0 (0.1 M or 0.01 M), PB pH 7.0 containing 2 mM EDTA, DIW – deionised water.

	A (230 nm)				
Reaction solutions	0.1 M PB pH 7.0	0.01 M PB pH 7.0	0.1 M PB pH 7.0 + EDTA	0.01 M PB pH 7.0 + EDTA	DIW
MBC-SpnHL (20 µL)	2.354	1.197	1.733	1.568	1.76
MBC-IDA-SpnHL (20 µL)	2.429	2.055	1.752	1.826	1.477

the MBC-SpnHL bead preparation was higher than that of the MBC-IDA-SpnHL preparation (651 mU/mL settled beads and 216 mU/mL settled beads, respectively). Contrary to our expectations, the final activity of SpnHL immobilised orientally (MBC-IDA-SpnHL) was lower than the activity of enzyme immobilised randomly to the MBC beads. We suppose the cause of lower final enzyme activity per mL of settled carrier could be lower binding capacity per mL of settled MBC-IDA functionalised beads. Contrary to MBC-IDA-SpnHL, it is not guaranteed that the enzyme molecules are bound only in a monolayer in case of MBC-SpnHL beads. Both these factors could contribute to the final activity of carriers. However, the quality and utility of the carriers should be evaluated comprehensively, the operational and storage stabilities including (see chapter 3.4).

We also tested the effectiveness of the MBC-SpnHL and MBC-IDA-SpnHL beads for the degradation of highly viscous HA solutions, expecting that the high ferrous oxide content and large diameter (80–100 µm) of the beads would enable them to be homogenously resuspended even in highly viscous reaction mixtures. Indeed, both carriers were confirmed to be functional in highly viscous HA solutions (1.5 mg/mL and 2.5 mg/mL; Fig. 3).

For application of the newly prepared carriers in routine HMW-HA fragmentation, we measured the kinetic parameters (Michaelis constant, K_M, and maximal velocity, v_{max}) of soluble SpnHL (K_M 3.49 E-5 M, v_{max} 1.16 E-1 s) and both carriers (Fig. 4). These parameters reflect the affinity of the enzyme for the substrate (K_M) and the maximal reaction rate achieved when the enzyme is saturated with substrate (v_{max}). Kinetic parameters were tested at same ranges of substrate

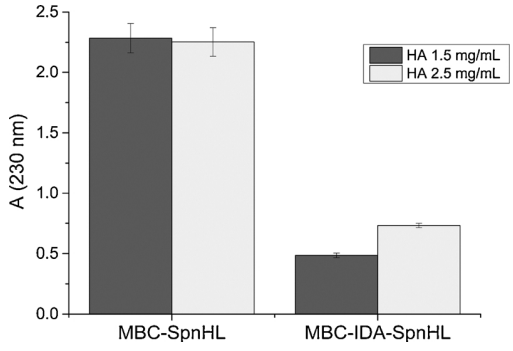

Fig. 3. Evaluation of MBC-SpnHL and MBC-IDA-SpnHL enzyme activity in highly viscous high molecular weight hyaluronic acid (HA) solutions using spectrophotometric enzyme assays. Reaction mixtures contained 1.5 mg/mL or 2.5 mg/mL HA and 20 µL of settled MBC-SpnHL (corresponding to enzyme activity equal to 13 mU) or MBC-IDA-SpnHL (corresponding to enzyme activity equal to 4.3 mU). Reaction was performed in 1 mL deionised water, reaction time 10 min. Experiments were performed in three aliquots of one sample series. Error bars represent standard deviation.

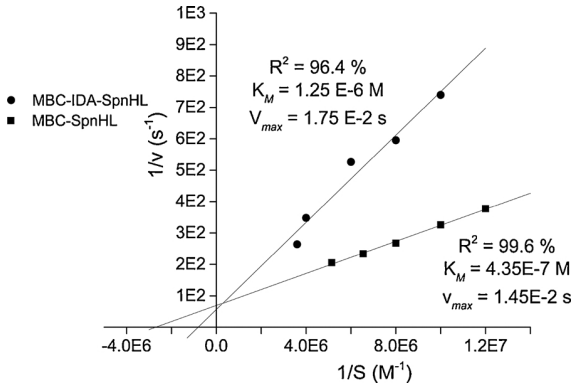

Fig. 4. Lineweaver-Burk plot for evaluation of kinetic parameters of MBC-SpnHL and MBC-IDA-SpnHL carriers. Both carriers MBC-SpnHL (squares), MBC-IDA-SpnHL (dots), were applied in 20 µL aliquots. Measurements were performed in triplicate. K_M, Michaelis constant; v_{max}, maximum velocity.

concentrations. To compare the kinetic parameters, the soluble SpnHL was used in amount of 6 mU ranging to total enzyme activities of both carries (561 mU per mL, resp. 13 mU per used aliquot of MBC-SpnHL beads; 231 mU per mL, resp. 4.3 mU per used aliquot of MBC-IDA-SpnHL beads). The results showed that the catalytic activity of the enzyme was not negatively influenced by immobilisation. Moreover, the kinetic parameters showed higher affinity as well as fragmentation velocity for both carriers in comparison with soluble enzyme. The substrate specificity even after immobilization of the enzyme to selected magnetic beads was unchanged as it was confirmed by three analytical methods, spectrophotometrically, high performance liquid chromatography with fluorescent as well as mass spectrometry detection (data not shown).

3.4. Stability of MBC-SpnHL and MBC-IDA-SpnHL

For routine and reproducible application of the MBC-SpnHL and MBC-IDA-SpnHL carriers in HA fragmentation, storage and operational stabilities are essential. We therefore assessed the stability of these carriers using spectrophotometric enzyme assays, aiming to identify storage and reaction conditions under which the enzyme activity remained > 80% of the initial enzyme activity (measured immediately after immobilisation).

Operational stability was tested using the optimised reaction buffer (0.1 M phosphate buffer pH 7.0), as well as a model solution, 1 mM NaCl, to assess whether the prepared carriers would be suitable for applications requiring low-salt reaction mixtures. Both MBC-SpnHL and MBC-IDA-SpnHL showed high operational stability in 0.1 M phosphate buffer pH 7.0, with enzyme activity remaining over 80% of the initial enzyme activity after five consecutive runs (Fig. 5) and after subsequent overnight storage, both carriers were successfully used for further fragmentation reactions. Conversely, 1 mM NaCl as a reaction solution achieved comparable results only for MBC-IDA-SpnHL.

It is also necessary for the SpnHL carriers to have reproducible long-term storage stability to minimise the time spent on carrier preparation. We monitored the storage stability of both carriers in deionised water at 4 °C; this temperature was chosen to minimise any potential microbial overgrowth and is usually used for storage of ready-to-use carriers. The enzyme activity of each bead preparation was periodically measured in 0.1 M phosphate buffer pH 7.0 and compared with the initial enzyme activity. Whereas the enzyme activity of MBC-SpnHL decreased rapidly during storage, MBC-IDA-SpnHL retained 95% activity even after 6 weeks of storage (Fig. 6). Similar results were obtained when the carriers were stored in 0.1 M phosphate buffer pH 7.0 (data not shown). Our results suggest that the immobilisation strategy (random covalent vs. site-directed affinity-based immobilisation) can significantly

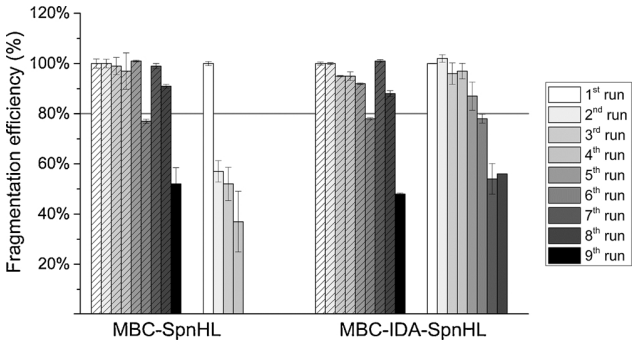

Fig. 5. Operational stability of MBC-SpnHL and MBC-IDA-SpnHL. The reaction mixtures contained 225 µg hyaluronic acid and 20 µL settled carrier in 0.1 M phosphate buffer pH 7.0 (dashed) or 1 mM NaCl (solid). Experiments were performed in three aliquots of one sample series using spectrophotometric enzyme assay. After 6th run overnight incubation followed due to analysis time and measurement continued next day. Straight horizontal line represented 80% of the initial enzyme activity. Error bars represent standard deviation.

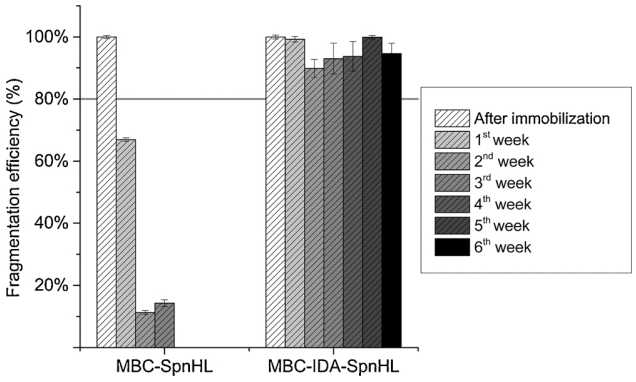

Fig. 6. Storage stability of MBC-SpnHL and MBC-IDA-SpnHL at 4 °C in deionised water. The reaction mixtures contained 225 µg hyaluronic acid and 20 µL settled carrier in 0.1 M phosphate buffer pH 7.0. Experiments were performed in three aliquots using spectrophotometric enzyme assay. Straight horizontal line represented 80% of the initial enzyme activity. Error bars represent standard deviation.

influence the operational and storage stability of SpnHL carriers.

Altogether, our results confirm the advantages of immobilisation of SpnHL on magnetic beads for controllable fragmentation of highly viscous HMW-HA. The magnetic properties of macroporous bead cellulose combined with the characteristics resulting from the natural origin of cellulose, including its low price, yielded an excellent tool for large-scale HA fragmentation for *in vivo* applications. The use of magnetically active carriers simplifies all procedures related to mixing of reagents and solid-phase separation and avoids the limitations of soluble enzyme related to the requirements for enzyme inactivation and quantitative separation.

4. Conclusion

The dependence of the immunological properties of HA on its molecular weight, together with the biotechnological requirements for HA, prompted the preparation and thorough characterisation of enzymatically active carriers presenting immobilised *Streptococcus pneumoniae* hyaluronan lyase (SpnHL). SpnHL was successfully immobilised on hydrophilic and non-toxic magnetic beads, specifically magnetic macroporous bead cellulose (MBC) and MBC with fixed iminodiacetic acid (MBC-IDA). Both enzymatically active carriers (MBC-SpnHL and MBC-IDA-SpnHL) were characterised in terms of enzyme activity, kinetic parameters, operational stability, and storage stability. Both carriers exhibited high operational stability, with the enzyme retaining > 80% of its initial activity over five consecutive runs in phosphate buffer. Moreover, MBC-IDA-SpnHL displayed comparable stability in phosphate buffer and 1 mM NaCl solution. Both carriers were functional in highly viscous HA solutions, which would be beneficial for further industrial applications. Whereas MBC-SpnHL displayed low storage stability, MBC-IDA-SpnHL retained > 80% of its initial enzyme activity even after 6 weeks of storage at 4 °C.

Altogether, our results show that immobilisation of SpnHL on magnetic beads yields enzymatically active carriers with high stability, activity, and specificity that can be used under mild reaction conditions. The carriers developed in this study combine the operational advantages of magnetic beads, including rapid, simple, and accurate manipulation, with the controllable catalysis of enzymes, even in highly viscous HA solutions. Moreover, the use of enzymes immobilised on magnetic beads, which are quickly and easily separated from the product, minimises the possibility of protein contaminants and residual enzyme activity in the final product. Compare to soluble enzyme, the developed enzyme carriers reduce the total cost of the catalytic process, make the catalytic process simpler and more robust for end-users, and should enable the routine production of low molecular weight HA or even HA oligosaccharides from high molecular weight HA.

Acknowledgement

This work was supported by research project of University of Pardubice SGS_2017_004.

References

[1] M.K. Cowman, H.-G. Lee, K.L. Schwertfeger, J.B. McCarthy, E.A. Turley, The content and size of hyaluronan in biological fluids and tissues, Front. Immunol. 6 (2015) 261, https://doi.org/10.3389/fimmu.2015.00261.
[2] D. Vigetti, E. Karousou, M. Viola, S. Deleonibus, G. De Luca, A. Passi, Hyaluronan: biosynthesis and signaling, Biochim. Biophys. Acta - Gen. Subj. 1840 (2014) 2452–2459, https://doi.org/10.1016/j.bbagen.2014.02.001.
[3] P.L. Bollyky, M. Bogdani, J.B. Bollyky, R.L. Hull, T.N. Wight, The role of hyaluronan and the extracellular matrix in islet inflammation and immune regulation, Curr. Diab. Rep. 12 (2012) 471–480, https://doi.org/10.1007/s11892-012-0297-0.
[4] D. Jiang, J. Liang, P.W. Noble, Hyaluronan as an immune regulator in human diseases, Physiol. Rev. 91 (2011) 221–264, https://doi.org/10.1152/physrev.00052.2009.
[5] S. Kaya, D. Schmidl, L. Schmetterer, K.J. Witkowska, A. Unterhuber, V. Aranha, C. Baar, G. Garho, Effect of hyaluronic acid on tear film thickness as assessed with ultra-high resolution optical coherence tomography, Acta Ophthalmol. (2015) 439–443, https://doi.org/10.1111/aos.12647.
[6] A. Sionkowska, B. Kaczmarek, M. Michalska, K. Lewandowska, Conference paper preparation and characterization of collagen/chitosan/hyaluronic acid thin films for application in hair care cosmetics, Pure Appl. Chem. 89 (2017) 1829–1839.
[7] S. Bowman, M.E. Awad, M.W. Hamrick, M. Hunter, S. Fulzele, Recent advances in hyaluronic acid based therapy for osteoarthritis, Clin. Transl. Med. (2018), https://doi.org/10.1186/s40169-017-0180-3.
[8] N. Volpi, J. Schiller, R. Stern, L. Soltés, Role, metabolism, chemical modifications and applications of hyaluronan, Curr. Med. Chem. 16 (2009) 1718–1745, https://doi.org/10.2174/092986709788186138.
[9] R. Stern, a Asari, K. Sugahara, Hyaluronan fragments: an information-rich system, Eur. J. Cell. Biol. 85 (2006) 699–715, https://doi.org/10.1016/j.ejcb.2006.05.009.
[10] R. Fernandez-Lafuente, Stabilization of multimeric enzymes: strategies to prevent subunit dissociation, Enzyme Microb. Technol. 45 (2009) 405–418, https://doi.org/10.1016/j.enzmictec.2009.08.009.
[11] B. Brena, P. González-Pombo, F. Batista-Viera, Immobilization of enzymes: a literature survey, Methods Mol. Biol. 1051 (2013) 15–31, https://doi.org/10.1007/978-1-62703-550-7_2.
[12] C. Mateo, J.M. Palomo, G. Fernandez-lorente, J.M. Guisan, R. Fernandez-lafuente, Improvement of enzyme activity, stability and selectivity via immobilization techniques, Enzyme Microb. Technol. 40 (2007) 1451–1463, https://doi.org/10.1016/j.enzmictec.2007.01.018.
[13] D. Šmejkalová, M. Hermannová, R. Buffa, D. Čožíková, L. Vištejnová, Z. Matulková, J. Hrabica, V. Velebný, Structural characterization and biological properties of degradation byproducts from hyaluronan after acid hydrolysis, Carbohydr. Polym. 88 (2012) 1425–1434, https://doi.org/10.1016/j.carbpol.2012.02.031.
[14] M.S. Akhtar, V. Bhakuni, Streptococcus pneumoniae hyaluronate lyase contains Two Non-cooperative independent Folding/Unfolding structural domains: characterization of functional domain and inhibitors of enzyme, J. Biol. Chem. 278 (2003) 25509–25516, https://doi.org/10.1074/jbc.M301894200.
[15] Y. Tokita, A. Okamoto, Hydrolytic degradation of hyaluronic acid, Polym. Degrad.

Stab. 48 (1995) 269–273, https://doi.org/10.1016/0141-3910(95)00041-J.
[16] P.-F. Yang, C.-K. Lee, Direct purification and immobilization of recombinant hyaluronan lyase from unclarified feedstock using immobilized metal affinity magnetite for oligo-hyaluronan preparation, Biochem. Eng. J. 37 (2007) 108–115, https://doi.org/10.1016/j.bej.2007.04.001.
[17] F. Wang, C. Guo, C.Z. Liu, Functional magnetic mesoporous nanoparticles for efficient purification of laccase from fermentation broth in magnetically stabilized fluidized bed, Appl. Biochem. Biotechnol. 171 (2013) 2165–2175, https://doi.org/10.1007/s12010-013-0503-9.
[18] M.A.M. Gijs, F. Lacharme, U. Lehmann, Microfluidic applications of magnetic particles for biological analysis and catalysis, Chem. Rev. 110 (2010) 1518–1563, https://doi.org/10.1021/cr9001929.
[19] N. Pamme, On-chip bioanalysis with magnetic particles, Curr. Opin. Chem. Biol. 16 (2012) 436–443, https://doi.org/10.1016/j.cbpa.2012.05.181.
[20] M.M. Bradford, A rapid and sensitive method for the quantitation of microgram quantities of protein utilizing the principle of protein-dye binding, Anal. Biochem. 72 (1976) 248–254, https://doi.org/10.1016/0003-2697(76)90527-3.
[21] W.L. Hynes, J.J. Ferretti, Assays for hyaluronidase activity, Methods Enzymol. 235 (1994) 606–616, https://doi.org/10.1016/0076-6879(94)35174-0.
[22] M.J. Jedrzejas, R.B. Mewbourne, L. Chantalat, D.T. McPherson, Expression and purification of streptococcus pneumoniae hyaluronate lyase from Escherichia coli, Protein Expr. Purif. 13 (1998) 83–89, https://doi.org/10.1006/prep.1997.0864.
[23] S.J. Kelly, K.B. Taylor, S. Li, M.J. Jedrzejas, Kinetic properties of streptococcus pneumoniae hyaluronate lyase, Glycobiology 11 (2001) 297–304, https://doi.org/10.1093/glycob/11.4.297.
[24] T. Takahashi, M. Ikegami-Kawai, R. Okuda, K. Suzuki, A fluorimetric morgan-elson assay method for hyaluronidase activity, Anal. Biochem. 322 (2003) 257–263, https://doi.org/10.1016/j.ab.2003.08.005.
[25] L. Holubova, L. Korecka, S. Podzimek, V. Moravcova, J. Rotkova, T. Ehlova, V. Velebny, Z. Bilkova, Enhanced multiparametric hyaluronan degradation for production of molar-mass-defined fragments, Carbohydr. Polym. 112 (2014) 271–276, https://doi.org/10.1016/j.carbpol.2014.05.096.
[26] M. Ikegami-Kawai, T. Takahashi, Microanalysis of hyaluronan oligosaccharides by polyacrylamide gel electrophoresis and its application to assay of hyaluronidase activity, Anal. Biochem. 311 (2002) 157–165 http://www.ncbi.nlm.nih.gov/pubmed/12470675.
[27] L. Kuchař, J. Rotková, B. Asfaw, J. Lenfeld, D. Horák, L. Korecká, Z. Bílková, J. Ledvinová, Semisynthesis of C17:0 isoforms of sulphatide and glucosylceramide using immobilised sphingolipid ceramide N-deacylase for application in analytical mass spectrometry, Rapid Commun. Mass. Spectrom. 24 (2010) 2393–2399, https://doi.org/10.1002/rcm.4659.
[28] P. Přikryl, D. Horák, M. Tichá, Z. Kučerová, Magnetic IDA-modified hydrophilic methacrylate-based polymer microspheres for IMAC protein separation, J. Sep. Sci. 29 (2006) 2541–2549, https://doi.org/10.1002/jssc.200600248.
[29] G. Kozlov, R. Vinaik, K. Gehring, Triosephosphate isomerase is a common crystallization contaminant of soluble his-tagged proteins produced in Escherichia coli, Acta Crystallogr. Sect. F Struct. Biol. Cryst. Commun. 69 (2013) 499–502, https://doi.org/10.1107/S1744309113010841.
[30] G.T. Hermanson, Bioconjugate Techniques, Third ed., (2013), pp. 1–1146, https://doi.org/10.1016/C2009-0-64240-9.

Příloha P4

Kuchař L., Rotková J., Asaw B., Lenfeld J., Horák D., **Korecká L.**, Bílková Z., Ledvinová J. Semisynthesis of C17:0 isoforms of sulphatide and glucosylceramide using immobilised sphingolipid ceramide N-deacylase for application in Analytical mass spectrometry. *Rapid Communications in Mass Spectrometry,* **24**, 2010, 2393-2399

IF_{2018} = 2,045; Q2 – Chemical sciences; 10 citací [1. 7. 2020]

- podíl na experimentální práci a vyhodnocení výsledků 15 %
- dílčí příprava a revize článku

RAPID COMMUNICATIONS IN MASS SPECTROMETRY
Rapid Commun. Mass Spectrom. 2010; **24**: 2393–2399
Published online in Wiley InterScience (www.interscience.wiley.com) DOI: 10.1002/rcm.4659

RCM

Semisynthesis of C17:0 isoforms of sulphatide and glucosylceramide using immobilised sphingolipid ceramide N-deacylase for application in analytical mass spectrometry

L. Kuchař[1], J. Rotková[2], B. Asfaw[1], J. Lenfeld[3], D. Horák[3], L. Korecká, Z. Bílková[2] and J. Ledvinová[1]***

[1]Institute of Inherited Metabolic Disorders, General Faculty Hospital and Charles University First Faculty of Medicine, Prague, Czech Republic
[2]University of Pardubice, Faculty of Chemical Technology, Department of Biological and Biochemical Sciences, Academy of Sciences of the Czech Republic, Prague, Czech Republic
[3]Institute of Macromolecular Chemistry, Academy of Sciences of the Czech Republic, Prague, Czech Republic

Received 21 April 2010; Revised 2 June 2010; Accepted 7 June 2010

Sphingolipid ceramide N-deacylase (SCDase, EC 3.5.1.69) is a hydrolytic enzyme isolated from *Pseudomonas* sp. TK 4. In addition to its primary deacylation function, this enzyme is able to reacylate lyso-sphingolipids under specific conditions. We immobilised this enzyme on magnetic macroporous cellulose and used it to semisynthesise C17:0 glucosylceramide and C17:0 sulphatide, which are required internal standards for quantification of the corresponding glycosphingolipids (GSL) by tandem mass spectrometry. A high rate of conversion was achieved for both lipids (80% for C17:0 sulphatide and 90% for C17:0 glucosylceramide). In contrast to synthesis with a soluble form of the enzyme, use of immobilised SCDase significantly reduced the contamination of the sphingolipid products with other isoforms, so further purification was not necessary. Our method can be effectively used for the simple preparation of specifically labelled sphingolipids of high isoform purity for application in mass spectrometry. Copyright © 2010 John Wiley & Sons, Ltd.

Sphingolipids (SFL) are complex molecules composed of a hydrophobic ceramide (N-acylsphingoid) and a hydrophilic portion, with either a saccharide or phosphorylcholine moiety. In glycosphingolipids (GSL), oligosaccharide chains of varying complexity are attached by their reducing end to the terminal hydroxyl group of the sphingoid.[1]

Recently, tandem mass spectrometry (MS/MS) has become very useful for analysis and quantification of sphingolipids in different biological materials. For this purpose, sphingolipid species that are not abundant in nature are required as internal standards (IST).

In recent years, an enzymatic reaction catalyzed by sphingolipid ceramide N-deacylase (SCDase, EC 3.5.1.69) was found to be effective for the preparation of specific sphingolipid molecules.[2–7] The enzyme is an acid hydrolase isolated from the culture medium of the bacteria *Pseudomonas* sp. TK4 by ammonium sulphate precipitation and high-performance liquid chromatography (HPLC) purification. Its substrate specificity is not identical to that of acid ceramidase (EC 3.5.1.23).[4]

**Correspondence to*: J. Ledvinová, Ke Karlovu 2 (Building D), 128 00 Prague 2, Czech Republic.
E-mail: jledvin@cesnet.cz
***Correspondence to*: Z. Bílková, Studentska 95, 532 10 Pardubice, Czech Republic. E-mail: Zuzana.Bilkova@upce.cz

The molecular mass of the SCDase protein is 52 kDa. SCDase has optimal activity at pH 5–6 (hydrolysis) and is stable between pH 4–9; it is potently inhibited by Hg^{2+}, Cu^{2+} and Zn^{2+}, maintains 80% of its initial activity after 30 min at 60°C and can be stored at −85°C for 2 months without any loss of activity. The addition of Triton X-100 at concentrations of 0.4–0.8% increases its hydrolytic activity by approximately 10-fold.[4]

SCDase catalyses the conversion of GSL into lyso-derivatives (N-deacylated GSL, lyso-GSL) under acidic conditions (pH 5, detergent concentrations up to 0.8%) by splitting the amide bond between the sphingoid and fatty acid in the ceramide. Under modified conditions (pH 7, detergent concentrations up to 0.1%) the enzyme catalyses the reverse reaction, i.e., reacylation. The effectiveness of the condensation is influenced by the type of lyso-GSL and fatty acid.[5]

This work was primarily prompted by the demand for convenient sphingolipid internal standards (ISTs) for MS/MS analysis, which is applicable to laboratory diagnostics of inherited lysosomal disorders of sphingolipid storage (especially prosaposin and saposin B deficiencies, metachromatic leukodystrophy, and Gaucher and Fabry diseases).[2,6–10]

SCDase is the most important and expensive component of the reaction mixture, so we looked for conditions that would enable us to reuse the enzyme, e.g., by utilising the principle of enzyme immobilisation on the surface of solid particles.

The use of carriers with magnetic properties overcomes problems associated with liquid gel slurries in high-throughput and standard laboratory applications.[11] Magnetic particles provide an universal system that is consistent, stable, easy to handle and exceptionally flexible compared to standard chromatographic resins. These particles serve as carriers of surface-immobilised enzymes and can be easily recovered in a magnetic field when the reaction is terminated.

Here we describe the immobilisation of SCDase on magnetic carriers using standard procedures, and its utilisation for the preparation of the specific sphingolipid isoforms C17:0 SGalCer and C17:0 GlcCer as ISTs for MS/MS.

EXPERIMENTAL

Abbreviations

Gangliotetraosylceramide – Gg4Cer, globotriaosylceramide – Gb3Cer, glucosylceramide – GlcCer, sulphatide - SGalCer. For deacylated derivatives, the prefix lyso- is used, i.e., lyso-globotriaosylceramide – lyso-Gb3Cer. Glycosphingolipids are abbreviated according to the IUPAC-IUB Commission on Biochemical Nomenclature.[12]

Materials

Sphingolipid ceramide N-deacylase (SCDase) was purchased from TAKARA Bio. Inc. (Otsu, Japan). Magnetic macroporous cellulose beads (op. L 1680; 125–250 μm) were kindly provided by Dr. J. Lenfeld from the Institute of Macromolecular Chemistry, Academy of Sciences of the Czech Republic, Prague, Czech Republic, and are available upon request by e-mail (lenfeld@imc.cas.cz). Macroporous PERLOZA® MT 100 cellulose beads provided by Iontosorb (Prague, Czech Republic) can be used as an equivalent alternative. The enzyme substrates Gg4Cer, lyso-Gb3Cer and stearic acid (C18:0) used for optimisation reactions and lyso-GlcCer were purchased from Matreya LLC (Pleasant Gap, PA, USA). Lyso-SGalCer was from Calbiochem-Novabiochem GmbH (Schwalbach, Germany), and margaric acid (C17:0) acid was obtained from Larodan Fine Chemicals AB (Malmö, Sweden). Sodium cyanoborohydride ($NaCNBH_3$) and bovine serum albumin (BSA) were from Sigma-Aldrich Co. (St. Louis, MO, USA). Sodium periodate was from Fluka (Seelze, Germany). HPTLC-Fertigplatten, Kieselgel 60 and orcinol were purchased from Merck Chemicals Ltd. (Darmstadt, Germany). All other chemicals were of p.a. grade quality. Organic solvents for tandem mass spectrometry were of mass spectrometry grade.

Substrates and products of the enzyme reaction were evaluated with a CAMAG II TLC scanner (Camag Scientific, Switzerland) equipped with CATS3 analytical software and an AB/MDS SCIEX API 3200 triple quadrupole tandem mass spectrometer (Foster City, CA, USA) equipped with Analyst 1.4.1 software.

Immobilisation of sphingolipid ceramide N-deacylase on magnetic macroporous bead cellulose (MMB cellulose)

SCDase was immobilised onto MMB cellulose using a standard enzyme immobilisation procedure.[13,14] Briefly: 100 μL of settled particles was washed five times with distilled water and then was activated with $NaIO_4$ by mixing with an equal volume (100 μL) of freshly prepared 0.2 M $NaIO_4$ before starting the binding reaction. The mixture was incubated for 1.5 h at room temperature while mixing on a rotator (Multi Bio RS-24, Biosan, Riga, Latvia). The activated particles were washed 10 times with 0.1 M phosphate buffer at pH 7 (PB), and then 250 mI.U. of SCDase (5 mI.U./μL) and 200 μL of PB were added. The mixture was incubated for 10 min at room temperature while mixing on a rotator. Next, 200 μL of $NaCNBH_3$ was added to stabilise the formed Schiff base, and the reaction was incubated overnight on a rotator at 4°C. The particles with immobilised enzyme were washed with PB, followed by 1 M NaCl in PB and finally with PB again. After that, the activation of immobilised SCDase was done by incubation with 100 nmol of Gg4Cer substrate in 300 μL of 50 mM acetate buffer containing 0.8% Triton X-100 at 37°C for 1 h. Then the products were washed three times with 50 mM phosphate buffer (pH 7) containing 0.1% Triton X-100 (storage buffer). Immobilised SCDase was stored in storage buffer at 4°C.

Examination of SCDase catalytic activity: hydrolysis and synthesis for estimation of optimum molar ratio of substrates

For examination of the *hydrolytic activity* of the immobilised SCDase, the substrate Gg4Cer was incubated with the bio-activated particles using the same standard procedure as described for the soluble enzyme.[3,4] Briefly, 20 nmol of Gg4Cer with 20 μL of settled MMB cellulose containing bound SCDase was incubated in 50 mM acetate buffer (pH 5) with 0.8% Triton X-100 for 30 min at 37°C with mixing on a rotator.

The *reverse synthetic reaction* was performed under standard conditions[5] using lyso-Gb3Cer as the substrate because a high rate of conversion has been reported for soluble enzyme.[6] To optimise the reaction, different molar ratios of the precursors, lyso-derivative and fatty acid were tested. Briefly, SCDase immobilised on MMB cellulose (100 μL of settled particles) was distributed into four tubes. Each 25 μL aliquot was mixed with a precise molar ratio of the substrates (20 nmol of the lyso-Gb3Cer mixed with C18:0 fatty acid in molar ratios of 1:1, 1:2, 1:3 and 1:4) in 200 μl of phosphate buffer (pH 7.0) containing 0.1% Triton X-100. The reaction was incubated for 20 h at 37°C while mixing on a rotator.[5]

Magnetic particles were separated with a magnetic separator (Dynal MPC-S, Dynal Biotech ASA, Oslo, Norway), and the supernatant containing the reaction product was evaporated under a stream of nitrogen and resuspended in 300 μL of chloroform/methanol (2:1, v/v; C:M). A 20 μL aliquot of chloroform:methanol solution, which corresponded to approximately 2 nmol of the reaction product, was evaporated under nitrogen. The reaction products were analyzed using HPTLC (chloroform/methanol/10% acetic acid, 5:4:1, v/v/v[6]) with orcinol detection and densitometry.

Semisynthesis of specific sphingolipid isoforms: C17:0 sulphatide and C17:0 glucosylceramide

For the semisyntheses, 50 nmol of lyso-SGalCer or lyso-GlcCer and 50 nmol of C17:0 fatty acid were incubated with immobilised SCDase (0.1 mI.U./20 μL of settled particles) in

DOI: 10.1002/rcm

300 μL phosphate buffer (pH 7.0) containing 0.1% Triton X-100. For comparison, the reaction with soluble SCDase for semisynthesis of C17:0 GlcCer was performed. The reaction mixture was incubated for 20 h at 37°C while mixing on a rotator. The magnetic particles were separated and the supernatant processed as described above. A 5 μL aliquot of C:M solution, which corresponded to approximately 0.5 nmol of the reaction product, was evaporated under a stream of nitrogen and analysed with electrospray ionisation tandem mass spectrometry (ESI-MS/MS) and HPTLC (to determine the overall purity of the lipid preparation).

The macroporous character of the cellulose beads requires exhaustive washing before each subsequent use; therefore, either twenty 1-min washes or overnight elution with storage buffer was required to produce clean particles.

Tandem mass spectrometry of C17:0 sulphatide and C17:0 glucosylceramide

Instrument settings

Samples of semisynthesised SFL were applied by direct injection with a syringe pump into the SCIEX API 3200 tandem mass spectrometer equipped with an ESI source. Analysis 1.4.1 software was used to operate the instrument and process the data. Sphingolipids were analysed by precursor ion scan in the negative ion mode for SGalCer and in the positive ion mode for GlcCer. Pauses between the ranges for mass scans were set to 5.007 ms with Q1 and Q3 operating in unit resolution mode. The settling time (ms) and intensity threshold (counts per second (cps)) were set to 0.

The curtain gas pressure was 10 psi in both ion modes. Nitrogen was used as the collision gas with the pressure set to 10 and 5 psi in negative and positive ion modes, respectively. The capillary spray voltage was 4.5 kV with different polarities depending on the ion mode. The temperature of the nebulising gas was 200°C. The ion source gas pressure was adjusted to 20 psi for source gas 1 in both modes and 45 psi in negative mode or 25 psi in positive ion mode for source gas 2. The interface heater was turned on for analysis of both lipids.

Ion optics settings for SGalCer measurements were −140 V for the declustering potential and −10.4 V for the entrance potential. The collision energy was set to −130 V with a collision cell exit potential of −2 V. GlcCer was measured with a declustering potential of 47 V. The entrance potential of the collision cell was 4.9 V and the collision energy was 48 V. The collision cell exit potential was set to 5.6 V.

Sample analysis

Approximately 0.5 nmol of the reaction products in 500 μL of the appropriate solvent (see below) was continuously injected by a syringe pump into the ESI-MS/MS system at a flow rate of 50 μL/min. GlcCer was resuspended in methanol with 10 mM NH_4COOH to create $[M+H]^+$ ions in the positive ion mode, whereas SGalCer was re-suspended in methanol to create $[M–H]^-$ ions in the negative ion mode. The precursor ion scan was performed for a fragment of *m/z* 264.4 (the sphingosine base fragment) for GlcCer and a fragment of *m/z* 97 (the sulphate group) for the SGalCer.

RESULTS

Examination of the hydrolytic activity of the immobilised SCDase

The rate of hydrolysis of Gg4Cer by SCDase-activated MMB cellulose was 62% after 20 h as compared to 48% with the soluble enzyme under the same reaction conditions. This result confirmed the superiority of the immobilised enzyme over the soluble enzyme in a standard hydrolysis reaction.

SCDase reacylation activity: optimisation of the fatty acid to lyso-sphingolipid ratio

A series of reactions was carried out to identify the best ratio of substrates for enzymatic semisynthesis of bioactivated MMB cellulose. Various molar ratios of lyso-Gb3Cer and stearic acid (1:1, 1:2, 1:3 and 1:4) were tested for the synthesis of C18:0 Gb3Cer. The reaction products were analysed using HPTLC and evaluated by densitometry. A 1:1 ratio of fatty acid to lyso-sphingolipid was found to produce the best results (Table 1).

Preparation of C17:0 GlcCer by soluble SCDase: purity of the product

To compare both methods of synthesis, C17:0 GlcCer was prepared in bulk solution containing a soluble form of SCDase. Mass spectra revealed a considerable amount of contaminants in the final product; the contaminants were identified as GlcCer isoforms with C16:0 and C18:0 fatty acids (see Fig. 1(A)). The total yield of GlcCer synthesis was 99% (data not shown), but only 36% of the lyso-GlcCer was converted into the desired C17:0 isoform. The remaining 63% of the product consisted of contaminating isoforms.

MS analysis of a lipid extract of commercial SCDase (2:1 chloroform/methanol, v/v) confirmed the presence of C16:0 and C18:0 fatty acids, indicating that the crude enzyme preparation was the main source of the fatty acid contaminants (data not shown).

Table 1. The effects of different molar ratios of substrates on the formation of the C18:0 Gb_3Cer product. Reactions were catalysed by the SCDase-activated MMB cellulose

Ratio lyso-Gb_3Cer/stearic acid	1:1	1:2	1:3	1:4
*lyso-Gb_3Cer**	143	216	219	310
*C18:0 Gb_3Cer**	1401	1478	1403	1307
synthesis (%)	**91**	**87**	**86**	**81**

* Evaluated by densitometry in arbitrary units.

Reaction conditions: 20 nmol lyso-Gb_3Cer, different molar amounts of stearic acid and 0.48 mI.U./100 μL of bioactivated MMB cellulose in 200 μL of 50 mM phosphate buffer (pH 7) containing 0.1% Triton X-100 were incubated for 20 h at 37°C.

TLC analysis: the solvent system was chloroform/methanol/10% acetic acid (5:4:1); Detection: orcinol.

Substrates: lyso-Gb_3Cer and stearic acid. Product: C18:0 Gb_3Cer.

DOI: 10.1002/rcm

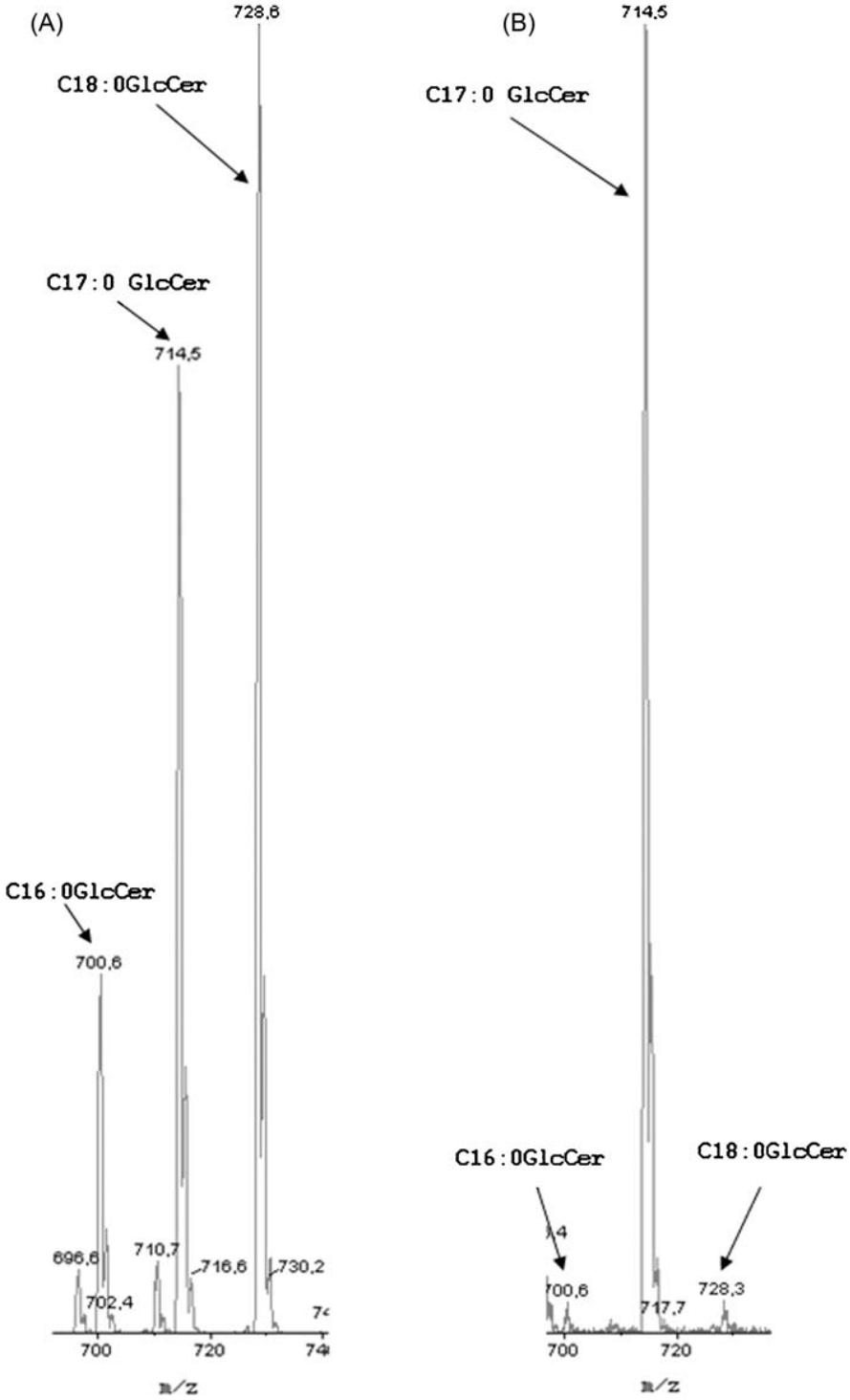

Figure 1. ESI-MS/MS analysis of C18:0 and C16:0 isoform contaminants and comparison of the soluble and immobilised SCDase reaction products. Semisynthesis of C17:0 GlcCer using (A) soluble SCDase and (B) SCDase-activated MMB cellulose. Reaction conditions: 50 nmol lyso-glucosylceramide and 50 nmol C17:0 fatty acid either with (A) 0.5 mI.U. of soluble SCDase or with (B) 0.1 mI.U./20 μl of bioactivated MMB cellulose in 300 μL of phosphate buffer at pH 7 with 0.1% Triton X-100 were incubated for 20 h at 37°C. ESI-MS/MS: the sample was directly injected by a syringe pump at a flow rate of 10 μL/min. C17:0 glucosylceramide was dissolved in methanol with 10 mM NH_4COOH and scanned for precursor ions at *m/z* 264 (specific fragment of C18:1 sphingoid base) in positive ion mode for 1 min.

DOI: 10.1002/rcm

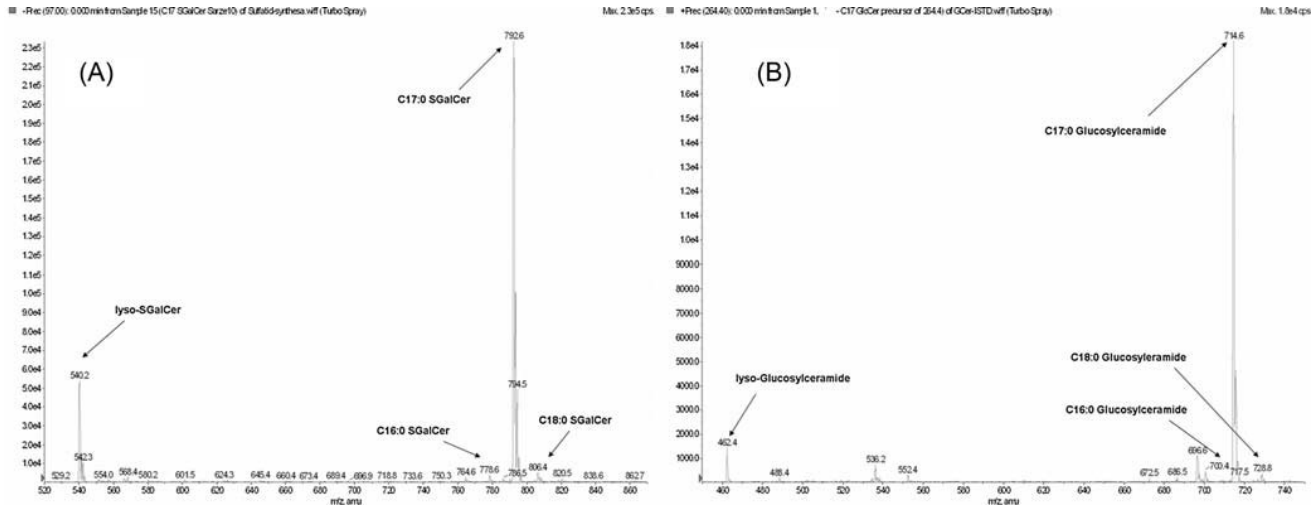

Figure 2. ESI-MS/MS analysis of C17:0 sulphatide (A) and C17:0 glucosylceramide (B) prepared with the SCDase-activated MMB cellulose. Reaction conditions: 50 nmol lyso-SGalCer or lyso-GlcCer, 50 nmol C17:0 fatty acid and 0.1 mI.U./20 μL of bioactivated MMB cellulose were incubated in 300 μL of phosphate buffer at pH 7 with 0.1% Triton X-100 for 20 h at 37°C. ESI-MS/MS: the sample was directly injected by a syringe pump at a flow rate of 10 μL/min. C17:0 SGalCer was dissolved in methanol and scanned for precursor ions at *m/z* 97 (sulphate group) in negative ion mode for 1 min. C17:0 GlcCer was dissolved in methanol with 10 mM NH_4COOH and scanned for precursor ions at *m/z* 264 (sphingoid fragment) in positive ion mode for 1 min.

Preparation of C17:0 sulphatide and C17:0 GlcCer using SCDase-activated macroporous bead cellulose

C17:0 SGalCer and C17:0 GlcCer ISTs were prepared from the respective lyso-derivatives using the immobilised SCDase.

Each reaction was repeated three times. Mass spectra (Figs. 1(A), 1(B) and Figs. 2(A), 2(B)) clearly demonstrated that the enzymatic semisynthesis effectively produced specific sphingolipids with much higher isoform purities (minimum production of molecular species other than the desired isoform) in comparison to catalysis by the soluble enzyme. With the immobilised enzyme, 80% of lyso-SGalCer and 90% of lyso-GlcCer were acylated and converted into C17:0 SGalCer and GlcCer, respectively. Only trace amounts of contaminating isoforms (about 3% in both lipid preparations) were detected when using carefully washed SCDase-activated MMB cellulose. In Figs. 3(A)–3(C), the results from three subsequently performed semisyntheses of SGalCer using newly prepared unwashed SCDase-activated MMB cellulose are presented. During these steps, almost all of the contaminating C16:0 and C18:0 isoforms were removed (Figs. 3(A)–3(C)). Different commercial batches of SCDase may contain different amounts of fatty acids, but the 'pre-run procedure' with lyso-SFL is recommended before every synthesis of specific glycosphingolipids on new SCDase-activated MMB cellulose.

Products were also analyzed by HPTLC to examine contamination by other compounds, especially sphingolipids. The purities of the synthesised ISTs were satisfactory (data not shown).

SCDase immobilised on MMB cellulose maintained its activity without any loss after 15 uses. Long-term stability was also achieved, since the enzyme retained the same activity after 1.5 years in storage buffer at 4°C.

DISCUSSION

Immobilisation of SCDase: preparation of SCDase-activated magnetic macroporous bead cellulose

A carrier with superparamagnetic properties was chosen for the simple and gentle separation of products from the reaction mixture. MMB cellulose was selected for its hydrophilic properties and high specific surface area, which provides maximum binding activity. The character of the particles and the chosen method of immobilisation resulted in a system with many advantages.

The standard procedure used for enzyme immobilisation was based on the creation of a Schiff base between the primary amino group of the enzyme and the aldehyde group of the activated MMB cellulose. The advantage of this method is that the reactive aldehyde groups are formed on the solid phase, while the enzyme molecule is not affected by the oxidation. The resulting Schiff base is mildly reduced with cyanoborohydride to form a stable bond.[15]

The prepared SCDase-activated MMB cellulose had a higher rate of substrate conversion for both the deacylation and reacylation reactions than the soluble enzyme using standard conditions.[5] The optimal substrate ratio for synthesis was 1:1.

This result and the ability to use the immobilised enzyme multiple times make it a promising tool for the preparation of specific sphingolipid species, especially if only a moderate amount of product is needed.

Advantages and disadvantages of SCDase-activated magnetic macroporous bead cellulose compared to the soluble enzyme

Although it has been successfully applied to sphingolipid semisynthesis,[2,5–7,16,17] the use of soluble SCDase results in the presence of contaminating fatty acids in the reaction mixture (resulting in low isoform purity of the product),

DOI: 10.1002/rcm

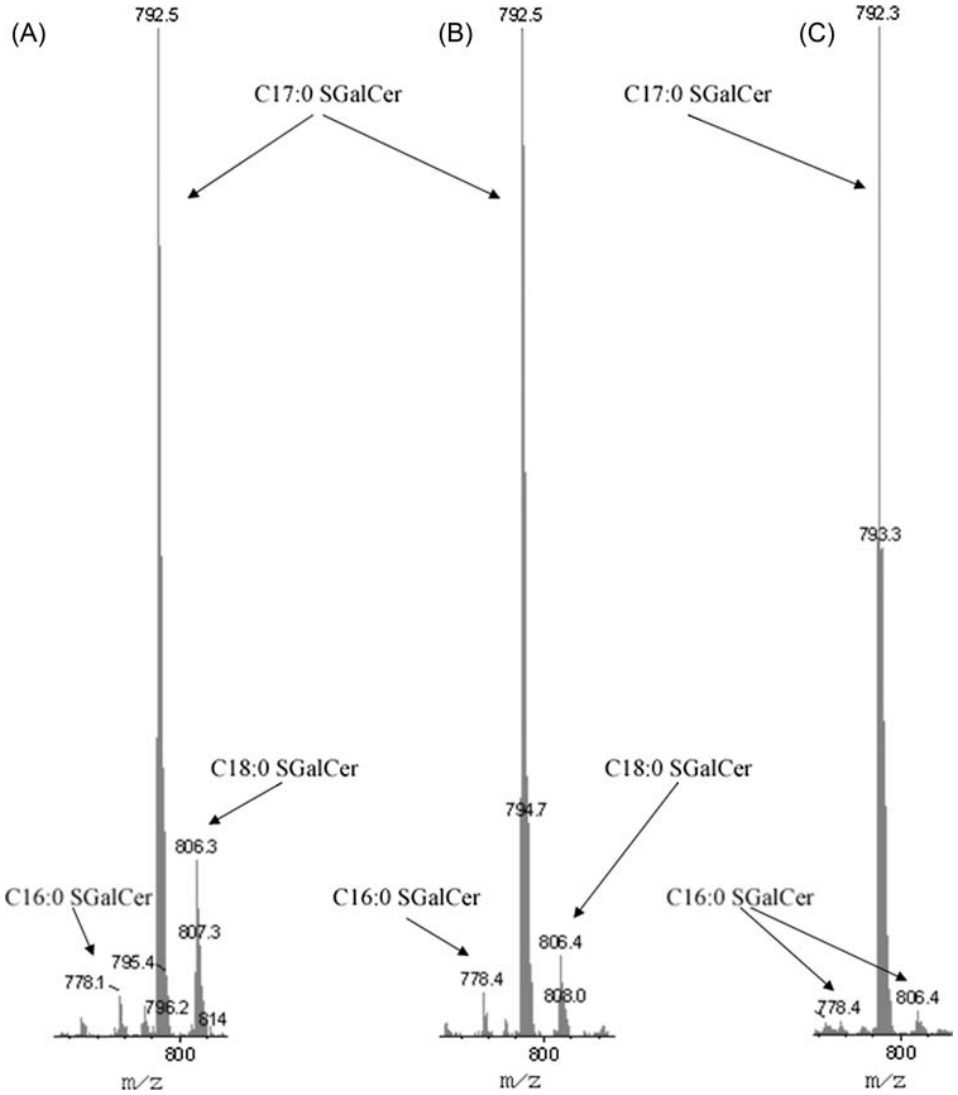

Figure 3. ESI-MS/MS analysis of C18:0 and C16:0 isoform contaminants in the course of preparation of new SCDase-activated MMB cellulose. Lyso-sulphatide was used as the optimisation compound. First (A), second (B) and third (C) semisyntheses of C17:0 SGalCer on new SCDase-activated MMB cellulose. Reaction conditions: 50 nmol lyso-SGalCer, 50 nmol C17:0 fatty acid and 0.1 mI.U./20 μL of bioactivated macroporous cellulose beads were incubated in 300 μL of phosphate buffer at pH 7 containing 0.1% Triton X-100 for 20 h at 37°C. ESI-MS/MS: sample was directly injected by syringe pump at a flow rate of 10 μL/min. C17:0 SGalCer was dissolved in methanol and scanned for precursor ions of *m/z* 97 (sulphate group) in negative ion mode for 1 min.

which may hinder some studies. In some of our experiments with the soluble enzyme, the amounts of co-synthesised C16:0, and particularly of C18:0 isoforms, were even greater than those of the target glycolipid, C17:0 GlcCer (Fig. 1(A)), especially when small amounts (up to 100 μg) of sphingolipids were synthesised. Because commercial SCDase is prepared by ammonium sulphate precipitation of culture media from the bacterium *Pseudomonas* sp. TK4 and C16:0 and C18:0 are generally abundant fatty acids, the presence of these compounds in the enzyme preparation is not surprising. However, there is only one paper that mentions the presence of some impurities in newly synthesised glycolipids, and the contaminating compounds were not characterised.[2] It is difficult to remove fatty acid contaminants from the soluble enzyme preparation without unfavourably affecting its activity. Immobilisation of the enzyme onto the surface of the carrier allows the majority of lipid and non-lipid contaminants to be washed away without affecting enzyme function.

The situation is more complicated for the reverse reaction than for hydrolysis if only one specific isoform is synthesised. Soluble SCDase gave a relatively low yield for the final product (e.g., 36% for C17:0 GlcCer) and a large amount of isoform by-products (see Fig. 1(A)), which are hardly removable. In contrast, the yields of the reacylation reaction of lyso-derivatives in terms of the C17:0 isoforms were

DOI: 10.1002/rcm

80% for SGalCer and 90% for GlcCer using the SCDase-activated MMB cellulose.

Fauler *et al*.[2] moved the reaction equilibrium of the soluble enzyme towards the desired molecular species of Gb3Cer under reaction conditions of high substrate saturation. Nevertheless, only 25% of lyso-Gb3Cer was converted into the pure Gb3Cer isoform under these conditions, with high consumption of the enzyme and precursor substrates.

The main advantages of the SCDase-activated carrier were its stability and availability for immediate use. SCDase-activated MMB cellulose with particles sizes of 125–250 μm did not show any decrease in activity after 15 reuses and was still active after 1.5 years of storage in storage buffer at 4°C.

A limitation of the MMB cellulose is that it generally exists in a narrow range of mechanical stability; however, this can be easily overcome by using dilute suspensions, handling gently and avoiding high-pressure applications (e.g., centrifugation). In addition, thorough washing is required for the removal of residual lipids (and fatty acids) before the next reaction. This is an imperative but routine step in all procedures with reusable carriers (e.g., HPLC and affinity chromatography).

For some studies, separation of the product from the remaining lipid precursors and other, mostly non-lipid contaminants might be required (this is not necessary for MS/MS). This requirement is easily accomplished by simple chromatographic procedures.[6]

Another way to prepare sphingolipid isoforms is chemical synthesis utilising acid chlorides and lyso-sphingolipids;[18] however, the acid chlorides are highly reactive compounds that can react not only with the amino group of the sphingosine moiety, but also with the hydroxyl groups of the saccharide.[19] These products would have the same mass as the required sphingolipids and would be indistinguishable by mass spectrometry. Only NMR spectra can show the position of the fatty acid in the compound. Other procedures for organic synthesis have also been applied for the preparation of sphingolipid species,[20] but time expenditure and relatively low yields were always the main disadvantages.

In summary, SCDase immobilised on a magnetic carrier was used for the first time for preparation of the specific molecular species C17:0 SGalCer and C17:0 GlcCer, that are useful standards for MS/MS quantification. The SCDase-activated MMB cellulose has the following advantages: reusability, long-term stability, high rate of conversion, low production of by-products and effectiveness for preparation of low amounts of sphingolipids. The isoform purities of the synthesised sphingolipid species were about 97%. This immobilised system can be universally used for the preparation of sphingolipids that are specifically labelled in the fatty acid moiety and could be further applied in different fields of sphingolipid biochemistry.

Acknowledgements

This work was supported by the grant projects GAUK 19509 from the Grant Agency of Charles University and MSM 0021620806 and MSM 0021627502 from the Ministry of Education and Youth of the Czech Republic.

REFERENCES

1. Stults CL, Sweeley CC, Macher BA. *Methods Enzymol*. 1989; **179**: 167.
2. Fauler G, Rechberger GN, Devrnja D, Erwa W, Plecko B, Kotanko P, Breunig F, Paschke E. *Rapid Commun. Mass Spectrom*. 2005; **19**: 1499.
3. Ito M, Kita K, Kurita T, Sueyoshi N, Izu H. *Methods Enzymol*. 2000; **311**: 297.
4. Ito M, Kurita T, Kita K. *J. Biol. Chem*. 1995; **270**: 24370.
5. Kita K, Kurita T, Ito M. *Eur. J. Biochem*. 2001; **268**: 592.
6. Mills K, Johnson A, Winchester B. *FEBS Lett*. 2002; **515**: 171.
7. Mills K, Morris P, Lee P, Vellodi A, Waldek S, Young E, Winchester B. *J. Inherit. Metab. Dis*. 2005; **28**: 35.
8. Fuller M, Sharp PC, Rozaklis T, Whitfield PD, Blacklock D, Hopwood JJ, Meikle PJ. *Clin. Chem*. 2005; **51**: 688.
9. Kuchar L, Ledvinova J, Hrebicek M, Myskova H, Dvorakova L, Berna L, Chrastina P, Asfaw B, Elleder M, Petermoller M, Mayrhofer H, Staudt M, Krageloh-Mann I, Paton BC, Harzer K. *Am. J. Med. Genet. A* 2009; **149A**: 613.
10. Whitfield PD, Sharp PC, Johnson DW, Nelson P, Meikle PJ. *Mol. Genet. Metab*. 2001; **73**: 30.
11. Bilkova Z, Slovakova M, Horak D, Lenfeld J, Churacek J. *J. Chromatogr. B Analyt. Technol. Biomed. Life Sci*. 2002; **770**: 177.
12. Chester MA. *Eur. J. Biochem*. 1998; **257**: 293.
13. Bilkova Z, Castagna A, Zanusso G, Farinazzo A, Monaco S, Damoc E, Przybylski M, Benes M, Lenfeld J, Viovy JL, Righetti PG. *Proteomics* 2005; **5**: 639.
14. Korecka L, Jezova J, Bilkova Z, Benes M, Horak D, Hradcova O, Slovakova M, Viovy JL. *J. Magn. Magn. Mater*. 2005; **293**: 349.
15. Hermanson GT. *Bioconjugate Techniques* (1st edn). Academic Press, Inc.: New York, 1996.
16. Mitsutake S, Kita K, Nakagawa T, Ito M. *J. Biochem. (Tokyo)* 1998; **123**: 859.
17. Mitsutake S, Kita K, Okino N, Ito M. *Anal. Biochem*. 1997; **247**: 52.
18. Mills K, Eaton S, Ledger V, Young E, Winchester B. *Rapid Commun. Mass Spectrom*. 2005; **19**: 1739.
19. Thevenet S, Wernicke A, Belniak S, Descotes G, Bouchu A, Queneau Y. *Carbohydr. Res*. 1999; **318**: 52.
20. Zhou X, Turecek F, Scott CR, Gelb MH. *Clin. Chem*. 2001; **47**: 874.

DOI: 10.1002/rcm

Příloha P5

Rotková J., Šuláková R., Korecká L., Zdražilová P., Jandová M., Lenfeld J., Horák D., Bílková Z.: Laccase immobilized on magnetic carriers for biotechnology applications. *Journal of Magnetism and Magnetic Materials*, **321**, 2009, 1335-1340

IF_{2018} = 2,683; Q2 – Materials engineering; 26 citací [1. 7. 2020]

- podíl na experimentální práci a vyhodnocení výsledků 20 %
- dílčí příprava a revize článku

Journal of Magnetism and Magnetic Materials 321 (2009) 1335–1340

Contents lists available at ScienceDirect

Journal of Magnetism and Magnetic Materials

journal homepage: www.elsevier.com/locate/jmmm

Laccase immobilized on magnetic carriers for biotechnology applications

Jana Rotková [a], Romana Šuláková [b], Lucie Korecká [a], Pavla Zdražilová [a], Miroslava Jandová [a], Jiří Lenfeld [c], Daniel Horák [c], Zuzana Bílková [a,*]

[a] Department of Biological and Biochemical Sciences, University of Pardubice, Štrossova 239, 530 03 Pardubice, Czech Republic
[b] Department of Technology of Organic Compounds, Doubravice 41, 533 53 Pardubice, Czech Republic
[c] Institute of Macromolecular Chemistry, Academy of Sciences of the Czech Republic, Heyrovského nám. 2, 162 06 Praha, Czech Republic

ARTICLE INFO

Available online 20 February 2009

Keywords:
Macroporous bead cellulose
Laccase
Oriented immobilization
Enzyme carrier
Textile dye

ABSTRACT

Laccase catalyzing the oxidation of *p*-diphenols has been applied in many industrial and biotechnology areas. Immobilized form of laccase has overcome the problem with contamination of the final product. Nevertheless sensitive enzymes immobilized to the matrix can be inactivated by the environmental conditions. The aim of this research was to prepare carrier with improved activity and responsible stability even under extreme reaction conditions. Laccase immobilized through carbohydrate moieties on magnetic hydrazide bead cellulose with a final activity of 0.63 I.U./1 ml of settled carrier confirmed that carriers with oriented immobilized enzyme might be useful in routine biocatalytic applications.

Laccase is an attractive, industrially relevant enzyme, which can be applied for a number of diverse biocatalytic applications such as delignification of lignocellulosics, cross-linking of polysaccharides, bioremediation, including waste detoxification or textile dye transformation [1,2]. Colored waste water from the paper and textile industries represents a major environmental problem [3]. Azo dyes represent the largest group of organic dyes accounting for about 70% of all textile dyes produced. They are not toxic, but after release into the water environment they may be converted into potentially carcinogenic amines with impact on the ecosystem downstream from the mill [4]. Most existing processes to treat dye waste water are ineffective and not economical [5]. The development of processes based on laccase seems an attractive solution due to its potential in degrading dyes of diverse chemical structure [6], including synthetic dyes currently employed in the industry [7].

Laccase (*p*-diphenol:O_2 oxidoreductase; EC 1.10.3.2) is an enzyme belonging to the family of multicopper oxidases. It catalyzes oxidation of *p*-diphenols with the concomitant reduction of molecular oxygen to water [8]. Laccase is found in plants, insects and bacteria, but the most important sources of this enzyme are fungi. It can remove potentially toxic phenols formed during degradation of lignin. Laccase often occurs as isoenzyme that oligomerizes to functional multimeric complexes. Its molecular weight ranges from about 50 to 110 kDa [9]. Laccase is a glycoprotein; covalently linked carbohydrate moieties (10–45%) contribute to the high stability of the enzyme [10].

Laccase was already used for degradation of azo dyes immediately after dyeing [6]. This, however, is not convenient in the textile industry, due to the contamination and low stability of free enzyme in waste water. One of possible solutions to eliminate this drawback is to immobilize laccase on appropriate support. Immobilization thus allows decouple the enzyme location from the flow of the liquid carrying the reagents and products. But sensitive enzymes even they are immobilized can be inactivated by the wide variety of environmental conditions such as extreme pH, ionic concentration, inhibitors, detergents and other contaminants [11]. It was already proved that covalent capturing of bioactive molecules through their glycosidic moieties improves the stability of them and extends the reaction conditions as pH, temperature and resistance to detergent [12]. To prepare laccase carrier with desired stability, with simple and efficient processing and economical reusability we decided to combine oriented immobilization of laccase with magnetic form of macroporous bead cellulose.

Micro/nanosized particles with superparamagnetic properties overcome many of the problems associated with the use of liquid gel slurries in high throughput and standard biotechnology application. Magnetic particles provide a universal system with additional convenience, consistency, stability, ease of handling and exceptional flexibility compared to standard chromatography resinos. Hydrophilic macroporous bead cellulose is carrier with a high surface area, with easily modified OH– groups for covalent ligand attachment, minimal nonspecific binding for common protein and peptide molecules, no tendency to aggregate and excellent flow characteristics [13]. Such characteristics of carrier combined with improved immobilization strategy could significantly improve the conditions for

* Corresponding author. Tel.: +420 466 037 700; Fax: +420 46 603 7068.
E-mail address: Zuzana.Bilkova@upce.cz (Z. Bílková).

0304-8853/$ - see front matter © 2009 Elsevier B.V. All rights reserved.
doi:10.1016/j.jmmm.2009.02.034

enzyme catalysis of azo dyes degradation and other industrial applications.

1. Chemicals and methods

Laccase from *Trametes versicolor* and *Pycnoporus cinnabarinus* (EC 1.10.3.2) was purchased from Jena Bios GmbH, Germany. Substrates SGZ, syringaldazine (4-hydroxy-3,5-dimethoxybenzaldehyde azine) and 2,2′-azino-bis(3-ethylbenzthiazoline-6-sulfonic acid) (ABTS) were obtained from Sigma-Aldrich, St. Louis, MO, USA. BCA Protein Assay Kit was purchased from Pierce, Rockford, IL, USA. Magnetic macroporous bead cellulose (125–250 μm) with hydroxyl or hydrazide functional groups (20 μmol of hydrazide moieties per 1 ml of settled carrier) were obtained as the generous gift from the Institute of Macromolecular Chemistry, Academy of Sciences, Prague, Czech Republic. Non-magnetic form of macroporous bead cellulose (Perloza MT) was provided by Iontosorb, Ústí n/L, Czech Republic. Anthraquinone dye (ANTD) $C_{20}H_{15}N_3O_8S_2$ was a product of Aliachem a.s., division Synthesia, Czech Republic. Azo dye (Dye I) $C_{16}H_{13}N_3O_7S_2$ was synthesized in the Department of Technology of Organic Compounds, University of Pardubice, Czech Republic.

1.1. Determination of laccase activity using substrate syringaldazine (SGZ)

SGZ solution was pre-incubated before its addition to the enzyme solution for 5 min.

(a) *Soluble form of laccase*: 0.1 ml of soluble laccase was mixed with 0.9 ml of SGZ in 0.05 M K–acetate buffer pH 4.5 (35 μM SGZ in 1 ml of reaction mixture). The activity was measured at 30 s intervals at 525 nm on spectrophotometer Agilent HP 8453 (Agilent Technologies, Waldbronn, Germany) at room temperature.
(b) *Immobilized laccase:* 30 μl of settled carrier with immobilized laccase was mixed with 0.97 ml of SGZ in 0.05 M K–acetate buffer pH 4.5 (35 μM SGZ in 1 ml of reaction mixture). The activity was measured at 30 s intervals at 525 nm on spectrophotometer MODEL V 200-RS visible light (LW Scientific, USA) at room temperature. Between individual measurements reaction mixture was hand-stirred; before measuring the absorbance, the magnetic beads were separated using magnetic separator and non-magnetic form of them by gentle centrifugation.

1.2. Determination of laccase activity using substrate 2,2′-azino-bis(3-ethylbenzthiazoline-6-sulfonic acid) (ABTS)

A total of 0.1 ml of soluble laccase was mixed with 0.9 ml of ABTS in 0.05 M K–acetate buffer pH 4.5 (45 μM ABTS in 1 ml of reaction mixture). Reaction was measured. The activity was measured at 30 s intervals at 414 nm on spectrophotometer Agilent HP 8453 (Agilent Technologies, Waldbronn, Germany) at room temperature.

1.3. Determination of K_m for laccase using substrate SGZ

A total of 0.1 ml of soluble laccase (0.2 I.U. laccase from *T. versicolor* and 0.0075 I.U. laccase from *P. cinnabarinus*) was mixed with 0.9 ml of SGZ in 0.05 M K–acetate buffer pH 4.5 (4, 6, 8, 10, 12 and 14 μM for *T.v.* laccase and 4, 8, 12, 16 and 20 μM SGZ for *P.c.* laccase in 1 ml of reaction mixture). The activity was measured at 30 s intervals at 525 nm on spectrophotometer Agilent HP 8453 (Agilent Technologies, Waldbronn, Germany) at room temperature. K_m was calculated from enzyme activity data using a Lineweaver–Burk plot.

1.4. Determination of K_m for laccase using substrate ABTS

A total of 0.1 ml of soluble enzyme isolated from *Trametes versicolor (T.v.)* and/or *Pycnoporus cinnabarinus (P.c.)* was mixed with 0.9 ml of ABTS in 0.05 M K–acetate buffer pH 4.5 (45 μM ABTS in 1 ml of reaction mixture). Initial enzyme activity were 4.5×10^{-3}, 6×10^{-3}, 7.5×10^{-3}, 9×10^{-3}, 10.5×10^{-3} I.U. for *T.v.* and 1.8×10^{-3}, 2.25×10^{-3}, 2.7×10^{-3} and 3.15×10^{-3} I.U. for *P.c.*

The activity was measured at 10 s intervals at 414 nm on spectrophotometer Biochrom Libra S22 at room temperature. Kinetic data were analyzed using software GEPASI.

1.5. Decolorization of model dyes with soluble laccase

Lyophilized enzyme was dissolved in 0.2 M citrate–phosphate buffer, for laccase from *P. cinnabarinus* pH 3.0, for laccase from *T. versicolor* pH 3.5).

(a) *Decolorization of anthraquinone dye*: aqueous solution of ANTD (product of Aliachem a.s., division Synthesia, Czech Republic) at concentrations of 1, 2, 3, 4 and 5 μM in reaction mixture (25 ml) was mixed with 5 I.U. of laccase in citrate–phosphate buffer at pH given for each laccase, reaction was done at room temperature. Decrease of ANTD concentration was determined by monitoring the absorbance at 604 nm.
(b) *Decolorization of azo dye (dye I):* aqueous solution of dye I (synthetized in laboratory of Department of Technology of Organic Compounds, University of Pardubice), 1 μM in 25 ml of reaction mixture was mixed with 2.5 I.U. of laccase in citrate–phosphate buffer pH 3, 4, 5 and 8. Reaction was done at room temperature. Decrease of dye I concentration was determined by monitoring the absorbance at 528 nm.

1.6. Magnetic macroporous bead cellulose

Magnetic bead cellulose (125–250 μm) with hydroxyl or hydrazide functional groups (20 μmol of hydrazide moieties per 1 ml of settled carrier) was prepared from viscose and ferrite powder by employing the suspension procedure using the thermal sol–gel transition [14]. The amount of hydrazide groups were quantificated by the elemental analysis and the reaction with TNBS.

1.7. Non-oriented immobilization of laccase

A total of 0.25 ml of settled magnetic macroporous bead cellulose (size of particles 125–250 μm) was washed with distilled water and then oxidized by 0.1 M $NaIO_4$ in the dark for 90 min under gentle stirring. After properly washing with 0.05 M K–acetate buffer pH 4.5, 3 I.U. of laccase were added. Reaction mixture was incubated 10 min at room temperature under gentle stirring. Finally, 1.5 mg of $NaCNBH_3$ in 0.05 M K–acetate buffer pH 4.5 was added and reaction mixture (0.8 ml) was incubated overnight at 4 °C under gentle stirring. After incubation carrier with immobilized laccase was washed with 0.05 M K–acetate buffer pH 4.5, then 0.05 M K–acetate buffer pH 4.5 containing 1 M NaCl and finally 0.05 M K–acetate buffer pH 4.5 containing 5 mM $CuCl_2$. Immobilized laccase can be stored at 4 °C in 0.05 M

K–acetate buffer pH 4.5 containing 5 mM $CuCl_2$. The immobilized laccase content was determined using the BCA kit (Sigma-Aldrich, St. Louis, MO, USA) for the determination of protein content, soluble form of enzyme used as standard for calibration.

1.8. Oriented immobilization of laccase

A total of 0.25 ml of settled magnetic form of hydrazide macroporous bead cellulose (size of particles 125–250 μm, 20 μmol of hydrazide moieties per 1 ml of settled carrier) was washed with 0.05 M K–acetate buffer pH 4.5. A total of 3 I.U. of laccase in 1 ml of 0.1 M K-acetate buffer pH 5.5 were mixed with $NaIO_4$ at final concentration 0.01 M in reaction mixture. Enzyme was oxidized 30 min at 4 °C. Reaction was stopped by addition of 3 μl of ethylene glycol and reaction mixture was incubated 10 min at 4 °C. Enzyme was then dialyzed to 0.05 M K–acetate buffer pH 4.5 containing 0.5 M NaCl overnight at 4 °C (alternatively enzyme was equilibrated to 0.05 M K–acetate buffer pH 4.5 by SEC using MicroSpin G-25 column). Solution of oxidized enzyme was added to 0.25 ml of settled carrier washed with 0.05 M K–acetate buffer pH 4.5 and reaction mixture was incubated overnight at 4 °C under gentle stirring. After incubation carrier with immobilized laccase was washed with 0.05 M K–acetate buffer pH 4.5 containing 5 mM $CuCl_2$.

2. Results

The aim of the present work was to prepare and characterize laccase carrier. But at first the kinetic characteristics of free form of laccase have been verified. The enzyme activity of laccase originated from white rot fungi *T. versicolor* or *P. cinnabarinus* was measured using two substrates, 4-hydroxy-3,5-dimethoxybenzaldehyde azine (syringaldazine, SGZ) and 2,2′-azino-bis(3-ethylbenzthiazoline-6-sulfonic acid). In view of precipitation of the colored oxidative product of SGZ oxidation [15], the kinetic measurement of enzyme activity is preferred (Fig. 1). The linear ascendant part of the curve corresponding to the product addition was used for construction of calibration curve as a function of absorbance change in time on the addition of enzyme I.U. To evaluate the conversion of ABTS substrate, the software GEPASI was used. Experimental data were examined on validity of Michaelis–Menten equation $v = V_m.\ S/(K_m+S)$ in modification of Briggs–Haldane ($V_m = k_2.\ [E]_0$). Optimal K_m, V_m and $[S]_0$ values were determined. Experimental curves and theoretical dependencies of substrate conversion by laccase were compared. The experimental curves for ABTS were calculated by software GEPASI, kinetic characteristics for substrate SGZ were calculated from enzyme activity data using a Lineweaver–Burk plot (Fig. 2).

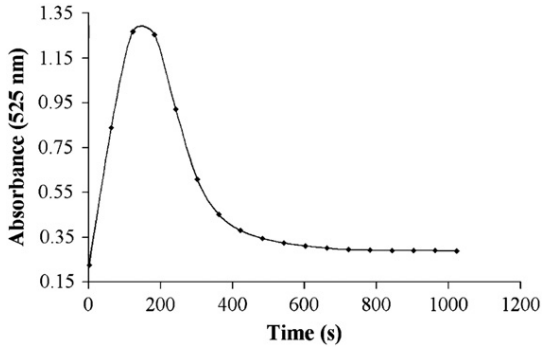

Fig. 1. Time dependence of syringaldazine conversion by soluble laccase. A total of 0.1 ml of soluble laccase was mixed with 0.9 ml of SGZ in 0.05 M K–acetate buffer pH 4.5, kinetic measurement at 30 s intervals, at 525 nm, at room temperature.

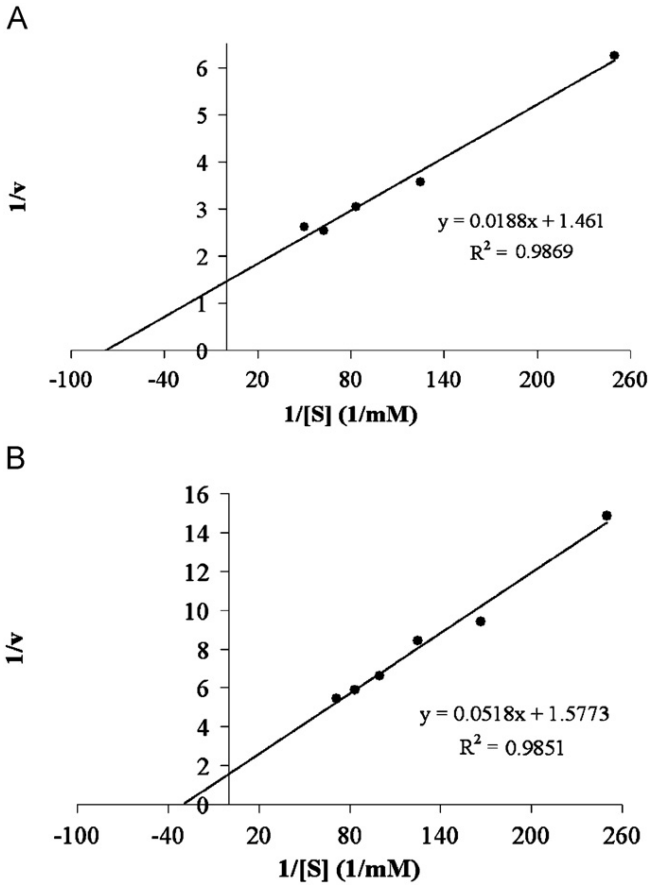

Fig. 2. Kinetic characterization of enzyme for substrate SGZ: 0.1 ml of soluble laccase was mixed with 0.9 ml of SGZ in 0.05 M K–acetate buffer pH 4.5, kinetic measurement at 30 s intervals at 525 nm, at room temperature. K_m was calculated from enzyme activity data using a Lineweaver–Burk plot.

Kinetic characteristics of laccase isolated from *P.c.* and *T.v.* for the substrate ABTS are summarized in Table 1, for substrate SGZ in Table 2. On the basis of our experimentally determined K_m values, the enzyme originated from *P.c.* and *T.v.* has comparable affinity for both substrates. The agreement exists also between experimental K_m values and K_m values already published (database Brenda), for both laccase and SGZ (Table 2), but comparing our experimental K_m values with already published data (Table 1) more than ordinal discrepancy in K_m values for *T.v.* laccase and ABTS was observed.

The optimum pH of laccase reaction varies depending on the type of substrate [8]. The pH values for the reaction of laccase from *T.v.* and *P.c.* with substrates SGZ and ABTS were verified. Optimal pH of reaction environment for laccase lies between 5.0–5.5 for substrate SGZ and 3.5–4.0 for substrate ABTS (Fig. 3A). The optimal pH of the reaction for enzyme with SGZ was slightly different in comparison with already published pH values (4.0–5.0) [1,3]. Record et al. (2002) studied the effect of pH on laccase activity and concluded that with ABTS activity of enzyme increased when pH decreased [8]. In this report, optimal pH value of reaction environment for reaction of laccase with ABTS is lower than that for reaction with SGZ (Fig. 3B).

To know more about the oxidation ability to detoxificate textile azo dyes soluble laccase was used for the decolorization of model anthraquinone dye ANTD (Fig. 4) and simple azo dye Dye I (Fig. 5). After ANTD oxidation by laccase (*T.v.* or *P.c.*), the new peak of products (similar, unknown structure) at 480 nm appeared in

Table 1
Kinetic characterization of laccase isolated from *P.c.* and *T.v.* for substrate ABTS, compared with K_m already published and summarized in database Brenda.

Laccase	Experimental K_m (mM)	Experimental V_m (mM/s)	Published K_m (mM)
Trametes versicolor	0.0337	1.98×10^{-4}	0.62 [23]
Pycnoporus cinnabarinus	0.0508[a]	7.47×10^{-5}[a]	0.041 [24]

[a] Average value from five measurements.

Table 2
Kinetic characterization of laccase *T.v.* and *P.c.* for substrate SGZ, compared with K_m already published and summarized in database Brenda.

Source of laccase	Experimental K_m (mM)	Experimental V_m (mM/s)	Published K_m (mM)
Trametes versicolor	0.0328	0.0106	0.028[a] [16]
Pycnoporus cinnabarinus	0.0129	0.0114	0.004 ± 0.001 [25]

[a] *Trametes* sp. AH28-2.

decolorization spectra. Degradation of azo dye (Dye I) is not quite effective, although it can be easily oxidized. One of the possible reasons could be the fact that azo dye Dye I have higher redox potential than laccase and do not operate as a mediator.

Soluble laccase is sensitive (even inactivated) towards high salt concentrations, high pH and inhibitors characteristic for effluents [11]. Therefore, the improvement of the laccase stability as well as the possibility to reuse it in consecutive catalyzed cycles was needed. The oriented immobilization of laccase to a water-insoluble support could be a promising solution.

Initial phase was focused on the choice of suitable support and selecting convenient immobilization technique. Previously laccase was immobilized on various types of carriers, preferably magnetic ones. Magnetic particles are convenient, consistent, stable, easy to handle and offer exceptional flexibility compared with conventional chromatographic resins. With respect to chosen method of enzyme quantification on the carrier, kinetic measurement, magnetic macroporous bead cellulose and its hydrazide derivative were used for laccase immobilization (Fig. 6). Advantage of this carrier consists in large specific surface area due to high porosity, low nonspecific sorption of proteins and peptides, simplicity and excellent flow rate property [14]. Low cost and good handling are indisputable advantages for routine laboratories and biotechnology application.

Next, suitable immobilization strategy has to be selected with the aim to achieve high enzyme activity and stability of the carrier. Oriented immobilization, where all active sites of enzyme remain sterically accessible also for high-molecular-weight substrates can be a promising choice [17]. Enzymes–glycoproteins—can be immobilized through their glycosidic chains. Increased stability of orientedly immobilized enzymes already confirmed for various bioactive glycoproteins (antibodies, enzymes) [18]. The proper orientation of all enzyme molecules is assured due to the fact that enzyme active sites are always situated outside the glycosidic part of enzyme. The hydrazide derivatives of carriers are presently provided by many companies and they are in common use for oriented immobilization of glycoproteins.

In order to evaluate the effect of immobilization strategy to the activity and stability, two covalent binding strategies were applied: immobilization of enzyme molecules orientedly through carbohydrate moieties, immobilization of laccase non-orientedly through NH_2- groups located on the surface of laccase molecules (Table 3). In this case, the enzyme molecules were bound to the aldehyde groups of oxidized cellulose creating Schiff base formation with subsequent stabilization of the linkage by reductive amination [19]. The improved immobilization strategy

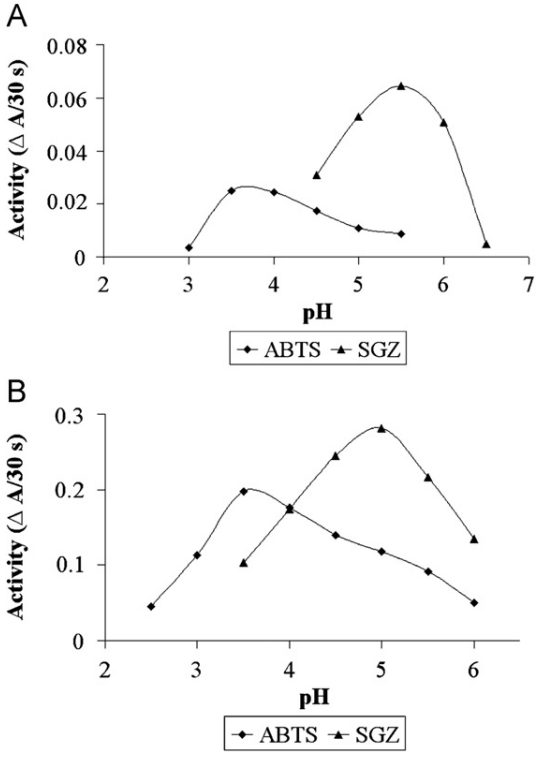

Fig. 3. Optimization of pH conditions for the reaction of laccase with substrates SGZ and ABTS. The reactions of 0.2 I.U. (laccase from *T.v.*) and 0.0075 I.U. (laccase from *P.c.*) with SGZ (35 μM) and ABTS (45 μM) in 1 ml of reaction mixture proceeded in glycine–HCl buffer (pH 2–3), acetate buffer (pH 3.5–6) and phosphate buffer (pH 6.5). (A) Laccase from *T.v.* and (B) Laccase from *P.c.*.

is based on the activation of terminal monosaccharide of glycosidic chains by specific oxidizing agent, e.g. sodium peroxidate or oxidizing enzyme galactose oxidase [20]. Both approaches lead to the formation of aldehyde groups which can react with hydrazide functional groups on the carrier. The resulting condensation product is a stable hydrazone. The total amount of immobilized protein was estimated by bicinchoninic acid (BCA) test modified in our laboratory for solid phase. The enzyme activity was measured using SGZ or ABTS as substrates. The average activity of oriented immobilized laccase from *P.c.* (0.63 ± 0.111 I.U./ml of settled carrier) in comparison with the

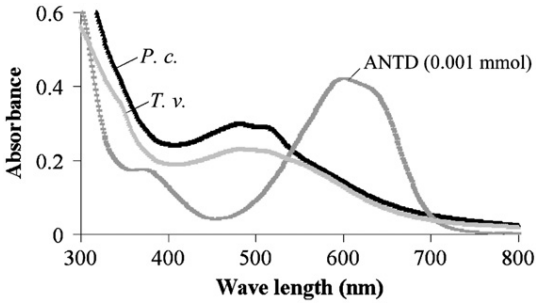

Fig. 4. Spectra of ANTD decolorization by soluble laccase (5 I.U. in 25 ml of reaction mixture), *P.c.* = *Pycnoporus cinnabarinus*, *T.v.* = *Trametes versicolor*.

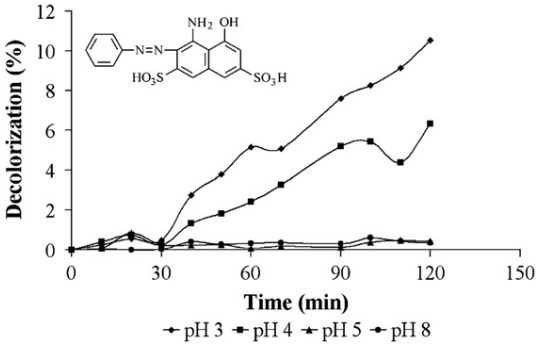

Fig. 5. Decolorization of Dye I by soluble laccase from *P.c.* (2.5 I.U. in 25 ml of reaction mixture, pH 3, 4, 5 and 8).

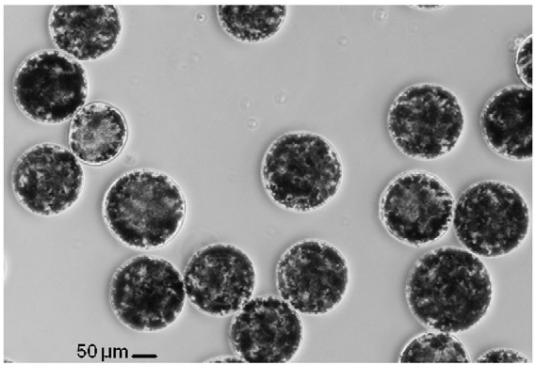

Fig. 6. Magnetic macroporous bead cellulose, particle size 125–250 μm with 20 μmol of hydrazide moieties per 1 ml of settled carrier, magnification 400 ×.

average activity of non-oriented immobilized laccase (0.22 ± 0.005 I.U./ml of settled carrier) confirmed the predicted preferences of oriented enzyme immobilization (Table 3). The enzyme activity of laccase immobilized to non-magnetic form of bead cellulose was determined also by kinetic measurement, but the total activity was not quantified due to the color instability of product and time-consuming separation of carrier from supernatant by centrifugation.

Storage stability of an enzyme is a significant parameter for carriers applied in biotechnology processes [21]. The enzyme carriers were stored at 5–10 °C. The oxidation activity was determined every week with new aliquots of carrier. No loss in activity of the laccase immobilized orientedly was observed after one month. The results indicated that the immobilized enzyme had much better storage stability than the free enzyme. Operational stability is also parameter needed for application in practice. The enzyme activity was measured repeatedly with the same aliquots of the carrier. The activities were almost the same after 7th repetition. During repeated catalysis of the reaction, the actual activity of immobilized enzymes temporarily increased (about 10–15% of origin activity measured immediately after immobilization). Presumably the repeated contact of enzyme molecules with substrate can enhance the renaturation of native conformation of enzyme molecules negatively affected during immobilization and also can give support for oligomerization of functional multimeric complexes [9].

For estimation of suitable storage conditions, the effect of sodium azide in storage buffer was tested. Minussi et al. (2007) investigated the inactivation of laccase isolated from *T. versicolor* by various concentrations of potential inhibitors and discovered that the activity of laccase is strongly inhibited by the addition of sodium azide, L-cysteine or dithiothreitol [22]. After one week storage of laccase carrier in presence of sodium azide, the immobilized laccase activity decreased almost to zero. After washing the carrier and elimination of sodium azide, the laccase activity was regenerated after 1 week, stored in 0.05 M K–acetate buffer pH 4.5 with 5 mM $CuCl_2$. Although laccase is strongly inhibited by sodium azide, the inhibition is reversible. The immobilized laccase with provided good storage and operational stability has a potential to be tested for practical biotechnology application. At present, the testing of additional reaction conditions as temperature, pH and detergent stability using the newly developed laccase reactor is in progress.

3. Conclusions

On the basis of the provided results, the magnetic laccase carrier for industrial or biotechnology applications was developed.

Table 3
Summary of carriers with immobilized laccase.

Carrier	Particle size	Function group	Immobilization technique	Laccase activity[a]
Bead cellulose (non-magnetic)	80–100 μm	–OH	Schiff base formation with subsequent reductive amination	⩽0.10 I.U./ml of s. c. (see text)
Bead cellulose (magnetic)	125–250 μm	–OH	Schiff base formation with subsequent reductive amination	0.22 ± 0.005 I.U./ml of s. c.
Bead cellulose (non-magnetic)	80–100 μm	–NH–NH_2 15 μmol ADH/ml of s. c.	First aldehyde groups formation Second formation of stable hydrazone	0.15–0.20 I.U./ml of s. c. (see text)
Bead cellulose (magnetic)	125–250 μm	–NH–NH_2 20 μmol ADH/ml of s. c.	1st aldehyde groups formation 2nd formation of stable hydrazone	0.63 ± 0.11 I.U./ml of s. c.

ADH—adipic acid dihydrazide
s. c.—settled carrier
[a] Kinetic measurement of enzyme activity (Fig. 1).

The highest enzyme activity (0.63 ± 0.111 I.U./ml of settled carrier) was achieved with laccase immobilized in an oriented fashion through the glycosidic moieties. Hydrophilic macroporous bead cellulose with defined size, dispersity and ferrite content provide versatile and robust carrier for by laccase catalyzed oxidation reaction.

The suitability of oriented immobilization for the preparation of highly active enzyme carrier was confirmed.

Acknowledgements

This work was supported by the Ministry of Education of Czech Republic, Project no. MSMT 0021627502 and by the Czech Science Foundation, Project no. 203/08/1536.

References

[1] Ch. Galhaup, S. Goller, C.K. Peterbauer, et al., Microbiology 148 (2002) 2159.
[2] C. Crecchio, P. Ruggiero, M.D.R. Pizzigallo, Biotechnol. Bioeng. 48 (1995) 585.
[3] K. Schliephake, D.E. Mainwaring, G.T. Lonergan, et al., Enzyme Microb. Technol. 27 (2000) 100.
[4] G.M.B. Soares, M.T.P. Amorim, R. Hrdina, et al., Process Biochem. 37 (2002) 581.
[5] J.A. Stephen, J. Chem. Technol. Biotechnol. 62 (1995) 111.
[6] E. Abadulla, T. Tzanov, S. Costa, et al., Appl. Environ. Microbiol. 66 (2000) 3357.
[7] S. Rodríguez Couto, D. Hofer, M.A. Sanromán, et al., Eng. Life Sci. 4 (2004) 233.
[8] E. Record, P.J. Punt, M. Chamkha, et al., Eur. J. Biochem. 269 (2002) 602.
[9] C.F. Thurston, Microbiology 140 (1994) 19.
[10] N. Durán, M.A. Rosa, A. D'Annibale, et al., Enzyme Microb. Technol. 31 (2002) 907.
[11] A. D′Annibale, S.R. Stazi, V. Vinciguerra, et al., Process Biochem. 34 (1999) 697.
[12] J. Turková, Z. Kučerová, M.J. Beneš, J. Mol. Recognition 9 (1998) 360.
[13] L. Korecká, J. Ježová, Z. Bílková, et al., J. Magn. Magn. Mater. 293 (2005) 349.
[14] J. Lenfeld, Angew. Makromol. Chem. 212 (1993) 147.
[15] L. Setti, S. Giuliani, G. Spinozzi, et al., Enzyme Microb. Technol. 25 (1999) 285.
[16] Y.Z. Xiao, Q. Chen, J. Hang, et al., Mycologia 96 (2004) 26.
[17] J. Turková, I. Vinš, M.J. Beneš, et al., Int. J. Bio-Chromatogr. 1 (1994) 1.
[18] D.J. O′Shannessy, J. Chromatogr. 510 (1990) 13.
[19] G.T. Hermanson (Ed.), Bioconjugate Techniques, Academic Press, San Diego, 1996.
[20] Z. Bílková, M. Slováková, A. Lyčka, et al., J. Chromatogr. B 770 (2002) 25.
[21] I. Chibata (Ed.), Immobilized Enzymes, A Halsted Press Book, Tokyo, 1978.
[22] R.C. Minussi, M.A. Miranda, J.A. Silva, et al., Afr. J. Biotechnol. 6 (2007) 1248.
[23] N.K. Pazarlioglu, M. Sariisik, A. Telefoncu, Process Biochem. 40 (2005) 1673.
[24] C. Sigoillot, E. Record, V. Belle, et al., Appl. Microbiol. Biotechnol. 64 (2004) 346.
[25] K. Li, F. Xu, K.-E.L. Eriksson, Appl. Environ. Microbiol. 65 (1999) 2654.

Příloha P6

Čadková M., Metelka R., Holubová L., Horák D., Dvořáková V., Bílková Z., **Korecká L.*** Magnetic beads-based electrochemical immunosensor for monitoring allergenic food proteins. *Analytical Biochemistry,* **484**, 2015, 4-8

IF_{2018} = 2,507; Q2 – Chemical sciences, Q3 – Biological sciences – Biochemistry;

25 citací [1. 7. 2020]

- koncepce výzkumu, plánování experimentů
- podíl na experimentální práci a vyhodnocení výsledků 30 %
- dílčí příprava článku, revize, korespondující autor

Analytical Biochemistry 484 (2015) 4–8

Contents lists available at ScienceDirect

Analytical Biochemistry

journal homepage: www.elsevier.com/locate/yabio

Magnetic beads-based electrochemical immunosensor for monitoring allergenic food proteins

Michaela Čadková [a], Radovan Metelka [b], Lucie Holubová [a], Daniel Horák [c], Veronika Dvořáková [a], Zuzana Bílková [a], Lucie Korecká [a,*]

[a] Department of Biological and Biochemical Sciences, Faculty of Chemical Technology, University of Pardubice, 532 10 Pardubice, Czech Republic
[b] Department of Analytical Chemistry, Faculty of Chemical Technology, University of Pardubice, 532 10 Pardubice, Czech Republic
[c] Institute of Macromolecular Chemistry, Academy of Sciences of the Czech Republic, 162 06 Prague, Czech Republic

ARTICLE INFO

Article history:
Received 6 February 2015
Received in revised form 10 April 2015
Accepted 30 April 2015
Available online 9 May 2015

Keywords:
Electrochemical immunosensor
Magnetic particles
Ovalbumin

ABSTRACT

Screen-printed platinum electrodes as transducer and magnetic beads as solid phase were combined to develop a particle-based electrochemical immunosensor for monitoring the serious food allergen ovalbumin. The standard arrangement of enzyme-linked immunosorbent assay became the basis for designing the immunosensor. A sandwich-type immunocomplex was formed between magnetic particles functionalized with specific anti-ovalbumin immunoglobulin G and captured ovalbumin molecules, and secondary anti-ovalbumin antibodies conjugated with the enzyme horseradish peroxidase were subsequently added as label tag. The electrochemical signal proportional to the enzymatic reaction of horseradish peroxidase during the reduction of hydrogen peroxide with thionine as electron mediator was measured by linear sweep voltammetry. The newly established method of ovalbumin detection exhibits high sensitivity suitable for quantification in the range of 11 to 222 nM and a detection limit of 5 nM. Magnetic beads-based assay format using external magnets for rapid and simple separation has been proven to be an excellent basis for electrochemical detection and quantification of food allergens in highly complex sample matrices.

Adverse food reaction, including food intolerance or allergy, is a broad term referring to any abnormal clinical response associated with ingestion of a food [1] and results in life-threatening reactions [2]. One of the most serious allergic reactions to foods is egg hypersensitivity in children caused by the major allergens ovalbumin (OVA)[1] and ovomucoid [1,3–9].

Ovalbumin, a water-soluble phosphoglycoprotein with molecular mass of approximately 45 kDa [7,8,10], is often present in various foods as an emulsifying and foaming agent [11]. A rapid and sensitive ovalbumin detection method, therefore, would be of great value. Methods commonly used for ovalbumin determination consist of laborious, time-consuming, and often expensive procedures [8,11,12] such as radioimmunoelectrophoresis [10,13,14], immunoblotting [15], competitive immunoassay [16], Western blot [17], and enzyme-linked immunosorbent assay (ELISA) [18–20]. An element common to all of the aforementioned methods is the use of specific antibodies for selective capture of the target antigen. Such traditional methods also are instrumentally challenging and must be performed by analytical experts in fully equipped laboratories. Combinations of immunochemical and electrochemical methods are becoming more attractive today, mainly for their wide accessibility, ease of implementation, and ability to perform measurements even outside of laboratories.

The great advantage of electrochemical methods is the possibility they offer to use screen-printed sensors, characterized by factors such as low-cost fabrication, low sample consumption, and possible surface modification [21,22]. The electrode surface used as a solid phase for incubation of target antigen and transduction of the electrochemical signal has certain restrictions consisting in a limited number of accessible recognizing biomolecules, its influence on the kinetics of the antibody–antigen reaction, and the possibility of electrode defects caused by washing steps [23]. All of

* Corresponding author. Fax: +420 466 037 068.
E-mail address: lucie.korecka@upce.cz (L. Korecká).

[1] *Abbreviations used:* OVA, ovalbumin; ELISA, enzyme-linked immunosorbent assay; IgG, immunoglobulin G; EDC, 1-ethyl-3-(3-dimethylaminopropyl)carbodiimide hydrochloride; sulfo-NHS, *N*-hydroxysulfosuccinimide sodium salt; BSA, bovine serum albumin; OPD, *o*-phenylenediamine; Mes, 2-morpholinoethane-1-sulfonic acid; HRP, horseradish peroxidase; anti-OVA^{HRP}, anti-ovalbumin IgG antibodies labeled with horseradish peroxidase; p(GMA-MOEAA)-NH_2, poly[glycidylmethacrylate-(methacryloyloxy)ethoxy]acetic acid)-NH_2; HA, hyaluronic acid; SDS–PAGE, sodium dodecyl sulfate–polyacrylamide gel electrophoresis; LSV, linear sweep voltammetry.

http://dx.doi.org/10.1016/j.ab.2015.04.037
0003-2697/

these drawbacks could be overcome by the use of magnetic beads [21,23–25] having large specific surface areas and functional groups for the attachment of various ligands [26]. Magnetic particles with all of these advantages already have been successfully coupled with electrochemical sensors [21,23–25].

To date, there have been only a few published articles devoted to electrochemical detection of the allergen ovalbumin. These studies used different analytical approaches enabling demonstration of the presence or even quantification of the desired allergen in biological samples such as by using a specific electrode modification with concanavalin A in combination with an aminoferrocene mediator [27], a covalently bound ovalbumin antibody with 4-carboxyphenyl film [28], peptides labeled with the electroactive compound daunomycin [29], pulsed electrochemical detection on a rotating gold electrode after high-performance liquid chromatography separation [30], and a reagentless immunosensor based on a multifunctional conjugated quinone-type copolymer [31]. Kuramitz and coworkers [32] used hydrodynamic voltammetry with a rotating disc electrode for detecting ovalbumin captured by magnetic particles modified by anti-ovalbumin immunoglobulin G (IgG) molecules.

We present here a selective and sensitive magnetic beads-based electrochemical immunosensor for rapid assay of ovalbumin using screen-printed platinum electrodes. The novelty of the current work lies in its combining the advantages of magnetic separation, selectivity of specific antibodies, and sensitivity of electrochemical detection. All of this is performed without the need for any additional preanalytical steps. To achieve sufficient shuttling of electrons between the substrate and redox center of the enzyme [33], an electron mediator could be used. We selected thionine for this purpose. Moreover, this approach avoids prolonged preparation steps (e.g., direct grafting of the electrodes with ovalbumin [31]) or other various modifications [27,29].

Materials and methods

Chemicals

Albumin from chicken egg (OVA), Oligo-HA4, thionine acetate, 1-ethyl-3-(3-dimethylaminopropyl)carbodiimide hydrochloride (EDC), *N*-hydroxysulfosuccinimide sodium salt (sulfo-NHS), hydrogen peroxide, bovine serum albumin (BSA), *o*-phenylenediamine (OPD), 2-morpholinoethane-1-sulfonic acid (Mes), and Tween 20 were purchased from Sigma–Aldrich (St. Louis, MO, USA). Horseradish peroxidase (HRP, 800 IU/mg) was provided by Fluka (Buchs, Switzerland). Affinity purified rabbit monoclonal anti-OVA IgG antibodies and secondary rabbit polyclonal anti-OVA IgG antibodies labeled with HRP (anti-OVA^{HRP}) were obtained from Patricell (Nottingham, UK). Precision Plus Protein unstained standard 10 to 250 kDa was a product of Bio-Rad (Hercules, CA, USA). Sera-Mag Double Speed magnetic carboxylate-modified microparticles (0.771 μm in diameter) were supplied by Thermo Fisher Scientific (Indianapolis, IN, USA), and poly[glycidylmethacrylate-(methacryloyloxy)ethoxy]acetic acid)-NH_2 (p(GMA-MOEAA)-NH_2) magnetic particles (4.5 μm in diameter) were kindly provided by the Institute of Macromolecular Chemistry (Academy of Sciences of the Czech Republic, Prague, Czech Republic) [34,35]. All other chemicals were supplied by Sigma–Aldrich or Penta (Chrudim, Czech Republic) and were of reagent grade.

Apparatus

All electrochemical measurements were performed with a PalmSens compact electrochemical sensor interface (PalmSens, Utrecht, Netherlands) connected to screen-printed three-electrode sensors (BST-120) composed of working and auxiliary electrodes made of platinum and Ag/AgCl pseudo-reference electrode (Bio Sensor Technology, Berlin, Germany).

Immobilization of anti-OVA antibodies on carboxylate-modified magnetic microparticles

The two kinds of magnetic particles—p(GMA-MOEAA)-NH_2 coated with hyaluronic acid (HA) [36] and commercially available carboxylate-modified Sera-Mag magnetic particles—were exploited for covalent coupling of specific antibodies using a slightly modified two-step carbodiimide method and with EDC as zero-length cross-linker and sulfo-NHS according to Hermanson [37]. Here, 1 mg of magnetic particles was washed five times with 50 mM Mes buffer (pH 5.0). EDC (2 mg) and sulfo-NHS (2.2 mg) were then dissolved in 500 μl of Mes buffer, and the reaction mixture was stirred for 30 min at room temperature. Particles were then washed two times with 0.5 M Mes buffer with the addition of 100 μg of affinity-purified monoclonal anti-OVA antibodies (IgG) dissolved in 1 ml of 50 mM Mes buffer in the final step. This was incubated overnight at 4 °C (with gentle mixing) and then washed three times with Mes buffer, followed by four times with 0.1 M phosphate buffer (pH 7.3). Immobilization efficiency was estimated using Tris/glycine sodium dodecyl sulfate–polyacrylamide gel electrophoresis (SDS–PAGE).

Immobilization of HRP on Sera-Mag microparticles

Similarly, the modified common carbodiimide method described by Hermanson [37] was used for covalent immobilization of HRP onto carboxylate-modified Sera-Mag magnetic particles. Here, 1 mg of magnetic particles was washed five times with 0.1 M phosphate buffer (pH 7.3) and activated by 7.5 mg of EDC and 1.25 mg of sulfo-NHS dissolved in 1 ml of phosphate buffer for 10 min at room temperature with gentle mixing. After removing the supernatant, 1.5 mg of HRP in 1 ml of phosphate buffer was added. After overnight incubation at 4 °C with gentle mixing, the magnetic particles were washed with phosphate buffer five times. The activity of immobilized HRP was determined as published previously [38] with slight modification. Here, 50 μg of magnetic beads with immobilized HRP was incubated with substrate solution (5 mg OPD with 5 μl of 30% hydrogen peroxide in 10 ml of 0.1 M phosphate buffer, pH 6.2) protected from light using gentle mixing for 10 min at 37 °C. This was followed by spectrophotometric measurement of 100 μl of supernatant in a microwell plate at 492 nm.

Sandwich-type immunocomplex formation

Immunocomplex formation was performed as the mixture of OVA and Sera-Mag with immobilized monoclonal anti-OVA antibodies in molar ratio 2:1 (OVA/anti-OVA) within 0.1 M phosphate buffer (pH 7.0) was incubated for 1 h at room temperature under gentle mixing. It was then washed three times with phosphate buffer. Afterward, secondary anti-OVA^{HRP} IgG in 0.1 M carbonate buffer (pH 9.49) (1:10,000, v/v) with 0.1% BSA and 0.05% Tween 20 was added. Incubation followed for 1 h at 37 °C [39]. In parallel, the blank sample eliminating the negative effect of nonspecific sorption of secondary anti-OVA^{HRP} IgG was prepared by the same protocol without antigen addition.

Electrochemical measurement

Linear sweep voltammetry (LSV) was selected as the most suitable voltammetric technique. It was used for all electrochemical recordings of current decrease during hydrogen peroxide oxidation

caused by enzymatic conversion using HRP. Potential range of 0 to 0.8 V, potential step of 0.005 V, scan rate of 50 mV/s, and equilibration time of 2 s were the optimized experimental LSV parameters.

With regard for the surface of screen-printed electrodes and their possible reuse, minimal hydrogen peroxide concentration (1 mg/L) in 0.1 M phosphate buffer (pH 7.3) with 0.15 M NaCl as substrate solution and different concentrations of thionine acetate (25, 50, 100, 250, and 1000 μM) were used. Substrate solution with thionine (800 μl) was subsequently added to the suspension of S eraMag–anti-OVA–OVA–anti-OVA^{HRP} mixture. For measurements, 40 μl of supernatant was pipetted onto the electrode; the remaining content was still mixed on a rotator. The current response of hydrogen peroxide oxidation with or without the addition of thionine was recorded at the potential 0.4 V and monitored at 5-min intervals for a total time of 15 min.

Results and discussion

The aim of our work was to develop a sensitive immunosensor for ovalbumin detection that could be potentially exploited also for detecting any other clinically significant protein with the aid of a corresponding antibody and by mere change of the specific reagents used. Attaining detection limits as low as possible is the main challenge in developing sensors for protein detection with respect to the low concentrations of analyzed proteins in complex biological samples. The combination of selective immunochemical reaction with sensitive electrochemical techniques offers a very promising approach in comparison with methods based on a standard ELISA arrangement, especially due to the potential for miniaturization, low sample volumes, rapid analysis, and possible automation of analysis and the possibility of measurement outside the laboratory maintaining the sensitivity and specificity.

First, we focused on preparing the immunosensor based on covalent attachment of antibodies specific to the target antigen to the surface of magnetic microparticles. Such an approach enables easy and fast isolation and separation of ovalbumin directly from the complex matrix and removes unwanted impurities without any further sample pre-purification using external magnet. Subsequently, ovalbumin detection is based on electrochemical monitoring of hydrogen peroxide consumption in the substrate solution by the enzyme HRP, used as a label for specific anti-OVA antibodies. The decreased response of the hydrogen peroxide oxidation current is then related to the amount of ovalbumin in the sample. Considering the current trend toward miniaturizing analytical devices, we used miniaturized screen-printed three-electrode sensors with platinum working electrodes. This approach is feasible for detection of hydrogen peroxide oxidation.

For immunomagnetic protein isolation, specific anti-OVA IgG was covalently immobilized onto the surface of magnetic particles via EDC/sulfo-NHS chemistry. Two types of magnetic carriers were selected. The first was commercial carboxylate-modified Sera-Mag Double Speed microparticles made of encapsulated magnetite and characterized by increased speed of response to a magnetic field. Second, amino-modified magnetic particles made of p(GMA-MOEAA)-NH_2 and 4.5 μm in diameter were tested. The immobilization efficiency of anti-OVA IgG was verified by densitometric evaluation of polyacrylamide gels after SDS–PAGE analysis by Chemi-Doc XRS with Image Lab software by comparing the density of the bands before and after immobilization (see Fig. 1), and simultaneously the amount of immobilized anti-OVA IgG was assessed by absorbance measurement at 260/280 nm. Both methods confirmed the immobilization efficiency as 86% for Sera-Mag and 90% for HA-coated p(GMA-MOEAA)-NH_2 acquired from SDS–PAGE evaluation, which correspond to 89 and 98 μg of anti-OVA IgG (based on 260/280-nm measurement).

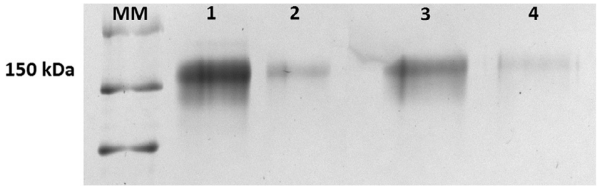

Fig.1. Tris/glycine SDS–PAGE of fractions from anti-OVA immobilization onto Sera-Mag (positions 1 and 2) and onto p(GMA-MOEAA)-NH_2 magnetic particles coated by HA (positions 3 and 4). MM, Precision Plus Protein standard; positions 1 and 3: anti-OVA IgG before immobilization; positions 2 and 4: anti-OVA IgG after immobilization. Materials and conditions: 10% polyacrylamide separation gel, 5% polyacrylamide focusing gel, silver staining, samples mixed with Laemmli sample buffer (1:1, v/v).

It has been repeatedly verified that naked p(GMA-MOEAA)-NH_2 particles cause instability in current response during subsequent electrochemical measurements, probably due to residues of electrochemically active iron oxides on the surface of particles that were not sufficiently encapsulated in a polymer shell. Such is the case of carboxylate-modified Sera-Mag particles. In view of these microparticles' other excellent characteristics, such as good response to the magnetic field and high binding capacity, we decided to perform post-synthetic surface coating using HA as described previously [36]. Surface coating with such a glycosaminoglycan improves colloidal stability, provides a compact layer covering the surface iron oxides, and (last but not least) inserts free carboxylic functional groups enough for effective binding of specific antibodies. That is why HA-coated p(GMA-MOEAA)-NH_2 particles were subsequently used in addition to the carboxylate-modified Sera-Mag magnetic particles.

Electrochemical measurements were performed using miniaturized screen-printed electrodes, thereby enabling measurement in a small droplet of 40 μl [39]. Two features were critical for electrochemical detection of the allergen using the ELISA sandwich approach, namely high selectivity and sensitivity. Although in our previous study the immunosensor showed high selectivity [39], the sensitivity of the final electrochemical analysis was insufficient.

In the current work, we focused on substantially increasing the sensitivity of electrochemical detection. One promising strategy is to promote electron transfer between the molecule of interest and the electrode using an electron mediator. For signal amplification of the aforementioned electrochemical immunosensor based on HRP as a label of secondary antibodies, thionine was selected as the mediator (see Fig. 2). Thionine exhibits pronounced electrocatalytic activity toward both the reduction and oxidation of hydrogen peroxide. The electrocatalytic properties of thionine were used mainly during reduction of hydrogen peroxide [40,41], although enhanced sensitivities in the case of hydrogen peroxide oxidation also have been reported [42].

First, the effect of thionine addition on the current level during measurement of hydrogen peroxide (1 mg/L) was evaluated in 0.1 M phosphate buffer (pH 7.3) with 0.15 M NaCl and different concentrations of thionine (25, 50, 100, and 250 μM and 1 mM). All measurements were performed in triplicate. The increasing oxidation current response correlates with a higher amount of thionine in the substrate solution (see Fig. 3). Even though the strongest response was observed with 1 mM thionine, the maximum concentration of 100 μM thionine was chosen as sufficient due to the limited solubility of the mediator at high concentrations.

For simplicity, the signal amplification effect was also tested by the subsidiary simulation of the final step using HRP-modified Sera-Mag particles. The aim was to electrochemically monitor the current change induced by HRP's conversion of hydrogen peroxide. For the experiment, 50 μg of particles with immobilized HRP

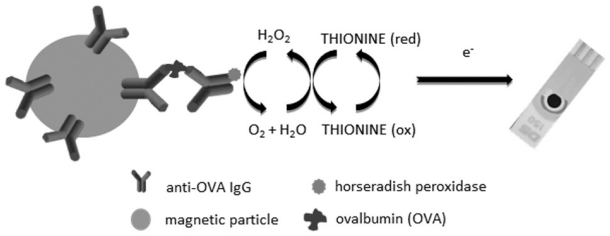

Fig.2. Scheme of electrochemical immunomagnetic biosensor for ovalbumin detection. H_2O_2, hydrogen peroxide.

(4.5 IU) was taken into the reaction and incubated with hydrogen peroxide for 15 min. The current change induced by the enzyme reaction was monitored at 5-min intervals with the aid of the LSV technique after the separation of magnetic particles onto the working electrode of the screen-printed sensor. All measurements were performed in triplicate. The addition of electron mediator produces increased oxidation currents compared with measurements without thionine, which improved sensitivity in the detection step of the proposed electrochemical immunoassay.

Finally, a magnetic beads-based electrochemical immunosensor for ovalbumin detection was constructed. The monitored decrease in current response over time caused by enzymatic consumption of the substrate was related to the amount of target antigen in the sample. The negative effect of nonspecific sorption of secondary anti-OVA IgG has been eliminated by subtraction of current registered for blank sample.

The decrease of electrochemical response of substrate hydrogen peroxide consumed by HRP, the label of secondary anti-OVA IgG, in the presence of target antigen (OVA) in the sample was evident. Moreover, the positive effect of thionine as mediator in the substrate solution, and thus mediation of the electron transfer between enzyme and surface of electrode, was confirmed. Each immunoassay was performed using new screen-printed sensor to avoid unwanted passivation of working electrode surface area between experiments. To correct unequal background currents of used working electrodes, the difference between the current value measured at the beginning of the detection step and after 10 min of substrate conversion was plotted against the ovalbumin

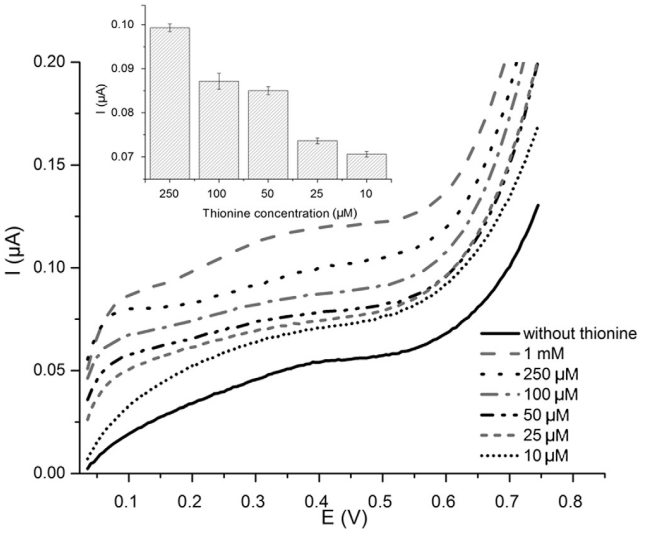

Fig.3. Effect of thionine addition on the current response for hydrogen peroxide oxidation. Medium and conditions: 0.1 M phosphate buffer (pH 7.3) containing 0.15 M NaCl and hydrogen peroxide (1 mg/L), thionine concentrations (10 μM to 1 mM), linear sweep voltammetry, thick film sensor (Pt/Pt/Ag/AgCl).

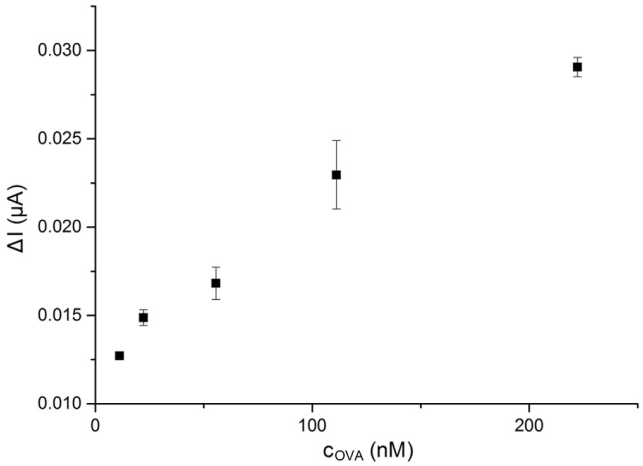

Fig.4. Increase in current response due to hydrogen peroxide consumption by HRP on ovalbumin in the sample with 100 μM thionine. All measurements were performed in triplicate.

concentration. Using such a transformation, a current difference was then proportional to the concentration of ovalbumin, which enables simpler evaluation of the amount of target analyte in the sample (Fig. 4).

The presented immunosensor for ovalbumin determination exhibits linear range from 11 to 200 nM. The linear regression equation was $I\,(\mu A) = 7.77 * 10^{-5}\, c_{OVA}\,(nM) + 0.012$ with a correlation coefficient of 0.9856. The ovalbumin detection limit using the presented system was calculated as 5 nM ovalbumin (estimated for a signal-to-noise ratio of 3) in the sample. This system using magnetic particles enables capture of desired allergen molecules from the highly complex biological material; thus, pre-concentrated molecules can be effectively eluted into the minimum volume and further analyzed electrochemically.

Conclusion

In this article, we have demonstrated a highly selective and sensitive magnetic beads-based electrochemical immunosensor for rapid detection of food proteins with allergenic potential using screen-printed platinum electrodes. The electron mediator thionine was employed with the aim to increase sensitivity of the analysis. The immunosensor could be reused after simple regeneration and washing steps; therefore, the overall costs of the analysis could be reduced substantially. The design of the proposed magnetic beads-based electrochemical immunosensor constitutes a potentially universal system applicable to any other antigen so long as specific antibodies are available.

Acknowledgment

This work was supported by the grant from the Czech Science Foundation, No. P206/12/0381.

References

[1] A. Cianferoni, J.M. Spergel, Food allergy: review, classification, and diagnosis, Allergol. Int. 58 (2009) 457–466.
[2] A.W. Burks, M. Tang, S. Sicherer, A. Muraro, P.A. Eigenmann, M. Ebisawa, A. Fiocchi, W. Chiang, K. Beyer, R. Wood, J. Hourihane, S.M. Jones, G. Lack, H.A. Sampson, ICON: food allergy, J. Allergy Clin. Immunol. 129 (2012) 906–920.
[3] W.A. Żukiewicz-Sobczak, P. Wróblewska, P. Adamczuk, P. Kopczyński, Causes, symptoms, and prevention of food allergy, Postepy Dermatol. Alergol. 30 (2013) 113–116.
[4] M.D. Chapman, Anna Pomés, H. Breiteneder, F. Ferreira, Nomenclature and structural biology of allergens, J. Allergy Clin. Immunol. 119 (2007) 414–420.

[5] J.H. Seo, J.W. Lee, J.H. Kim, E.B. Byun, S.Y. Lee, I.J. Kang, M.W. Byun, Reduction of allergenicity of irradiated ovalbumin in ovalbumin-allergic mice, Radiat. Phys. Chem. 76 (2007) 1855–1857.
[6] J.C. Caubet, R. Bencharitiwong, E. Moshier, J.H. Godbold, H.A. Sampson, A. Nowak-Węgrzyn, Significance of ovomucoid- and ovalbumin-specific IgE/IgG(4) ratios in egg allergy, J. Allergy Clin. Immunol. 129 (2012) 739–747.
[7] W.X. Su, J. Rick, T.C. Chou, Selective recognition of ovalbumin using a molecularly imprinted polymer, Microchem. J. 92 (2009) 123–128.
[8] Y. Mine, M. Yang, Recent advances in the understanding of egg allergens: basic, industrial, and clinical perspectives, J. Agric. Food Chem. 56 (2008) 4874–4900.
[9] Y. Kato, E. Oozawa, T. Matsuda, Decrease in antigenic and allergenic potentials of ovomucoid by heating in the presence of wheat flour: dependence on wheat variety and intermolecular disulfide bridges, J. Agric. Food Chem. 49 (2001) 3661–3665.
[10] V. Lechevalier, T. Croguennec, F. Nau, C. Guérin-Dubiard, Part I, Chapter: Ovalbumin and gene-related proteins, in: R. Huopalahti, R. López-Fandiño, M. Anton, R. Schade (Eds.), Bioactive Egg Compounds, Springer, Heidelberg, Germany, 2007, pp. 51–60.
[11] S. Purushothama, S. Kradtap, C.A. Wijayawardhana, H.B. Halsall, W.R. Heineman, Small volume bead assay for ovalbumin with electrochemical detection, Analyst 126 (2001) 337–341.
[12] S.R. Raz, H. Liu, W. Norde, M.G.E.G. Bremer, Food allergens profiling with an imaging surface plasmon resonance-based biosensor, Anal. Chem. 82 (2010) 8485–8491.
[13] T. Langeland, A clinical and immunological study of allergy to hen's egg white: III. Allergens in hen's egg white studied by crossed radio-immunoelectrophoresis (CRIE), Allergy 37 (1982) 521–530.
[14] J.R. Cann, Electrophoretic analysis of ovalbumin, J. Am. Chem. Soc. 71 (1949) 907–909.
[15] V. Leduc, C. Demeulemester, B. Polack, C. Guizard, L. Le Guern, G. Peltre, Immunochemical detection of egg-white antigens and allergens in meat products, Allergy 54 (1999) 464–472.
[16] S.W. Zhang, X.T. Lai, G.W. Yang, Enzyme-linked Fab' fragment based competitive immunoassay for ovalbumin in hot-processed food, J. Immunoassay Immunochem. 34 (2013) 393–403.
[17] M.A. Romero-Rodríguez, R. Barcia-Vieitez, M.L. Vázquez-Odériz, An immunochemical technique for the detection of ovalbumin in surimi-derived products, J. Sci. Food Agric. 82 (2002) 1614–1616.
[18] C. Breton, L. Phan Thanh, A. Paraf, Immunochemical properties of native and heat denatured ovalbumin, J. Food Sci. 53 (1988) 222–225.
[19] S. Azarnia, J.I. Boye, V. Mongeon, H. Sabik, Detection of ovalbumin in egg white, whole egg, and incurred pasta using LC–ESI–MS/MS and ELISA, Food Res. Int. 52 (2013) 526–534.
[20] G. Edevåg, M. Eriksson, M. Granström, The development and standardization of an ELISA for ovalbumin determination in influenza vaccines, J. Biol. Stand. 14 (1986) 223–230.
[21] F. Ricci, G. Volpe, L. Micheli, G. Palleschi, A review on novel developments and applications of immunosensors in food analysis, Anal. Chim. Acta 605 (2007) 111–129.
[22] P. Fanjul-Bolado, D. Hernández-Santosa, P.J. Lamas-Ardisanaa, A. Martín-Perníab, A. Costa-Garcíaa, Electrochemical characterization of screen-printed and conventional carbon paste electrodes, Electrochim. Acta 53 (2008) 3635–3642.
[23] F. Ricci, G. Adornetto, G. Palleschi, A review of experimental aspects of electrochemical immunosensors, Electrochim. Acta 84 (2012) 74–83.
[24] S. Centi, S. Laschi, M. Mascini, Improvement of analytical performances of a disposable electrochemical immunosensor by using magnetic beads, Talanta 73 (2007) 394–399.
[25] S. Centi, S. Laschi, M. Fránek, M. Mascini, A disposable immunomagnetic electrochemical sensor based on functionalised magnetic beads and carbon-based screen-printed electrodes (SPCEs) for the detection of polychlorinated biphenyls (PCBs), Anal. Chim. Acta 538 (2005) 205–212
[26] L. Stanciu, Y.H. Won, M. Ganesana, S. Andreescu, Magnetic particle-based hybrid platforms for bioanalytical sensors, Sensors 9 (2009) 2976–2999
[27] Y. Wu, S. Liu, L. He, Electrochemical biosensing using amplification-by-polymerization, Anal. Chem. 81 (2009) 7015–7021
[28] S. Eissa, L. L'Hocine, M. Siaj, M. Zourob, A graphene-based label-free voltammetric immunosensor for sensitive detection of the egg allergen ovalbumin, Analyst 138 (2013) 4378–4384
[29] K. Sugawara, T. Kadoya, H. Kuramitz, S. Tanaka, Voltammetric detection of ovalbumin using a peptide labeled with an electroactive compound, Anal. Chim. Acta 834 (2014) 37–44
[30] M.P. Olson, L.R. Keating, W.R. LaCourse, Indirect pulsed electrochemical detection of amino acids and proteins following high performance liquid chromatography, Anal. Chim. Acta 652 (2009) 198–204
[31] B. Piro, Q.D. Zhang, S. Reisberg, V. Noel, L.A. Dang, H.T. Duc, M.C. Pham, Direct and rapid electrochemical immunosensing system based on a conducting polymer, Talanta 82 (2010) 608–612
[32] H. Kuramitz, H.B. Halsall, W.R. Heineman, Magnetic microbead-based enzyme immunoassay for ovalbumin using hydrodynamic voltammetry and fluorometric detection, Anal. Methods 4 (2012) 1783–1789
[33] A.J. Saleh Ahammad, Hydrogen peroxide biosensors based on horseradish peroxidase and hemoglobin, J. Biosens. Bioelectron. (2013) S9
[34] D. Horák, Z. Svobodová, J. Autebert, B. Coudert, Z. Plichta, K. Královec, Z. Bílková, J.L. Viovy, Albumin-coated monodisperse magnetic poly(glycidyl methacrylate) microspheres with immobilized antibodies: application to the capture of epithelial cancer cells, J. Biomed. Mater. Res. A 101 (2013) 23–32
[35] Q. Gao, F. Yang, Y. Ma, X. Yang, The modification of screen-printed carbon electrodes with amino group and its application to construct a H_2 biosensor, Electroanalysis 16 (2004) 730–735
[36] L. Holubová, P. Knotek, J. Palarcik, M. Cadkova, P. Belina, M. Vlcek, L. Korecka, Z. Bilkova, Magnetic microparticles post-synthetically coated by hyaluronic acid as an enhanced carrier for microfluidic bioanalysis, Mater. Sci. Eng. C 44 (2014) 345–351
[37] G.T. Hermanson, Zero-length crosslinkers, in: G.T. Hermanson (Ed.), Bioconjugate Techniques, 2nd ed., Academic Press, San Diego, 2008, pp. 213–233
[38] J.H. Bovaird, T.T. Ngo, H.M. Lenhoff, Optimizing the *o*-phenylenediamine assay for horseradish peroxidase: effects of phosphate and pH, substrate and enzyme concentrations, and stopping reagents, Clin. Chem. 28 (1982) 2423–2426
[39] P. Šálek, L. Korecká, D. Horák, E. Petrovský, J. Kovářová, R. Metelka, M. Čadková, Z. Bílková, Immunomagnetic sulfonated hypercrosslinked polystyrene microspheres for electrochemical detection of proteins, J. Mater. Chem. 21 (2011) 14783–14792
[40] C. Ruan, R. Yang, X. Chen, J. Deng, A reagentless amperometric hydrogen peroxide biosensor based on covalently binding horseradish peroxidase and thionine using a thiol-modified gold electrode, J. Electroanal. Chem. 455 (1998) 121–125
[41] X. Chen, X. Chen, J. Zhang, B. Wang, G. Cheng, S. Dong, Hydrogen peroxide biosensor based on sol–gel-derived glasses doped with Eastman AQ polymer, Anal. Chim. Acta 434 (2001) 255–260
[42] R. Yu, L. Wang, Q. Xie, S. Yao, High-performance amperometric sensors using catalytic platinum nanoparticles–thionine–multiwalled carbon nanotubes nanocomposite, Electroanalysis 22 (2010) 2856–2861.

Příloha P7

Šálek P., **Korecká L.**, Horák D., Petrovský E., Kovářová J., Metelka R., Čadková M., Bílková Z. Immunomagnetic sulfonated hypercrosslinked polystyrene microspheres for electrochemical detection of proteins. *Journal of Materials Chemistry,* **21**, 2011, 14783-14792

IF_{2013} = 6,626; Q1 – Physical sciences, Materials sciences; 12 citací [1. 7. 2020]

- koncepce výzkumu, plánování experimentů 50 %
- podíl na experimentální práci a vyhodnocení výsledků 40 %
- dílčí příprava a revize článku

Journal of Materials Chemistry

Dynamic Article Links

Cite this: *J. Mater. Chem.*, 2011, **21**, 14783

www.rsc.org/materials

PAPER

Immunomagnetic sulfonated hypercrosslinked polystyrene microspheres for electrochemical detection of proteins

Petr Šálek,[a] Lucie Korecká,[b] Daniel Horák,*[a] Eduard Petrovský,[c] Jana Kovářová,[a] Radovan Metelka,[d] Michaela Čadková[b] and Zuzana Bílková[b]

Received 1st June 2011, Accepted 28th July 2011
DOI: 10.1039/c1jm12475g

Poly(styrene-*co*-divinylbenzene) microspheres of narrow size distribution were prepared by (2-hydroxypropyl)cellulose-stabilized dispersion copolymerization of styrene and divinylbenzene in a 2-methoxyethanol/ethanol mixture under continuous addition of divinylbenzene. The copolymerization was initiated with dibenzoyl peroxide. The obtained microspheres were chloromethylated using several chloromethylation agents and then hypercrosslinked. Their porous structure was analyzed by nitrogen adsorption and mercury porosimetry. Superparamagnetic iron oxide nanoparticles were precipitated within the pores of microspheres from Fe(II) and Fe(III) chloride solution. The Fe content in the microspheres was determined by carbon analysis, atomic absorption spectroscopy and thermogravimetric analysis. Magnetic properties of the microspheres were characterized by magnetization curves and the temperature dependence of magnetic susceptibility. Finally, sulfo groups were introduced into the microspheres to prepare an immunomagnetic electrochemical biosensor for protein detection with ovalbumin as a model substance.

Introduction

Separation of polymer or inorganic sorbents from complex mixtures is generally difficult. To alleviate the problem, magnetic microspheres providing large specific surface area (S_{BET}) for covalent binding and narrow size distribution ensuring homogeneous properties were developed. They have been widely used in biological practice, *e.g.*, for protein separation,[1] antibody and enzyme immobilization,[2] cell sorting,[3] nucleic acid[4,5] and protein purification,[6] and in immunoassays.[7] The interest in magnetic separations stems from the fact that they provide easy manipulation and fast isolation using magnetic field; the possibility to obtain desired biological compounds in sufficient purity and concentration necessary for polymerase chain reaction,[8] quantification of biomarkers by mass spectroscopy,[9,10] *etc.* Magnetic microspheres are suitable also as electrochemical biosensors in enzyme-linked immunosorbent assays (ELISA) where the microspheres replace colorimetric end-point measurement. Electrochemical immunosensors based on coupling of immunochemical reactions and appropriate transducers[11] have become attractive due to their simple use, fast analysis and the possibility of miniaturization.[12] Application of magnetic microspheres in immunosensors prevents their poor regeneration and reproducibility, which are often caused by direct adsorption of antibodies on the electrode surface that is commonly used in the immunosensor arrangement.[13] Moreover, screen-printed electrodes (SPEs), which are produced by printing on various polymer or ceramic supports,[14] have advantages of high sensitivity and selectivity, portable size and low cost.

Several methods have been developed to prepare magnetic polymer microspheres including surface-initiated polymerization,[15–17] suspension,[18] dispersion,[19] emulsion,[20] miniemulsion[21,22] and emulsifier-free emulsion[23] polymerization in the presence of magnetic nanoparticles. The magnetic microspheres (size 1–5 μm) have to fulfill requirements for low toxicity (biocompatibility) and non-interference with the chemical environment in diagnostics. Moreover, they should be stable in solutions, show narrow size distribution and minimum non-specific adsorption. Last but not least, an appropriate functionalization of magnetic polymer microspheres is required for intended applications in biochemistry[24] and immunochemistry.[25,26] There is a wide range of different options, such as introduction of basic or acid groups to facilitate desirable adsorption[27] or separation.[28] Ferrites are well known as appropriate magnetic cores of magnetic polymer microspheres. In particular, maghemite and magnetite are often used[29] because of a high saturation magnetization (80–100 A m^2 kg^{-1}). The iron oxides are conveniently prepared in the presence of oleic acid which prevents nanoparticle aggregation in

[a]*Institute of Macromolecular Chemistry, Academy of Sciences of the Czech Republic, Heyrovsky Sq. 2, 162 06 Prague 6, Czech Republic*
[b]*Department of Biological and Biochemical Sciences, Faculty of Chemical Technology, University of Pardubice, Studentská 573, 532 10 Pardubice, Czech Republic*
[c]*Geophysical Institute, Academy of Sciences of the Czech Republic, Boční II/1401, 141 31 Prague 4, Czech Republic*
[d]*Department of Analytical Chemistry, Faculty of Chemical Technology, University of Pardubice, Studentská 573, 532 10 Pardubice, Czech Republic*

organic media.[30] They can be made by precipitation of ferrous and ferric salts with alkali hydroxides[31] or by thermal decomposition of organometal compounds.[32]

Dispersion polymerization has been known as a suitable technique for preparation of monodisperse polymer microspheres in the range 0.1–15 μm.[33] The concentration of monomer and initiator as well as the stabilizer and solvent (hydrocarbon or polar solvent) plays an important role in controlling the microsphere size. Many applications require microspheres crosslinked with another multifunctional monomer to prevent their dissolution in the medium. However, the addition of a crosslinking agent to the reaction system often interferes with the nucleation mechanism of the dispersion polymerization and the resulting particles have then an irregular morphology and a broad size distribution.[34] To overcome this drawback of the polymerization, steric stabilizer or monomer was added to the reaction mixture in several portions[35] or a bifunctional monomer was continuously dosed in certain time periods after beginning of polymerization.[36]

If magnetic nanoparticles are precipitated in the porous structure of polymer microspheres,[37] only limited amounts of a magnetic compound can be incorporated and, moreover, the release of iron oxide from the pores is often a serious problem. For this purpose it is suitable to make the microspheres with micro- (< 2 nm) or mesopores (2–50 nm) in which the iron oxide can be easily kept and thus the incorporated amount of magnetic nanoparticles can be raised. Hypercrosslinking is a convenient method for preparation of micro- and mesoporous microspheres. This reaction was introduced by Davankov in 1970s.[38] Since that time, hypercrosslinked particles have been employed in many fields, such as ion exchangers,[39] water treatment[40] and hydrogen storage.[41] Hypercrosslinked styrene–divinylbenzene copolymers with the size of hundreds of micrometres, so-called Hypersol-Macronet™ sorbent resins, are commercially available from Purolite.[42]

The aim of this work was to investigate the preparation of magnetic polymer microspheres of narrow size distribution from sulfonated hypercrosslinked styrene–divinylbenzene copolymers in which an iron oxide was further precipitated. The microspheres with immobilized anti-OVA antibody were then integrated in a sandwich-type electrochemical immunosensor and ovalbumin was isolated and detected as a model protein (Scheme 1).

Experimental

Materials

Styrene (S) and divinylbenzene (DVB; 54% *meta*- and 20% *para*-isomers, 24% ethylvinylbenzene) from Kaučuk (Kralupy nad Vltavou, Czech Republic) were vacuum distilled; 1,2-dichloroethane (DCE), ethanol (EtOH) for UV spectroscopy, 2-methoxyethanol (MetCel), 25% aqueous solution of ammonia, diethyl ether and cyclohexane were from Lach-Ner (Neratovice, Czech Republic). Chloromethyl methyl ether (CMME), chloromethyl ethyl ether (CMEE), chloromethyl octyl ether (CMOE), (2-hydroxypropyl)cellulose (HPC; M_w = 100 000), $FeCl_2 \cdot 4H_2O$, $FeCl_3 \cdot 6H_2O$, $SnCl_4$ and 2-morpholinoethane-1-sulfonic acid (MES) were from Aldrich (St Louis, USA). Dibenzoyl peroxide (BPO; moistened with 20% of water; crystallized from ethanol), horseradish peroxidase (HRP), chicken egg albumin (ovalbumin, OVA) and bovine serum albumin (BSA) were supplied by Fluka (Buchs, Switzerland). Rabbit anti-ovalbumin (anti-OVA) IgG and rabbit anti-ovalbumin HRP-labeled anti-ovalbumin (anti-OVA-HRP) were obtained from Patricell Ltd. (Nottingham, UK) and purified by affinity chromatography. All other chemicals were supplied by Aldrich or Penta (Chrudim, Czech Republic) and used without further purification.

Preparation of microspheres

Dispersion copolymerization of styrene and divinylbenzene. Poly-(styrene-*co*-divinylbenzene) (PS) microspheres were prepared by modified Ober's procedure.[33] Polymerization was conducted in a glass 100 ml reaction vessel equipped with an anchor-type stirrer. In a typical experiment, HPC (1.09 g) was dissolved in a mixture of MetCel (19.3 g) and EtOH (38.9 g) and separately BPO (0.48 g) was dissolved in S (10.9 g). Both the solutions were mixed and placed in a reaction vessel and purged with nitrogen for 15 min. The reaction was allowed to proceed at 75 °C for 24 h under stirring (100 rpm). Five minutes after the start of the polymerization, DVB (0.11 g; 1 wt%) was added at various rates: 0.11 g in one portion, 2 μl every 30 s for 30 min, 2 μl every 45 s for 45 min, 2 μl every 60 s for 60 min and 2 μl every 75 s for 75 min. At the end of the reaction, the resulting PS microspheres were separated by centrifugation (600 rpm) and washed ten times with ethanol (100 ml each) to ensure complete removal of impurities (excessive stabilizer, unreacted monomer, initiator residues), and finally dried at room temperature.

Preparation of hypercrosslinked PS microspheres. PS microspheres were hypercrosslinked according to the modified Davankov's procedure.[43,44] In a typical experiment, the PS microspheres (2 g) were swollen in anhydrous DCE (32 ml) for 20 h in a 100 ml round-bottomed flask. The mixture was cooled to −15 °C in an ice/NaCl bath under magnetic stirring, chloromethyl methyl ether (0.727 ml) was added and the mixture

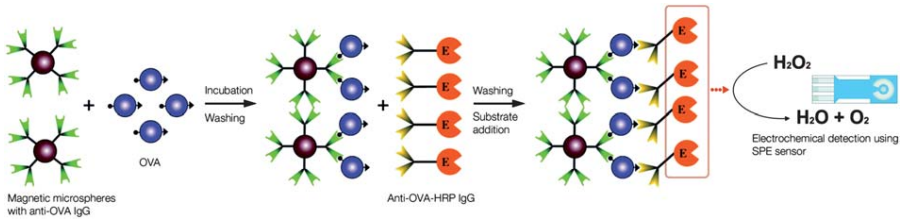

Scheme 1 System for detection of ovalbumin based on ELISA combined with electrochemical monitoring.

was kept at this temperature for 1 h. $SnCl_4$ (1.12 ml) was added and the mixture refluxed at 80 °C for 20 h. The hypercrosslinked (HPSX; X = M, E or O for chloromethylation with CMME, CMEE or CMOE, respectively) microspheres were then kept in anhydrous DCE for 12 h, filtered and washed successively with 1,2-dichloroethane, ethanol and diethyl ether before vacuum drying at 40 °C.

Sulfonation of HPSX microspheres. HPSX (X = M, E or O for chloromethylation with CMME, CMEE or CMOE, respectively) microspheres (1 g) were placed in a 50 ml round-bottomed flask, swollen in DCE (16 ml) for 10 h, 96% H_2SO_4 (4 g) and Ag_2SO_4 (12.5 mg) were added and the mixture was refluxed at 80 °C for 2 h. After completing the sulfonation, the microspheres (denoted as HPSX-SO_3^-) were washed five times with 0.2 M H_2SO_4 and water and vacuum-dried at 40 °C for 24 h. The content of SO_3^- groups was determined by sulfur analysis.

Precipitation of iron oxide in HPSX-SO_3^- microspheres. HPSX-SO_3^- microspheres were charged in a 100 ml round-bottomed reaction vessel equipped with an anchor-type stirrer (150 rpm). The microspheres (1 g) were dispersed in water (40 ml) at room temperature for 4 h. Subsequently, $FeCl_3 \cdot 6H_2O$ and $FeCl_2 \cdot 4H_2O$ (the amounts are given in Table 1) were dissolved in the above-mentioned suspension ($FeCl_3/FeCl_2$ = 2/1 mol/mol), which was then evacuated (2.7 kPa) at 23 °C for 1 h. Vacuum was removed and the reaction mixture was heated up to 80 °C. 25% aqueous ammonia (50% excess) was then dropwise added and the mixture refluxed for 30 min. After completing the reaction, the mixture was cooled to room temperature. The resulting magnetic (HPSX-M-SO_3^-) microspheres were separated using a magnet, ten times washed with water and finally vacuum dried at 40 °C for 24 h.

Immobilization of HRP on HPSM-M4-SO_3^- microspheres and determination of enzyme activity. HPSM-M4-SO_3^- microspheres (1 mg, 29 μl of suspension with a concentration of 35 mg particles per ml) were washed five times with 0.1 M phosphate buffer (pH 7.3). HRP (3 mg) in 0.1 M phosphate buffer (1 ml) was added and the mixture incubated at 4 °C for 16 h under mild shaking. After completion of the immobilization, the resulting HRP-HPSM-M4-SO_3^- microspheres were washed eight times with phosphate buffer.

The activity of immobilized enzyme was determined using hydrogen peroxide as a substrate and 1,2-phenylenediamine (OPD) as a chromogen according to an earlier published method.[45] A solution of the substrate was prepared from 0.1 M phosphate buffer (20 ml, pH 6.2), 30% hydrogen peroxide (10 μl) and OPD (10 mg). The solution (100 μl) was added to the suspension of HRP-HPSM-M4-SO_3^- microspheres (100 μl) and after incubation at 37 °C for 10 min under mild shaking UV absorbance of the supernatant was measured at 492 nm.

Direct immobilization of primary antibodies (anti-OVA IgG) on HPSM-M4-SO_3^- microspheres. HPSM-M4-SO_3^- microspheres (1 mg, 29 μl of suspension with concentration 35 mg ml^{-1}) were washed five times with 0.1 M MES buffer (pH 5) and a solution of anti-OVA IgG (100 μg) in MES buffer (500 μl) was added. The immobilization proceeded at 4 °C for 16 h under mild shaking. The anti-OVA-HPSM-M4-SO_3^- microspheres were washed five times with MES buffer, non-specifically adsorbed antibodies were removed after incubation with 0.05% trifluoroacetic acid (TFA; 2 × 200 μl) at 23 °C for 5 min. Finally, the microspheres were washed five times with 0.1 M MES buffer.

The immobilization efficiency was estimated by SDS-PAGE in Tris/glycine according to the following procedure. Electrophoresis was performed on a linear 12% SDS–polyacrylamide gel of 0.75 mm thickness. The samples were mixed with Laemmli buffer (1 : 1 v/v) and boiled at 100 °C for 2 min. SDS-PAGE proceeded in a Mini-PROTEAN electrophoresis cell (Bio-Rad, Philadelphia, USA) at 180 V with Tris/glycine/SDS running buffer (25 mM Tris, 192 mM glycine, 0.1 wt% SDS). Gels were stained by a conventional silver staining method.

Affinity isolation of ovalbumin and electrochemical detection. A solution of antigen ovalbumin (OVA) in 0.1 M phosphate buffer (500 μl; pH 7) was added to the suspension of anti-OVA-HPSM-M4-SO_3^- microspheres (OVA : anti-OVA 2 : 1 mol/mol) and the mixture was incubated at 23 °C for 45 min under mild shaking. The microspheres were then washed with 0.1 M phosphate buffer (pH 7), 0.1 M phosphate buffer (pH 7) containing 1 M NaCl and 0.1 M phosphate buffer (pH 7), three times each. To detect specifically bound OVA, the secondary antibody (anti-OVA-HRP conjugate) diluted 1 : 20 000 with 0.1 M hydrogencarbonate buffer (pH 9.49) containing 0.1% BSA and 0.05% Tween 20 was added. The reaction proceeded at 37 °C for 45 min under gentle shaking. Finally, to electrochemically monitor the signal decrease of substrate due to enzymatic reaction of conjugate label and substrate, unbound conjugate was removed by washing five times with 0.1 M phosphate buffer. Hydrogen peroxide (800 μl; 15 mg l^{-1}) was added for final electrochemical measurement depending on the above mentioned conditions. HPSM-M4-SO_3^- microspheres were used as a control.

Electrochemical linear sweep voltammetry (LSV) measurement. All electrochemical measurements were performed on a PalmSens

Table 1 Preparation of HPSX-M-SO_3^- microspheres containing γ-Fe_2O_3; Fe(III)/Fe(II) = 2/1 (mol/mol)

Microspheres	Fe(II) + Fe(III) salts[a] (wt%)	Fe (wt%) in microspheres		
		CA[b]	AAS[c]	TGA[d]
HPSM-M1-SO_3^-	2.2	26	23	45
HPSM-M2-SO_3^-	3.4	35	33	25
HPSM-M3-SO_3^-	5.6	46	41	31
HPSM-M4-SO_3^-	6.8	54	53	52
HPSM-M5-SO_3^-	8.0	55	53	46
HPSE-M1-SO_3^-	2.2	23	16	16
HPSE-M2-SO_3^-	3.4	24	17	15
HPSE-M3-SO_3^-	5.6	44	40	38
HPSE-M4-SO_3^-	6.8	37	32	31
HPSE-M5-SO_3^-	8.0	40	38	35
HPSO-M1-SO_3^-	2.2	26	23	23
HPSO-M2-SO_3^-	3.4	36	37	34
HPSO-M3-SO_3^-	5.6	45	46	39
HPSO-M4-SO_3^-	6.8	45	45	41
HPSO-M5-SO_3^-	8.0	44	44	42

[a] Content of ferrous and ferric chlorides in reaction mixture. [b] By carbon analysis. [c] By AAS. [d] By TGA.

compact electrochemical sensor interface (Palm Instruments BV; Houten, Netherlands). Screen-printed three-electrode sensors (SPEs) comprised reference Ag/AgCl electrode, platinum working and auxiliary electrodes (type AC1.W2.R1, BVT Technologies, Brno, Czech Republic) for sensing substrate hydrogen peroxide after its enzymatic conversion by HRP. 0.1 M phosphate buffer (pH 7.3) containing 0.15 M NaCl was used in all assays. Measurement conditions were the following: potential range 0–1 V with 0.005 V steps, scan rate 0.1 V s^{-1}, equilibration time 2 s. The current value at the potential 0.5 V was read-out for evaluation of results.

Characterization

The microspheres were observed in an Opton III light microscope (Oberkochen, Germany) and photographed using a Canon EOS 400D camera (Tokyo, Japan). The microsphere size in the dry state and their size distribution were analyzed by scanning electron microscopy (SEM; JEOL JSM 6400; TEM Tecnai Spirit G2, FEI, Brno, Czech Republic) and the number-average diameter (D_n), weight-average diameter (D_w) and uniformity (D_w/D_n) were calculated using an Atlas software (Tescan Digital Microscopy Imaging, Brno, Czech Republic) by counting at least 500 individual microspheres on SEM micrographs. The D_n and D_w can be expressed as follows:

$$D_n = \sum n_i D_i / \sum n_i \quad (1)$$

$$D_w = \sum n_i D_i^4 / \sum n_i D_i^3 \quad (2)$$

where n_i and D_i are the number and diameter of the i^{th} microsphere, respectively.

S_{BET} of microspheres was determined by nitrogen adsorption in liquid nitrogen (77 K) using a Gemini VII 2390 Analyzer (Micromeritics, Norcross, USA).

The specific pore volumes and the pore size distribution of dry microspheres were determined with a Pascal 140 and 440 mercury porosimeter (Thermo Finigan, Rodano, Italy) in two pressure intervals, 0–400 kPa and 1–400 MPa, allowing evaluation of meso- and macropores. Because macropores are not pertinent in this study, only the volume and size of mesopores were considered. The pore volume and the most frequent mesopore diameter were calculated from the cumulative pore volume curves assuming a cylindrical pore model by the Pascal program using Washburn's equation describing capillary flow in porous materials.[46]

The microspheres were analyzed using a Perkin Elmer 2400 Series CHNS/O elemental analyzer (Shelton, CN, USA). The absorbance was measured with a Biochrom Libra S22 UV/VIS spectrophotometer (Cambridge, UK). The content of Fe was analyzed by atomic absorption spectroscopy (AAS). The relative content of polystyrene and iron oxide was determined using a Perkin Elmer TGA 7 Thermogravimetric Analyzer (Norwalk, CT, USA). The magnetic microspheres were heated from room temperature to 860 °C at a heating rate of 10 °C min^{-1} in air, allowing the polymer to completely decompose while the inorganic iron oxides were determined as the residue.

Magnetic measurements. Magnetization curves were measured at room temperature using an EV9 vibrating magnetometer (DSM Magnetics, ADE Corporation, Lowell, MA, USA) with the maximum magnetic field of 2 T. The temperature dependence of magnetic susceptibility, κ, was measured from liquid nitrogen temperature (77 K) to *ca.* 1000 K using a KLY-4S/CS-3 kappabridge (AGICO Brno, Czech Republic) according to a previously described procedure.[47] The measurements were carried out in ambient atmosphere; the heating rate was 8.5 K min^{-1}.

Results and discussion

Dispersion copolymerization of styrene and divinylbenzene

Dispersion polymerization is a convenient single-step technique for preparation of monodisperse micrometre-sized particles. Here, PS microspheres with size ranging from 2.5 to 5.2 μm were prepared by dispersion copolymerization of S and DVB in a MetCel/EtOH mixture. The dispersion was stabilized with (2-hydroxypropyl)cellulose and the polymerization was initiated with dibenzoyl peroxide. The concentrations of the stabilizer, initiator and MetCel/EtOH ratio were kept constant throughout the experiments at 1.58 wt%, 4.4 wt% and 0.5 w/w, respectively. In order to make the microspheres insoluble in organic solvents, a small amount of DVB (1 wt%) was added to the reaction mixture for obtaining lightly crosslinked non-porous microspheres ($S_{BET} \approx 5$ m^2 g^{-1}). Because DVB in the polymerization mixture can interfere with a homogeneous nucleation mechanism resulting in wrinkled particles in an undesirable secondary nucleation,[36] continuous addition of DVB at various rates was investigated.

After addition of the whole amount of DVB five minutes after beginning of the polymerization in one portion, 5.2 μm PS microspheres with a very broad size distribution ($D_w/D_n = 1.91$; Fig. 1a) were obtained. One of the reasons for formation of polydisperse particles may be ascribed to different reactivity ratios for DVB isomers and S. As *p*-DVB has a higher reactivity ratio ($r_2 = 1.18$) than S ($r_1 = 0.26$),[48] *p*-DVB is capable of formation of new nuclei broadening thus the distribution. Polydispersity may be also caused by slow initiation of the system.[49]

When DVB was added continuously, at a rate of 2 μl every 30 s for 30 min, the primary particles aggregated in 2.5 μm cauliflower-like structures (Fig. 1b). The aggregation could be caused by very fast addition of DVB which was not completely accommodated in polymer–monomer particles. As a result, new particles were attached to the primary ones forming cauliflower morphology. If DVB was continuously added at a rate of 2 μl every 45 s for 45 min, PS microspheres had an average size of 3.7 μm and $D_w/D_n = 1.16$ (Fig. 1c). The microspheres were almost monodisperse; it could be thus assumed that this mode of DVB addition was appropriate for preparation of the particles. Such microspheres were tested for immobilization of anti-OVA and subsequent detection of OVA. *Ca.* 4.5 μm PS microspheres ($D_w/D_n = 1.34$) were obtained at a dosing rate of 2 μl DVB every 60 s in the course of 60 min (Fig. 1d). The presence of small amounts of tiny (0.7 μm) particles among larger microspheres indicated that the nucleation was not fast enough. Finally, DVB was continuously added at a rate of 2 μl every 75 s for 75 min and 4.8 μm PS microspheres of a rather narrow size distribution ($D_w/D_n = 1.17$) were obtained (Fig. 1e). It could be thus stated

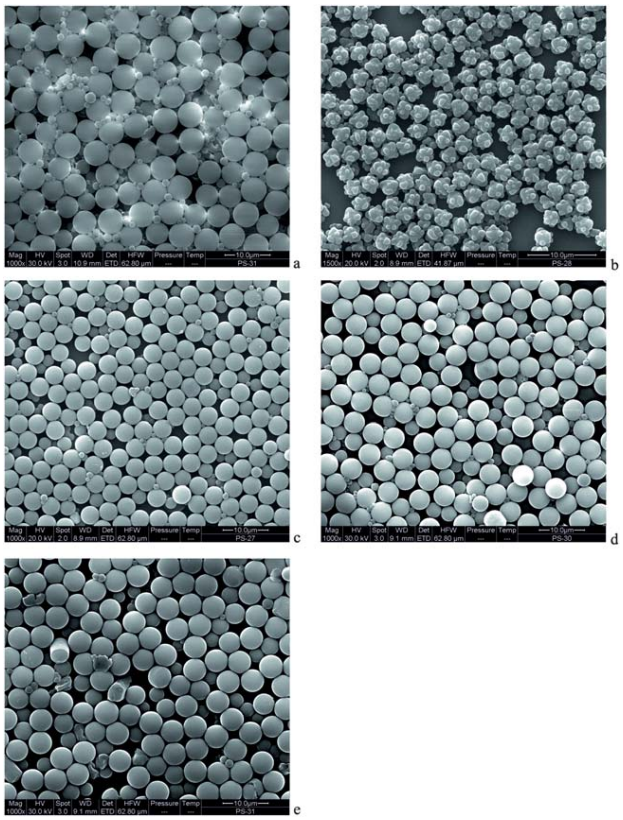

Fig. 1 SEM micrographs of (a–e) PS microspheres prepared by dispersion polymerization of styrene and DVB in 2-methoxyethanol/ethanol mixture. DVB was added 5 min after starting of the polymerization: (a) 0.11 g (120 μl) in one portion, (b) 2 μl every 30 s for 30 min, (c) 2 μl every 45 s for 45 min, (d) 2 μl every 60 s for 60 min and (e) 2 μl every 75 s for 75 min. The polymerization was stabilized by 1.58 wt% HPC.

that the particle size increased with prolonging time of DVB addition. The result could be explained by decreasing *in situ* DVB concentration with increasing rate of DVB addition which is in agreement with literature data.[50] Moreover, the narrowing of the particle size distribution could be ascribed to a decrease in solubility of polymer chains in the medium with increasing concentration of DVB in the reaction mixture leading to the formation of more nuclei. However, their size was smaller.[51]

Hypercrosslinking of PS microspheres and sulfonation of HPSX microspheres

With the aim to efficiently modify benzene rings of PS and subsequently produce large S_{BET} in the microspheres, three chloromethylated ethers were investigated. PS microspheres were chloromethylated with CMME, CMEE or CMOE in DCE and hypercrosslinked using the $SnCl_4$ catalyst. The resulting HPSX microspheres had large S_{BET} ranging from 367 to 1212 $m^2\ g^{-1}$ as determined by BET isotherm obtained by adsorption of nitrogen. Some of them, however, partly aggregated. Hypercrosslinked CMME-chloromethylated polystyrene microspheres (HPSM) had the largest S_{BET} = 1212 $m^2\ g^{-1}$. This could be ascribed to the fact that small CMME molecule easily penetrated into the swollen PS network. CMME was the most reactive of all the investigated chloromethylation agents. Due to its highly efficient Friedel–Crafts alkylation (0.65 mmol Cl g^{-1}), many chloromethyl groups were introduced bridging the benzene rings of PS microspheres. Fine porous structure of HPSM microspheres with pore size in the range of tens of nanometres was confirmed by a TEM micrograph of the cross-section (Fig. 2a). Every HPSX microsphere consisted of *ca.* 10 nm PS globules between which *ca.* 10–40 nm pores were formed.

Hypercrosslinking of CMEE-chloromethylated microspheres (HPSE) produced somewhat lower, but still sufficient, S_{BET} = 929 $m^2\ g^{-1}$. Also CMEE molecule was small enough and its access into the network was easy to chloromethylate PS microspheres (0.55 mmol Cl per g). The smallest S_{BET} = 367 $m^2\ g^{-1}$ was achieved with microspheres obtained by hypercrosslinking CMOE-chloromethylated particles (HPSO). The CMOE reagent was obviously not as reactive as CMME and CMEE providing insufficient amounts of chloromethyl groups (0.27 mmol Cl per g).

Determination of micro/mesoporous structure of hypercrosslinked HPS microspheres by nitrogen adsorption was completed by characterization of mesoporous structure by mercury porosimetry measurements. Macroporosity was not considered due to a small size of the microspheres. The most frequent pore radius of HPSM microspheres was mostly in the range 8–24 nm (Fig. 3), the cumulative pore volume was 0.4 ml g^{-1} and the mesoporosity amounted to 29%. Porous properties of the HPSO microspheres resembled those of HPSM particles. The most frequent pore radius was 6–20 nm, the cumulative pore volume 0.3 ml g^{-1} and mesoporosity 23%. Compared with HPSM and HPSO microspheres, mesoporosity of the HPSE microspheres was higher (34%). Their most frequent pore radius was also larger ranging from 7 nm to 25 nm, which was accompanied by a high cumulative pore volume of 0.43 ml g^{-1}.

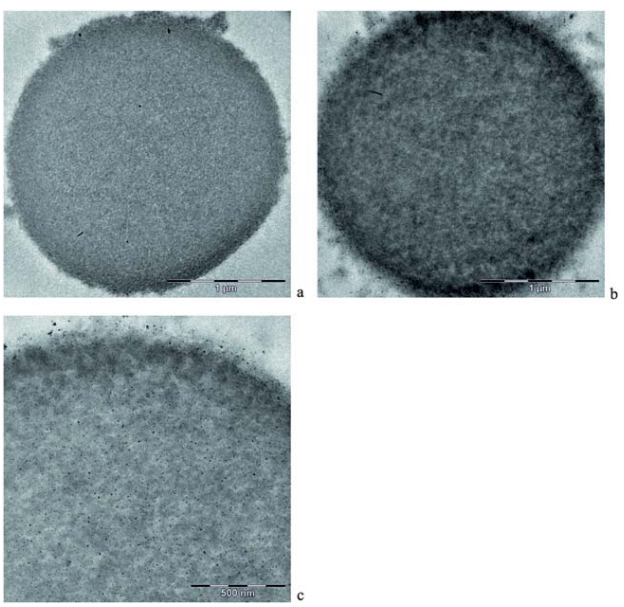

Fig. 2 TEM micrographs of cross-sections of (a) HPSM and (b and c) HPSM-M5-SO_3^- microspheres. Magnification 37 000× (a and b) and 59 000× (c).

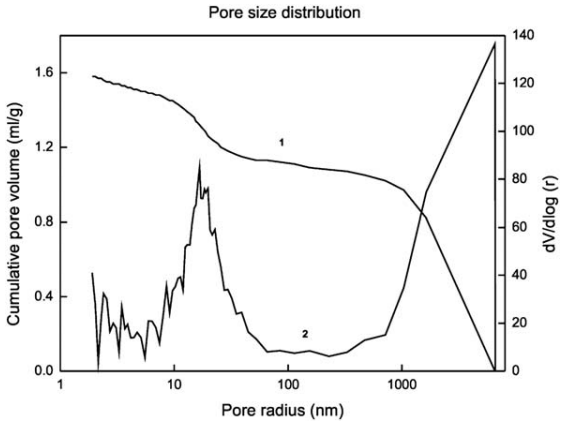

Fig. 3 (1) Cumulative pore volume V and (2) pore size distribution dV/dlog(r) curves of CMME-hypercrosslinked HPSM (1 wt% DVB) microspheres determined by mercury porosimetry; pore radii range 1.9 nm–10 μm (mesopore radii analyzed up to 25 nm).

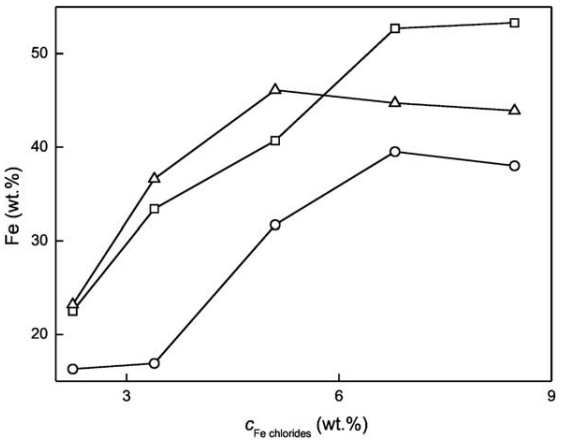

Fig. 4 Dependence of Fe content (by AAS) in HPSX-SO3$^-$ microspheres on $FeCl_x$ concentration c in the reaction mixture. Chloromethylation with (□) CMME, (○) CMEE and (△) CMOE.

Functionalization of microsphere surface is necessary to make coupling of antibody (anti-ovalbumin) on the surface by covalent bonds possible. In this report, sulfonation was selected for modification of hypercrosslinked PS microspheres because it is an easy and reliable reaction. Silver sulfate-catalyzed reaction of 96% sulfuric acid yielded HPSX-SO_3^- microspheres containing *ca.* 4 mmol SO_3^- per g according to sulfur analysis.

Precipitation of iron oxide within HPSX-SO_3^- microspheres

Fe(II) and Fe(III) salts were precipitated in the pores of the HPSX-SO_3^- microspheres by alkaline medium performed by Massart's procedure.[52] Ferrous and ferric chloride solutions were first imbibed in the porous structure in vacuum and precipitation was achieved by aqueous ammonia. Although the concentration of ferrous and ferric chlorides in the aqueous phase was varied from 2 to 8.5 wt%, the Fe^{2+}/Fe^{3+} ratio was kept constant (2/1 mol/mol).

Successful embedding of iron oxide in the PS matrix was documented by TEM of cross-sections in HPSM-M5-SO_3^- microspheres (Fig. 2b and c as an example). Both non-magnetic HPSM and magnetic HPSM microspheres are composed of globules (dark spots in Fig. 2a–c) between which the pores (light spots) appear. Iron oxides in the pores can be observed as black dots (Fig. 2b and c); their size is around 9 nm, which is comparable with the pore size. This finding favors retention of the iron oxide nanoparticles inside the porous structure. However, iron oxide was precipitated also on the particle surface. As expected, filing of the pores with iron oxide nanoparticles led to a significant decrease of specific surface area. For example, S_{BET} of HPSM-M1, HPSE-M1 and HPSO-M1 microspheres decreased to 62, 58 and 20 $m^2\ g^{-1}$, respectively.

Fig. 4 shows the dependence of the iron content determined by AAS in the 3.7 μm HPSX-M-SO_3^- microspheres on the concentration of iron salts in the reaction mixture. As expected, with an increasing concentration of ferrous and ferric chlorides in the reaction mixture, the content of Fe precipitated in the microspheres increased reaching a plateau at high iron chloride concentration (5.1 wt% for HPSO-M3-SO_3^- and 6.8 wt% for HPSM-M4-SO_3^- and HPSE-M4-SO_3^-). This could be explained by washing out of iron oxides from the microspheres at higher iron salt concentrations. It can be assumed that the precipitated iron oxide was in the form of maghemite (γ-Fe_2O_3) due to the presence of oxygen in the aqueous medium which oxidized the primarily formed Fe_3O_4. The amount of iron in the microspheres was determined not only by AAS but by elemental analysis and thermogravimetric analysis (TGA) as well. Elemental analysis, in particular the percentage of carbon, can be used for calculating the percentage of γ-Fe_2O_3 in HPSX-M-SO_3^- microspheres since the original neat PS microspheres do not contain Fe. The following equation was used:

$$\%(\gamma\text{-}Fe_2O_3) = 100 - \text{PS}\ (\%) = 100 - [\text{C}\ (\%)/89.8)] \times 100, \quad (3)$$

where % of C was obtained from elemental analysis of HPS-M-SO_3^- microspheres and 89.8 was the content of C found in neat PS microspheres. For example, the C content in HPSE-M1-SO_3^- microspheres was 61.1% and the calculated PS content in the magnetic microspheres was 68 wt%, *i.e.*, the γ-Fe_2O_3 content was 32 wt% which corresponds to 23.1 wt% Fe (Table 1). The contents of Fe determined by elemental analysis were in rough agreement with those obtained by AAS (Table 1). The iron content determined in the microspheres by the above mentioned three methods decreased in the order HPSM ≈ HPSO > HPSE (Table 1).

TGA of HPSX-M-SO_3^- microspheres was measured at temperatures ranging from 40 to 860 °C. As an example, the temperature-dependent decomposition of HPSE-M4-SO_3^- microspheres is shown in Fig. 5. A temperature increase was accompanied by a gradual mass loss. The main decomposition started at around 330 °C where the HPSE-M4-SO_3^- microspheres began to rapidly lose weight with the mass loss around 50% up to 420 °C (Fig. 5). In the degradation of polystyrene, random main-chain scission occurs below 300 °C, where the weak links play a significant role.[53] At temperatures above 300 °C, volatile products are formed, containing monomers (45%) and oligomers. The value 125.5 kJ mol^{-1} was determined by DSC for the activation energy of polystyrene degradation[53]

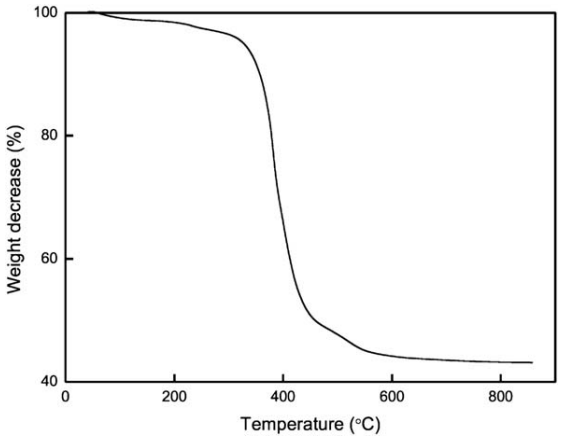

Fig. 5 Thermogravimetric analysis of HPSE-M4-SO_3^- microspheres.

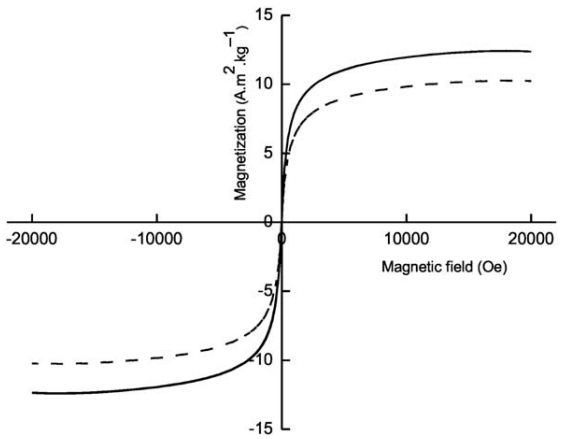

Fig. 6 Induced magnetization of HPSM-M5-SO_3^- (full line) and HPSE-M5-SO_3^- (dashed line) microspheres.

and this value was found to be independent of the atmosphere in which the degradation took place (air, nitrogen or oxygen). At the end of the TGA analysis performed in air, the organic phase of HPSE-M4-SO_3^- microspheres was completely decomposed around 600 °C, allowing one to calculate the iron oxide content as the inorganic residue. The determination of iron in magnetic microspheres by the three methods was mostly in agreement. Generally, the content of precipitated iron oxide increased with increasing concentration of Fe salts in the feed. However, some differences between the results, obtained from TGA, AAS or elemental analysis, were observed, *e.g.*, in HPSM-M1-SO_3^- microspheres where the Fe content as determined by TGA was higher compared with the other two methods. This might be due to inaccurate results of TGA of microspheres containing low amounts of precipitated iron oxides. The data scattering in Table 1 could be explained by a release of iron oxide captured on the particle surface during washing. HPSM-M4-SO_3^- microspheres contained the highest amount of iron ($\sim$ 53 wt%).

Magnetic properties

The induced magnetization curves of HPSM-M5-SO_3^- and HPSE-M5-SO_3^- microspheres at room temperature are shown in Fig. 6. Negligible hysteresis in the magnetization curves suggests a significant superparamagnetic contribution of the iron oxide precipitated inside the hypercrosslinked microsphere pores. As expected, HPSM-M5-SO_3^- microspheres displayed higher saturation magnetization (M_s) than the HPSE-M5-SO_3^- ones. The γ-Fe_2O_3 content in the microspheres estimated from magnetic measurements (Table 2) was lower than that from the Fe contents obtained by carbon analysis (CA), AAS and TGA (Table 1). The reduced M_s values could be ascribed to various surface effects, such as oxidation resulting in low-magnetic compounds, imperfections in the crystal structure, deviation from stoichiometry and adsorbed materials.[54] It should be noted that the saturation magnetization of small particles is always lower than that of the bulk. Magnetic parameters obtained from measurements of magnetization curves included also mass-specific magnetic susceptibility χ measured at room temperature (Table 2). The value of saturation magnetization M_s, which is a direct measure of the concentration of atomic magnetic moments, was used to estimate the relative concentrations of magnetic iron oxide nanoparticles in HPSM-M5-SO_3^-, HPSE-M4-SO_3^-, HPSE-M5-SO_3^- and HPSO-M5-SO_3^- microspheres (Table 2), assuming that the reported saturation magnetization of bulk maghemite (γ-Fe_2O_3) is 84 $Am^2\ kg^{-1}$ (ref. 55) and that of pure maghemite nanoparticles is 55.9 $Am^2\ kg^{-1}$.[56]

Thermomagnetic analysis revealed analogous behavior of all analyzed magnetic microspheres. As an example, the temperature dependence of magnetic susceptibility of HPSM-M5-SO_3^- is shown in Fig. 7. A pronounced maximum of magnetic susceptibility was observed at 120 °C, followed by a sharp decrease with a local minimum between 350 °C and 450 °C and an increase with different intensity. Finally, the decrease starting at about 550–570 °C indicated the presence of magnetite, which was obviously the final product of thermal transformations. The absence of the Verwey transition around −150 °C suggested a lack of multidomain magnetic particles. The interpretation is

Table 2 Characteristics of HPSX-M-SO_3^- microspheres containing γ-Fe_2O_3

Microspheres	$\chi^a \times 10^{-4}/m^3\ kg^{-1}$	$H_c{}^b$/Oe	$M_{rs}{}^c/10^{-1}$ A $m^2\ kg^{-1}$	$M_s{}^d$/A $m^2\ kg^{-1}$	$(M_{rs}/M_s)^e \times 10^{-2}$	γ-$Fe_2O_3{}^f$ (wt%)
HPSM-M5-SO_3^-	5.17	3.78	0.592	11.80	0.501	21.2
HPSE-M4-SO_3^-	5.50	15.16	2.060	8.71	2.360	15.3
HPSE-M5-SO_3^-	4.18	4.92	0.772	9.70	0.796	17.3
HPSO-M5-SO_3^-	5.50	4.39	0.844	11.60	0.727	20.8

[a] Magnetic susceptibility. [b] Coercive force. [c] Remanent saturation magnetization. [d] Saturation magnetization. [e] Remanent saturation/saturation magnetization ratio. [f] The γ-Fe_2O_3 content in the microspheres was calculated relative to M_s of pure γ-Fe_2O_3 nanoparticles (55.9 $Am^2\ kg^{-1}$).

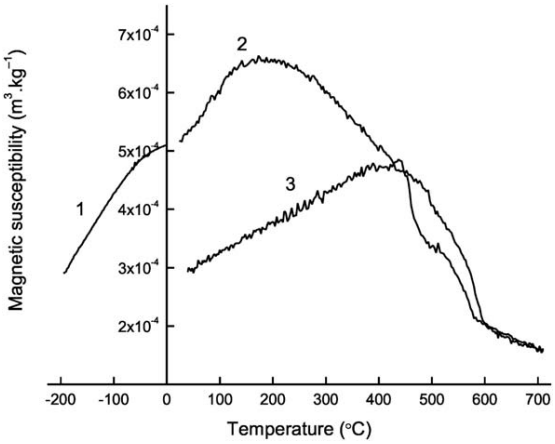

Fig. 7 Temperature dependence of magnetic susceptibility of HPSM-M5-SO_3^- microspheres. (1) Low-temperature curve, (2) heating curve and (3) cooling curve.

unclear, but this could be probably related to disintegration of microspheres and subsequent reduction of maghemite to magnetite.

Direct immobilization of HRP and anti-OVA on HPSM-M4-SO_3^- microspheres

As a model system for construction of immunomagnetic biosensor for sandwich ELISA-based protein detection, primary antibody (anti-OVA)/antigen (OVA)/secondary antibody (anti-OVA-HRP) was selected. Anti-OVA was therefore immobilized on HPSM-M4-SO_3^- microspheres. The immobilization efficiency investigated by the standard Tris/glycine SDS-PAGE[57] with silver staining[58] was higher than 90% (Fig. 8).

In lane 1, there was pure anti-OVA as a positive control. The supernatant after immobilization was in lane 2. This lane was compared with the first lane and it was concluded that almost all anti-OVA was immobilized on HPSM-M4-SO_3^- microspheres. The first and second eluents were in lanes 3 and 4, respectively. Blind runs confirmed that anti-OVA was not released from HPSM-M4-SO_3^- microspheres after immobilization.

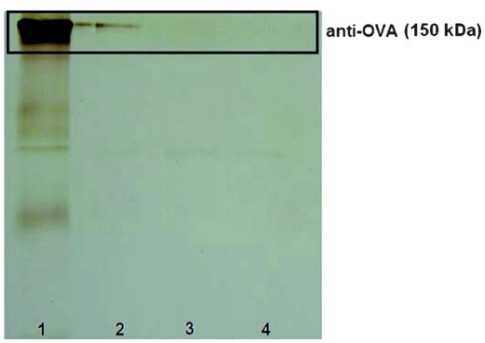

Fig. 8 Tris/glycine SDS-PAGE of anti-OVA antibodies immobilized onto M-PS-SO_3H microspheres. Original anti-OVA IgG (lane 1), supernatant after immobilization (lane 2), first (lane 3) and second washing after immobilization (lane 4).

Electrochemical measurements

The reaction between antigen and antibody proceeds generally on the surface of the working electrode, where the limiting factors are regeneration of the sensor and reusability.[59] The problems can be avoided by using magnetic microspheres with immobilized antibodies enabling us to perform immunoreactions separately from electrochemical detection.

From a variety of tested sweep and pulse electrochemical techniques, linear sweep voltammetry (LSV) was found to be the most suitable for hydrogen peroxide detection (Fig. 9). The conditions of electrochemical measurements, such as potential range, steps, equilibration time and scan rate, with SPEs were optimized using HRP-HPSM-M4-SO_3^- microspheres. The advantage of HRP-HPSM-M4-SO_3^- microspheres is the incorporation of superparamagnetic iron oxide cores within PS particles. Substrate is then protected from the contact with iron oxide suppressing thus possible electrocatalytic oxidation of hydrogen peroxide.

Finally, affinity isolation of ovalbumin was performed and electrochemically detected after recognition of the specific secondary antibodies (conjugate) of the formed immunocomplex. A complete immunomagnetic biosensor for electrochemical determination of protein (OVA) based on sandwich ELISA was constructed using a model system primary antibody (anti-OVA)/antigen (OVA)/secondary antibody (anti-OVA-HRP). Anti-OVA IgG was immobilized on HPSM-M4-SO_3^- microspheres and used for affinity isolation of OVA antigen at the anti-OVA/OVA ratio 1 : 2 (mol/mol). To confirm the affinity OVA isolation, the HRP-labeled secondary antibody (anti-OVA-HRP) diluted 1 : 20 000 was added. Hydrogen peroxide (substrate) was then used to verify the immunocomplex formation and the corresponding current decrease was electrochemically monitored (Fig. 10). Anti-OVA-HPSM-M4-SO_3^-/OVA/anti-OVA-HRP microspheres were compared with HPSM-M4-SO_3^- microspheres (as control) to validate the system functionality. The current decrease in time induced by oxidation of hydrogen peroxide with the HRP-labeled conjugate proved that HPSM-M4-SO_3^- microspheres are suitable for combination of

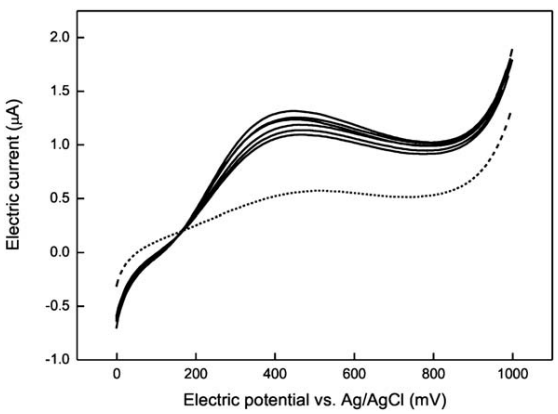

Fig. 9 Electric current change induced by the conversion of hydrogen peroxide by HRP-HPSM-M4-SO_3^- microspheres. Medium: 0.1 M phosphate buffer (pH 7) containing 0.15 M NaCl and hydrogen peroxide (substrate; 20 mg l^{-1}).

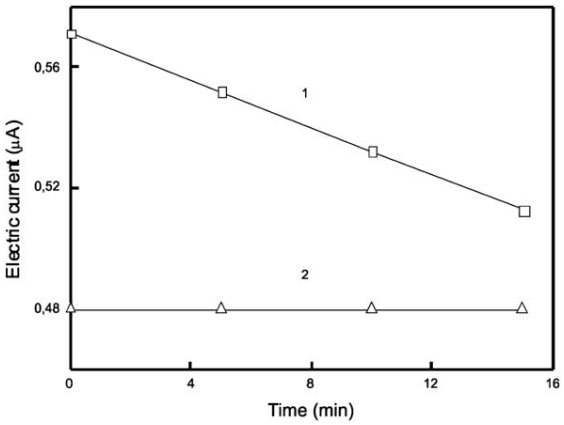

Fig. 10 Electrochemical detection of H_2O_2 consumption using anti-OVA-HPSM-M4-SO_3^-/OVA/anti-OVA-HRP microspheres (curve 1). HPSM-M4-SO_3^- microspheres served as a control (curve 2). Medium: 0.1 M phosphate buffer (pH 7) containing 0.15 M NaCl; anti-OVA/OVA 1/2 (mol/mol), conjugate dilution 1 : 20 000, 15 mg of H_2O_2 per l.

ELISA-based protein detection with a highly sensitive electrochemical determination. At present, OVA detection was only qualitative; quantitative determination is in progress.

Conclusions

Homogeneous (non-porous) PS microspheres with a rather narrow size distribution were prepared by controlled polymerization of styrene with small amounts of divinylbenzene (1 wt%) as a crosslinking agent. Porous structure was then formed by hypercrosslinking of chloromethylated PS microspheres providing sufficiently large space for precipitation of iron oxides. Subsequent hypercrosslinking was, however, accompanied by partial aggregation of the microspheres. In the next steps, the microspheres were sulfonated with sulfuric acid and iron oxide subsequently incorporated into pores of the sulfonated hypercrosslinked microspheres by precipitation of Fe(II)/Fe(III) salts. As far as we know, this is the first example of preparation of strongly magnetic supports by taking advantage of highly microporous structure of hypercrosslinked microspheres. As the sulfo groups enable immobilization of biomolecules, an anti-OVA antibody was attached to the surface of the magnetic microspheres without adversely influencing the functions of immobilized ligands, *e.g.*, enzyme activity and capability of antibodies of affinity interactions. The specific model system served for construction of an electrochemical immunosensor for detection of ovalbumin protein, which can be easily assayed using linear sweep voltammetry with a three-electrode screen-printed sensor with platinum working electrode. Systems based on electrochemical monitoring of proteins are promising, *e.g.*, for detection of biomarkers specific to various diseases.

Acknowledgements

The financial support of the European Union (grants CaMiNEMS no. 228980 and NaDiNe no. 246513), Grant Agency of the Czech Republic (grants 203/09/0857 and 203/09/1242) and Ministry of Education, Youth and Sports (grants 0021627502 and LC06035) is gratefully acknowledged.

References

1 B. Hickstein and U. A. Peuker, *Biotechnol. Prog.*, 2008, **24**, 409.
2 M. Slováková, J. M. Peyrin, Z. Bílková, M. Jukličková, L. Hernychová and J. L. Viovy, *Bioconjugate Chem.*, 2008, **19**, 966.
3 R. Handgretinger, P. Lang, M. Schumm, G. Taylor, W. Schwinger, E. Koscielniak, A. Reiter, C. Peters, D. Niethammer and T. Klingebiel, *Bone Marrow Transplant.*, 1998, **21**, 987.
4 B. Rittich, A. Španová, D. Horák, M. J. Beneš, L. Klesnilová, K. Petrová and A. Rybníkář, *Colloids Surf., B*, 2006, **52**, 143.
5 Z. C. Zhang, L. M. Zhang, L. Chen, L. G. Chen and Q. H. Wan, *Biotechnol. Prog.*, 2006, **22**, 514.
6 M. Franzreb, M. Siemann-Herzberg, T. J. Hobley and O. R. T. Thomas, *Appl. Microbiol. Biotechnol.*, 2006, **70**, 505.
7 R. P. Liu, J. T. Liu, L. Xie, M. X. Wang, J. P. Luo and X. X. Cai, *Talanta*, 2010, **81**, 1016.
8 B. Rittich, A. Španová, P. Šálek, P. Němcová, Š. Trachtová and D. Horák, *J. Magn. Magn. Mater.*, 2009, **321**, 1667.
9 J. R. Whiteaker, L. Zhao, H. Y. Zhang, L. C. Feng, B. D. Piening, L. Anderson and A. G. Paulovich, *Anal. Biochem.*, 2007, **362**, 44.
10 J. F. Peter and A. M. Otto, *Proteomics*, 2010, **10**, 628.
11 P. B. Luppa, L. J. Sokoll and D. W. Chan, *Clin. Chim. Acta*, 2001, **314**, 1.
12 S. Centi, S. Laschi and M. Mascini, *Talanta*, 2007, **73**, 394.
13 W. Liang, W. Yi, Y. Li, Z. Zhang, M. Yang, C. Hu and A. Chen, *Mater. Lett.*, 2010, **64**, 2616.
14 O. D. Renedo, M. A. Alonso-Lomillo and M. J. A. Martínez, *Talanta*, 2007, **73**, 202.
15 F. H. Chen, Q. Gao, G. Y. Hong and J. Z. Ni, *J. Magn. Magn. Mater.*, 2008, **320**, 1921.
16 Y. Zhou, S. X. Wang, B. J. Ding and Z. M. Yang, *Chem. Eng. J.*, 2007, **138**, 578.
17 Y. B. Sun, X. B. Ding, Z. H. Zheng, X. Cheng, X. H. Hu and Y. X. Peng, *Eur. Polym. J.*, 2007, **43**, 762.
18 H. X. Liu, C. Y. Wang, Q. X. Gao, X. X. Liu and Z. Tong, *Acta Biomater.*, 2010, **6**, 275.
19 D. Horák and N. Benedyk, *J. Polym. Sci., Part A: Polym. Chem.*, 2004, **42**, 5827.
20 C. Oh, Y. G. Lee, C. U. Jon and S. G. Oh, *Colloids Surf., A*, 2009, **337**, 208.
21 Y. Mori and H. Kawaguchi, *Colloids Surf., B*, 2007, **56**, 246.
22 J. S. Nunes, C. L. de Vasconcelos, F. A. O. Cabral, J. H. de Araujo, M. R. Pereira and J. L. C. Fonseca, *Polymer*, 2006, **47**, 7646.
23 S. Lu, J. Ramos and J. Forcada, *Langmuir*, 2007, **23**, 12893.
24 M. Slováková, J.-M. Peyrin, Z. Bílková, M. Juklíčková, L. Hernychová and J.-L. Viovy, *Bioconjugate Chem.*, 2008, **19**, 966.
25 B. Jankovicova, S. Rosnerova, M. Slovakova, Z. Zverinova, M. Hubalek, M. Hernychova, M. Rehulka, J.-L. Viovy and Z. Bilkova, *J. Chromatogr., A*, 2008, **1206**, 64.
26 Z. Bílková, M. Slováková, N. Minc, C. Fütterer, R. Cecal, D. Horák, M. J. Beneš, I. le Potier, J. Křenková, M. Przybylski and J.-L. Viovy, *Electrophoresis*, 2006, **27**, 1811.
27 B. Hickstein and U. A. Peuker, *Biotechnol. Prog.*, 2008, **24**, 409.
28 S. S. Sun, G. L. Yang, T. Wang, Q. Z. Wang, C. Chen and Z. Li, *Anal. Bioanal. Chem.*, 2010, **396**, 3071.
29 D. Horák, M. Babič, H. Macková and M. J. Beneš, *J. Sep. Sci.*, 2007, **30**, 1751.
30 S. S. Pappel, *US Pat.*, 3 215 572, Washington, 1965.
31 R. Massart, *C. R. Acad. Sci., Ser. III*, 1980, **291**, 1.
32 M. Gonzales and K. M. Krishnan, *J. Magn. Magn. Mater.*, 2005, **293**, 265.
33 C. K. Ober, K. P. Lok and M. L. Hair, *J. Polym. Sci.*, 1985, **23**, 103.
34 C. M. Tseng, Y. Y. Lu, M. S. El-Aasser and J. W. Vanderhoff, *J. Polym. Sci., Part A: Polym. Chem.*, 1986, **24**, 2995.
35 J. Choi, S. Y. Klak, S. Kang, S. S. Lee, M. Park, S. Lim, J. Kim, C. R. Choe and S. I. Homg, *J. Polym. Sci., Part A: Polym. Chem.*, 2002, **40**, 4368.
36 B. Thomson, A. Rudin and G. Lajoie, *J. Appl. Polym. Sci.*, 1996, **59**, 2009.
37 J. Ugelstad, T. Ellingsen, A. Berge and B. Helgée, *PCT Pat.*, WO 83/03920, 1983.

38 V. A. Davankov, S. V. Rogozhin and M. P. Tsyurupa, *Vysokomol. Soedin., Ser. B*, 1973, **15**, 463.
39 N. Fontanals, P. A. G. Cormack and D. C. Sherrington, *J. Chromatogr., A*, 2008, **1215**, 21.
40 N. Fontanals, R. M. Marcé, P. A. G. Cormack, D. C. Sherrington and F. Borrull, *J. Chromatogr., A*, 2008, **1191**, 118.
41 J. Germain, J. M. J. Fréchet and F. Svec, *Small*, 2009, **5**, 1098.
42 Purolite Technical Bulletin, in *Hypersol-Macronet Sorbent Resins*, Purolite Int Ltd, UK, 1999.
43 V. A. Davankov and M. P. Tsyurupa, *Pure Appl. Chem.*, 1989, **61**, 1881.
44 M. P. Tsyurupa and V. A. Davankov, *React. Funct. Polym.*, 2002, **53**, 193.
45 J. H. Bovaird, T. T. Ngo and H. M. Lenhoff, *Clin. Chem.*, 1982, **28**, 2423.
46 S. P. Rigby, D. Barwick, R. S. Fletcher and S. N. Riley, *Appl. Catal., A*, 2003, **238**, 303.
47 F. Hrouda, *Geophys. J. Int.*, 1994, **118**, 604.
48 J. Brandrup, E. H. Immergut and E. A. Grulke, in *Polymer Handbook*, John Wiley, New York, 4th edn, 1999.
49 D. Horák, F. Švec and J. M. J. Fréchet, *J. Polym. Sci., Polym. Chem. Ed.*, 1995, **33**, 2961.
50 J. S. Song, F. Tronc and M. A. Winnik, *J. Am. Chem. Soc.*, 2004, **126**, 6562.
51 H. T. Zhang, J. X. Huang and B. B. Jiang, *J. Appl. Polym. Sci.*, 2002, **85**, 2230.
52 R. Massart, *IEEE Trans. Magn.*, 1981, **17**, 1247.
53 E. A. Turi, in *Thermal Characterization of Polymeric Materials*, Academic Press, San Diego, 2nd edn, 1981, vol. 1, p. 692.
54 F. Vereda, J. de Vicente, M. del Perto Morales, F. Rull and R. Hidalgo-Ivarez, *J. Phys. Chem. C*, 2008, **112**, 5843.
55 K. Kluchova, R. Zboril, J. Tucek, M. Pecova, L. Zajoncova, I. Safarik, M. Mashlan, I. Markova, D. Jancik, M. Sebela, H. Bartonkova, V. Bellesi, P. Novak and D. Petridis, *Biomaterials*, 2009, **30**, 2855.
56 E. Pollert, K. Knížek, M. Maryško, K. Závěta, A. Lančok, J. Boháček, D. Horák and M. Babič, *J. Magn. Magn. Mater.*, 2006, **306**, 241.
57 U. K. Laemmli, *Nature*, 1970, **227**, 680.
58 B. R. Oakley, D. R. Kirsch and N. R. Morris, *Anal. Biochem.*, 1980, **105**, 361.
59 N. Jaffrezie-Renault, C. Martelet, Y. Chevelot and J. P. Cloarec, *Sensors*, 2007, **7**, 589.

Příloha P8

Čadková M., Dvořáková V., Metelka R., Bílková Z., **Korecká L.*** Alkaline phosphatase labeled antibody-based electrochemical biosensor for sensitive HE4 tumor marker detection. *Electrochemistry Communications,* **59**, 2015, 1-4

IF_{2018} = 4,197; Q1 – Chemical sciences; 18 citací [1. 7. 2020]

- koncepce výzkumu, plánování experimentů
- podíl na experimentální práci a vyhodnocení výsledků 20 %
- dílčí příprava článku, revize, korespondující autor

Electrochemistry Communications 59 (2015) 1–4

Contents lists available at ScienceDirect

Electrochemistry Communications

journal homepage: www.elsevier.com/locate/elecom

Alkaline phosphatase labeled antibody-based electrochemical biosensor for sensitive HE4 tumor marker detection

Michaela Čadková [a], Veronika Dvořáková [a], Radovan Metelka [b], Zuzana Bílková [a], Lucie Korecká [a,*]

[a] Department of Biological and Biochemical Sciences, Faculty of Chemical Technology, University of Pardubice, Studentska 573, 532 10 Pardubice, Czech Republic
[b] Department of Analytical Chemistry, Faculty of Chemical Technology, University of Pardubice, Studentska 573, 532 10 Pardubice, Czech Republic

ARTICLE INFO

Article history:
Received 20 April 2015
Received in revised form 19 June 2015
Accepted 23 June 2015
Available online 27 June 2015

Keywords:
Electrochemical immunosensor
Magnetic particles
Tumor biomarker HE4
Alkaline phosphatase

ABSTRACT

Quantitative determination of the serum level of human epididymis protein 4 (HE4), a tumor marker for ovarian carcinoma, has come to the fore of interest mainly due to the possibility for its detection in early stages of the disease when the sensing of other biomarkers is limited. We present a simple ELISA based approach for rapid HE4 detection including its immunomagnetic capturing accompanied by sensitive electrochemical detection of the electroactive product formed after enzymatic conversion of the substrate by alkaline phosphatase used as a label of anti-HE4 IgG. The proposed immunosensor offers stability in time and due to excellent limit of detection at 6.8 fM HE4, and limit of quantification of 23 fM meets the requirements for the early detection of this biomarker.

1. Introduction

Ovarian cancer is one of the leading causes of cancer-related mortality among women [1], a frequent cause of death in oncological diseases, and the first cause of death in cases of gynecological cancer [2,3]. Because ovarian cancers typically manifest few specific symptoms, more than 70% of patients are diagnosed at an advanced course of the disease [4] and only 20–30% of patients in such cases can be cured [5]. Current diagnoses habitually rely on histological evaluation of tumor masses and determination of specific serum biomarkers by enzyme-linked immunosorbent assay (ELISA), radioimmunoassay, as well as western blot [6,7]. Laboratory diagnosis is mostly based on quantitative determination of cancer antigen 125 [2,3], which is the standard tumor marker for the detection of ovarian cancer in current clinical practice [8] and also employed for the evaluation of biomarker serum level before treatment, for therapeutic response evaluation during chemotherapy, and in patient monitoring during follow-up to detect recurrences [2,3].

Recently, human epididymis protein 4 (HE4), a promising biomarker has entered the field of diagnostic markers for ovarian cancer. HE4, encoded by the WFDC2 gene [9–11], is a protein abundantly secreted in human epididymis [12,13] where it was first identified [14]. HE4 is commonly overexpressed in patients with serous endometriosis as well as epithelial ovarian and uterine cancer, and it is elevated in the serum of patients with ovarian cancer [12,13]. The main advantages in using HE4 for ovarian cancer detection reside in its high specificity for malignancy compared to the benign form of the disease [15] as well as in the fact that it is not only expressed in the disease's early stages but also serves as an early indicator of disease recurrence [12,13]. Therefore, HE4 is today of particular interest for recognizing early stages of epithelial ovarian cancer [15].

As a protein with molecular weight 25 kDa, HE4 is routinely detected by such common methods as enzyme immunoassay [2,8,16] and chemiluminescent microparticle immunoassay [2,17]. An ELISA-based microchip with a portable system (cell phone/charge-coupled device) has been utilized for HE4 detection in urine [1]. Moreover, electrochemical immunosensors based on the technique of rolling circle amplification of captured biotinylated DNA primer and detection of intercalated DNA redox indicator have been also used [18].

The most common enzyme used as a label of antibody in imunoanalytical methods (ELISA) is horseradish peroxidase. Nevertheless to achieve the desired sensitivity electrochemical detection usually requires the presence of a suitable electron mediator in substrate solution [19]. Thus, alkaline phosphatase (ALP) can be used as a preferable alternative, as it can convert a number of substrates to electroactive compounds with various redox potentials.

The presented approach to HE4 detection is based on immunomagnetic separation accompanied by sensitive electrochemical detection of the electroactive product formed after the enzymatic conversion of a suitable substrate by alkaline phosphatase, which is conjugated with anti-HE4 IgG serving for immunocomplex visualization. The use of

* Corresponding author at: Department of Biological and Biochemical Sciences, Faculty of Chemical Technology, University of Pardubice, Studentska 573 (HB/C), 532 10 Pardubice, Czech Republic. Tel.: +420 466 037 711.
E-mail addresses: michaela.cadkova@upce.cz (M. Čadková), veronika.dvorakova@upce.cz (V. Dvořáková), radovan.metelka@upce.cz (R. Metelka), zuzana.bilkova@upce.cz (Z. Bílková), lucie.korecka@upce.cz (L. Korecká).

http://dx.doi.org/10.1016/j.elecom.2015.06.014
1388-2481/

magnetic particles offers such advantages as simple and rapid separation of the target antigen from the real sample and its preconcentration. Many disadvantages, such as lower reproducibility and time-consuming procedures, are also avoided.

2. Experimental

2.1. Chemicals

Alkaline phosphatase (ALP, bovine intestinal mucosa, 8407 U/mg), 1-ethyl-3-(3-dimethylaminopropyl) carbodiimide hydrochloride (EDAC), *N*-hydroxysulfosuccinimide sodium salt (sulfo-NHS), *p*-nitrophenyl phosphate (PNPP), 2-morpholinoethane-1-sulfonic acid (MES), and TWEEN 20 were purchased from Sigma-Aldrich (Germany), amino- (SiMAG-NH_2) and carboxylate-modified (SiMAG-COOH) magnetic particles (1 μm diameter) from Chemicell (Germany), Precision Plus Protein™ Unstained standard (10–250 kDa) from Bio-Rad (USA), monoclonal and polyclonal anti-HE4 IgG and standard HE4 from Sino Biological (USA), Lightning-Link™ ALP conjugation kit from Innova Biosciences (UK), Biochemistry Control Serum Level II from BioSystems (Spain), *p*-aminophenyl phosphate (PAPP) and hydroquinone diphosphate (HQDP) from DropSens (Spain). All other chemicals were supplied by Penta (Czech Republic) and were of reagent grade.

2.2. Apparatus

PalmSens electrochemical analyzer (PalmSens BV, the Netherlands) and DRP-150 screen-printed three-electrode sensors comprised of carbon working, platinum auxiliary, and silver pseudo reference electrodes (DropSens, Spain) were used. Gels were evaluated using the ChemiDoc™ XRS + system with Image Lab™ Software (Bio-Rad, USA).

2.3. Biofunctionalization of SiMAG-NH_2 magnetic particles with ALP

One milligram of SiMAG-NH_2 magnetic particles was washed ten times with 0.1 M MES buffer (pH 6.0), activated by 7.5 mg EDAC and 1.25 mg sulfo-NHS, incubated overnight at 4 °C together with 700 U of ALP (overall volume 1 ml) under gentle mixing and then washed five times with 50 mM Tris–HCl buffer (pH 8.5). Enzyme activity was estimated using 50 μg of particles with immobilized ALP and 15.2 mM PNPP in 0.1 M Tris–HCl buffer as a substrate (reaction volume 1 ml). The reaction was performed at 37 °C for 20 min, stopped by the addition of 6 M NaOH and the colored product was measured at 405 nm.

2.4. Biofunctionalization of SiMAG-COOH magnetic particles by anti-HE4 IgG

Monoclonal anti-HE4 IgGs were immobilized to SiMAG-COOH magnetic particles using a standard two-step carbodiimide/sulfo-NHS method. Particles (1 mg) were washed five times with 0.1 M MES buffer (pH 5.0) and mixed with 7.5 mg of EDAC and 1.25 mg of sulfo-NHS (each in 500 μl of buffer). After 30 min incubation at room temperature and five times washing with MES buffer, 100 μg of monoclonal anti-HE4 IgG in MES buffer (1 ml) was added and incubated under gentle mixing overnight at 4 °C. Afterwards, biofunctionalized particles were washed five times with 50 mM MES buffer and transferred to 0.1 M phosphate buffered saline (pH 7.4). Immobilization efficiency was estimated by polyacrylamide gel electrophoresis with sodium dodecyl sulfate (SDS-PAGE) with the silver staining.

2.5. Electrochemical detection of HE4 by immunocomplex formation

The detection of antigen HE4 is based on immunocomplex formation with monoclonal anti-HE4 IgG immobilized on SiMAG-COOH magnetic microparticles with visualization by secondary polyclonal anti-HE4 IgG conjugated with ALP (anti-HE4 IgG^{ALP}) as follows: Labelling of secondary antibodies with ALP was carried out using a commercial labelling kit (Lightning-Link™) according to the recommended protocol. The proportion of magnetic immunosorbent with monoclonal anti-HE4 IgG taken to the reaction was set for the maximum amount of analyzed protein (molar ratio Ab:Ag 1:2). Precisely, the suspension of magnetic particles with 1.5 μg of immobilized anti-HE4 IgG (washed five times with 0.1 M phosphate buffer pH 7.0) was incubated with corresponding amount of HE4 (4 pM–20 nM) 1 h at room temperature (final volume of 1 ml) with following washing of the formed immunocomplex with 0.1 M phosphate buffer, phosphate buffer containing 0.15 M NaCl, and phosphate buffer (follows behind, three times each). Thereafter incubation with secondary anti-HE4 IgG^{ALP} (diluted 1:1000) in 0.1 M carbonate buffer (pH 9.49) for 1 h at 37 °C followed. Finally, electrochemical detection after washing with carbonate buffer and 0.1 M Tris–HCl (pH 8.9) (three times each) was performed.

Square-wave voltammetry was employed as the measuring technique to detect the electroactive product formed after enzymatic hydrolysis of specific substrates (dissolved in 500 μl of Tris–HCl) by ALP bound to secondary anti-HE4 IgG in an immunocomplex. The parameters of the voltammetric technique were as follows: initial potential −0.3 V, final potential 0.3 V, step potential 0.005 V, amplitude 0.02805 V, and frequency 20 Hz. Electrochemical sensing of the formed electroactive product was performed with 50 μl of supernatant in 5 min intervals (total detection time 15 min). The remainder of the tube's content was kept incubated at room temperature. The peak height evaluated at the tenth minute and potential 0.045 V was recorded.

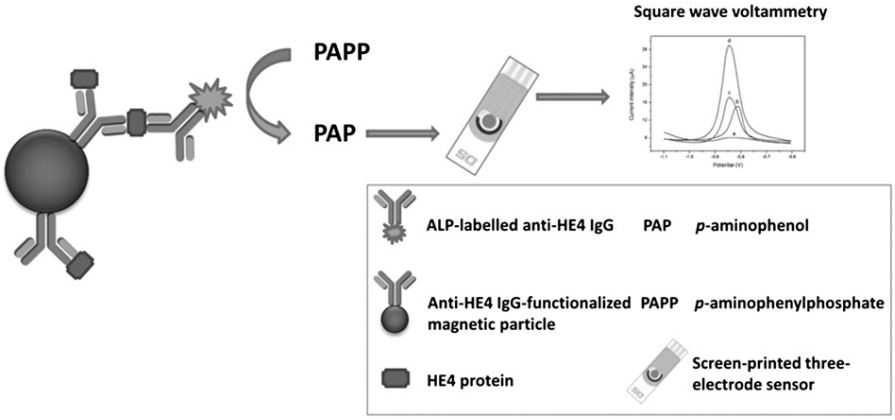

Fig. 1. Scheme of the magnetic bead-based electrochemical immunosensor for HE4 detection.

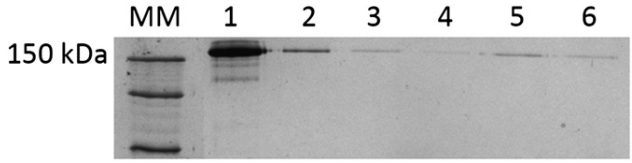

Fig. 2. Immobilization of anti-HE4 IgG on SiMAG-COOH particles using SDS-PAGE (10% gel, silver staining method). Sample order: MM) molecular marker (10–250 kDa), 1) mAb anti-HE4 prior to immobilization, 2) mAb after immobilization, 3–6) washing fractions.

3. Results and discussion

The scheme of the presented electrochemical biosensor for detecting HE4 based on the ELISA principle in combination with immunomagnetic separation is shown in Fig. 1.

Although ALP has already been used in a number of immunoassays [20,21] including electrochemical immunosensors, it has never been used previously to detect HE4. One of the key aspects of designing an immunomagnetic biosensor for HE4 with high sensitivity was the choice of an appropriate substrate for enzymatic hydrolysis in the presence of ALP. The reaction's electroactive product was then detected using square-wave voltammetry and the intensity of the recorded signal (peak height) was related to antigen concentration in the analyzed sample.

Two substrates for alkaline phosphatase, PAPP and HQDP, were selected as the most convenient owing to the low oxidation potentials of the corresponding hydrolysis products, (i.e., *p*-aminophenol [PAP] and hydroquinone [HQ]) [22,23]. Therefore, ALP activity was evaluated by monitoring the oxidation current of PAP or HQ at suitable peak potentials (0.01 V and −0.15 V, respectively) where PAPP or HQDP is not oxidized and interferences from other electroactive species which might be present in the sample are minimized [22].

The effect of different substrates on the resulting electrochemical response was first tested using ALP immobilized on SiMAG-NH_2 magnetic particles in connection with a three-electrode screen-printed sensor. The concentration of both PAPP and HQDP was 3 mM in 0.1 M Tris–HCl pH 8.9 (upon supplier recommendation). Although the experiments with HQDP provided an increase of electrochemical signal in time, the use of PAPP showed much higher oxidation currents. The difference in the substrates used was readily observed after 5 min of substrate hydrolysis and can be described by corresponding linear regressions equations for HQDP (I (μA) = 0.0612 t (min) − 0.074) and PAPP (I (μA) = 1.4035 t (min) + 0.4678). PAPP was used for all subsequent measurements in order to achieve the highest possible sensitivity in electrochemical monitoring of ALP activity.

To ensure maximum enzyme activity, the following solutions and pH were tested: 0.1 M Tris–HCl buffer, 0.1 M Tris–HNO_3 buffer (pH 8.9 and 9.8 in both), and finally 0.1 M carbonate buffer (pH 9.0). Although all buffers seemed to be suitable for detecting PAPP after hydrolysis by ALP, electrooxidation of PAPP in 0.1 M Tris–HCl buffer (pH 8.9) exhibited the highest peak currents and therefore it was used in further experiments.

The crucial step in immunosensor construction was specific antibody immobilization while maintaining the antibody's ability to capture HE4 antigen from the sample. Specific monoclonal anti-HE4 IgGs were covalently immobilized on SiMAG-COOH magnetic particles. Immobilization efficiency was estimated using SDS-PAGE after comparing the bands density before and after immobilization (Fig. 2) as 94.7%.

Since specific antibodies against HE4 conjugated with ALP are not commercially available, polyclonal anti-HE4 IgG were labelled using an ALP labelling kit. Labelling efficiency was evaluated using SDS-PAGE with silver staining, and it was estimated as 32.41% by comparing the band densities (Fig. 2, lanes 1 and 2). An appropriate dilution of prepared anti-HE4 IgG^{ALP} conjugate was optimized electrochemically using a limited amount of HE4 (2 nM) in various dilutions (1:750–1:2500). Electrochemical detection was performed according to the aforementioned protocol at a screen-printed electrode with 3 mM PAPP in 0.1 M Tris–HCl (pH 8.9). Peak currents values at 10 min were evaluated and compared. To keep analysis costs as low as possible with respect to the expensive secondary anti-HE4 IgG, the optimal dilution of anti-HE4 IgG^{ALP} conjugate at 1:1000 was chosen.

The stability of immunosensors is a key parameter in the analysis of corresponding antigens. Prepared immunosorbent and labelled antibodies were stored for 6 months at 4 °C and a slight decrease in enzyme activity of 11% was noted. Measurement with material stored in such manner provided comparable results. Therefore, the developed immunosensor has excellent analytical performance for the detection of HE4 antigen and thus meets the demanding requirements for diagnostic tests of the tumor marker in human serum.

The final electrochemical immunomagnetic biosensor for HE4 detection was constructed on the basis of the described preliminary

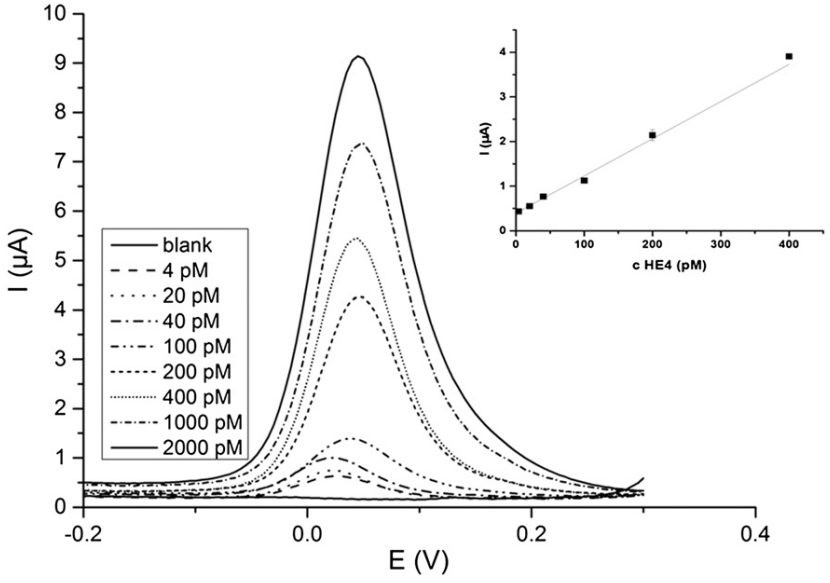

Fig. 3. Square-wave voltammograms of HE4 detection by immunomagnetic biosensor and corresponding calibration curve (inset). Experimental conditions were as follows: 0.1 M Tris–HCl (pH 8.9) with 3 mM PAPP, detection at 10th minute, using DRP-150 screen-printed sensor.

experiments. The calibration curve in Fig. 3 was obtained by plotting the current response for PAP oxidation in 0.1 M Tris–HCl (pH 8.9) with 3 mM PAPP substrate versus HE4 concentration. Linear dependence was observed up to 400 pM HE4 with corresponding regression equation I (μA) = $0.0833c_{HE4}$ (pM) + 0.39613 and the correlation coefficient of 0.973.

The limit of detection, defined as LOD = $3s_B/m$, where m is the slope of the calibration curve and s_B is the standard deviation of the blank ($n = 6$) [24], was calculated as 6.8 fM. The limit of quantification (defined as LOQ = $10s_B/m$) was estimated at 23 fM. The functionality of the proposed immunosensor was also tested by using standard human serum spiked with known additions of HE4 which simulates the complex biological matrix. Recoveries ranged from 87% to 93% within HE4 concentration levels shown in the calibration curve (Fig. 3).

4. Conclusion

We developed a magnetic bead-based immunosensor for detecting the ovarian cancer biomarker HE4 that achieved a limit of detection of 6.8 fM HE4, which is lower than the levels determined by the commonly used enzyme immunoassay and chemiluminescent microparticle immunoassay methods. The crucial step in immunosensor construction, specific antibody immobilization without restriction of the antibody's ability to capture HE4, was optimized. All measurements were performed using standard HE4, additionally standard human serum spiked with HE4 was used to simulate a real complex sample. The achieved analytical performance meets the requirements for detecting this biomarker at an early stage of cancer.

Conflict of interest

There are no conflict of interest.

Acknowledgement

This work was supported by the project of Czech Science Foundation P206/12/0381.

References

[1] S.Q. Wang, X.H. Zhao, I. Khimji, R. Akbas, W.L. Qiu, D. Edwards, D.W. Cramer, B. Ye, U. Demirci, Integration of cell phone imaging with microchip ELISA to detect ovarian cancer HE4 biomarker in urine at the point-of-care, Lab Chip 11 (2011) 3411–3418.
[2] G. Ruggeri, E. Bandiera, L. Zanotti, S. Belloli, A. Ravaggi, C. Romani, E. Bignotti, R.A. Tassi, G. Tognon, C. Galli, L. Caimi, S. Pecorelli, HE4 and epithelial ovarian cancer: comparison and clinical evaluation of two immunoassays and a combination algorithm, Clin. Chim. Acta 412 (2011) 1447–1453.
[3] S. Aebi, M. Castiglione, E.G.W. Grp, Newly and relapsed epithelial ovarian carcinoma: ESMO clinical recommendations for diagnosis, treatment and follow-up, Ann. Oncol. 20 (2009) 21–23.
[4] Z. Yurkovetsky, S. Skates, A. Lomakin, B. Nolen, T. Pulsipher, F. Modugno, J. Marks, A. Godwin, E. Gorelik, I. Jacobs, U. Menon, K. Lu, D. Badgwell, R.C. Bast, A.E. Lokshin, Development of a multimarker assay for early detection of ovarian cancer, J. Clin. Oncol. 28 (2010) 2159–2166.
[5] R. Macuks, I. Baidekalna, S. Donina, An ovarian cancer malignancy risk index composed of HE4, CA125, ultrasonographic score, and menopausal status: use in differentiation of ovarian cancers and benign lesions, Tumour Biol. 33 (2012) 1811–1817.
[6] I. Diaconu, C. Cristea, V. Harceaga, G. Marrazza, I. Berindan-Neagoe, R. Sandulescu, Electrochemical immunosensors in breast and ovarian cancer, Clin. Chim. Acta 425 (2013) 128–138.
[7] I. Hellstrom, E. Swisher, K.E. Hellstrom, Y.Y. Yip, K. Agnew, J.L. Luborsky, Anti-HE4 antibodies in infertile women and women with ovarian cancer, Gynecol. Oncol. 130 (2013) 629–633.
[8] J.M. Escudero, J.M. Auge, X. Filella, A. Torne, J. Pahisa, R. Molina, Comparison of serum human epididymis protein 4 with cancer antigen 125 as a tumor marker in patients with malignant and nonmalignant diseases, Clin. Chem. 57 (2011) 1534–1544.
[9] D. Trudel, B. Tetu, J. Gregoire, M. Plante, M.C. Renaud, D. Bachvarov, P. Douville, I. Bairati, Human epididymis protein 4 (HE4) and ovarian cancer prognosis, Gynecol. Oncol. 127 (2012) 511–515.
[10] I. Hellstrom, J. Raycraft, M. Hayden-Ledbetter, J.A. Ledbetter, M. Schummer, M. McIntosh, C. Drescher, N. Urban, K.E. Hellstrom, The HE4 (WFDC2) protein is a biomarker for ovarian carcinoma, Cancer Res. 63 (2003) 3695–3700.
[11] I. Hellstrom, P.J. Heagerty, E.M. Swisher, P. Liu, J. Jaffar, K. Agnew, K.E. Hellstrom, Detection of the HE4 protein in urine as a biomarker for ovarian neoplasms, Cancer Lett. 296 (2010) 43–48.
[12] E. Anastasi, T. Granato, G.G. Marchei, V. Viggiani, B. Colaprisca, S. Comploj, M.G. Reale, L. Frati, C. Midulla, Ovarian tumor marker HE4 is differently expressed during the phases of the menstrual cycle in healthy young women, Tumor Biol. 31 (2010) 411–415.
[13] D.J. Brennan, A. Hackethal, A.M. Metcalf, J. Coward, K. Ferguson, M.K. Oehler, M.A. Quinn, M. Janda, Y. Leung, M. Freemantle, P.M. Webb, A.B. Spurdle, A. Obermair, A. Grp, Serum HE4 as a prognostic marker in endometrial cancer – a population based study, Gynecol. Oncol. 132 (2014) 159–165.
[14] S. Kondalsamy-Chennakesavan, A. Hackethal, D. Bowtell, A. Obermair, A.O.C.S. Grp, Differentiating stage 1 epithelial ovarian cancer from benign ovarian tumours using a combination of tumour markers HE4, CA125, and CEA and patient's age, Gynecol. Oncol. 129 (2013) 467–471.
[15] A. Fritz-Rdzanek, W. Grzybowski, J. Beta, A. Durczynski, A. Jakimiuk, HE4 protein and SMRP: potential novel biomarkers in ovarian cancer detection, Oncol Lett 4 (2012) 385–389.
[16] B. Kristjansdottir, K. Levan, K. Partheen, K. Sundfeldt, Diagnostic performance of the biomarkers HE4 and CA125 in type I and type II epithelial ovarian cancer, Gynecol. Oncol. 131 (2013) 52–58.
[17] S. Lawicki, G.E. Bedkowska, E. Gacuta-Szumarska, M. Szmitkowski, The plasma concentration of VEGF, HE4 and CA125 as a new biomarkers panel in different stages and sub-types of epithelial ovarian tumors, J Ovarian Res 6 (2013) 45.
[18] L.S. Lu, B. Liu, Z.H. Zhao, C.X. Ma, P. Luo, C.G. Liu, G.M. Xie, Ultrasensitive electrochemical immunosensor for HE4 based on rolling circle amplification, Biosens. Bioelectron. 33 (2012) 216–221.
[19] N. Djellouli, M. Rochelet-Dequaire, B. Limoges, M. Druet, P. Brossier, Evaluation of the analytical performances of avidin-modified carbon sensors based on a mediated horseradish peroxidase enzyme label and their application to the amperometric detection of nucleic acids, Biosens. Bioelectron. 22 (2007) 2906–2913.
[20] C. Nistor, J. Emneus, An enzyme flow immunoassay using alkaline phosphatase as the label and a tyrosinase biosensor as the label detector, Anal. Commun. 35 (1998) 417–419.
[21] M.P. Kreuzer, C.K. O'Sullivan, G.G. Guilbault, Alkaline phosphatase as a label for immunoassay using amperometric detection with a variety of substrates and an optimal buffer system, Anal. Chim. Acta 393 (1999) 95–102.
[22] H.T. Tang, C.E. Lunte, H.B. Halsall, W.R. Heineman, P-aminophenyl phosphate: an improved substrate for electrochemical enzyme immunoassay, Anal. Chim. Acta 214 (1988) 187–195.
[23] M.S. Wilson, R.D. Rauh, Hydroquinone diphosphate: an alkaline phosphatase substrate that does not produce electrode fouling in electrochemical immunoassays, Biosens. Bioelectron. 20 (2004) 276–283.
[24] A.E. Radi, J.L.A. Sanchez, E. Baldrich, C.K. O'Sullivan, Reagentless, reusable, ultrasensitive electrochemical molecular beacon aptasensor, J. Am. Chem. Soc. 128 (2006) 117–124.

Příloha P9

Čadková M., Dvořáková V., Metelka R., Bílková Z., **Korecká L.*** Verification of antibody labelling efficiency as an important step in ELISA/QLISA development. *Monatshefte für Chemie – Chemical Monthly,* **147**, 2016, 69-73

IF_{2018} = 1,501; Q3 – Chemical sciences; 8 citací [1. 7. 2020]

- koncepce výzkumu, plánování experimentů
- podíl na experimentální práci a vyhodnocení výsledků 15 %
- dílčí příprava článku, revize, korespondující autor

Monatsh Chem (2016) 147:69–73
DOI 10.1007/s00706-015-1598-1

ORIGINAL PAPER

Verification of antibody labelling efficiency as an important step in ELISA/QLISA development

Michaela Čadková[1] · Veronika Dvořáková[1] · Radovan Metelka[2] · Zuzana Bílková[1] · Lucie Korecká[1]

Received: 5 September 2015 / Accepted: 27 October 2015 / Published online: 19 November 2015

Abstract A simple and effective method for validation of antibody labelling procedure as well as for optimal conjugate dilution assessment based on electrochemical detection is presented. Enzyme alkaline phosphatase and core-shell CdSe/ZnS quantum dots are used as sensitive tag exploitable as detection tool of antibody-antigen complex in magnetic microbead-based immunoassays. Square-wave voltammetry for detection of the electroactive product that is induced by conversion of appropriate substrate by alkaline phosphatase and square-wave anodic-stripping voltammetry for signal of Cd in case of quantum dots, respectively, was elected. Anti-Apo E IgG antibodies were selected as model molecules for method optimizations.

Graphical abstract

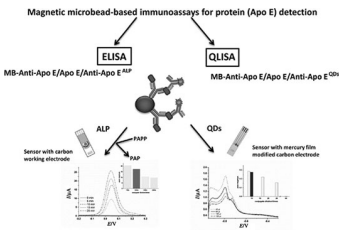

M. Čadková and V. Dvořáková contributed equally to this work.

✉ Lucie Korecká
lucie.korecka@upce.cz

[1] Department of Biological and Biochemical Sciences, Faculty of Chemical Technology, University of Pardubice, Pardubice, Czech Republic

[2] Department of Analytical Chemistry, Faculty of Chemical Technology, University of Pardubice, Pardubice, Czech Republic

Keywords Biosensors · Immunoassays · Proteins · Alkaline phosphatase · Quantum dots

Introduction

Currently the immunoassays, whose principle consists in specific reaction between antigen and antibody, are used in many areas for determination of various ligands [1, 2]. Randomly, they include a wide range of disease biomarkers in clinical diagnoses, pharmaceutical, environmental or food compounds. In principle, for successful analysis of given antigen (usually protein), two specific antibodies are needed [3]. A primary antibody serving for antigen capture from the sample and usually fixed onto solid phase (microtiter plate, magnetic beads, electrode surface, etc.) is supplemented by a secondary antibody, also called conjugate, which is labeled by an eligible tag, such as enzyme, fluorescent, chemiluminescent probes or other small detectable molecules [4–7].

Due to limited commercial availability of specific conjugates, especially enabling sensitive detection and quantification of significant biomarkers, techniques of covalent linkage exploiting EDC/NHS-based [8, 9] or click-chemistry [10] labelling reactions are used for its in-house preparation. Moreover, the choice of appropriate conjugation methodology along with post-immobilization characterization of product from the perspective of optimal dilution adjustment and maintaining of affinity properties are the cornerstone for further bioapplications.

For enzyme-based immunosensors, horseradish peroxidase (HRP), alkaline phosphatase (ALP), or glucose oxidase (GOx) are the most commonly used for antibody labelling. Compared to HRP and GOx, the main

advantages of ALP use lie in higher sensitivity and also broad spectrum of substrates easily convertible to electroactive products [11–13].

During the last few years, ever-increasing number of works exploiting the semiconductor quantum dots (QDs) nanolabels for designing the electrochemical immunosensors characterized by high sensitivity were published. Surface-functionalized QDs made of various materials (Zn, Cd, Pb, Cu, In, Ga) are used for conjugate preparation based on the same methods as for enzymes [13–16]. The proteins are quantified by sandwich-type quantum dot-linked immunosorbent assay (QLISA) along with stripping voltammetry of given metal. Moreover, the relatively broad potential windows, over which heavy metals are oxidized/stripped and provide sharp stripping peaks, offers the possibility of simultaneous detection of up to five metals with minimal peak overlap. The size of each peak than reflects the concentration of the corresponding target to allow convenient multi-target quantification.

Here, we present a simple approach for characterization of prepared anti-Apo E IgG conjugate, labeled by ALP or CdSe/ZnS QDs, by electrochemical detection in development of magnetic bead-based electrochemical biosensors for sensitive protein detection.

Results and discussion

Because a successful analysis of proteins by sandwich-type immunoassay and its sensitivity, mainly of low amount disease biomarkers, depends on detection of eligible label of antibody, our most important goal in development of magneto-immunoassay for analysis of various antigens was such labeled antibody preparation and characterization. The commercial unavailability of number of specific labeled antibodies enabling achieve low detection limits is another reason of this work. System of Apo E/anti-Apo E* IgG as a model affinity pair was chosen for methodology testing and optimizations, and variable with different antigen–antibody systems.

Enzyme alkaline phosphatase (ALP) and core shell CdSe/ZnS quantum dots (QDs) were selected for anti-Apo E IgG labelling to gain anti-Apo E^{ALP} IgG, anti-Apo E^{QDs} IgG, respectively. Because the proposed application of developed immunosensor is for disease biomarker detection, ALP has been used due to higher sensitivity compare to HRP as well as possibility of more substrates alternatives, and QDs for high sensitivity and possibility of multi-target analysis. The principles of both approaches are schematically described in Fig. 1.

For preparation of anti-Apo E^{ALP} IgG the commercial Lightning-Link^{TM} ALP conjugation kit has been used for antibody tagging. Labelling efficiency was verified by square-wave voltammetry by detection of electroactive product formed after enzymatic hydrolysis of appropriate substrate. Substrates, such as *p*-aminophenyl phosphate (PAPP), *p*-nitrophenyl phosphate (PNPP), hydroquinone diphosphate (HQDP) are the most common [2, 17]. For our purpose, two of them, PAPP and HQDP, were tested and based on results (published already), PAPP in 3 mM concentration was selected for further applications [18]. PAPP is converted to *p*-aminophenol (PAP) by ALP action. The enzymatic reaction was monitored by square-wave voltammetry with use of screen-printed three-electrode sensors composed of carbon working, platinum auxiliary and silver pseudoreference electrode. Measurements conditions are described in experimental part. The height of resulted (characteristic) peak evaluated at potential 0.045V. Even though the labelling procedure is based on oriented linkage between antibody and tag utilizing the glycosidic chain of antibody with no effect to its binding site, the post-labelling functionality of prepared conjugate should be verified. Moreover, maintained affinity properties of conjugated antibodies were confirmed through specific reaction with Apo E-modified magnetic microparticles (MB-Apo E). This approach enables also easy manipulation and acquired signal corresponds to only molecules specifically bound to antigen, while unbound molecules are washed out. Also optimal conjugate dilution necessary for its efficient application could be determined in this manner, where dilutions ranging from 1/2500 to 1/750 were tested. Results in Fig. 2 show a square-wave voltammogram for anti-Apo E^{ALP} dilution 1/1000, which was set to be optimal. The economic aspect has been taken into account (compared to 1/750 dilution).

Also for preparation of anti-Apo E^{QDs} IgG the commercial conjugation kit has been used (SiteClick^{TM} Qdot$^{®}$ 565 Antibody Labelling Kit). The kit is designed for conjugation with 100 μg of specific antibodies finally reached in volume of 150 mm^3. Labelling efficiency was verified by square-wave voltammetry analysis of Cd(II) ions released from core shell CdSe/ZnS Qdot$^{®}$ 565 ITK^{TM} quantum dots by dissolution in 0.1 M HCl. Measurements were proceeded upon conditions mentioned in experimental part and peak heights at potential -0.722 V obtained with screen-printed three-electrode sensors with the mercury film were compared. It was verified that signals observed in negative potential range starting from −800 mV are associated with the modification of working electrode containing mercury precursor compound, which is reduced to mercury during accumulation period. The composition of the layer coated on the electrode surface is unknown. The background response diminishes with the repetitive stripping measurements in pure supporting electrolyte, probably due to the dissolution of the coating. As for ALP-conjugates, the functionality of prepared anti-

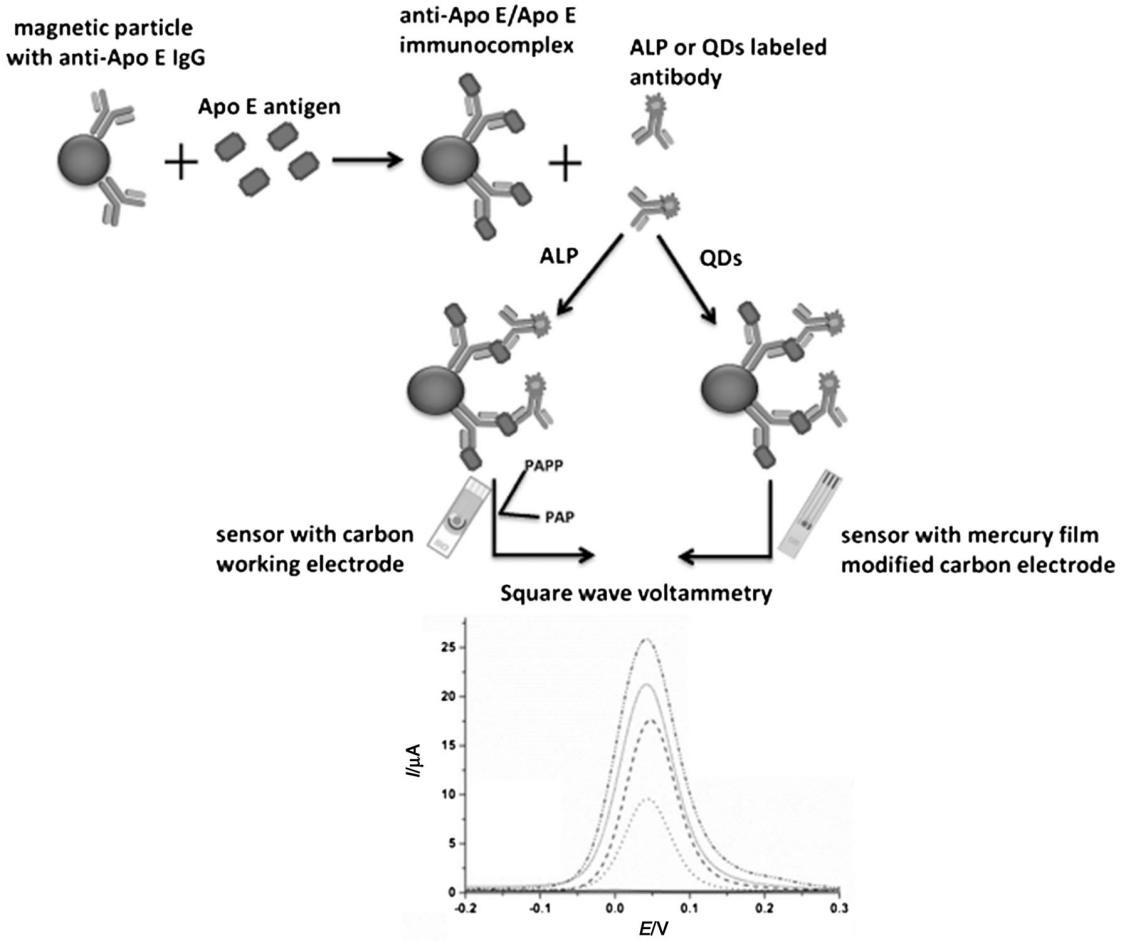

Fig. 1 The scheme of developed magnetic bead-based ELISA/QLISA system for protein detection

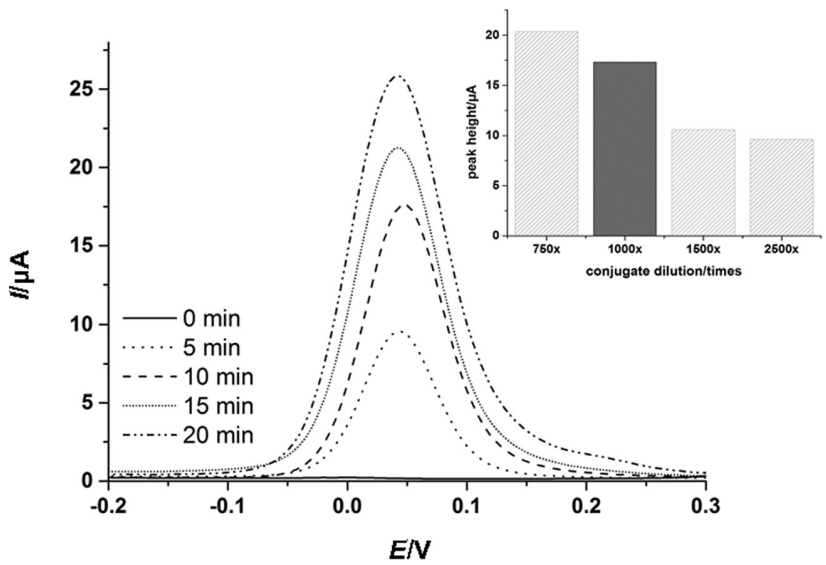

Fig. 2 Square-wave voltammogram of anti-Apo E^{ALP} conjugate diluted 1/1000 and optimal dilution determination (inserted graph). Experimental conditions were as follows: 0.1 M Tris–HCl (pH 8.9), 3 mM PAPP, DRP-150 screen-printed three-electrode sensor, detection time 0–10th minute

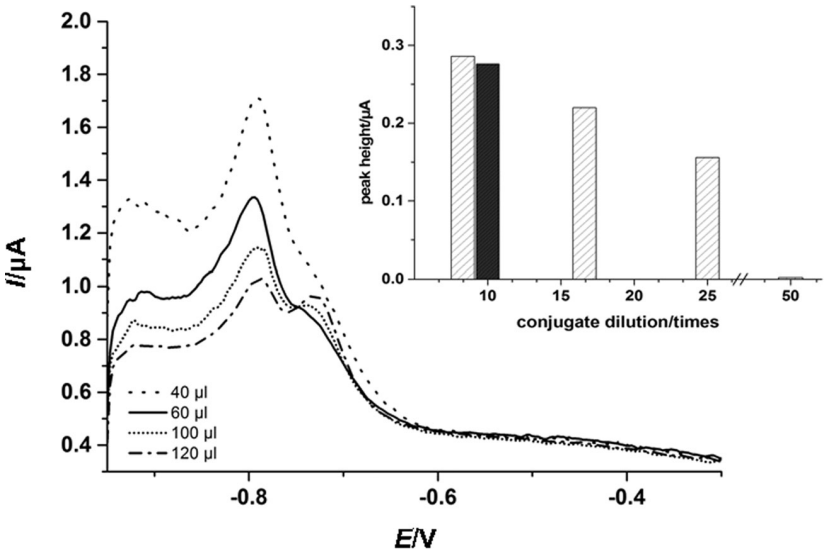

Fig. 3 Square-wave voltammogram of anti-Apo E^{QDs} conjugate in amounts ranging from 40 to 120 mm^3. Optimal conjugate amount (inserted graph). Experimental conditions were as follows: 0.1 M HCl, screen-printed three-electrode sensor with the mercury film, evaluation of peak height at potential −0.722 V

Apo E^{QDs} IgG as well as optimal amount to be taken into the reaction was determined using antigen modified magnetic beads. The typical square-wave voltammogram of MB-Apo E/anti-Apo E^{QDs} IgG analysis with various amounts of conjugate in the reaction is presented in Fig. 3 that shows the 100 µl of QDs labeled anti-Apo E IgG is optimal for sufficiently sensitive protein analysis in arrangement of magnetic bead-based QLISA.

To conclude, electrochemical detection of proteins by sandwich-type ELISA/QLISA with use of in-lab prepared specific ALP or QDs labeled antibodies bring comparable alternative to the official spectrophotometric or fluorescence assay. It is characterized by simplicity, short analysis time, low reagents consumption and could be successfully used not only for final detection but also for optimization of intermediate steps such as functionality verification and/or optimal dilution for construction of complete magneto-immuno assay.

Experimental

Chemicals

Human recombinant Apo E3 was supplied by BioVision (USA). Rabbit polyclonal affinity purified anti-Apo E antibodies were produced by Moravian-Biotechnology (Czech Republic). SiteClick™ Qdot® 565 Antibody Labeling Kit and core shell CdSe/ZnS Qdot® 565 ITK™ quantum dots were from Thermofisher (USA) and Lightning-Link™ ALP conjugation kit from Innova Biosciences (UK). Sigma–Aldrich (USA) was supplier of 1-ethyl-3-(3-dimethylaminopropyl) carbodiimide hydrochloride, N-hydroxysulfosuccinimide sodium salt, 2-morpholinoethane-1-sulfonic acid (MES), bovine serum albumin (BSA), and TWEEN 20. Carboxylate-modified (SiMAG-COOH) magnetic particles (1 µm diameter) were provided by Chemicell (Germany), Precision Plus Protein™ Unstained standard (10-250 kDa) by Bio-Rad (USA), *p*-aminophenyl phosphate (PAPP) by DropSens (Spain). All other chemicals were of analytical grade purity and were from Sigma-Aldrich (Germany) or Penta (Czech Republic).

Apparatus

All electrochemical measurements were performed using a PalmSens electrochemical analyzer (PalmSens BV, the Netherlands) and two types of screen-printed three-electrode sensors were used. DRP-150 sensors (DropSens, Spain) comprise of carbon working (4 mm diameter), platinum auxiliary, and silver pseudoreference electrodes. MF-SPCE (ItalSens, Italy) are composed of a mercury film modified carbon working electrode, a platinum auxiliary and a silver pseudoreference electrode.

Labelling of anti-ApoE IgG by CdSe/ZnS quantum dots and electrochemical detection by square-wave anodic-stripping voltammetry

Specific anti-Apo E IgG antibodies were labeled by core shell CdSe/ZnS QDs according to standard protocol recommended by supplier of commercially available SiteClick™ Qdot® 565 Antibody Labeling Kit (Thermofisher, USA) [19] to prepare conjugate anti-Apo E^{QDs} IgG.

Labelling efficiency was verified by square-wave anodic-stripping voltammetry as detection technique where post-labelling fraction was mixed with 0.1 M HCl in ratio

sample:HCl 10:40 mm^3. After 3 min incubation, the sample was applied to screen-printed three-electrode sensor, containing a carbon working electrode coated with mercury precursor compound (ItalSens, IT), which is reduced to mercury film during accumulation period. Detection conditions were as follows: condition potential 0 V, condition time 0 s, deposition potential −1 V, dep. time 120 s, potential range from −0.95 to −0.15 V, step potential 0.005 V, frequency 20 Hz, and amplitude 0.0285 V. Before experiment, the sensor was subjected to stripping procedure in pure electrolyte three times to lower high background currents, which appeared in negative potential range starting from −800 mV. Peak heights at potential −0.722 V were evaluated. The functionality of labeled conjugate (the preserved antigen binding ability) was verified using antigen-modified magnetic microparticles. Specific antigen Apo E (50 μg) was immobilized on SiMAG-COOH magnetic microparticles (1 mg) by two-step immobilization procedure in presence of *N*-(3-dimethylaminopropyl)-*N*′-ethylcarbodiimide hydrochloride (EDC) and *N*-hydroxysulfosuccinimide sodium salt (sulfo-NHS) in ratio 6 : 1 according to Hermanson [8]. Preventive blocking by 0.1 M ethanolamine (1 cm^3, 30 min, room temperature with gentle rotation) followed to avoid non-specific sorption. Then the portion of magnetic particles with immobilized 0.5 μg of Apo E was taken to the reaction for creation of immunocomplex between antigen and anti-Apo E^{QDs} IgG of various dilutions. Reaction was proceeded in 0.1 M carbonate buffer pH 9.4 containing 0.1 % BSA and 0.05 % Tween-20 (500 mm^3) for 1 h at room temperature supplemented by gentle rotation. After washing three times with 0.1 M phosphate buffer pH 7.3 (500 mm^3 each), three times with 0.1 M phosphate buffer pH 7.3 containing 0.15 M NaCl (500 mm^3 each) and five times with deionized water (500 mm^3 each), 50 mm^3 of 0.1 M HCl was added and analysed in the same way as mentioned above.

Labelling of anti-Apo E IgG antibodies by alkaline phosphatase and electrochemical detection by square-wave voltammetry

Specific anti-Apo E IgG antibodies were labeled by enzyme alkaline phosphatase to prepare anti-Apo E^{ALP} IgG according to standard protocol recommended by supplier of commercially available Lightning-Link® Alkaline Phosphatase kit (Innova Bioscience Ltd, Cambridge, UK) [20]. Functionality of conjugate labeled by ALP (anti-Apo E^{ALP} IgG) was then verified using antigen modified magnetic microparticles prepared in the same way as it is described in previous section with difference in the final step of detection where square-wave voltammetry was employed as the measuring technique for the detection of electroactive product formed after enzymatic hydrolysis of substrate *p*-aminophenyl phosphate (PAPP, 3 mM in 0.1 M Tris–HCl pH 8.9, reaction volume 500 mm^3). Screen-printed three-electrode sensors DRP-150 comprised of carbon working (4 mm diameter), platinum auxiliary and silver pseudoreference electrode (DropSens, Spain) were used and 50 mm^3 of the sample was applied. Parameters of voltammetric technique were as follows: potential range from −0.3 to 0.3 V, step potential 0.005 V, amplitude 0.02805 V, and frequency 20 Hz. Enzyme activity was monitored by the recording the peak height evaluated at tenth minute and potential 0.045 V.

Acknowledgments Support of the Czech Science Foundation Grant No. 15-16549S and University of Pardubice, Faculty of Chemical Technology (Project No. SGFChT07/2015) is gratefully acknowledged.

References

1. Zhu GN, Jin MJ, Gui WJ, Guo YR, Jin RY, Wang CM, Liang CZ, Liu YH, Wang ST (2008) Food Chem 107:1737
2. Xue-Mei L, Xiao-Yan Ym Shu-Sheng Z (2008) Trends. Anal Chem 27:543
3. Wang R, Chen X, Ma J, Ma Z (2013) Sens Actuators B 176:1044
4. Rusling JF, Sotzing G, Papadimitrakopoulosa F (2009) Bioelectrochemistry 76:189
5. Abuknesha RA, Luk CY, Griffith HHM, Maragkou A, Iakovaki D (2005) J Immunol Methods 306:211
6. Cappione A, Mabuchi M, Briggs D, Nadler T (2015) J Immunol Methods 419:48
7. Kuramitz H (2009) Anal Bioanal Chem 394:61
8. Hermanson GT (ed) (2008) Bioconjugate techniques, 2nd edn. Academic Press, New York, p 213
9. Čadková M, Metelka R, Holubová L, Horák D, Dvořáková V, Bílková Z, Korecká L (2015) Anal Biochem 484:4
10. Hein CD, Liu X-M, Wang D (2008) Pharm Res 25:2216
11. Cleland WW, Hengge AC (2006) Chem Rev 106:3252
12. Djellouli VN, Rochelet-Dequaire M, Limoges B, Druet M, Brossier P (2007) Biosens Bioelectron 22:2906
13. Holzinger M, Le Goff A, Cosiner S (2014) Front Chem. doi:10.3389/fchem.2014.00063
14. Sun H, Wang M, Wang J, Tian M, Wang H, Sun Z, Huang P (2015) J Trace Elem Med Biol 30:37
15. Yu C, Kim G-B, Clark PM, Zubkov L, Papazoglou ES, Noh M (2015) Sens Actuator B-Chem 209:722
16. Zhu X, Duan D, Publicover NG (2010) Analyst 135:381
17. Pemberton RM, Hart JP, Stoddard P, Foulkes JA (1999) Biosens Bioelectron 14:495
18. Čadková M, Dvořáková V, Metelka R, Bílkková Z, Korcká Z (2015) Electrochem Commun 59:1
19. http://www.thermofisher.com/order/catalog/product/S10450?ICID=search-product. Accessed 05 Sep 2015
20. http://www.innovabiosciences.com/antibody-labeling-kits/enzymes/lightning-link-alkaline-phosphatase-ap.html. Accessed 05 Sep 2015

Příloha P10

Cadková M., Kovarova A., Dvorakova V., Metelka R., Bilkova Z., **Korecka L.*** Electrochemical quantum dots-based magneto-immunoassay for detection of HE4 protein on metal film-modified screen-printed carbon electrodes. *Talanta,* **182**, 2018, 111-115

IF_{2018} = 4,916; Q2 – Chemical sciences; 13 citací [1. 7. 2020]

- koncepce výzkumu, plánování experimentů
- podíl na experimentální práci a vyhodnocení výsledků 15 %
- dílčí příprava článku, revize, korespondující autor

Talanta 182 (2018) 111–115

Contents lists available at ScienceDirect

Talanta

journal homepage: www.elsevier.com/locate/talanta

Electrochemical quantum dots-based magneto-immunoassay for detection of HE4 protein on metal film-modified screen-printed carbon electrodes

Michaela Cadkova[a], Aneta Kovarova[a], Veronika Dvorakova[a], Radovan Metelka[b], Zuzana Bilkova[a], Lucie Korecka[a,*]

[a] Department of Biological and Biochemical Sciences, Faculty of Chemical Technology, University of Pardubice, Studentska 573, 532 10 Pardubice, Czech Republic
[b] Department of Analytical Chemistry, Faculty of Chemical Technology, University of Pardubice, Studentska 573, 532 10 Pardubice, Czech Republic

ARTICLE INFO

Keywords:
Magneto-immunoassay
HE4 biomarker
Quantum dots
Metal-film electrode
Anodic stripping voltammetry

ABSTRACT

A novel enzyme-free electrochemical immunosensor was developed for highly sensitive detection and quantification of human epididymis protein 4 (HE4) in human serum. For the first time, core/shell CdSe/ZnS quantum dots were conjugated with anti-HE4 IgG antibodies for subsequent sandwich-type immunosensing with superparamagnetic microparticles functionalized with anti-HE4 IgG antibodies, which allow rapid and efficient HE4 capture from the sample. Electrochemical detection of anti-HE4 IgG – HE4 – anti-HE4 $IgG^{CdSe/ZnS}$ immunocomplex was performed by recording the current response of Cd(II) ions, released from dissolved quantum dots at screen-printed carbon electrode (SPCE), modified with mercury or bismuth film. The linear range of the detection was from 20 pM to 40 nM with limit of detection of 12 pM using three times the standard deviation of blank criterion at mercury-film SPCE and from 100 pM to 2 nM with limit of detection of 89 pM at bismuth-film SPCE. Proposed electrochemical immunosensor meets the requirements for fast and sensitive quantification of HE4 biomarker in early stage of ovarian cancer and due to the proper sensitivity and specificity presents a promising alternative to enzyme-based probes used routinely in clinical diagnostics.

1. Introduction

For ovarian cancer, where reliable diagnosis and differentiation between benign and malignant forms significantly influence survival rate, the analysis of as low as possible level of serum cancer biomarkers is essential [1]. Such analysis is routinely based on Enzyme Linked Immunosorbent Assay (ELISA). The selection of an appropriate antibody label is crucial to the sensitivity of the detection. Commonly used labels of antibodies are enzymes, primarily horseradish peroxidase [2,3], alkaline phosphatase [4] or β-galactosidase [5]. Although all of them generally provide adequate sensitivity, nowadays nanomaterials such as materially diverse nanoparticles [6] and nanotubes [7,8] are increasingly used, as well as various types of quantum dots (QDs) [9], which provide indisputable benefits, particularly when exploited in electrochemical analyses.

Quantum dots in the form of semiconductor nanocrystals, which are composed of heavy metals,have already been employed as labels of various biomolecules due to their unique optical properties [10,11], usable in many applications from fluorescent [12,13], western blot [14] or electrochemiluminescence methods [15] to the recently presented inductively coupled plasma mass spectrometry (ICP-MS) [16]. The metallic core-shell composition of quantum dots is favorable for electrochemical detection in biosensors [11,17]. Comparing to the above-mentioned methods, the electrochemical detection of quantum dots is versatile, robust, cost-effective and easy to manipulate and miniaturize [11,18]. Moreover, its combination with screen-printed electrodes modified with different metal films (mercury, bismuth, gold, antimony and copper) [19] and square wave anodic stripping voltammetry (SWASV) represents a significant contribution in sensitive detection methods for quantum dots [20–23]. Although mercury film electrodes offer high sensitivity, less toxic electrode materials are being tested as a viable alternative. Bismuth film electrodes are promising analogues to mercury counterparts due to their favorable electrochemical properties and easy preparation by the electrodeposition of Bi(III) ions on the surface of the selected substrate (glassy carbon, carbon paste, screen-printed carbon ink, gold, etc.) [24,25].

Human epididymis protein 4 (HE4) as a newly approved biomarker of ovarian cancer is currently of great importance not only for its potential to distinguish malignant and benign forms but also for its ability to reflect the differentiation stage of this cancerous disease [26–28].

* Correspondence to: Department of Biological and Biochemical Sciences, Faculty of Chemical Technology, University of Pardubice, Studentska 573 (HB/C), 532 10 Pardubice, Czech Republic.
E-mail address: lucie.korecka@upce.cz (L. Korecka).

https://doi.org/10.1016/j.talanta.2018.01.054
Received 6 October 2017; Received in revised form 18 January 2018; Accepted 20 January 2018
Available online 31 January 2018

Only a few reports on the electrochemical detection of HE4 protein have been published so far. Lu et al. described an electrochemical immunosensor for HE4 based on an indium tin oxide electrode with electrodeposited chitosan-titanium carbide and gold nanoparticles [29]. An electrochemical immunomagnetic biosensor based on sandwich-type ELISA with alkaline phosphatase-labeled antibodies was developed by Čadková and co-authors [30]. Recently, screen-printed carbon electrodes modified with graphene sheets and gold nanoparticles were applied for electrochemical enzyme-based sandwich immunoassay for HE4 analysis, where horseradish peroxidase was used as enzyme label [31]. Here we present its improvement by the inclusion of quantum dots as the sensitive antibody label instead of an enzyme. This novel HE4 biosensor exploited the specificity of classical immunospecific reaction and the signal sensitivity provided by quantum dots (quantum dot-linked immunosorbent assay - QLISA). Electrochemical detection was performed using two configurations of metal film-modified screen-printed carbon electrodes. First sensor utilizes a recent approach in preparation of mercury film electrodes, traditionally used for sensitive stripping analysis of heavy metals [32,33]. Mercury compound is immobilized directly on the surface of screen-printed carbon working electrode and it is reduced to mercury film during accumulation of heavy metals at negative potentials. In such configuration, manipulation with liquid mercury or mercury salt solutions is avoided while desired electrochemical properties of film electrodes are still maintained. Second sensor was an in situ bismuth-film screen-printed carbon electrode, which has manifested nowadays as the most favorable non-toxic replacement of mercury electrodes in stripping analysis of heavy metals [33,34]. Analytical performance of both configurations in HE4 detection was compared and critically discussed.

2. Experimental

2.1. Chemicals

Monoclonal and polyclonal anti-HE4 IgG antibodies and standard human HE4 protein were provided by Sino Biological (USA) (www.sinobiological.com). SiteClick™ Qdot® 565 Antibody Labeling Kit and Qdot® 565 ITK™ Carboxyl CdSe/ZnS Quantum Dots were purchased from Life Technologies (USA) (www.thermofisher.com), 1-Ethyl-3-(3-dimethylaminopropyl) carbodiimide hydrochloride (EDC), N-hydroxysulfosuccinimide sodium salt (sulfo-NHS), 2-morpholinoethane-1-sulfonic acid (MES), bovine serum albumin (BSA), bismuth(III) nitrate pentahydrate and TWEEN 20 were from Sigma–Aldrich (USA) (www.sigmaaldrich.com). Carboxylate-modified (SiMAG-COOH) magnetic particles (1 μm in diameter) were bought from Chemicell (Germany) (www.chemicell.com). Precision Plus Protein™ unstained standard (10–250 kDa) was produced by Bio-Rad (USA) (www.bio-rad.com). Biochemistry Control Serum Level II was from BioSystems (Spain) (www.biosystems-sa.com). All other chemicals were of analytical grade purity and were supplied by Penta (www.penta.cz) or Lachema (www.lach-ner.com) (Czech Republic).

2.2. Apparatus

All electrochemical measurements were performed with screen-printed three-electrode sensors. First type was C110 from DropSens (Spain) (www.dropsens.com) consisted of carbon working and auxiliary electrodes and a silver pseudoreference electrode, which served as a substrate for preparation of in situ bismuth film electrode (Bi-SPCE). Second type HM1, manufactured by ItalSens (Italy) (www.palmsens.com), comprised carbon working electrode modified with a mercury salt (unspecified by the producer), platinum auxiliary and silver pseudoreference electrode (Hg-SPCE). The sensors were connected to a PalmSens2 compact electrochemical analyzer with PSTrace software (PalmSens BV, the Netherlands) (www.palmsens.com). SDS-PAGE separation was performed in a Mini-PROTEAN® cell (Bio-Rad, USA) (www.bio-rad.com) and gels were evaluated using the ChemiDoc™ XRS + System with Image Lab™ Software (Bio-Rad, USA) (www.bio-rad.com).

2.3. Labeling of anti-HE4 IgG with CdSe/ZnS quantum dots

Polyclonal anti-HE4 IgG (100 μg) was labeled by CdSe/ZnS quantum dots using a commercially available SiteClick™ Qdot® 565 Antibody Labeling Kit according to the manufacturer´s instructions or by the common one-step carbodiimide method adjusted for the required antibody amount, using Qdot® 565 ITK™ Carboxyl CdSe/ZnS Quantum Dots. Labeled anti-HE4$^{CdSe/ZnS}$ antibodies were affinity purified using antigen HE4-modified SiMAG-COOH magnetic particles.

2.4. Anti-HE4 IgG-HE4-anti-HE4$^{CdSe/ZnS}$ immunocomplex formation

The immobilization of monoclonal anti-HE4 IgG antibodies onto the surface of SiMAG-COOH magnetic beads (MBs) and the determination of immobilization efficiency were performed according to the already published protocol in [30]. Briefly, 50 μg of antibodies were immobilized to 1 mg of magnetic particles. A two-step protocol was used, consisting of 30 min of particles activation with EDC and sulfo-NHS, followed by washing and then the addition of antibodies in 0.1 M MES buffer, pH 5.0, and incubation overnight at 4 °C with gentle mixing.

Subsequently, the immunocomplex was formed by incubation of appropriate amount of magnetic particles with immobilized monoclonal anti-HE4 IgG (10 μg anti-HE4 IgG) with different amounts of standard HE4 protein (1 h, room temperature) and followed by incubation with anti-HE4 IgG$^{CdSe/ZnS}$ in 0.1 M phosphate buffer, pH 7.3, containing 0.1% BSA and 0.05% TWEEN 20 (1 h, room temperature) prepared beforehand as described in 2.3. Dilution 1:500 (v/v) was used for labeled antibodies prepared via commercially available kit, or 1:10 (v/v) for antibodies prepared by the carbodiimide method, respectively.

Magnetic particles with the formed immunocomplex anti-HE4 IgG–HE4–anti-HE4 IgG$^{CdSe/ZnS}$ were washed five times with 1 ml of 0.1 M phosphate buffer, pH 7.3, containing 0.15 M NaCl and five times with distilled water. 50 μl of 0.1 M HCl was added to a sample and incubated at room temperature for 3 min, to release Cd(II) ions for voltammetric measurement.

2.5. Electrochemical measurements

Square wave anodic stripping voltammetry (SWASV) was used as the detection technique for the analysis of Cd(II) ions released from CdSe/ZnS by acid hydrolysis at disposable screen-printed carbon electrodes with a mercury salt (Hg-SPCE) or in situ formed bismuth film (Bi-SPCE). First, the electrode surface of Hg-SPCE was pre-treated by applying the conditional potential −1.1 V for 300 s for reduction of immobilized mercury salt to mercury film with subsequent detection of Cd (II) ions under the following conditions: deposition potential −1 V, deposition time 120 s, potential range from −1 V to −0.15 V, frequency 25 Hz and amplitude 0.0285 V.

The in-situ bismuth film was formed after the addition of Bi(III) ions (500 ppb in a final volume of analyzed solution) to each sample just before its application to SPCE. Measurements were performed in the presence of 0.1 M hydrochloric acid and 0.1 M acetate buffer (pH 4.5) and conducted using the experimental conditions mentioned above, but without the prior electrode pretreatment.

3. Results and discussion

The development of an electrochemical magneto-immunoassay using disposable screen-printed electrodes with the potential to become part of a point-of-care device in the early diagnostics of ovarian cancer is of great interest nowadays. Such an electrochemical immunoassay is presented here, based on square wave voltammetric monitoring of the

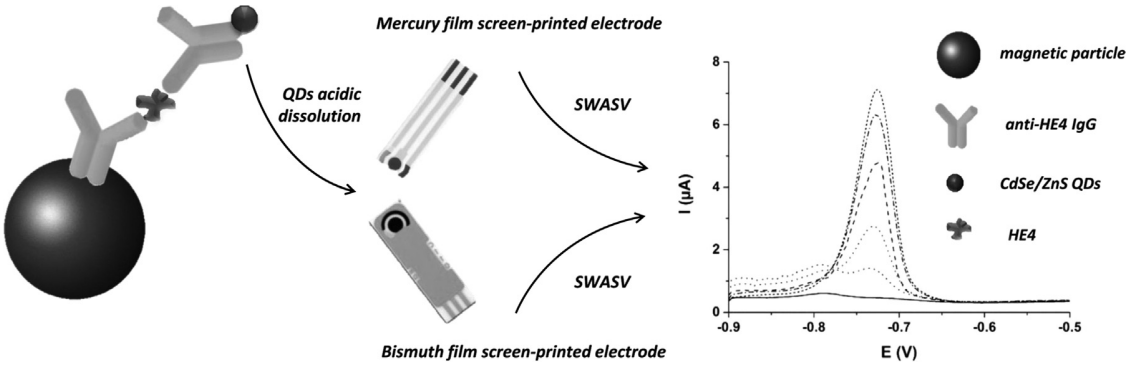

Fig. 1. Scheme of electrochemical magneto-immunoassay for HE4 protein detection.

current response of Cd(II) ions, released from the core of carboxylated CdSe/ZnS quantum dots used as the label probe of antibodies, which are an integral part of the immunoassays. The protein HE4, an ovarian cancer tumor marker, is a molecule of interest to be determined. Fig. 1 shows the assay arrangement, where antibody-modified magnetic particles serve as the solid phase for the efficient capture of the determined HE4 protein from the sample, followed by reaction with antibodies labeled with quantum dots. After the acidic dissolution of the quantum dots, the released Cd(II) ions are detected electrochemically. The use of magnetic particles instead of direct immunocomplex formation onto working electrode brings even more benefits related to covalent attachment of antibodies and higher surface area of prepared immunosorbent compare to limited area of working electrode.

Before assessing the conditions for specific HE4 immunocomplex formation, the parameters of the square wave anodic stripping voltammetry (SWASV) of CdSe/ZnS quantum dots had to be optimized since the multi elemental composition of core-shell QDs as well as the additional surface modifiers needed for conjugation with antibodies could influence the final current response. Deposition potential, deposition time, square wave frequency and the medium for dissolution of QDs was optimized using solution of 50 nM QDs and disposable Hg-SPCE sensor. Despite the fact that the Hg-SPCEs are conveniently used for the trace analysis of heavy metals [19,33], the application of bismuth film electrodes (either in situ or *ex* situ), introduced in 2001 [34], was proposed as an alternative to comply with the current trend of "green chemistry". These sensors offer similar analytical advantages to mercury-modified electrodes while eliminating the need to use toxic mercury or its salts. For that reason, we also utilized disposable screen-printed carbon electrodes with an in situ formed bismuth film (Bi-SPCEs).

We tested that it is possible to measure up to seven samples using one mercury film-modified carbon electrode without any negative impact onto subsequent measurement. With bismuth-film electrodes, only one reliable measurement was attained. Nevertheless, a reuse of working electrode is not expected in case of clinical samples due to possible contamination from previous analysis. Therefore, a new screen-printed sensor was used for each sample.

Hydrochloric and nitric acid were tested as the medium for the acidic dissolution of QDs varying their effective concentration range from 0.01 to 1 M and time of action from 1 min to 10 min. Effective dissolution was achieved using 0.1 M HCl for 3 min. The dissolution of QDs for less than 1 min gave a decreased peak height of Cd(II), whereas a prolonged action lasting from 5 to 10 min did not produce a significant increase in the stripping signal (Fig. S1 in Supplementary data).

In the next step, applicable experimental parameters for the SWASV of Cd(II), namely deposition potential in the range −1.1 to −0.8 V with a step of 0.1 V, deposition time (60, 120 and 180 s) and square wave frequency (15, 20 and 25 Hz), were optimized in terms of the maximum current response and the character of the stripping response. Thus, the optimal conditions for the electrochemical detection of dissolved quantum dots were as follows: deposition potential −1 V for 120 s, square wave frequency 25 Hz and amplitude 0.0285 V for both types of disposable screen-printed electrodes (Hg-SPCE and Bi-SPCE). Peak height was monitored at the potential of the peak maximum.

For the labeling of anti-HE4 IgG antibodies by CdSe/ZnS QDs (anti-HE4 $IgG^{CdSe/ZnS}$), two different linkage approaches were compared in terms of functionality, each with certain pros and cons. A commercial SiteClick™ Qdot® 565 Antibody Labeling Kit using click-chemistry ensures the linkage through the glycosidic part of antibody without affecting the binding sites, however it is limited to only CdSe/ZnS QDs and it needs to be emphasized that both labeled and non-labeled antibodies are present in the final product. The second approach combining well-known carbodiimide chemistry with the affinity purification [35]. It has a lower labeling yield but is versatile and it enables the pure product of labeled antibodies to be obtained with the simultaneous washing of free QDs, which could negatively affect the final signal. Labeling efficiency was verified by standard SDS-PAGE (10% gel) with densitometry evaluation in UV light as a comparison of the intensity of protein bands provided by the fractions before and after the labeling procedure. Moreover, the shift in molecular weight of the sample of antibodies after labeling indicates a successful protocol. The labeling efficiency was evaluated to be 75% with a commercially available kit and approximately 30% by the in-lab carbodiimide-based labeling strategy.

Thereafter, the proper dilution of anti-HE4 $IgG^{CdSe/ZnS}$ used for the immunoassay was determined with the aid of HE4 protein-modified magnetic particles according to an already published procedure [36] adapted for this system. The dilution of labeled anti-HE4 $IgG^{CdSe/ZnS}$ antibodies for experiments was in the range 1:10 − 1:1000 (v/v, final volume 1 ml). As for the labeling approach, the highest response obtained for the lowest possible amount of labeled antibodies provides the optimal dilution. This was determined to be 1:500 (v/v) for the commercial kit and 1:10 (v/v) for the carbodiimide-based in-lab approach (Fig. S2 and S3 in Supplementary data).

The cornerstone of the entire biosensor is the magnetically active carrier, modified with monoclonal anti-HE4 IgG antibodies (described in 2.4) and designed for the capture of HE4 molecules. The immunocomplexes consisting of anti-HE4 IgG - modified magnetic beads - HE4 (see 2.4) react with labeled specific antibodies (anti-HE4 $IgG^{CdSe/ZnS}$) and electrochemical detection then follows under the optimized conditions (see 2.5). For quantification of standard HE4 protein with anti-HE4 $IgG^{CdSe/ZnS}$ antibodies labeled by commercial kit and measured on Hg-SPCE, a calibration curve was constructed in concentrations ranging from 2 nM to 40 nM (Fig. 2). The limit of detection for HE4 biomarker was calculated to be 2.94 pM. It is defined as LOD = $3s_B/m$, where m is the slope of the calibration curve with the corresponding regression equation $I\ (\mu A) = 3.637 \log c_{HE4}$ (nM) + 0.359, s_B is the standard deviation of the blank ($n = 5$). The limit of quantification, defined as LOQ = $10s_B/m$, was 9.79 pM HE4.

Comparing to the analysis of the HE4 biomarker on Hg-SPCE, the

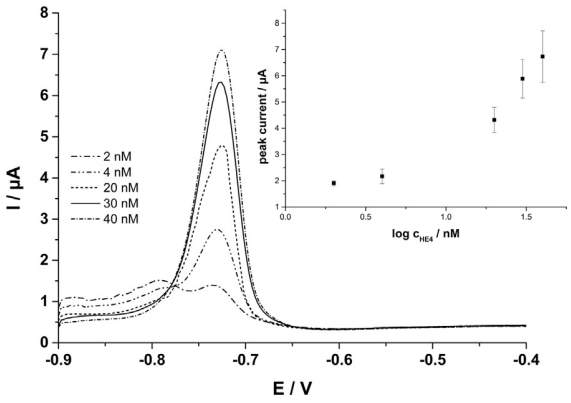

Fig. 2. SWASV voltammogram of HE4 detection using anti-HE4 IgG$^{CdSe/ZnS}$ antibodies labeled by commercial kit on Hg-SPCE in 0.1 M HCl; peak height evaluation at the potential of the peak maximum (−0.75 V).

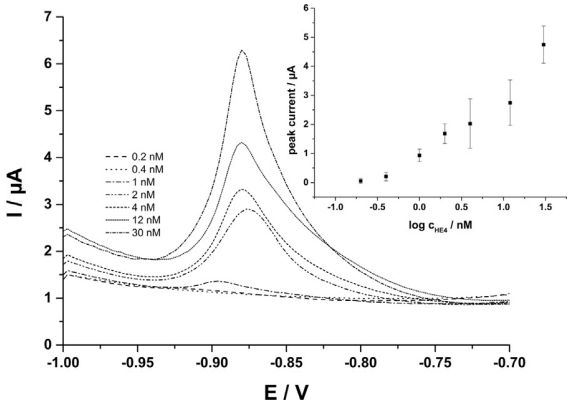

Fig. 3. SWASV voltammogram of HE4 analysis using anti-HE4 IgG$^{CdSe/ZnS}$ antibodies labeled by commercial kit on Bi-SPCE (500 ppb Bi(III)) in 0.1 M acetate buffer (pH 4.5) with 0.1 M HCl; peak height evaluation at the potential of the peak maximum (−0.88 V).

use of Bi-SPCE showed slight shift in peak evaluation potential (−0.88 V) and broader reoxidation peak was observed. The working concentration range with Bi-SPCE and anti-HE4 IgG$^{CdSe/ZnS}$ prepared in the same way was from 0.2 to 30 nM HE4 with the corresponding regression equation $I\ (\mu A) = 0.902 \log c_{HE4}$ (nM) −0.077 (see Fig. 3). The limit of detection 5.27 pM and the limit of quantification 17.55 pM, respectively, were calculated ($n = 5$) for developed HE4 immunosensor. Although the lower limit of detection was attained with the mercury compound modified screen-printed carbon electrode the results with Bi-SPCE provided wider working concentration range and better linearity.

Additionally, antibodies prepared by the in-lab carbodiimide-based labeling strategy were utilized for HE4 quantification on Hg-SPCE and compared with results obtained by commercially available labeling kit. The corresponding regression equation was $I\ (\mu A) = 3.694 \log c_{HE4}$ (nM) + 0.895 (see Fig. 4). Linear range for HE4 biomarker was estimated from 0.02 to 20 nM. The of limit detection for HE4 biomarker ($n = 4$) was calculated to be 3.7 pM and the limit of quantification 12 pM HE4. The best analytical performance in terms of concentration range over three orders of while maintaining linearity were achieved with this labeling strategy.

Moreover, this system was also proven in the analysis of standard human serum spiked with a known concentration of HE4 protein to simulate the complex biological matrix for which the system should be utilized as part of a point-of-care device. The recovery of HE4 standard addition (20; 40; 200; 4000; 2000 and 4000 pM) was within range 80 – 91% (measured in triplicate), which is favorable and comparable with literature [37,38].

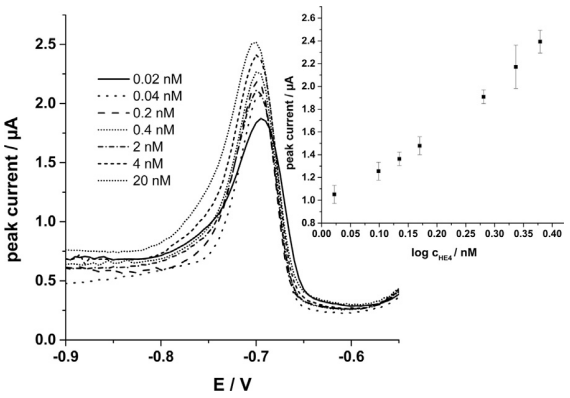

Fig. 4. HE4 analysis using anti-HE4 IgG$^{CdSe/ZnS}$ antibodies prepared by in-lab strategy and Hg-SPCE in 0.1 M HCl; peak height evaluation at potential of the peak maximum.

All the above-mentioned combinations of modified electrodes and different labeling approaches met the requirements for sensitive HE4 analysis with the possibility of the early-stage diagnosis of ovarian cancer. Analytical characteristics of developed immunosensor were compared with those of already published setups (Table 1). According to the literature, the cut-off limit is 150 pM for active malignant disease [39]. Moreover, our designed electrochemical magneto-immunoassay provides advantages in terms of the potential analysis of multiple serum biomarkers important in cancer diagnostics. Its multiple detection potential is due to the possibility of applying various specific antibodies labeled with QDs differing in their metal ion composition, which results in specific current responses at particular potentials without peak overlapping. In this way the stripping voltammetric analysis would surpass commonly used enzyme-based immunoassays.

4. Conclusions

Two qualitatively different labeling approaches and metal film-modified screen-printed carbon electrodes were tested for developing electrochemical immunosensor for HE4 protein detection using quantum dots as electrochemically active labels of specific antibodies. Two labeling strategies were used, namely commercially available labeling kit and in-lab developed carbodiimide method-based protocol. Disposable screen-printed carbon electrodes modified with mercury salt, reduced to the mercury film during accumulation period of stripping analysis, and in situ electrodeposited bismuth film in conjunction with SWASV were utilized for the detection of cadmium ions released from quantum dots. Both options contributed significantly to the analytical performance of tumor marker detection and met the exacting

Table 1
Comparison of recently published electrochemical sensors for HE4 quantification with results obtained in the proposed arrangement.

Sensor	LOD (HE4)	Linear range	Reference
AuNPs/CS–TiC/nanocomposite film modified ITO electrode	0.06 pM	3–300 pM	[29]
graphene sheets/AuNPs modified SPCE	0.5 pM	0–400 pM	[31]
Hg-SPCE	6.8 fM	23 fM – 400 pM	[30]
Hg-SPCE	2.94 pM[a]	2 nM – 40 nM	presented work
	3.7 pM[b]	0.2 nM – 20 nM	
Bi-SPCE	5.27 pM[a]	0.02 nM – 20 nM	

[a] anti-HE4 IgG$^{CdSe/ZnS}$ antibodies labeled by commercial kit.
[b] anti-HE4 IgG$^{CdSe/ZnS}$ antibodies prepared by in-lab strategy.

requirements for HE4 protein clinical monitoring. Lower detection limits in HE4 determination were attained with mercury salt-modified screen-printed carbon electrodes compared to that coated with in situ bismuth film. Moreover, the capability of the detection in the complex matrix was examined in the simulated real sample of human serum, where recovery rate was 80 − 91% for wide concentration range of HE4 protein.

Acknowledgements

This work was financially supported by the Czech Science Foundation (project 15–16549S).

Appendix A. Supporting information

Supplementary data associated with this article can be found in the online version at http://dx.doi.org/10.1016/j.talanta.2018.01.054.

References

[1] R. Laocharoensuk, Development of electrochemical immunosensors towards point-of-care cancer diagnostics: clinically relevant studies, Electroanalysis 28 (2016) 1716–1729.
[2] S.K. Vashist, E.M. Schneider, J.H.T. Luong, Rapid sandwich ELISA-based in vitro diagnostic procedure for the highly-sensitive detection of human fetuin A Biosens, Bioelectron 67 (2015) 73–78.
[3] M. Ihara, A. Yoshikawa, Y.S. Wu, H. Takahashi, K. Mawatari, K. Shimura, K. Sato, T. Kitamori, H. Ueda, Rapid noncompetitive detection of a small biomarker peptide by open-sandwich enzyme-linked immunosorbent assay (OS-ELISA) integrated into microfluidic device, Lab on Chip 10 (2010) 92–100.
[4] L. Liu, N. Xia, Me Jiang, N. Huang, S. Guo, S. Li, S. Zhang, Electrochemical detection of amyloid-β oligomer with the signal amplification of alkaline phosphatase plus electrochemical–chemical–chemical redox cycling, J. Electroanal. Chem. J. Electroanal. Chem. 754 (2015) 40–45.
[5] Z. Liu, T. Gurlo, H. von Grafenstein, Cell-ELISA using beta-galactosidase conjugated antibodies, J. Immunol. Methods 234 (2000) 153–167.
[6] Z.F. Wang, N. Liu, Z.F. Ma, Platinum porous nanoparticles hybrid with metal ions as probes for simultaneous detection of multiplex cancer biomarkers, Biosens. Bioelectron 53 (2014) 324–329.
[7] D.X. Feng, L.H. Li, J.Q. Zhao, Y.Z. Zhang, Simultaneous electrochemical detection of multiple biomarkers using gold nanoparticles decorated multiwall carbon nanotubes as signal enhancers, Anal. Biochem. 482 (2015) 48–54.
[8] S. Kruss, A.J. Hilmer, J.Q. Zhang, N.F. Reuel, B. Mu, M.S. Strano, Carbon Nanotub. Opt. Biomed. Sens. Adv. Drug Deliv. Rev. 65 (2013) 1933–1950.
[9] X. Li, D.W. Deng, J.P. Xue, L.Z. Qu, S. Achilefu, Y.Q. Gu, Quantum dots based molecular beacons for in vitro and in vivo detection of MMP-2 on tumor, Biosens. Bioelectron 61 (2014) 512–518.
[10] K. Brazhnik, Z. Sokolova, M. Baryshnikova, R. Bilan, A. Efimov, I. Nabiev, A. Sukhanova, Quantum dot-based lab-on-a-bead system for multiplexed detection of free and total prostate-specific antigens in clinical human serum samples Nanomedicine: nanotechnology, Biol. Med. 11 (2015) 1065–1075.
[11] J. Wang, G.D. Liu, H. Wu, Y.H. Lin, Quantum-dot-based electrochemical immunoassay for high-throughput screening of the prostate-specific antigen, Small 4 (2008) 82–86.
[12] C.J. Murphy, Optical sensing with quantum dots, Anal. Chem. 74 (2002) 520A–526A.
[13] P.K. Bae, K.N. Kim, S.J. Lee, H.J. Chang, C.K. Lee, J.K. Park, The modification of quantum dot probes used for the targeted imaging of his-tagged fusion proteins, Biomaterials 30 (2009) 836–842.
[14] K.L. Gilroy, S.A. Cumming, A.R. Pitt, A simple, sensitive and selective quantum-dot-based western blot method for the simultaneous detection of multiple targets from cell lysates, Anal. Bional. Chem. 398 (2010) 547–554.
[15] J.J. Zhang, T.F. Kang, Y.C. Hao, L.P. Lu, S.Y. Cheng, Electrochemiluminescent immunosensor based on CdS quantum dots for ultrasensitive detection of microcystin-LR, Sens. Actuators B: Chem. 214 (2015) 117–123.
[16] A.R.M. Bustos, M. Garcia-Cortes, H. Gonzales-Iglesias, J.R. Encinar, J.M. Costa-Fernandes, M. Coca-Prados, A. Sanz-Medel, Sensitive targeted multiple protein quantification based on elemental detection of Quantum Dots, Anal. Chim. Acta 879 (2015) 77–84.
[17] M. Medina-Sanchez, S. Miserere, S. Marin, G. Aragay, A. Merkoci, On-chip electrochemical detection of CdS quantum dots using normal and multiple recycling flow through modes, Lab on a Chip 12 (2012) 2000–2005.
[18] K. Pinwattana, J. Wang, C.T. Lin, H. Wu, D. Du, Y.H. Lin, O. Chailapakul, CdSe/ZnS quantum dots based electrochemical immunoassay for the detection of phosphorylated bovine serum albumin, Biosens. Bioelectron. 26 (2010) 1109–1113.
[19] N.Y. Stozhko, N.A. Malakhova, M.V. Fyodorov, K.Z. Brainina, Modified carbon-containing electrodes in stripping voltammetry of metals, J. Solid State Electr. 12 (2008) 1185–1204.
[20] S.B. Hocevar, B. Ogorevc, J. Wang, B. Pihlar, A study on operational parameters for advanced use of bismuth film electrode in anodic stripping voltammetry, Electroanalysis 14 (2002) 1707–1712.
[21] A. Merkoci, U. Anik, S. Cevik, M. Cubukcu, M. Guix, Film combined with screen-printed electrode as biosensing platform for phenol detection, Electroanalysis 22 (2010) 1429–1436.
[22] G. Kefala, A. Economou, A. Voulgaropoulos, M. Sofoniou, A study of bismuth-film electrodes for the detection of trace metals by anodic stripping voltammetry and their application to the determination of Pb and Zn in tapwater and human hair, Talanta 61 (2003) 603–610.
[23] N. Serrano, A. Alberich, J.M. Diaz-Cruz, C. Arino, M. Esteban, Coating methods, modifiers and applications of bismuth screen-printed electrodes Trac-Trend, Anal. Chem. 46 (2013) 15–29.
[24] J. Wang, Stripping analysis at bismuth electrodes: a review, Electroanal. 17 (2005) 1341–1346.
[25] I. Švancara, C. Prior, S.B. Hočevar, J. Wang, A decade with bismuth-based electrodes in electroanalysis, Electroanalysis 22 (2010) 1405–1420.
[26] B. Kristjansdottir, K. Levan, K. Partheen, K. Sundfeldt, Diagnostic performance of the biomarkers HE4 and CA125 in type I and type II epithelial ovarian cancer, Gynecol. Oncol. 131 (2013) 52–58.
[27] A. Stiekema, C.A.R. Lok, G.G. Kenter, W.J. van Driel, A.D. Vincent, C.M. Korse, A predictive model combining human epididymal protein 4 and radiologic features for the diagnosis of ovarian cancer, Gynecol. Oncol. 132 (2014) 573–577.
[28] D. Trudel, B. Tetu, J. Gregoire, M. Plante, M.C. Renaud, D. Bachvarov, P. Douville, I. Bairati, Human epididymis protein 4 (HE4) and ovarian cancer prognosis, Gynecol. Oncol 127 (2012) 511–515.
[29] L. Lu, B. Liu, Z. Zhao, C. Ma, P. Luo, C. Liu, G. Xie, Ultrasensitive electrochemical immunosensor for HE4 based on rolling circle amplification, Biosens. Bioelectron 33 (2012) 216–221.
[30] M. Čadková, V. Dvořáková, R. Metelka, Z. Bílková, L. Korecká, Alkaline phosphatase labeled antibody-based electrochemical biosensor for sensitive HE4 tumor marker detection, Electrochem. Commun. 59 (2015) 1–4.
[31] L. Lu, B. Liu, J. Leng, K. Wang, X. Ma, S. Wu, Electrochemical sandwich immunoassay for human epididymis-specific protein 4 using a screen-printed electrode modified with graphene sheets and gold nanoparticles, and applying a modular magnetic detector device produced by 3D laser sintering, Microchim. Acta 183 (2016) 837–843.
[32] C. Ari~no, N. Serrano, J.M. Díaz-Cruz, M. Esteban, Voltammetric determination of metal ions beyond mercury electrodes, Anal. Chim. Acta 990 (2017) 11–53.
[33] J. Barton, M.B. González García, D. Hernández Santos, P. Fanjul-Bolado, A. Ribotti, M. McCaul, D. Diamond, P. Magni, Screen-printed electrodes for environmental monitoring of heavy metal ions: a review, Microchim. Acta 183 (2016) 503–517.
[34] (a) W. Zhang, S. Zhu, R. Luque, S. Han, L. Hua, G. Xu, Recent development of carbon electrode materials and their bioanalytical and environmental applications, Chem. Soc. Rev. 45 (2016) 715–752;
(b) J. Wang, J.M. Lu, U. Anik, S.B. Hocevar, B. Ogorevc, Insights into the anodic stripping voltammetric behavior of bismuth film electrodes, Anal. Chim. Acta 434 (2001) 29–34.
[35] V. Dvorakova, M. Cadkova, V. Datinska, K. Kleparnik, F. Foret, Z. Bilkova, L. Korecka, An advanced conjugation strategy for the preparation of quantum dot-antibody immunoprobes, Anal. Methods 9 (2017) 1991–1997.
[36] M. Čadková, V. Dvořáková, R. Metelka, Z. Bílková, L. Korecká, Verification of antibody labelling efficiency as an important step in ELISA/QLISA development, Mon. Chem. - Chem. Mon. 147 (2016) 69–73.
[37] X. Fua, Y. Liub, R. Qiuc, M.F. Fodab, Y. Zhangb, T. Wangb, J. Lib, The fabrication of magnetic particle-based chemiluminescence immunoassay for human epididymis protein-4 detection in ovarian cancer, Biochem. Biophys. Rep. 13 (2018) 73–77.
[38] H. Zhao, G. Lin, T. Liu, J. Liang, Z. Ren, R. Liang, B. Chen, W. Huang, Y. Wu, Rapid quantitation of human epididymis protein 4 in human serum by amplified luminescent proximity homogeneous immunoassay (AlphaLISA), J. Immunol. Meth. 437 (2016) 64–69.
[39] R. Molina, J.M. Escudero, J.M. Augé, X. Filella, L. Foj, A. Torné, J. Lejarcegui, J. Pahisa, HE4 a novel tumour marker for ovarian cancer: comparison with CA 125 and ROMA algorithm in patients with gynaecological diseases, Tumour Biol. 32 (6) (2011) 1087–1095.

Příloha P11

Dvorakova V., Cadkova M., Datinska V., Kleparnik K., Foret F., Bilkova Z., **Korecka L.*** An advanced conjugation strategy for the preparation of quantum dot-antibody immunoprobes. *Analytical Methods,* **9**, 2017, 1991-1997

IF_{2018} = 2,378; Q3 – Chemical sciences; 6 citací [1. 7. 2020]

- koncepce výzkumu, plánování experimentů
- podíl na experimentální práci a vyhodnocení výsledků 15 %
- dílčí příprava článku, revize, korespondující autor

Analytical Methods

PAPER

View Journal | View Issue

Cite this: *Anal. Methods*, 2017, **9**, 1991

An advanced conjugation strategy for the preparation of quantum dot-antibody immunoprobes

Veronika Dvorakova,[a] Michaela Cadkova,[a] Vladimira Datinska,[b] Karel Kleparnik,[b] Frantisek Foret,[b] Zuzana Bilkova[a] and Lucie Korecka*[a]

Received 9th December 2016
Accepted 1st March 2017

DOI: 10.1039/c6ay03322a

rsc.li/methods

An advanced site-specific conjugation strategy for the preparation of quantum dot-based antibody probes applicable in various immunoassays from fluorescence to electrochemical biosensors is described. The combination of antigen (protein ApoE) modified magnetic particles providing protection to antibody binding sites, simple carbodiimide chemistry and carboxylate quantum dots (QDs) made of CdSe/ZnS is used for efficient labelling of anti-ApoE antibodies representing a model system. Polyacrylamide gel electrophoresis, fluorescence spectra measurements, capillary electrophoresis-laser induced fluorescence (CE-LIF) and square wave anodic stripping voltammetry (SWASV) were used for experimental verification of labelling efficiency. A simple change in antibody type makes this approach versatile and exploitable in a wide range of applications.

1. Introduction

Immunoglobulins and alternative antigen binding formats have the key position in a wide range of conventionally designed immunoassays fully utilizing the natural characteristics of antibodies to specifically target molecules or antigens.[1–4] The conjugation of specific antibodies with signal generating molecules including conventional radioactive isotopes, organic dyes, reporter enzymes, biotin or new generation probes such as quantum dots, carbon- and graphene-based nanomaterials, dendrimers or fullerenes enables the detection of bioactive compounds of various physico-chemical nature occurring over a wide concentration range.[5,6]

Recently semiconductor QDs have been considered as a new class of luminescent probes well suited for biological research and clinical medicine.[7,8] Luminescent nanocrystal QDs represent spherical particles with diameters in the range of 1–15 nm.[9] Their typical core–shell structure and material composition reflect their impressive opto-chemical properties for instance size-tunable emission, excellent signal brightness, and nearly no-photobleaching[8] whereas charged ligands on the surface provide water solubility and biocompatibility.[10] The ability to link QDs with various bioactive molecules without losing the aforementioned characteristics provides wide-field applications. Quantum dot-based immunochromatographic assays[11,12] or QD-FRET biosensing devices[13] are only two examples of numerous methods using QDs as a signal generating probe. The improved sensitivity, selectivity and multiplexity of QD-based methods enabled us to meet the high demands of the requirements for diagnostic methods for detecting tumours and other clinically important biomolecules.[8,14]

The unique properties of QDs such as their ability to generate fluorescence, chemiluminescence, conductivity or electrochemical signals enable us to select an appropriate way of detection based on the characteristics of the biomarker to be detected, its expected concentration, and taking into account also the complexity of the biological material and laboratory instrumentation.[15,16]

The surface properties of QDs play an important role in the conjugation process through which QDs can be attached to biomolecules.[17,18] The structure of core–shell QDs with a "coating" made from polymer molecules provides enough active functional groups for covalent binding of various bioactive molecules. Generally, there is an effort to apply a user-friendly and low-cost conjugation strategy suited for routine production of quantum dot-based probes. In particular, traditional bioconjugation techniques including random, site-selective, covalent or non-covalent strategies are widely used in the case of core–shell QDs.[8,19]

Carbodiimide mediated coupling represents one of the top covalent strategies used for crosslinking between amine and carboxylic functional groups. Although this approach is quick and very effective due to the high reactivity of crosslinking reagents, the most common strategy is the combination of EDC with sulfo-NHS. The limited possibility to control the orientation of biomolecules to be conjugated, influencing the total

[a]*Department of Biological and Biochemical Sciences, Faculty of Chemical Technology, University of Pardubice, Studentska 573, 532 10, Pardubice, Czech Republic. E-mail: lucie.korecka@upce.cz; Tel: +420 466 037 711*

[b]*Institute of Analytical Chemistry of the CAS, v.v.i., The Czech Academy of Sciences, Veveri 967/97, 602 00, Brno, Czech Republic*

activity of the modified carrier, is a drawback needed to be taken into account in the case of use. Conjugates prepared *via* carbodiimide chemistry are suitable for *e.g.* cellular imaging and tracking, for cancer cell targeting.[20–22]

Thiol chemistry is another frequently used conjugation strategy for the preparation of QD-nanoprobes for example for immunolabeling of cells or tissue specimens. Maleimide coupling is an example of the site-specific method strictly dependent on pH aimed at the conjugation of primary amines with thiols. However, the modification of proteins before conjugation is required in many cases.[23,24]

The carboxyl conjugation technique fully exploits the presence of carbohydrate groups located on the Fc fragment of immunoglobulins, and the reactive aldehyde groups react with the hydrazide modified counterpart. Conjugates prepared *via* the carboxyl crosslinking procedure are biocompatible and fit very well for sensing and bioimaging.[25]

His-tag site-specific coupling *via* polyhistidine residues is a great option for recombinant proteins to be conjugated with QDs. In this case Ni-NTA represents a biofunctional adaptor covalently linked to the QD whereas histidine-tagged antibodies bind the nickel ion by the chelation process.[8] Low production cost is the main advantage. These conjugates have been already used for *in vivo* imaging applications.[8,25,26]

The coupling strategy based on the biospecific pair streptavidin-biotin belongs to the simplest and widely used non-covalent techniques. This technique provides quick and relatively stable binding among all cooperative partners. Despite the size of this conjugate, which could be limiting in some applications, usability in cell biology has already been mentioned.[27,28]

Besides the possibility to prepare a "lab-made" quantum dot-based conjugate by one of the methods mentioned above, there is also a commercially available labeling kit (SiteClick™ Antibody Labeling Kit) enabling specific conjugation of QDs with IgG molecules *via* modified carbohydrate domains. However, this antibody labeling system brings a few disadvantages such as the limited amount of QDs per 1 mol of IgG molecules and contamination of the final conjugation product by free non-conjugated QDs. Final purification steps are desired however with significant losses.

Our work is focused on the development of an advanced conjugation technique suitable for routine preparation of QD conjugates of various specificities. To prepare quantum dot-based probes of high quality is a necessary prerequisite for their integration into sensitive and robust bioassays.

As many frequently used conjugation techniques, our protocol benefits from a well-known carbodiimide-based chemistry. Our original procedure includes (i) the biofunctionalization of the solid phase based on magnetic microparticles, (ii) capturing of the molecules to be conjugated with QDs by the molecules of the biospecific partner located on the magnetic carrier and covalent binding of QDs with biomolecules to be labeled, and (iii) the elution step providing a ready-to-use fraction of biomolecules labeled with QDs, *i.e.*, probe molecules.

The main goal was to prepare specific probes for bioassay combined with highly sensitive electrochemical detection. Apolipoprotein E (ApoE) and rabbit polyclonal anti-ApoE IgGs were used as a model of the biospecific pair. Our intention was to develop such a labeling strategy to obtain a fraction of QD probes without the need to purify the product before use. Also the specific IgG molecules conjugated with QDs have to keep the characteristics such as high specificity and affinity for biomarkers to be detected. During the whole labeling procedure their binding activity has to remain unaffected. Their functionality was proven by a set of control methods based on luminescence spectra measurements, and electrophoretic and electrochemical analyses.

2. Materials and methods

2.1 Reagents and chemicals

Qdot® 565 ITK™ carboxyl quantum dots (CdSe/ZnS carboxyl QDs) were purchased from Thermo Fisher Scientific (Waltham, MA, USA). Magnetic particles SiMAG-carboxyl were from Chemicell GmbH (1 μm in size; Berlin, Germany). Recombinant human apolipoprotein E (ApoE) was obtained from BioVision (CA, USA) and rabbit polyclonal anti-apolipoprotein E IgG (polyclonal anti-ApoE IgGs) antibodies were the product of Moravian Biotechnology (Brno, CZ). Precision Plus Protein™ Standards Unstained were supplied by Bio-Rad (Bio-Rad, Hercules, CA, USA) and acrylamide, *N*,*N*,*N*′,*N*′-tetramethylethylenediamine (TEMED), ethylenediaminetetraacetic acid (EDTA), Tris(hydroxymethyl)aminomethane and *N*,*N*′-(1,2-dihydroxyethylene)bisacrylamide were supplied by Sigma-Aldrich (St. Louis, MO, USA). All other chemicals were of reagent grade and supplied by Lach-Ner (Neratovice, Czech Republic) or Penta (Chrudim, Czech Republic).

2.2 Instrumentation

A spectrofluorimeter Jasco FP-8500, SAF-851 was purchased from JASCO Inc. (Easton, MD, USA), electrophoresis equipment and a ChemiDoc™ XRS+ Imaging System with Image Lab™ Software were from Bio-Rad (Hercules, California, USA).

A diode laser, RLTMLL-405 Series was supplied by Roithner Lasertechnik GmbH (Vienna, Austria) and it was connected with a 405/10 nm laser clean-up filter MaxDiode™ provided by Semrock (Rochester, USA). A microscope (objective: 40 × 0.65 NA) was obtained from Oriel. The long pass edge filter EdgeBasic™ and a 607/70 nm band-pass filter BrightLine® were products of Semrock (Rochester, USA). A photomultiplier tube R647 was obtained from Hamamatsu (Iwata City, Japan). Silica capillaries (75 μm i.d., 375 μm o.d.) were purchased from Polymicro Technologies (Phoenix, AZ, USA) and CSW 1.6 software was guaranteed from Data Apex Dobrichovice (Dobrichovice, Czech Republic). A potentiostat/galvanostat PalmSens2 with PSTrace software was obtained from PalmSens, the Netherlands, and screen-printed carbon electrodes modified with mercury films (MeSPCE) were obtained from ItalSens, Italy.

2.3 Preparation of quantum dot-based anti-ApoE IgG conjugates

(a) Biofunctionalization of the magnetic carrier. The molecules of antigen ApoE were immobilized on the surface of SiMAG-carboxyl magnetic microparticles using a standard two-step carbodiimide/sulfo-NHS method. The particles (1 mg) were washed five times with 0.1 M MES buffer (pH 5.0) and mixed with 7.5 mg of EDC and 1.25 mg of sulfo-NHS (both in 500 μL of 0.1 M MES buffer). After 30 min incubation at room temperature and washing twice with 0.1 M MES buffer, 25 μg of antigen ApoE (amount appropriate for the formation of a monolayer) in 0.1 M MES buffer (1 mL) was added and incubated under gentle mixing overnight at 4 °C. Afterwards, biofunctionalized particles were washed two times with 0.1 M MES buffer and two times with 0.1 M phosphate buffer saline (pH 7.4) and transferred to 0.1 phosphate buffer (pH 7.3). The remaining active functional groups of prewashed particles were blocked with 0.1 M ethanolamine in the presence of 0.1 M phosphate buffer pH (1 mL). After 1 h incubation at room temperature, the biofunctionalized particles were washed ten times with 0.1 phosphate buffer. The SiMAG-carboxyl magnetic microparticles with ApoE were stored in phosphate buffer, pH 7.3 with sodium azide.

(b) Conjugation of poly anti-ApoE IgGs with quantum dots. Antibodies, polyclonal anti-ApoE IgGs (25 μg), were added to biofunctionalized particles (0.5 mg) and incubated for 1.5 h under gentle mixing in 0.1 M phosphate buffer (500 μL). Afterwards the particles with immunocomplexes on their surface were washed three times with 0.1 M phosphate and 0.1 M phosphate buffer with 0.2 M NaCl.

The particles with bound immunocomplexes ApoE–anti-ApoE IgG (0.5 mg) were mixed with 0.5 mg of EDC and 0.083 mg of sulfo-NHS (both in 500 μL of 0.1 M phosphate buffer). After 10 min incubation under gentle mixing at room temperature, 8 μL Qdot® 565 ITK™ carboxyl quantum dots (250 μM stock solution) mixed with 0.1 M phosphate buffer (500 μL) were added to the magnetic microparticles and incubated under gentle mixing overnight at 4 °C. After incubation, the particles were washed three times with 0.1 M phosphate and 0.1 M phosphate buffer with 0.2 M NaCl. The washing fractions were retained for subsequent analyses.

(c) Efficient elution of quantum dot-labeled polyclonal anti-ApoE IgGs. The effective elution of labeled antibodies (poly anti-ApoE IgG^{QD} conjugate) was realized by using 0.05% trifluoroacetic acid (TFA) containing 0.5% SDS. As the last step, the transfer of the final conjugate from the elution medium to 0.1 M phosphate buffer pH 7.3 with the use of ultracentrifugal filters (cut off 150 kDa) was performed.

2.4 Luminescence spectra measurements

The luminescence signals of pure QDs, and fractions related to the labeling protocol such as pure QDs, unbound QDs, washing fractions and poly anti-ApoE IgG^{QDs} conjugates were measured by using a spectrofluorimeter Jasco FP-8500 enabling one-drop measurement unit analysis at 25 °C. Luminescence emission spectra were recorded from 400 to 700 nm with excitation at 340 nm.

2.5 SDS-PAGE and native TBE-PAGE

Denaturing SDS-PAGE in a standard arrangement (10% Tris–glycine separating gel, 5% Tris–glycine focusing gel)[29] was performed mostly to control the purity and homogeneity of prepared conjugates. Whereas slightly modified native TBE-PAGE (15% Tris–borate separating gel, 5% Tris–borate focusing gel, both with addition of EDTA)[30] was performed in order to monitor the quality and quantity of QDs (Fig. 1). Electrophoretic separation was carried out under these conditions: 0.1 M TBE buffer pH 8.3 running buffer, 180 V, 30 mA per one gel, approximately 50 minutes. TBE gels with samples of QDs were evaluated by UV illumination using Molecular Imager® ChemiDoc™ XRS+ with Image Lab™ software from Bio-Rad (Bio-Rad, Hercules, California, USA). Software Image J was used for QD quantification.

2.6 CE-LIF analysis of poly anti-ApoE IgG^{QDs} conjugates

QDs and anti-ApoE IgG^{QDs} conjugates were analyzed by separation in a laboratory-built CE-LIF system. Prior to each analysis, a 40 cm long (30 cm effective length) bare fused silica capillary (75 μm i.d., 375 μm o.d.) was rinsed successively with 0.1 M NaOH, water and finally with the running buffer (50 mM TRIS/TAPS, pH 8.6). The CE separation was driven by a Spellman CZE 1000R high power supply at a voltage of 10 kV. The samples were introduced electrokinetically at 10 kV for 5 s. At the positive voltage, the dominant mobility of electro-osmotic flow (EOF) carried all negatively charged analytes to the detector. A diode laser, RLTMLL-405 Series with a 405/10 nm laser clean-up filter was used as the excitation source at 405 nm. The fluorescence emission was collected by using a microscope objective (40 × 0.65 NA). A system of two filters including a 405 nm long pass edge filter and a 607/70 nm band-pass filter was used to block the 405 nm laser line and allow the maximum

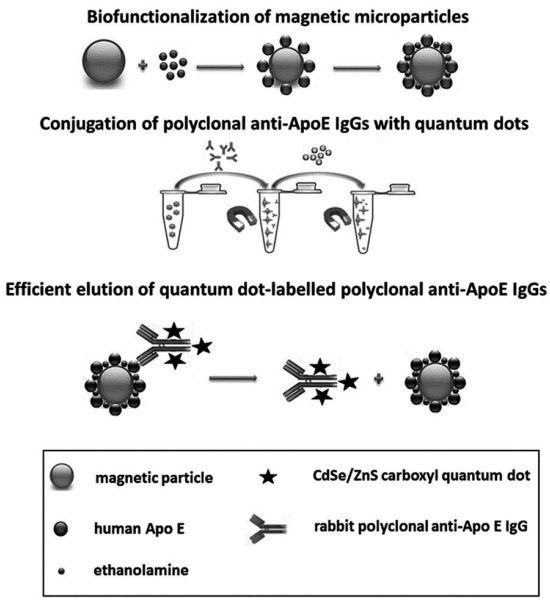

Fig. 1 Schematic of the advanced conjugation protocol.

intensity emission wavelength of QDs to enter the photomultiplier tube type R647 window. The detector signal was recorded at a sampling rate of 25 Hz with a data acquisition and evaluation system CSW 1.6. The value of EOF mobility was determined using coumarin (1,2-benzopyrone) as the neutral marker in all pH of background electrolytes used.

2.7 Electrochemical evaluation of anti-ApoE IgG^{QDs} conjugates

The conjugation efficiency was confirmed by square wave anodic stripping voltammetry (SWASV). All tested samples were mixed with 0.1 M HCl in a ratio of 10 : 40 μL (v/v) in the final volume of 50 μL and incubated for 3 minutes. Before sample application, the surface of MeSPCE was electrochemically pretreated at a potential of −1 V for 300 s followed by subsequent measurement of the blank (three times). In all cases, 0.1 M HCl was used. In each measurement, the surface of the screen-printed electrode was washed three times with 0.1 M HCl. Detection conditions for sample measurement were as follows: condition potential 0 V, condition time 0 s, deposition potential −1 V, dep. time 120 s, potential range from −0.95 to −0.15 V, frequency 20 Hz and amplitude 0.0285 V. The current response at potential (−0.72 V) characteristic of Cd(II) ions released after acidic dissolution of CdSe/ZnS QDs was monitored.

3. Results and discussion

Our work was aimed at the development of a versatile and highly efficient labeling protocol in order to prepare specific immunoprobes based on the conjugation of IgG molecules with Qdot® 565 ITK™ carboxyl quantum dots as an essential element of bioassays with electrochemical sensing.

Our strategy for IgG molecule labelling is based on the assumption which has been many times experimentally confirmed. This method is called hydrogen/deuterium (H/D) exchange for monitoring of biospecific interactions by mass spectrometry.[32,33] This method is used to localize the site of a molecule interacting with a ligand. To briefly summarize, the polypeptide chain forming the binding site of the IgG molecule is protected by ligand molecules (antigen) and H/D exchange does not occur. So our strategy was to protect the binding sites of specific antibodies by interactions with antigen molecules and perform the labeling with QDs only on sterically accessible parts of polypeptide chains.

According to our experience, the quality and stability of QDs used for conjugation were decisive for the final outcome of the whole conjugation procedure. Native TBE-PAGE was modified for separation and quality characterization of commercial QDs (Fig. 2A). TBE-PAA gel electrophoresis was also suited for QD quantification (Fig. 2B).

With the use of Qdot® 565 ITK™ carboxyl QDs we have successfully designed and validated the three stages of the IgG labeling approach which is schematically presented in Fig. 1. The biofunctionalization of SiMAG-carboxyl magnetic microparticles with antigen ApoE molecules was the first step, where the particle surface was fully covered with antigens

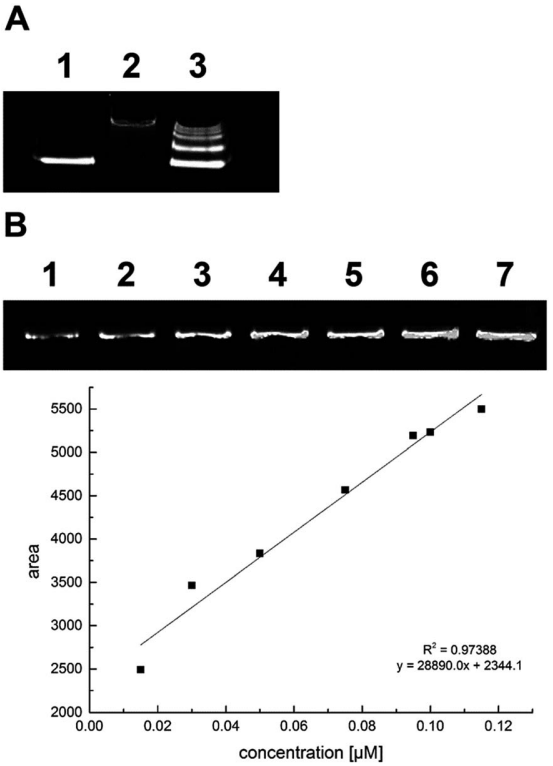

Fig. 2 TBE-PAGE (15% polyacrylamide separation gel, 5% polyacrylamide focusing gel) analysis of commercial carboxyl QDs (Qdot® 565 ITK™ carboxyl quantum dots). Data were obtained by UV detection: (A) quality control – QDs artificially affected in terms of aggregation and disintegration – (1) pure QDs without any modification, (2) QDs with simulated aggregation and (3) QDs with simulated disintegration. The tested concentration for all samples was 0.16 μM per well; (B) calibration curve of commercial carboxyl QDs (0.115–0.01 μM), UV detection and densitometric evaluation by Image J software.

corresponding to the specificity of antibodies to be labeled. The suitable amount of antigen was calculated with respect to the antigen molecular weight and the size of magnetic particles utilized for the reaction. In that case, we applied the following equation: $S = 6C/\rho_S\Delta d$ where S is the amount of representative protein (with respect to the molecular weight) required to achieve surface saturation (mg protein per g of microspheres), ρ_S is the density of the solid sphere (g cm^{-3}), d represents the mean particle diameter (μm) and C is the capacity of the microsphere surface for a given protein (mg of protein per m^2 of sphere surface).[31] For antigen binding, we applied the carbodiimide-mediated crosslinking reaction where EDC was combined with sulfo-NHS. We tested one- and two-step immobilization protocols with overnight incubation in both cases, whereas the two-step protocol with 30 min-long preactivation and application of 7.5 mg of EDC and 1.25 mg of sulfo-NHS has been considered as more beneficial, because of better immobilization efficiency. To avoid nonspecific binding and residual reactivity, an additional blocking step was added. Ethanolamine as an intact molecule of low molecular weight was used to block remaining activated carboxyl groups. Different time intervals (30–180 min, 24 hours) and

concentrations (0.01–1 M) were tested. The 60 min blocking time with 0.1 M ethanolamine was assumed as optimal.

Thus the ApoE biofunctionalized magnetic carrier was incubated with specific IgG molecules to create stable immunocomplexes with site-specific oriented IgG molecules. In the case of antigens with molecular weights in the range of 25–40 kDa the double molar amount of antibodies added into the binding mixture is the most efficient (data not shown). Also different times (30, 60, 90, 120 minutes and overnight incubation) required for the formation of specific immunocomplexes have been tested. In the case of rabbit polyclonal anti-ApoE IgG, the time of immunocomplex formation 90 min was evaluated as the sufficient time for maximal coverage. To label the specific IgG molecules fixed in immunocomplexes on magnetic particles, EDC, sulfo-NHS and an appropriate amount of carboxyl QDs was added. Incubation was performed under gentle mixing (see 2.3 b). Finally, the magnetic beads were repeatedly washed to remove all reagents and free QDs.

The third phase of the protocol followed immediately. The molecules of poly anti-ApoE IgG^{QDs} conjugates had to be released from the complexes with ApoE. Elution represents the disruption of many non-covalent bonds between the specific binding sites of IgG molecules and antigenic determinants of complex antigen molecules. We tested various elution reagents from the acidic and basic pH range (Table 1), and the time and number of elution steps were also optimized. Elution reagents were applied in three independent 15 minute-long intervals. The most efficient elution reagent has been determined based on spectrophotometric measurements of immunocomplexes before and after treatment with the elution reagent. The standard ELISA arrangement in a microtiter plate, with enzyme horseradish peroxidase as the antibody label, was used. To prove that the binding activity of antibodies is not affected by the used elution reagent, eluted antibodies were repeatedly used for immunocomplex formation (data not shown). Based on our results, the acidic medium namely 0.05% TFA with 0.5% SDS (pH 2.5) provided the strongest elution efficiency. Considering the very low pH the released conjugate was directly transferred to 0.1 M phosphate buffer (pH 7.3).

Fluorescence spectra measurements (Fig. 4A) and polyacrylamide gel analyses (Fig. 3 and 4B) supplemented by CE-LIF (Fig. 5) were chosen as fundamental methods for evaluating all the reactive compounds, bioactive molecules entering the reaction and also all the fractions obtained during the three steps of the labeling protocol. Square wave anodic stripping voltammetry (Fig. 6) was considered as the main confirmatory technique for the assessment of the functionality of the designed labeling protocol.

The luminescence emission spectra are shown in Fig. 4A. The pure QDs, unbound QDs and poly anti-ApoE IgG^{QDs} conjugates provided detectable signals in contrast to washing fractions, which did not contain any traces of QDs. The samples were also loaded into the slab gel to perform TBE-PAGE accompanied by UV detection (Fig. 4B). The results of the

Table 1 Summary of tested elution reagents with calculated elution efficiency

Elution reagents	Efficiency [%]
Acidic media	
0.1 M acetic acid with 20 mM $CaCl_2$ (pH 4)	41
0.1 M acetic acid with 0.2 M $MgCl_2$ (pH 4)	36
1 M arginine–hydrochloride (pH 4)	37
0.5 M citrate (pH 4.3)	9
0.1 M glycine with 0.2 M NaCl (pH 2.6)	65
0.05% TFA with 0.5% SDS (pH 2.5)	76
0.05% TFA with 1% SDS (pH 2.5)	73
Alkaline media	
0.1 M citrate with 0.1 M NaOH (pH 8)	73
0.1 M citrate with 0.1 M NaOH and 0.2 M $MgCl_2$ (pH 7)	16
0.1 M glycine with 0.1 M NaOH and 0.2 M $MgCl_2$ (pH 8)	12
1 M $MgCl_2$ (pH 7.5)	14
0.1 M NH_4OH (pH 11)	25
0.1 M NH_4OH with 0.2 M $MgCl_2$ (pH 11)	12
0.1 M triethanolamine (pH 9)	7

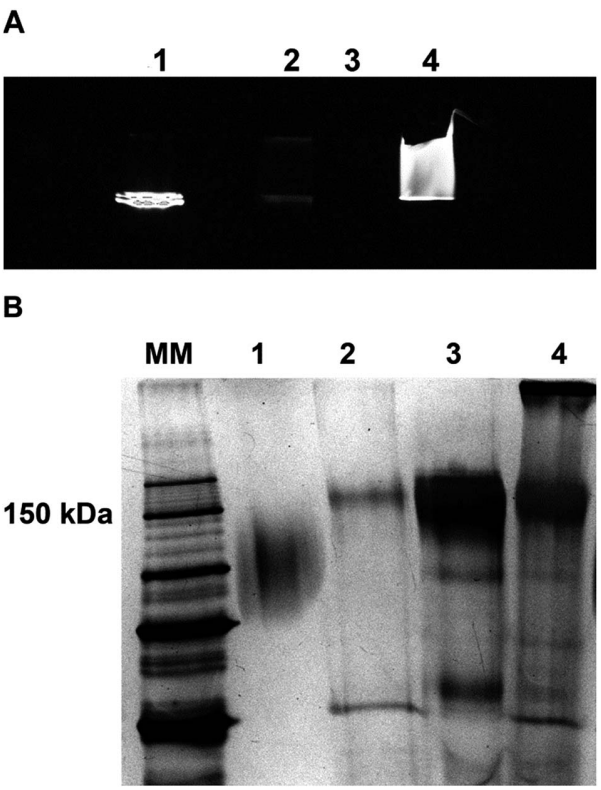

Fig. 3 PAGE analysis (A) TBE-PAGE (15% polyacrylamide gel, UV detection): (1) pure QDs (0.16 μM, Qdot® 565 nm ITK™), (2) poly anti-ApoE IgG^{QDs} conjugates (1 μg, home-made), (3) polyclonal anti-ApoE IgG antibodies (1 μg), (4) poly anti-ApoE IgG^{QDs} conjugates (1 μg, prepared by SiteClick™ Qdot® 565 Antibody Labeling Kit); (B) SDS-PAGE (10% polyacrylamide gel, silver staining): (MM) protein standard (10–250 kDa), (1) pure QDs (0.16 μM, Qdot® 565 nm ITK™), (2) polyclonal anti-ApoE IgG^{QDs} conjugates (1 μg, home-made), (3) polyclonal anti-ApoE IgG antibodies (1 μg), (4) polyclonal anti-ApoE IgG^{QDs} conjugates (1 μg, prepared by SiteClick™ Qdot® 565 Antibody Labeling Kit).

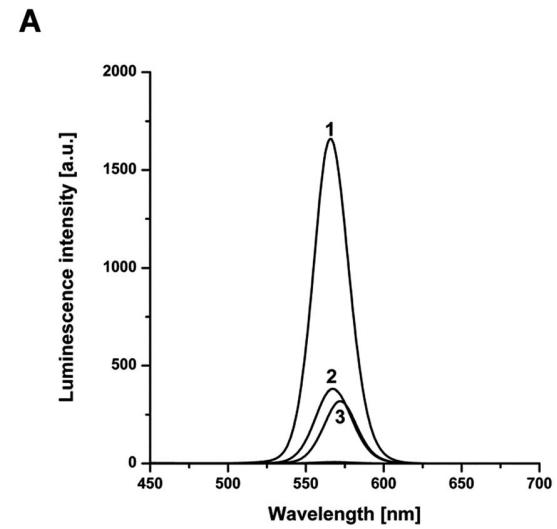

Fig. 4 Quality evaluation of poly anti-ApoE IgG^{QDs} conjugates: (A) luminescence emission spectra: (1) pure QDs (Qdot® 565 ITK™ carboxyl quantum dots, $c = 128$ nM), (2) unbound QDs and (3) poly anti-ApoE IgG^{QDs} conjugates; (B) TBE-PAGE (15% Tris–borate separating gel and 5% Tris–borate focusing gel, both with addition of EDTA): (1) pure QDs (Qdot® 565 ITK™ carboxyl quantum dots, $c = 128$ nM), (2) unbound QDs, (3–5) washing fractions and (6) poly anti-ApoE IgG^{QDs} conjugates.

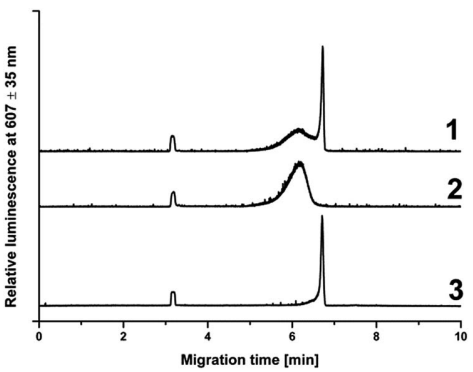

Fig. 5 CE-LIF analysis of pure QDs and poly anti-ApoE IgG^{QDs} conjugates: (1) mixture of pure QDs and poly anti-ApoE IgG^{QDs} conjugates, (2) poly anti-ApoE IgG^{QDs} conjugates and (3) pure QDs (Qdot® 565 ITK™ carboxyl quantum dots). Small peaks at 3.2 min represent neutral EOF (coumarin).

luminescence spectra and TBE-PAGE demonstrated the functionality of the designed labeling procedure.

The quality and purity of poly anti-ApoE IgG^{QDs} conjugates were confirmed by the CE-LIF assay. Due to the different

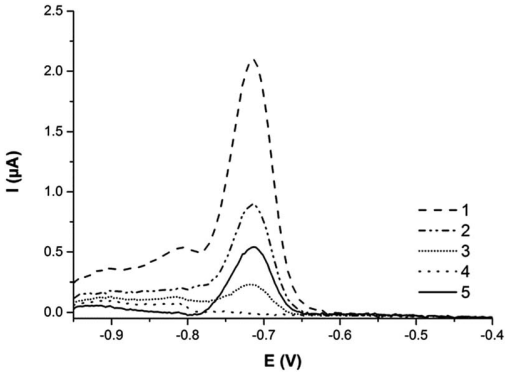

Fig. 6 SWASV voltammogram: (1) pure QDs (Qdot® 565 ITK™ carboxyl quantum dots, $c = 128$ nM), (2) unbound QDs, (3 and 4) washing fractions and (5) poly anti-ApoE^{QD}s IgG conjugates recorded at MeSPCE in 0.1 M HCl.

electrophoretic mobilities of pure QDs and conjugates this technique allowed us to confirm the high efficiency of the labeling procedure and prove the absence of free QDs in the conjugate fraction (Fig. 5).

Square wave anodic stripping voltammetry was another confirmation technique for labeling efficiency assessment. The current response at a potential of −0.72 V, characteristic of CdSe/ZnS quantum dots, was obtained by the use of a disposable miniaturized screen-printed three-electrode sensor with a mercury film modified carbon working electrode (MeSPCE) (Fig. 6). The efficiency of the conjugation of quantum dots with antibodies was calculated as the ratio of electrochemical current responses of quantum dots of all fractions connected with the performed labeling protocol. The difference of the electrochemical current responses of the original sample (the original fraction of quantum dots before conjugation), the fraction of conjugates (antibodies conjugated with QDs) and the sum of current responses of binding (fraction after conjugation – the rest of the unbound QDs) and washing fractions was calculated with a resulting conjugation efficiency of 30%.

The quality of the poly anti-ApoE IgG^{QDs} conjugate in terms of its ability to target the antigen specifically as well as further optimization of reaction conditions was verified.[34]

4. Conclusions

Here we have designed and validated a three-stage conjugation procedure to prepare QD-based immunoprobes for highly sensitive biosensors combined with electrochemical detection. This protocol fully exploited the benefits provided by superparamagnetic microparticles, *i.e.*, easy, rapid and quantitative separation of the liquid phase with reagents from the solid phase carrying the molecules of antigens, immunocomplexes or bioconjugates. The conjugation strategy was based on traditional carbodiimide chemistry but combined with site-specific immobilization of IgG molecules on the surface of antigen biofunctionalized magnetic microparticles. The binding sites of all IgG molecules to be labeled are protected by antigen molecules just in immunocomplexes, and IgG affinity and specificity

remained unaffected during all steps of the covalent coupling procedure. Another advantage of this labeling approach is the purity of the final product – the poly anti-ApoE IgG^{QDs} conjugate. Since no contamination of the conjugate by free QDs was observed, no additional separation step was needed. This protocol for the efficient conjugation of IgG molecules with QDs is suitable wherever there are high demands on quality and purity of signal generating probes.

Acknowledgements

At the Department of Biological and Biochemical Sciences, Faculty of Chemical Technology, University of Pardubice the work was supported by the Czech Science Foundation, project no. 15-16549S and project SGS-2016-004 of the Faculty of Chemical Technology (University of Pardubice, Czech Republic). At the Institute of Analytical Chemistry ASCR, v.v.i., the research was supported by the Czech Science Foundation, project no. 17-01995s.

References

1 I. Vainshtein and R. Lee, *Bioanalysis*, 2014, **6**, 1939–1951.
2 T. Fodey, P. Leonard, J. O'Mahony, R. O'Kennedy and M. Danaher, *TrAC, Trends Anal. Chem.*, 2011, **30**, 254–269.
3 F. Okda, S. Lawson, X. Liu, A. Singrey, T. Clement, K. Hain, J. Nelson, J. Christopher-Jennings and E. A. Nelson, *BMC Vet. Res.*, 2016, **12**, 95.
4 C. Spiess, Q. Zhai and P. J. Carter, *Mol. Immunol.*, 2015, **67**, 95–106.
5 T. Wróbel, G. Mazur, J. Diana, M. Biedro, R. Badowski and K. Kuliczkowski, *J. Oncol.*, 2005, **55**, 316–319.
6 M. Arruebo, M. Valladares and A. Gonzále-Fernandéz, *J. Nanomater.*, 2009, **2009**, 1–24.
7 A. M. Smith, S. Dave, S. Nie, L. True and X. Gao, *Expert Rev. Mol. Diagn.*, 2006, **6**, 231–244.
8 Y. Xing, Q. Chaudry, C. Shen, K. Y. Kong, H. E. Zhau, L. W. Chung, J. A. Petros, R. M. O'Regan, M. V. Yezhelyev, J. W. Simons, M. D. Wang and S. Nie, *Nat. Protoc.*, 2007, **2**, 1152–1165.
9 O. I. Mićić, H. M. Cheong, H. Fu, A. Zunger, J. R. Sprague, A. Mascarenhas and A. J. Nozik, *J. Phys. Chem.*, 1997, **101**, 4904–4912.
10 J. J. Beato-López, C. Fernández-Ponce, E. Blanco, C. Barrera-Solano, M. Ramírez-del-Solar, M. Domínguez, F. García-Cozar and R. Litrán, *Nanomater. Nanotechnol.*, 2012, **2**, 1–9.
11 L. Trapiella-Alfonso, J. M. Costa-Ferna, R. Pereiro and A. Sanz-Medel, *Talanta*, 2013, **106**, 243–428.
12 A. N. Berlina, N. A. Taranova, A. V. Zherdev, M. N. Sankov, I. V. Andreev, A. I. Martynov and B. B. Zantiev, *PLoS One*, 2013, **8**, 1–8.
13 D. Geißler and N. Hildebrandt, *Anal. Bioanal. Chem.*, 2016, **408**, 4475–4483.
14 U. Resch-Geger, M. Grabolle, S. Cavaliere-Jaricot and R. Nitschke, *Nat. Methods*, 2008, **5**, 763–775.
15 C. Frigerio, D. S. Ribeiro, S. S. Rodrigues, V. L. Abreu, J. A. Barbosa, J. A. Prior, K. L. Marques and J. L. Santos, *Anal. Chim. Acta*, 2012, **735**, 9–22.
16 D. Vasudevan, R. R. Gaddam, A. Trinchi and I. Cole, *J. Alloys Compd.*, 2015, **636**, 395–404.
17 H. Yukawa, R. Tsukamoto, A. Kano, Y. Okamoto, M. Tokeshi, T. Ishikawa, M. Mizuno and Y. Baba, *J. Cell Sci. Ther.*, 2013, **4**, 1–7.
18 K. Zhu, R. Dietrich, A. Didier, D. Doyscher and E. Märtlbauer, *Toxins*, 2014, **6**, 1325–1348.
19 K. T. Yong, Y. Wang, I. Roy, H. Rui, M. T. Swihart, W. C. Law, S. K. Kwak, L. Ye, J. Liu, S. D. Mahajan and J. L. Reynolds, *Theranostics*, 2012, **2**, 681–694.
20 T. A. Zdobnova, O. A. Stremovskiy, E. N. Lebedenko and S. M. Deyev, *PLoS One*, 2012, **7**, 2–9.
21 P. Suriamoorthy, X. Zhang, G. Hao, A. G. Joly, S. Singh, M. Hossu, X. Sun and W. Chen, *Cancer Nanotechnol.*, 2010, **1**, 19–28.
22 D. A. East, D. P. Mulvihill, M. Todd and I. J. Bruce, *Langmuir*, 2011, **27**, 13888–13896.
23 S. Avvakumova, M. Colombo, P. Tortora and D. Prosperi, *Trends Biotechnol.*, 2014, **32**, 11–20.
24 R. Bilan, K. braznik, P. Chames, D. Batyl, I. Nabiev and A. Sukhanova, *Phys. Procedia*, 2015, **73**, 228–234.
25 Y. Zhang and T. H. Wang, *Theranostics*, 2012, **2**, 631–654.
26 C. Schieber, A. Bestetti, J. P. Lim, A. D. Ryan, T. Nguyen, R. Eldridge, A. R. White, P. A. Gleeson, P. S. Donnelly, S. J. Williams and P. Mulvaney, *Angew. Chem., Int. Ed.*, 2012, **51**, 10523–10527.
27 A. Valizadeh, H. Mikaeili, M. Samiei, S. M. Farkhani, N. Zarghami, M. Kouhi, A. Akbarzadev and S. Davaran, *Nanoscale Res. Lett.*, 2012, **7**, 19–21.
28 J. L. Liu, S. A. Walper, K. B. Turner, A. Brozozog, I. L. Medintz, K. Susumu, E. Oh, D. Zabetakis, E. R. Goldman and G. P. Anderson, *Biotechnology Reports*, 2016, **10**, 56–65.
29 U. K. Laemmli, *Nature*, 1970, **227**, 680–685.
30 L. Holubova, L. Korecka, S. Podzimek, V. Moravcova, J. Rotkova, T. Ehlova, V. Velebny and Z. Bilkova, *Carbohydr. Polym.*, 2014, **112**, 271–276.
31 L. A. Cantarero, J. E. Butler and J. W. Osborne, *Anal. Biochem.*, 1980, **105**, 375–382.
32 A. J. Percy, M. Rey, K. M. Burns and D. C. Schriemer, *Anal. Chim. Acta*, 2012, **721**, 7–21.
33 A. C. Hogenboom, A. R. de Boer, R. J. E. Derks and H. Irth, *Anal. Chem.*, 2001, **73**(16), 3816–3823.
34 M. Cadkova, V. Dvorakova, R. Metelka, Z. Bilkova and L. Korecka, *Monatsh. Chem.*, 2016, **147**, 69–73.